

Institut für Nutzpflanzenwissenschaften und Ressourcenschutz (INRES)

– Allgemeine Bodenkunde und Bodenökologie –

**Coupled biotic-abiotic mechanisms of nitrous oxide production in
soils during nitrification involving the reactive intermediates
hydroxylamine and nitrite**

Inaugural-Dissertation zur Erlangung des Grades

Doktor der Agrarwissenschaften

(Dr. agr.)

der

Landwirtschaftlichen Fakultät

der

Rheinischen Friedrich-Wilhelms-Universität Bonn

vorgelegt von

Shurong Liu

aus Chongqing

Bonn 2017

Referent: Prof. Dr. Nicolas Brüggemann

Korreferentin: Prof. Dr. Claudia Knief

Tag der mündlichen Prüfung: 14.09.2017

Contents

Acknowledgements	i
Abstract	iii
Zusammenfassung.....	v
List of Figures	viii
List of Tables	xi
List of abbreviations	xiii
Chapter 1	1
1.1 Theory.....	2
1.2 Rationale.....	3
1.3 State of the art	5
1.3.1 Mechanisms of N ₂ O production from NH ₃ oxidation	5
1.3.2 Reactive N intermediates NH ₂ OH and NO ₂ ⁻	6
1.3.3 Effects of soil properties and environmental factors.....	8
1.4 Objectives and outline of the thesis	9
Chapter 2	11
2.1 Introduction	12
2.2 Materials and methods.....	15
2.2.1 Strains and cultivation	15
2.2.2 Incubation experiments.....	16
2.2.3 Determination of abiotic NH ₂ OH decay rates under ambient air conditions.....	16
2.2.4 Chemical assays	17
2.2.5 Calculation of the NH ₂ OH:final product ratio	17
2.2.6 Calculation of the fraction of NH ₄ ⁺ converted to N ₂ O during incubation	18
2.2.7 Data analyses.....	19
2.3 Results and discussion	19
2.3.1 Extracellular NH ₂ OH from autotrophic ammonia oxidizers.....	19
2.3.2 NH ₂ OH abiotic decay and NH ₂ OH:final product ratios during NH ₃ oxidation	24
2.3.3 Estimating the fraction of NH ₄ ⁺ converted to N ₂ O during NH ₃ oxidation under ambient air conditions	27
2.4 Conclusions	29
Chapter 3	31
3.1 Introduction	32

3.2 Materials and methods.....	33
3.2.1 Soils	33
3.2.2 Principle of the assay.....	34
3.2.3 Experimental design	35
3.2.4 Statistical analyses	37
3.3 Results and discussion	38
3.3.1 Soil NH ₂ OH extractions	38
3.3.2 Nitrite removal.....	40
3.3.3 NH ₂ OH concentration in forest soil samples and its correlation with aerobic N ₂ O emission rate.....	41
3.4 Conclusions	43
Chapter 4	45
4.1 Introduction	46
4.2 Materials and methods.....	48
4.2.1 Experimental site	48
4.2.2 Soil sampling.....	49
4.2.3 Analytical methods.....	50
4.2.4 Data analyses	51
4.3 Results	52
4.3.1 Potential soil N ₂ O emission rates, NH ₂ OH content and basic properties	52
4.3.2 Spatial patterns.....	54
4.3.3 Correlations and multiple stepwise regressions.....	55
4.3.4 Improvement of spatial estimation	57
4.4 Discussion	59
4.4.1 Spatial patterns of potential soil N ₂ O emission rates and soil NH ₂ OH content	59
4.4.2 The contribution of NH ₂ OH to soil potential N ₂ O emission.....	60
4.5 Conclusions	62
Chapter 5	63
5.1 Introduction	64
5.2 Methods	67
5.2.1 Preparation of the artificial soil mixtures	67
5.2.2 Preparation of artificial soil mixtures with different OM qualities.....	67
5.2.3 Addition of NH ₂ OH to the artificial soil mixtures and analysis of the N ₂ O formed ...	68
5.2.4 Calculation of the NH ₂ OH-to-N ₂ O conversion ratio	68

5.2.5 Determination of the basic properties of the organic materials.....	69
5.2.6 Data analyses	70
5.3 Results and discussion	70
5.3.1 $R_{\text{NH}_2\text{OH-to-N}_2\text{O}}$ at different pH, MnO_2 and OM contents (%)	70
5.3.2 $R_{\text{NH}_2\text{OH-to-N}_2\text{O}}$ at different pH, MnO_2 content, and OM quality	73
5.3.3 Development of a stepwise multiple regression model from the artificial soil mixtures and application to natural soils	76
Chapter 6	79
6.1 Introduction	80
6.2 Materials and methods.....	82
6.2.1 Soil collection.....	82
6.2.2 Oxidic and anoxic pre-treatment of soil	83
6.2.3 Addition of reactive N to freeze-dried soils.....	83
6.2.4 N_2O analysis	84
6.2.5 Soil chemical analyses	84
6.2.6 Data analyses	85
6.3 Results	85
6.3.1 Effect of reactive N addition on N_2O production in different soils.....	85
6.3.2 Effect of anoxic pre-incubation on N_2O production from reactive N addition	87
6.3.3 Contribution of abiotic pathways to N_2O production from reactive N addition	88
6.3.4 Controls of the effect of reactive N addition on N_2O production in soils after oxidic and anoxic pre-incubation.....	88
6.4 Discussion	90
6.4.1 The importance of NO_2^- and NH_2OH on biotic and abiotic N_2O formation in different soils.....	90
6.4.2 Effect of soil redox history on N_2O formation from NO_2^- and NH_2OH	91
6.5 Conclusions	93
Chapter 7	95
7.1 Introduction	96
7.2 Materials and methods.....	98
7.2.1 Soil collection.....	98
7.2.2 Experimental setup	99
7.2.3 Data analyses	102
7.3 Results	102

7.3.1 Soil basic properties	102
7.3.2 Mineral N and DOM content before and after drying.....	103
7.3.3 Rewetting effects on soil N ₂ O emissions.....	105
7.3.4 Influence of γ -irradiation on soil N ₂ O and CO ₂ emissions after rewetting.....	107
7.3.5 Control variables of soil N ₂ O emission upon rewetting	108
7.3.6 Isotopic ratio analyses of N ₂ O production during rewetting	109
7.4 Discussion	110
7.5 Conclusions	114
Chapter 8	115
8.1 Synopsis	116
8.2 Synthesis.....	119
8.3 Perspectives	123
References	126
Appendix	139
Figure S2.1	139
Figure S2.2	140
Figure S2.3	141
Figure S2.4	142
Figure S5.1	143
Figure S5.2	144
Figure S5.3	145
Figure S5.4	146
Table S2.1	147
Table S2.2	147
Table S2.3	148

Acknowledgements

This thesis represents not only my work at the keyboard, it is a milestone in more than four years of work in the Agrosphere Institute (IBG-3) at the Forschungszentrum Jülich. Every chapter of this thesis represents many questions, countless ideas, hard experimental work and a lot of discussions. The thesis would not exist without the support of my colleagues I have been lucky to meet during the past four years.

First and foremost I wish to thank my supervisor and first examiner of this thesis, Nicolas Brüggemann. I still remember he taught me the chemical reactions between different N compounds and the basic knowledge of isotope site preference. I also appreciate him for the excellent ideas, constructive criticisms and helpful suggestions during the experimental design, experiment conduction and paper writing. And during the most difficult times when I was frustrated by the experiments, he gave me moral support and the courage I needed to move on. Without the continuous support from him, I could not have finished so many papers during my Ph.D.

I am also thankful to Harry Vereecken, the director of the Agrosphere institute, for giving me the opportunity to do my research at the IBG-3, for the half-yearly discussions and the suggestions at the Ph.D seminar. Further, I would like to thank Jan Vanderborcht for the suggestions at the Ph.D seminar, and Claudia Knief for accepting to be the second examiner of this thesis.

My sincere gratitude is extended to the Chinese Scholarship Council (CSC) that supported the project both in finance and research training.

Dozens of my colleagues in IBG-3 have helped and taught me during my experiment conduction, data analysis, and paper discussion. I am sincerely grateful to Holger Wissel, Franz Leistner and Ulrike Langen for their technical support with the IRMS and GC measurement and ordering chemicals, Wolfgang Tappe and Sirgit Kummer for their technical support with the microbial experiments, Michael Herbst for the support on the Kriging and geostatistics, Anne Berns for the help with NMR analysis, Diana Hofmann, Martina Krause and Andrea Kubica for their assistance in the TOC/TN analysis, Wolfgang Kurtz for the technical support of R. A special thank goes to other colleagues in building 06.1, Jannis Heil, Maria Quade, Michael Stockinger, Di Wu, Kathrin Wagner, Minghua Zhou and Reichel Rüdiger, just to name a few, for the good times.

Further thanks go to colleagues at the University of Vienna, the University of Aberdeen and the Helmholtz center Munich. I appreciate Michael Wagner and James Prosser for welcoming

me in their labs in Vienna and Aberdeen, respectively, for letting me do the microbial experiments with pure ammonia oxidizers, and for their valuable comments and suggestions on the paper writing. I also appreciate Michael Schloter for the conduction of soil gamma-ray irradiation and the valuable comments and suggestions on the paper writing. I am also thankful to Linda Hink and Ping Han for the culture growth and their assistance with the operation of microbial experiments.

Last but not least, I would like to thank my husband Gaochao Cai. He is the warmest bay when I am tired from the research study and Ph.D work. I would not have finished this thesis smoothly without his support and nice companionship in Jülich.

Abstract

Nitrous oxide (N_2O) is an important greenhouse gas that can deplete the ozone layer. Microbial nitrification and denitrification have been long considered as the major contributors of soil N_2O production. However, the mechanisms responsible for N_2O production from nitrification are still not fully understood. The current understanding is that there are mainly two routes responsible for the N_2O production from nitrification: biological ammonia (NH_3) oxidation and nitrifier denitrification of nitrite (NO_2^-). However, so far it has been neglected that abiotic processes could also play an important role in the N_2O production during nitrification, involving the two reactive N intermediates hydroxylamine (NH_2OH) and NO_2^- via coupled biotic-abiotic mechanisms of N_2O production. While the abiotic N_2O production from NO_2^- has been studied in the last decades, the abiotic N_2O production involving NH_2OH has long been ignored. One possible reason could be that NH_2OH was not detected in soils in previous research. In addition, the release of NH_2OH during NH_3 oxidation in pure cultures of ammonia oxidizers has not been studied previously, which would be the prerequisite of abiotic N_2O production involving NH_2OH . Therefore, the aim of the present thesis was to study the relevance and mechanisms of coupled biotic-abiotic N_2O formation from NH_2OH and NO_2^- during nitrification in different soils.

By studying different types of ammonia oxidizers (ammonia-oxidizing bacteria (AOB), ammonia-oxidizing archaea (AOA), and complete ammonia oxidizers (comammox)), this thesis demonstrates NH_2OH release during NH_3 oxidation of various ammonia oxidizers. However, the NH_2OH :final product release ratios were different between the different microbial strains studied, ranging from 0.24% to 1.92%, and were also dependent on initial NH_3 concentrations in the medium. The presence of NO_2^- decreased the abiotic NH_2OH decay rate in the medium but increased abiotic N_2O production involving NH_2OH . The calculated fraction of NH_4^+ converted to N_2O via NH_2OH release during incubations ranged from 0.05% to 0.14%, which was consistent with published NH_4^+ -to- N_2O conversion ratios for certain ammonia oxidizers.

Hydroxylamine could not only be detected in pure cultures, but also be determined in natural soils by developing and applying a highly sensitive method using extraction under acidic conditions and oxidation of NH_2OH to N_2O with Fe^{3+} . The determined NH_2OH content in spruce forest soil samples ranged between 0.3 and 34.8 $\mu\text{g N kg}^{-1}$ dry soil, which was consistent with the magnitude of NO_2^- contents reported for forest soils. This thesis further shows a positive spatial correlation between NH_2OH concentrations and aerobic N_2O

production in Norway spruce forest soil, although aerobic N_2O production was also correlated with other soil basic properties, such as soil pH, NO_3^- , Mn, and soil organic carbon (SOC) content. Similar hotspots were identified for aerobic N_2O production itself as well as for the contribution of NH_2OH to aerobic N_2O production. The incorporation of the NH_2OH information largely improved the estimation of aerobic N_2O production in the study area.

In a systematic experiment with artificial soil mixtures with the aim to test the relevance of the control parameters identified in the forest soil study, the abiotic conversion of NH_2OH to N_2O was strongly dependent on soil organic matter (SOM) content, pH, and MnO_2 content. More NH_2OH was chemically converted to N_2O at low SOM content, low pH, and high MnO_2 content. Based on these results, the thesis presents a model to estimate abiotic NH_2OH -to- N_2O conversion in soils by considering the SOM and MnO_2 content as well as pH. It should be noted that not only the quantity, but also the quality of SOM, e.g. certain functional groups, such as carbonyl groups, can affect the abiotic conversion of NH_2OH to N_2O .

The thesis further explored the contribution of the two reactive N species NO_2^- and NH_2OH to abiotic N_2O production in different soils after oxic and anoxic pre-incubation. NO_2^- played the most important role in N_2O production in grassland soil, followed by the soils of upland forest, a riparian area, and cropland. Abiotic processes contributed about 10-40% to the conversion of NO_2^- to N_2O , but no significant factors responsible for the N_2O production from NO_2^- could be identified. N_2O production from NH_2OH played an important role in grassland and cropland soils, as well as partly in the forest soil. In contrast to NO_2^- , the conversion of NH_2OH to N_2O was mostly (>80%) abiotic and was correlated significantly with soil pH, MnO_2 and SOC content. After anoxic incubation, the contribution of NO_2^- to aerobic N_2O production increased, while the contribution of NH_2OH decreased depending on SOC content. Finally, a close relationship was found between pulse N_2O production after rewetting of air-dried soils and concentration of NO_2^- accumulated in the dry soils. Abiotic processes contributed 10-70% of N_2O production after rewetting of forest soil, but were even considerably higher in the grassland soil after gamma radiation.

In summary, this thesis describes the coupled biotic-abiotic mechanisms of N_2O production during nitrification in detail by studying the processes related to abiotic N_2O production from NH_2OH systematically with a series of experiments, and by exploring the contribution of NO_2^- and NH_2OH to abiotic N_2O production under various environmental conditions and for different soil types. The results of the thesis improve the understanding of the mechanisms as well as the quantification of aerobic N_2O production in soils, and could contribute to

developing more effective N₂O mitigation measures, such as increasing soil pH and adding organic soil amendments with appropriate functional groups that can react chemically with NH₂OH.

Zusammenfassung

Lachgas (N₂O) ist ein bedeutendes Treibhausgas, welches zum Abbau der Ozonschicht beitragen kann. Mikrobielle Nitrifikation und Denitrifikation wurden lange als die Hauptquellen der N₂O-Produktion im Boden angesehen. Allerdings sind die Mechanismen, welche für die N₂O-Produktion während der Nitrifikation im Boden verantwortlich sind, noch nicht vollständig entschlüsselt. Bisher ist man davon ausgegangen, dass hauptsächlich zwei Komponenten zur N₂O-Produktion während der Nitrifikation beitragen: biologische Ammoniak-(NH₃)-Oxidation und Nitrifizierer-Denitrifikation von Nitrit (NO₂⁻). Allerdings könnten auch abiotische Prozesse eine wichtige Rolle in der N₂O-Produktion während der Nitrifikation spielen, und zwar durch einen gekoppelten biotisch-abiotischen Mechanismus, ausgehend von den zwei reaktiven Zwischenprodukten Hydroxylamin (NH₂OH) und NO₂⁻. Obwohl die abiotische N₂O-Produktion aus NO₂⁻ in den letzten Jahrzehnten untersucht wurde, wurde die abiotische N₂O-Produktion aus NH₂OH bisher nicht beachtet. Eine mögliche Ursache könnte sein, dass in bisherigen Studien NH₂OH in Böden nicht nachgewiesen wurde. Ebenso wurde die Freisetzung von NH₂OH während der NH₃-Oxidation in reinen Kulturen von Ammoniakoxidierern bisher nicht untersucht, welche die Voraussetzung für die abiotische N₂O-Produktion aus NH₂OH wäre. Das Ziel der vorliegenden Arbeit war daher, die Relevanz und die Mechanismen gekoppelter biotischer-abiotischer N₂O-Bildung aus NH₂OH und NO₂⁻ während der Nitrifikation in unterschiedlichen Böden zu untersuchen.

In der vorliegenden Dissertation konnte anhand von Untersuchungen von Reinkulturen bzw. Anreicherungen unterschiedlicher Ammoniakoxidierer (ammoniakoxidierende Bakterien – AOB, ammoniakoxidierende Archaeen – AOA, sowie vollständige Ammoniakoxidierer – Comammox) eine der NH₂OH-Freisetzung während der NH₃-Oxidation gezeigt werden. Allerdings unterschieden sich die Verhältnisse zwischen NH₂OH-Freisetzung und Endproduktbildung zwischen den unterschiedlichen Mikroorganismenstämmen (0.24% bis zu 1.92%) und waren von der NH₃-Konzentration im Medium abhängig. Die Anwesenheit von NO₂⁻ verringerte im Mittel die abiotische NH₂OH-Zerfallsrate, erhöhte hingegen die abiotische N₂O-Produktion aus NH₂OH. Der Anteil von NH₄⁺, der dabei während der Inkubationszeit über NH₂OH in N₂O umgewandelt wurde, variierte zwischen 0.05% und

0.14%, und stimmte damit mit für verschiedene Ammoniakoxidierer veröffentlichten Werten von NH_4^+ -zu- N_2O -Umwandlungsverhältnissen überein.

Im Rahmen der vorliegenden Arbeit wurde die NH_2OH -Freisetzung nicht nur in Reinkulturen untersucht, sondern auch in natürlichen Böden. Hierzu wurde eine hochempfindliche Methode entwickelt und angewendet, bei der NH_2OH unter sauren Bedingungen extrahiert und anschließend mit Fe^{3+} zu N_2O oxidiert wird. Mit dieser neu entwickelten Methode konnte ein NH_2OH -Gehalt in Fichtenwaldböden zwischen 0.3 und 3.8 $\mu\text{g N kg}^{-1}$ Bodentrockengewicht nachgewiesen werden, der in der gleichen Größenordnung wie der NO_2^- -Gehalt in Waldböden lag. Zudem konnte in dieser Dissertation auch eine positive räumliche Korrelation zwischen NH_2OH -Konzentrationen im Boden und der aeroben N_2O -Produktion in einem Fichtenwald gefunden werden, wobei die aerobe N_2O -Produktion auch mit anderen Bodeneigenschaften, wie dem pH-Wert sowie dem NO_3^- -, Mn- und organischen Kohlenstoff- (SOC)-Gehalt, korrelierte. Hierbei wurden ähnliche Hotspots sowohl für die aerobe N_2O -Produktion selber als auch für den Beitrag von NH_2OH zur aeroben N_2O -Produktion identifiziert. Die Berücksichtigung der NH_2OH -Information in einem multiplen Regressionsmodell führte zu einer erheblichen Verbesserung der Abschätzung der N_2O -Produktion im Untersuchungsgebiet.

In einem systematischen Experiment mit künstlichen Bodenmischungen war die abiotische Umwandlung von NH_2OH in N_2O stark vom Gehalt an organischer Bodensubstanz (SOM), dem pH-Wert und dem MnO_2 -Gehalt abhängig. Bei geringem SOM-Gehalt, niedrigem pH-Wert und hohem MnO_2 -Gehalt wurde mehr NH_2OH chemisch zu N_2O umgewandelt. Basierend auf diesen Ergebnissen wurde in dieser Dissertation ein multiples Regressionsmodell entwickelt, welches die abiotische Umwandlung von NH_2OH zu N_2O in Böden unter Berücksichtigung des SOM- und MnO_2 Gehalts sowie dem pH-Wert abschätzt. Hierbei muss allerdings beachtet werden, dass nicht nur die Quantität, sondern auch die Qualität der SOM (z.B. bestimmte funktionale Gruppen) die abiotische Umwandlung von NH_2OH zu N_2O beeinflussen können.

Weiterhin wurde in dieser Dissertation der Beitrag der beiden reaktiven Nitrifikationsintermediate NO_2^- und NH_2OH zur abiotischen N_2O -Produktion in unterschiedlichen Böden nach oxidischer und anoxischer Vorinkubation untersucht. Es konnte gezeigt werden, dass NO_2^- eine wichtige Rolle in der N_2O -Produktion in Graslandböden spielte, gefolgt von Waldböden aus der ungesättigten Zone und dem Uferbereich sowie von Ackerlandböden. Abiotische Prozesse trugen zu 10-40% zur Umwandlung von NO_2^- zu N_2O bei. Es konnten allerdings keine signifikanten Faktoren, die für die N_2O -Produktion durch

NO_2^- verantwortlich waren, identifiziert werden. N_2O -Produktion aus NH_2OH spielte eine wichtige Rolle in Grasland- und Ackerböden, sowie auch teilweise in den untersuchten Waldböden. Die Umwandlung von NH_2OH zu N_2O war größtenteils (>80%) abiotisch und korrelierte signifikant mit dem pH-Wert des Bodens sowie mit dem MnO_2 - und SOC-Gehalt. Anoxische Vorinkubation führte zu einer Erhöhung des Beitrags von NO_2^- zur aeroben N_2O -Produktion, während der Beitrag von NH_2OH sich, abhängig vom SOC-Gehalt des Bodens, verringerte.

Schließlich konnte eine enge Beziehung zwischen pulsartiger N_2O -Produktion nach Wiederbefeuchtung von luftgetrockneten Waldböden und der Konzentration von NO_2^- , welches während der Trocknung der Böden akkumuliert worden war, beobachtet werden. Hierbei trugen abiotische Prozesse zu 10-70% zur N_2O -Produktion in den wiederbefeuchteten Waldböden bei. In wiederbefeuchteten Graslandböden war der Anteil abiotischer Prozesse an der N_2O -Produktion nach Gamma-Bestrahlung sogar noch erheblich größer.

Zusammenfassend beschreibt diese Dissertation die gekoppelten biotischen-abiotischen Mechanismen der N_2O -Produktion während der Nitrifikation. Hierzu wurden die Prozesse, die an der N_2O -Produktion aus NH_2OH beteiligt sind, systematisch in einer Reihe von Experimenten untersucht. Darüber hinaus wurde der Beitrag von NO_2^- und NH_2OH zur abiotischen N_2O -Produktion unter unterschiedlichen Umweltbedingungen und für unterschiedlichen Bodentypen näher untersucht. Die Ergebnisse dieser Dissertation verbessern das Verständnis der Mechanismen sowie die Quantifizierung der aeroben N_2O -Produktion in Böden und könnten zur Entwicklung effektiverer N_2O -Minderungsmaßnahmen beitragen, z.B. durch Erhöhung des Boden-pH-Wertes und Zugabe von organischen Bodenhilfsstoffen mit verschiedenen funktionellen Gruppen, welche mit NH_2OH chemisch reagieren können.

List of Figures

Figure 2.1 Dynamics of NH_4^+ (red squares), NO_2^- (yellow circles), NH_2OH (blue triangles) and total N (sum of NO_2^- and NH_4^+ , black diamonds) concentrations during incubation of four ammonia oxidizing bacteria. NH_4^+ , NO_2^- and total N are plotted using the left y-axis, while NH_2OH is plotted using the right y-axis. Please note that the left y-axes and the x-axes, respectively, are not always scaled identically to improve data presentation. The values are presented as mean \pm standard error (SE). 20

Figure 2.2 Dynamics of NH_4^+ (red squares), NO_2^- (yellow circles), NH_2OH (blue triangles) and total N (sum of NO_2^- and NH_4^+ , black diamonds) concentrations in the batch experiments with four ammonia oxidizing archaea. NH_4^+ , NO_2^- and total N are plotted using the left y-axis, while NH_2OH is plotted using the right y-axis. Please note that the left y-axes and the x-axes, respectively, are not always scaled identically to improve data presentation. The values are present as mean \pm standard error (SE). 22

Figure 2.3 Dynamics of NH_4^+ (red squares), NO_3^- (yellow circles), NH_2OH (blue triangles) and total N (sum of NO_3^- and NH_4^+ , black diamonds) concentrations during the incubation of the comammox organism *N. inopinata*. NH_4^+ , NO_3^- and total N are plotted using the left y-axis, while NH_2OH is plotted using the right y-axis. The values are present as mean \pm standard error (SE). 24

Figure 2.4 Abiotic decay of NH_2OH in the absence (hollow) or presence (solid) of 2 mM NO_2^- in HEPES-buffered and CaCO_3 -buffered media at different incubation temperatures. The NH_2OH concentrations were 0.5 (square), 1 (circle), 2.5 (triangle), and 5 (diamond) μM . Mean values of three replicates are presented. The relative standard deviation (RSD) of all data is smaller than 10%. Please note that the x-axes are not always scaled identically to improve data presentation. 25

Figure 2.5 Schematic representation of N_2O production pathways during NH_3 oxidation involving NH_2OH and NO_2^- (AMO, ammonia monooxygenase; HAO, hydroxylamine dehydrogenase; NIR, nitrite reductase; NOR, NO reductase). Please note that the schematic cell drawing includes the periplasm. 29

Figure 3.1 The final workflow of NH_2OH extraction in this study. 36

Figure 3.2 Effects of extraction time on NH_2OH concentration of the extract with shaking (a) and magnetic stirring (b) at 4 °C. Error bars indicate the range of measured concentrations (n = 2). 39

Figure 3.3 Effect of 10 and 100 μM NO_2^- on NH_2OH conversion with and without sulfanilamide (SA) in 0.05 M acetic acid + 0.01 M HCl solution (a) and soil extracts (b) at pH 2 and room temperature. Error bars indicate the standard deviation of the mean (n = 3). 40

Figure 3.4 Effect of different NO_2^- concentrations on NH_2OH determination in the presence of 2 mM sulfanilamide (SA) at pH 2 in 0.05 M acetic acid + 0.01 M HCl solution (n = 3). 41

Figure 3.5 Correlation between soil NH ₂ OH content and aerobic N ₂ O emission rates at room temperature of soil samples collected from Wüstebach forest (n = 44).	42
Figure 4.1 Map showing the location of the sampling area and the exact position of the sampling points within the Wüstebach catchment.	49
Figure 4.2 Semivariograms of log-transformed N ₂ O emission rates [$\ln(\mu\text{g}^{-1} \text{ N kg}^{-1} \text{ dry soil h}^{-1})^2$], NH ₂ OH content [$\ln(\mu\text{g}^{-1} \text{ N kg}^{-1} \text{ dry soil})^2$] and NO ₃ ⁻ content [$\ln(\text{mg N kg}^{-1} \text{ dry soil})^2$] in the Ah (A) and Oh (B) of the sampling area.	54
Figure 4.3 Spatial patterns of potential N ₂ O emission rates ($\mu\text{g}^{-1} \text{ N kg}^{-1} \text{ dry soil h}^{-1}$), NH ₂ OH content ($\mu\text{g}^{-1} \text{ N kg}^{-1} \text{ dry soil}$) and NO ₃ ⁻ content (mg N kg ⁻¹ dry soil) estimated using ordinary Kriging (OK) for the Ah and Oh layers of the sampling area. The grey smooth lines in the maps are contour lines. The black line represents the Wüstebach creek. The black points indicate the sampling points with valid data for each soil property.	55
Figure 4.4 Spatial patterns of potential N ₂ O emission rates estimated using external-drift Kriging (EDK) and conditional stochastic simulations (CSS) for the Ah and Oh layers. The EDK estimation is an extension of ordinary Kriging (OK) by using spatial regression estimates based on the regression models as auxiliary data. The CSS estimation is an estimation based on the spatial variability and spatial structure by checking the cumulative probability density function. The color code of the EDK maps represent N ₂ O emission rates in $\mu\text{g}^{-1} \text{ N kg}^{-1} \text{ dry soil h}^{-1}$, while the color code of the CSS maps represent the logarithm of N ₂ O emission rates in $\mu\text{g}^{-1} \text{ N kg}^{-1} \text{ dry soil h}^{-1}$	58
Figure 5.1 Hypothetical model of NH ₂ OH release by ammonia-oxidizing bacteria to the soil environment and potential reactions of NH ₂ OH with MnO ₂ and organic matter in the soil at different pH conditions (R ₁ R ₂ C=O represents carbonyl groups of SOM). AMO is ammonia monooxygenase; HAO is hydroxylamine oxidoreductase.	66
Figure 5.2 NH ₂ OH-to-N ₂ O conversion ratios (R _{NH₂OH-to-N₂O}) in artificial soil mixtures at different pH as well as MnO ₂ and organic matter (OM, peat moss) contents. The total amount of NH ₂ OH added was 5 nmol. Different symbols represent R _{NH₂OH-to-N₂O} at different OM content.	72
Figure 5.3 NH ₂ OH-to-N ₂ O conversion ratios (R _{NH₂OH-to-N₂O}) in artificial soils at different pH and MnO ₂ content, and for organic matter of different origins at a fixed content of 2.5% (w/w). The total amount of NH ₂ OH added was 5 nmol. Different symbols represent R _{NH₂OH-to-N₂O} for the artificial soil mixtures with the different organic materials.	74
Figure 5.4 The ¹³ C- and ¹⁵ N-CPMAS-NMR spectra of the different organic materials (cyanobacterium, clover, watermilfoil, peat moss) used in the experiment.	75
Figure 5.5 Results of the application of the artificial soil regression model for the NH ₂ OH-to-N ₂ O conversion ratios (R _{NH₂OH-to-N₂O}) to artificial soil mixtures amended with the different	

organic materials (n=22). The three points for which $R_{\text{NH}_2\text{OH-to-N}_2\text{O}}$ was determined at pH 3, 4, and 5 without MnO_2 addition were excluded for better simulation. 77

Figure 5.6 Application of the artificial soil regression model for the calculation of NH_2OH -to- N_2O conversion ratios to six natural fresh and fumigated soils as reported in Heil *et al.* (2015). 78

Figure 6.1 Net N_2O (ng N g^{-1} dry soil) production in forest (F1, F2, F3, F4, F5 and FR), grassland (G) and cropland (C) soils after NO_2^- (A: oxic, C: anoxic pre-incubation) and NH_2OH (B: oxic, D: anoxic pre-incubation) addition. Net N_2O production was calculated by subtracting N_2O emission after addition of pure water (as control) from the N_2O emission after addition of NO_2^- or NH_2OH solution. The values are presented as mean \pm standard deviation (SD). 86

Figure 6.2 Soil N_2O production (ng N g^{-1} dry soil) after MnO_2 and NH_2OH addition after oxic (A) and anoxic (B) pre-incubation for samples from forest (F1, F2, F3, F4, F5 and FR), grassland (G) and cropland (C). 89

Figure 7.1 Soil NH_4^+ (A) and NO_3^- (B) content before (W, grey) and after air-drying (AD, black) for forest (F_{Of} , F1, F2, F3, F4, F5, F6 and FR), grassland (G) and cropland (C) soil samples. Only one extraction was performed for the determination of soil NH_4^+ and NO_3^- content. 104

Figure 7.2 Rewetting effects by the addition of water (A), and aqueous solutions of NO_2^- (B), NO_3^- (C) and NH_4^+ (D) on soil N_2O production (ng N g^{-1} dry soil) of forest (F_{Of} , F1, F2, F3, F4, F5, F6 and FR), grassland (G) and cropland (C) soil samples for different (1 and 7 h) incubation times. The values are present as mean \pm standard deviation (SD). 106

Figure 7.3 Rewetting effects by the addition of water (A) and aqueous NO_2^- (B) solution on soil N_2O production (ng N g^{-1} dry soil) of forest (F_{Of} , F1, F2, F3, F4, F5, F6 and FR), grassland (G) and cropland (C) soil samples for different (1 h and 7 h) incubation times after γ -irradiation. The values are present as mean \pm standard deviation (SD). 107

List of Tables

Table 2.1 Total NH ₂ OH:final product (NO ₂ ⁻ or NO ₃ ⁻) ratios for different ammonia oxidizers. § For <i>N. inopinata</i> (a comammox organism), NO ₃ ⁻ is the final product of NH ₃ oxidation. # The NH ₂ OH concentration here is the total extracellular NH ₂ OH including the calculated concentration of NH ₂ OH that was abiotically converted during incubation.....	27
Table 2.2 Fraction (%) of N ₂ O abiotically produced from the added NH ₂ OH in the different media at various levels of NH ₂ OH (0.5, 1 and 2.5 μM) and NO ₂ ⁻ (0, 1 and 2 mM).....	28
Table 2.3 Estimated fraction of NH ₄ ⁺ converted to N ₂ O from the abiotic reactions between the biologically produced extracellular NH ₂ OH and substances in the medium for different ammonia oxidizers.	28
Table 3.1 Characteristics of the soil used in the experiments of this study (n = 3, ± sd).....	34
Table 3.2 pH and temperature effect on NH ₂ OH extraction during 10 min magnetic stirring at 4 °C (n = 3, ± sd).....	38
Table 4.1 Descriptive statistics of potential N ₂ O emission rates, NH ₂ OH concentrations and other soil variables of the Ah and Oh soil horizons.	53
Table 4.2 Spearman's rank correlation coefficients of the correlations of N ₂ O emission rates with NH ₂ OH, NO ₃ ⁻ , NH ₄ ⁺ , C, N, C/N, pH ₁ (H ₂ O),pH ₂ (CaCl ₂) and soil water content (SWC) in the Oh (grey area) and Ah (white area) layer, respectively.	56
Table 4.3 Stepwise multiple regression equations of potential N ₂ O emission rates in the Oh and Ah layer, respectively. The Akaike Information Criterion (AIC) was used for the model selection in the multiple linear regressions.	57
Table 4.4 Mean absolute error (MAE), root mean square error (RMSE), χ^2 and the improvement (<i>I_r</i>) percentage for the interpolation maps of ordinary Kriging (OK) and external drift Kriging (EDK).....	58
Table 5.1 Basic elemental properties of the organic materials used in this study.	68
Table 5.2 The chemical structures and their relative proportions derived from ¹³ C CPMAS NMR spectra of the different plant materials.	76
Table 6.1 Basic properties of the soils used in this study. For the determination of total C, N, Fe and Mn content, soils with oxic pre-incubation were used. Values are presented as mean of three replicates. The coefficient of variation of all data was smaller than 10% and is therefore not shown. For the determination of pH, DOC, DTN, A ₂₅₄ , NH ₄ ⁺ and NO ₃ ⁻ , soils with both oxic and anoxic pre-incubation were used, and only one extraction was carried out.	84

Table 6.2 Effect of anoxic pre-treatment on soil N ₂ O emissions after 1 and 7 h of incubation of soils with NO ₂ ⁻ additions. Values indicate the relative change (%) in N ₂ O emission in anoxic vs. oxic pre-treatment. Negative values indicate a decrease.	87
Table 6.3 Contribution (%) of abiotic pathways to soil N ₂ O emissions after 7 h incubation of soils with addition of aqueous solutions of NH ₂ OH or NO ₂ ⁻ to soil samples with oxic or anoxic pre-incubation and freeze-drying treatment. The data of F4 after γ-irradiation treatment is missing due to shortage of material.	88
Table 6.4 Spearman's correlation coefficients between soil N ₂ O emissions and basic soil properties in forest soil samples after 7 h incubation. Asterisks indicate a significant correlation (<i>P</i> < 0.05).	89
Table 7.1 Basic properties of air-dried soils. Data values are presented as mean (SD).	103
Table 7.2 Soil NO ₂ ⁻ -N (mg kg ⁻¹), dissolved organic carbon (DOC, mg kg ⁻¹), dissolved total nitrogen (DTN, mg kg ⁻¹) and A ₂₅₄ (cm ⁻¹ g ⁻¹ dry soil) after air-drying for forest, grassland and cropland soil samples. The standard deviation of the NO ₂ ⁻ assay is about 20% of the values (n.d. = not detectable). Only one extraction was performed for the determination of soil DOC, DTN and A ₂₅₄	104
Table 7.3 The inhibitory effect (%) of γ-irradiation on soil N ₂ O and CO ₂ emissions after 7 h incubation after rewetting of air-dried soils. Negative values represent a stimulating effect of γ-irradiation.	108
Table 7.4 Spearman's correlation coefficients between soil N ₂ O emission after 7 h incubation after rewetting and basic soil properties of air-dried soils (excluding Ca, Mg and K) across all soil samples. An asterisk indicates significance of the respective correlation coefficient at a level of <i>P</i> < 0.05.	109
Table 7.5 ¹⁵ N site preference (SP) values of N ₂ O production (peak height) upon water rewetting with different soil samples and incubation time. The peak height of ambient air and 400 ppb standard N ₂ O gas was about 1.9 and 2.4 nA, respectively.	109

List of abbreviations

A ₂₅₄	Absorption at a wavelength of 254 nm
Ah	humic mineral topsoil horizon
AIC	Akaike information criterion
AMO	ammonia monooxygenase
ANOVA	Analysis of variance
AOA	ammonia oxidizing archaea
AOA-TES	ammonia oxidizing archaea trace element solution
AOB	ammonia oxidizing bacteria
a.s.l.	above sea level
Ca	calcium
CaCl ₂	calcium chloride
CaCl ₂ ·2 H ₂ O	calcium chloride dehydrate
CaCO ₃	calcium carbonate
C/N	carbon-to-nitrogen ratio
CH ₄	methane
CO ₂	carbon dioxide
comammox	complete ammonia oxidation by bacterial nitrifiers
CPMAS	cross-polarisation magic-angle spinning
CSS	conditional stochastic simulation
cyt	cytochrome
Cu ²⁺	cupric ion
CV	coefficient of variation
δ	isotope ratio of a sample or substance relative to an isotope ratio of a standard
δ ¹⁵ N	¹⁵ N/ ¹⁴ N isotopic ratio of a sample relative to a standard
δ ¹⁵ N ^{bulk}	average δ ¹⁵ N of N ₂ O
δ ¹⁵ N ^α	δ ¹⁵ N of the central position of N ₂ O
δ ¹⁵ N ^β	δ ¹⁵ N of the terminal N position of N ₂ O
δ ¹⁸ O	¹⁸ O/ ¹⁶ O isotope ratio of a sample relative to a standard
DIN	Deutsches Institut für Normung
DNRA	dissimilatory nitrate reduction to ammonium
DOC	dissolved organic carbon

DOM	dissolved organic matter
DTPA	diethylenetriaminepentaacetic acid
DTN	dissolved total nitrogen
ECD	electron capture detector
EDK	external-drift Kriging
EFs	emission factors
FID	flame ionization detector
Fe	iron
Fe ²⁺	ferrous iron
Fe ₂ O ₃	hematite
Fe ³⁺	ferric iron
FeCl ₃	iron(III) chloride
FeNaEDTA	iron sodium ethylenediaminetetraacetate
F _{of}	fermented litter sample
FR	forest riparian
G	grassland
γ	gamma
GC	gas chromatography
H ⁺	proton
H ₂ O	water
H ₂ O ₂	hydrogen peroxide
HAO	hydroxylamine oxidoreductase
HCl	hydrogen chloride
He	helium gas
HEPES	4-(2-hydroxyethyl)-1-piperazineethanesulfonic acid
HNO	nitroxyl
HNO ₂	nitrous acid
HNO ₃	nitric acid
HSD	Tukey honest significant difference
ICP-OES	inductively coupled plasma optical emission spectrometry
IR	infrared
<i>I_r</i>	improvement index
IRMS	isotope ratio mass spectrometer

ISO	International Organization for Standardization
K	potassium
KCl	potassium chloride
KH ₂ PO ₄	potassium dihydrogen phosphate
L	litter layer
LD	left deviation
MAE	mean absolute error
MgSO ₄ ·7 H ₂ O	magnesium sulfate heptahydrate
Mn	manganese
Mn ²⁺	manganous ion
Mn ⁴⁺	manganese ion
MnO	manganese(II) oxide
MnO ₂	manganese(IV) dioxide
N	nitrogen
N ₂	nitrogen gas
Na	sodium
Na ₂ CO ₃	sodium carbonate
NaCl	sodium chloride
NaNO ₂	sodium nitrite
NaOH	sodium hydroxide
ND	normal distribution
NH ₂ OH	hydroxylamine
NH ₃	ammonia
NH ₄ ⁺	ammonium
NH ₄ Cl	ammonium chloride
(NH ₄) ₂ SO ₄	ammonium sulfate
NIR	nitrite reductase
NirK	nitrite reductase gene
NMR	Nuclear Magnetic Resonance
N ₂ O	nitrous oxide
NO	nitric oxide
NO ₂	nitrogen dioxide
NO ₂ ⁻	nitrite

NO_3^-	nitrate
NOB	nitrite-oxidizing bacteria
NOR	nitric oxide reductase
NorB	nitric oxide reductase subunit B
NUE	nitrogen use efficiency
O	organic soil horizon
O_2	oxygen gas
Oa	humus-rich organic soil horizon
Oh	humic organic topsoil horizon
OH^-	hydroxide
OK	ordinary Kriging
OM	organic matter
P	phosphate
QCLAS	quantum cascade laser absorption spectrometer
RD	right deviation
RF	radio frequency
RMSE	root mean square error
$R_{\text{NH}_2\text{OH-to-N}_2\text{O}}$	$\text{NH}_2\text{OH-to-N}_2\text{O}$ conversion ratio
rpm	revolutions per minute
$\text{R}^1\text{R}^2\text{CO}$	carbonyl group
$\text{R}^1\text{R}^2\text{CNOH}$	oxime group
RSD	relative standard deviation
S	sulfur
SA	sulfanilamide
SASIM	Simulated Annealing Simulation
SD	standard deviation
SE	standard error
SO_4^{2-}	sulfate ion
SOC	soil organic carbon
SOM	soil organic matter
S&W	Skinner and Walker
SWC	soil water content
SWS	selenium-tungsten solution

SP	site preference
T	temperature
TERENO	Terrestrial Environmental Observatories
TOC-TN	total organic carbon-total nitrogen
UV	ultraviolet
VESPER	Variogram Estimation and Spatial Prediction plus Error
VDLUFA	Verband Deutscher Landwirtschaftlicher Untersuchungs- und Forschungsanstalten
VSMOW	Vienna Standard Mean Ocean Water
WHC	water-holding capacity
WFPS	water-filled pore space

Chapter 1

Introduction

1.1 Theory

Nitrogen (N) is the dominant element in the atmosphere, which is essential for the synthesis of nucleic acids and proteins on earth. Despite the importance of N and its overwhelming abundance in the atmosphere, most of the N is stored in the earth's atmosphere as chemically inert triple bonded dinitrogen (N_2), making ~78% of the atmosphere. Two hundred years ago, the atmospheric N could only enter the biogeochemical N cycle through lightning and natural biological N fixation in the form of ammonia (NH_3). Since about 100 years, human activity has dramatically increased NH_3 production and release into the environment by fixing N_2 to NH_3 through the industrial Haber-Bosch method and by implementing new agricultural practices (e.g. increasing artificial fertilizer input) that boosted crop yields to fulfill the demand of the increasing world population. As fertilizer application rates increased, crop yield increased while nitrogen use efficiency (NUE) decreased to a certain degree. Zhang et al. (2015a) estimated that the global average NUE was 47% in 2009 and 42% in 2010, respectively. The low NUE is mainly due to unavoidable N losses by, e.g., gaseous N emission and nitrate (NO_3^-) leaching associated with soil biological activity. Gaseous N loss, e.g. in the form of nitric oxide (NO), nitrous oxide (N_2O) and NH_3 has resulted in substantial consequences for the atmospheric composition and severe effects on the environment and human health (Galloway *et al.*, 2008; Davidson, 2012).

The recent concern about global warming and ozone depletion has increased attention for research into N_2O . N_2O is a powerful greenhouse gas and is currently the third largest contributor to global warming, after carbon dioxide (CO_2) and methane (CH_4) (IPCC, 2013). While not as abundant in the atmosphere as CO_2 , an equivalent mass of it is nearly 300 times more potent in its global warming potential than CO_2 . Besides, N_2O has deleterious effects in the stratosphere, where it breaks down and acts as a catalyst in the destruction of atmospheric ozone. N_2O can stay in the stratosphere for hundreds of years. The global lifetime of N_2O is approximately 114 years according to the 5th Assessment report of the IPCC (IPCC, 2013). Since the industrial revolution, the N_2O mixing ratio in the atmosphere has increased about 20%, from 270 ± 7 ppb in 1750 to 324.2 ppb in 2011 (IPCC, 2013). It is reported that anthropogenic sources contribute about 40% of the total N_2O production, and agriculture contributes about 60% of the total anthropogenic N_2O production (IPCC, 2013). The increase is dominated by emissions from soils treated with synthetic and organic (manure) nitrogen fertilizer since the early 1950s according to measurements of N_2O and its isotopic

composition in firm air (Roeckmann & Levin, 2005; Ishijima *et al.*, 2007; Davidson, 2009; Syakila & Kroeze, 2011). The stimulating effect of N fertilization on the production of N₂O was shown in numerous studies (Shcherbak *et al.*, 2014). An exponential correlation was found between the N input and N₂O emissions from fertilized soils (Hoben *et al.*, 2011), and global emission factors (EFs) for fertilizer-induced direct N₂O emissions have been determined. For every 100 kg of fertilizer-N input, 1 kg of N in the form of N₂O is estimated to be emitted directly from soil (De Klein *et al.*, 2006). However, this EF was found to be strongly dependent on different fertilizer type, crop type, soil basic properties (e.g. soil C, pH) and environmental factors (e.g. water) (Bouwman *et al.*, 2002). Moreover, the mechanisms of N₂O formation in soils is not fully understood at present, and quantitative understanding of N₂O emissions remains an unresolved challenge at global, national and regional scales (Butterbach-Bahl *et al.*, 2013). To better estimate the N₂O emissions from soils and to provide theoretical support for the development of N₂O mitigation measures, a better understanding of the mechanisms responsible for N₂O production in soils is urgently required.

1.2 Rationale

According to the classic “hole-in-the-pipe” conceptual model (Firestone & Davidson, 1989), N₂O can leak out during nitrification (i.e., during NH₃ oxidation to nitrate (NO₃⁻)) and denitrification (i.e., during NO₃⁻ reduction to N₂), depending mainly on soil water content. This model generally shows the main processes responsible for soil N₂O production in soils. Until now, microbial nitrification and denitrification in managed and natural soils are widely accepted as the major sources of N₂O emissions from soil, contributing approximately 70% of global N₂O emissions (Braker & Conrad, 2011).

Denitrification is the microbial process that reduces NO₃⁻ anaerobically to nitrite (NO₂⁻), NO, N₂O and N₂. As an important intermediate of denitrification (NO₃⁻→NO₂⁻→NO→N₂O→N₂), the N₂O production from denitrification has been studied very early, together with the study of the denitrification process itself (Nömmik, 1956). The large contribution of denitrification to N₂O emissions in various ecosystems has been further demonstrated and summarized in a large number of studies (Bateman & Baggs, 2005; Baggs, 2011; Bouwman *et al.*, 2013), adding more detailed information on quantification and control of N₂O production via denitrification. However, one fundamental problem of the quantification of denitrification is

that it is very difficult to quantify the dominant end-product (N_2) of denitrification, given its high background concentration in the atmosphere, which makes the assessment of the efficiency of N_2O mitigation from denitrification difficult. Moreover, the proposed management options with consideration of denitrification only, such as application of copper (Cu) fertilizer to regulate Cu availability for the Cu-based nitrous oxide reductase enzyme, and liming of cropland or grassland, are ineffective in certain soils to promote the reduction of N_2O to N_2 (Richardson *et al.*, 2009).

On the other hand, although N_2O is not an intermediate of nitrification ($NH_3 \rightarrow NH_2OH \rightarrow NO_2^- \rightarrow NO_3^-$), Bremner & Blackmer (1978) showed that N_2O is also produced in soils as a side product by nitrifying bacteria. Within the last two decades, fostered by the development and application of stable isotope techniques to distinguish different N_2O sources, growing evidence was presented that NH_3 oxidation can be the predominant N_2O production process under certain conditions (Bremner *et al.*, 1980; Wrage *et al.*, 2004; Bateman & Baggs, 2005; Shaw *et al.*, 2006). NH_3 oxidation was found to contribute up to 80% of soil N_2O emissions in certain soils at relatively high temperature and moderate soil moisture content (Gödde & Conrad, 1999). This finding makes it possible to lower N_2O emission by inhibiting NH_3 oxidation, e.g. by applying nitrification inhibitors, and subsequently also denitrification by reducing the availability of NO_2^- as substrate (Bhatia *et al.*, 2010; Di *et al.*, 2010). Nevertheless, the mechanisms leading to the release of N_2O during nitrification are not clearly understood. Some researchers proposed that the two enzymes, i.e. hydroxylamine dehydrogenase (also known as hydroxylamine oxidoreductase, HAO) and NO reductase were responsible for the N_2O production during NH_3 oxidation through the oxidation of hydroxylamine (NH_2OH) to NO and the subsequent reduction of NO in a biological mechanism (Ritchie & Nicholas, 1972). Recently, researchers paid more attention to the mechanism of nitrifier denitrification, in which ammonia oxidizers use NO_2^- as a terminal electron acceptor to produce N_2O under oxygen-limited conditions (Ritchie & Nicholas, 1972; Wrage *et al.*, 2001; Shaw *et al.*, 2006). However, the potential contribution of abiotic processes, i.e. the chemical decomposition of nitrite (or chemodenitrification) and the chemical decomposition of NH_2OH , in an assumed coupled biotic-abiotic reaction mechanism, has been ignored until now. As an end product of NH_3 oxidation, small amounts of NO_2^- have been detected in natural soils, especially after N fertilizer application and under alkaline conditions (Shen *et al.*, 2003; Gelfand & Yakir, 2008; Ma *et al.*, 2015). For NH_2OH as an

intermediate product of NH_3 oxidation to NO_2^- existing in the periplasm of ammonia oxidizing bacteria (AOB), however, no detection in natural soil samples has been reported.

Recently, two review papers highlighted the role of abiotic processes, such as reactions of NO_2^- with reduced metal cations or certain soil organic matter (SOM) fractions, the reaction between NO_2^- and NH_2OH , and the oxidation of NH_2OH by Fe^{3+} or MnO_2 , which could also be important for soil N_2O production during nitrification (Zhu-Barker *et al.*, 2015; Heil *et al.*, 2016). These reactions can occur over a broad range of soil characteristics, but they are neglected in most current studies on N_2O production. The factors that regulate the activity of N-cycling microorganisms related to biotic N_2O formation, such as pH, quantity, and quality of SOM, oxygen availability, and supply of inorganic N, are also important factors responsible for the abiotic N_2O formation, which may lead to overlooking the contribution of abiotic processes to soil N_2O formation. Thus, a full understanding of N_2O production processes, including biotic and abiotic processes and their interactions, could improve the modeling of ecosystem N cycling and contribute to constraining atmospheric N_2O budgets and mitigation strategies. Moreover, a change in climatic conditions, such as drying-rewetting, freeze-thaw, and oxic-anoxic cycles, may enhance the contribution of abiotic processes on N_2O formation via the accumulation of highly reactive N intermediates (Clément *et al.*, 2005; Gelfand & Yakir, 2008). Therefore, the understanding the role of this coupled biotic-abiotic mechanism in N_2O formation involving NH_2OH and NO_2^- will also help to quantify the feedback of N_2O emissions to global climate change and other environmental problems.

1.3 State of the art

1.3.1 Mechanisms of N_2O production from NH_3 oxidation

Nitrification can be divided into two steps conducted by two sorts of microorganisms: (1) the oxidation of NH_3 to NO_2^- by ammonia oxidizers; (2) the further oxidation of NO_2^- to NO_3^- by nitrite oxidizers. N_2O production occurs usually in the first step, where NH_3 is oxidized to NO_2^- by ammonia oxidizers (Schreiber *et al.*, 2012). Chemolithotrophic ammonia oxidizers are an important component of the global N cycle. Until now, three microbial guilds responsible for the chemolithotrophic NH_3 oxidation have been enriched or purified responsible: AOB (Koops *et al.*, 1991), ammonia oxidizing archaea (AOA) (Walker *et al.*, 2010; Tourna *et al.*, 2011; Spang *et al.*, 2012) and the recently enriched complete bacterial

ammonia oxidizers (comammox) of the genus *Nitrospira* that perform ammonia oxidation via nitrite to nitrate (Daims *et al.*, 2015; van Kessel *et al.*, 2015). AOB are the earliest enriched and studied microorganisms among the three groups (Skinner & Walker, 1961; Ritchie & Nicholas, 1972; Poth & Focht, 1985). They are abundant in soil environments and have great potential in the production of N₂O. N₂O production has been measured from pure cultures of AOB of the genera of *Nitrosomonas* and *Nitrosospira* (Poth & Focht, 1985; Jiang & Bakken, 1999; Shaw *et al.*, 2006; Stieglmeier *et al.*, 2014). The mechanisms responsible for the N₂O production in AOB have been studied for a long time, mainly focusing on the oxidation of NH₂OH to NO by HAO (Ritchie & Nicholas, 1972) and the so-called nitrifier denitrification (Ritchie & Nicholas, 1972; Wrage *et al.*, 2001; Shaw *et al.*, 2006). The mechanisms responsible for the N₂O production from AOA were still poorly understood. AOA have received increasing attention recently, as AOA abundance has been found to exceed AOB abundance by orders of magnitude in soil ecosystems (Leininger *et al.*, 2006; He *et al.*, 2007). Until now, only a few pure AOA strains have been cultivated successfully from soil, marine and thermal spring environments (Walker *et al.*, 2010; Tourna *et al.*, 2011; Lehtovirta-Morley *et al.*, 2014; Palatinszky *et al.*, 2015), allowing to study the energy metabolism and general physiology of these microorganisms. Although production of N₂O has been observed for enrichment and pure cultures of AOA from marine and soil ecosystems (Santoro *et al.*, 2011; Jung *et al.*, 2014; Stieglmeier *et al.*, 2014), AOA must exhibit a totally different route of biotic N₂O production than AOB, as AOA lack genes for a homolog of HAO and lack genes encoding a potential nitric oxide reductase (NOR) which are assumed to be involved in biotic N₂O production in AOB (Walker *et al.*, 2010; Tourna *et al.*, 2011; Spang *et al.*, 2012). Recent research showed that the soil AOA *Nitrososphaera viennensis* is indeed not able to conduct nitrifier denitrification to produce N₂O (Stieglmeier *et al.*, 2014). Later, N₂O production from this AOA was observed under anoxic conditions that were attributed to abiotic reactions between NO and certain substances in the media (Kozłowski *et al.*, 2016a).

1.3.2 Reactive N intermediates NH₂OH and NO₂⁻

Hydroxylamine and NO₂⁻ are two reactive key N intermediates of nitrification, which can produce N₂O both biologically and chemically. NO₂⁻ can be reduced biologically to N₂O either by NO₂⁻ reductase through a pathway called “nitrifier denitrification” (Wrage *et al.*, 2001), as well as biologically or chemically by Fe²⁺ with the help of iron oxidizers and other microorganisms (Kampschreur *et al.*, 2011). Moreover, SOM fractions, e.g. fulvic acids,

lignin-building units and phenolic compounds can also react chemically with NO_2^- to form N_2O (Stevenson & Swaby, 1964). From NH_2OH , N_2O can be formed both biologically by the enzyme NH_2OH oxidoreductase (Ritchie & Nicholas, 1972) and chemically by O_2 and several soil oxidants (e.g., MnO_2 and Fe^{3+}) (Bremner, 1997; Heil *et al.*, 2016). Numerous studies have been conducted on the N_2O production from NO_2^- from the view of a biological process, i.e. nitrifier denitrification during nitrification (Wrage *et al.*, 2001; Wrage *et al.*, 2004; Zhu *et al.*, 2013a; Snider *et al.*, 2015). However, the importance of NH_2OH for N_2O production, especially from the view of an abiotic processes, has long been neglected, even though the abiotic conversion of NH_2OH to N_2O can be above 80% in a few hours under suitable conditions (e.g., low pH and in the presence of Fe^{3+}) given its chemically reactive nature (Butler & Gordon, 1986; Schreiber *et al.*, 2012).

Hydroxylamine has long been known as an important intermediate of chemolithoautotrophic AOB (Lees, 1952) and was recently also reported to be an intermediate of the marine AOA *Nitrosopumilus maritimus* (Vajrala *et al.*, 2013). NH_2OH may play a crucial role in N_2O production from soils under oxic conditions (Bremner *et al.*, 1980; Bremner, 1997; Schreiber *et al.*, 2012). Recently, Soler-Jofra *et al.* (2016) observed a significant contribution of the abiotic reaction between NH_2OH and NO_2^- to N_2O formation in a full-scale nitrification reactor. Further support for this hypothesis comes from the intramolecular distribution of ^{15}N within the linear, asymmetric NNO molecule, the so-called ^{15}N site preference (SP) (Toyoda & Yoshida, 1999), which is distinctly different between N_2O produced via denitrification and nitrification (Ostrom & Ostrom, 2011). Studies on the pure cultures and chemical reactions demonstrate that aerobic NH_3 and NH_2OH oxidation of AOB, aerobic NH_3 oxidation of a marine AOA and the chemical reactions of NH_2OH with Fe^{3+} , Cu^{2+} and NO_2^- yield similar SP values (30-33‰) (Shaw *et al.*, 2006; Santoro *et al.*, 2011; Heil *et al.*, 2014). All these findings indicate that chemical reactions involving NH_2OH may play an important role in N_2O production during chemolithoautotrophic NH_3 oxidation under oxic conditions. However, NH_2OH is very reactive and unstable in its natural environment. At neutral or slightly alkaline pH, about 30% of NH_2OH degrade within 3 h at room temperature in seawater samples at micromolar concentrations (Butler & Gordon, 1986). Therefore, determination of NH_2OH in natural soils is a very challenging step in the study of the mechanisms of abiotic conversion of NH_2OH to N_2O .

The abiotic N_2O production from NO_2^- has also obtained less attention as the biological processes, probably due to its low content in natural soils. NO_2^- does usually not accumulate in soil at moist or wet conditions (Robertson & Groffman, 2007), as then the oxidation of NO_2^- to NO_3^- proceeds faster than the conversion of NH_3 to NO_2^- . However, NO_2^- has a great potential to accumulate after pH increase, at high NH_3 levels and during drought stress (Smith *et al.*, 1997; Shen *et al.*, 2003; Gelfand & Yakir, 2008; Placella & Firestone, 2013). Accumulation of NO_2^- in soil can provide a substrate for certain biological processes, e.g. denitrification, nitrification and dissimilatory nitrate reduction to ammonium (DNRA) (Silver *et al.*, 2001; Rütting *et al.*, 2011). It also plays a major role in chemodenitrification, where NO_2^- reacts with phenolic compounds to form nitroso and nitro compounds (Thorn & Mikita, 2000). These nitroso and nitro compounds, in turn, can decompose to NO or N_2O , or be reduced by Fe^{2+} to N_2O (van Cleemput & Samater, 1995; Samarkin *et al.*, 2010).

1.3.3 Effects of soil properties and environmental factors

Certain environmental factors, such as oxygen conditions, pH, and drying-rewetting cycles have been long recognized as crucial factors of soil microbial N_2O production through their effects on nitrification and denitrification (Martikainen & de Boer, 1993; Parton *et al.*, 1996; Li *et al.*, 2000; Butterbach-Bahl *et al.*, 2013; Hu *et al.*, 2015). For instance, N_2O production from nitrification can increase by up to 700-fold when O_2 decreases to anoxic conditions (Remde & Conrad, 1990; Kool *et al.*, 2011; Stieglmeier *et al.*, 2014). In a complex soil environment, O_2 conditions determine the contribution of NH_3 oxidation, nitrifier denitrification and heterotrophic denitrification to total N_2O production, with heterotrophic denitrification becoming the only source of soil N_2O when O_2 is completely absent (Zhu *et al.*, 2013a). Furthermore, it has been revealed by a global meta-analysis that N_2O production in soils increases with decreasing pH values (Shcherbak *et al.*, 2014). The inhibition of N_2O reductase by low pH has been considered as one possible reason for the positive effects of increasing acidity on N_2O production (Bakken *et al.*, 2012). However, contributions of NH_3 oxidation to N_2O emissions as affected by soil pH have not been reported.

Rewetting of soil after longer dry periods is an important event triggering soil N_2O emissions (Smith & Parsons, 1985; Rudaz *et al.*, 1991; Ruser *et al.*, 2006). A single wetting event may be responsible for a large fraction of the annual N_2O emission for certain ecosystems (Priemé & Christensen, 2001; Berger *et al.*, 2013). The effects of environmental factors are usually dependent on soil basic properties. Different soil types may have different responses to the

change of environmental conditions. For example, soil rewetting effects were shown to be larger in grassland soils when compared to forest soils (Priemé & Christensen, 2001). Fluctuation of microbial and enzyme activities has long been considered as the main contributor to the increased soil N₂O production during the change of environmental conditions (Mørkved *et al.*, 2007; Bakken *et al.*, 2012; Zhu *et al.*, 2013a; Snider *et al.*, 2015). Nevertheless, varied environmental conditions could also lead to short-term accumulation of soil reactive N substances, such as NO₂⁻ (Clément *et al.*, 2005; Gelfand & Yakir, 2008). The accumulation of these substances may provide substrates for chemical reactions and result in a burst of N₂O production, which has been overlooked for a long time. Moreover, the accumulation of other reactive substrates, such as DOM and metal ions during environmental changes, may shift the contribution of NH₂OH and NO₂⁻ to abiotic N₂O production. For example, quality and quantity of SOM, especially the reactive part of SOM, i.e. phenol compounds, may have strong effects on N₂O formation from NH₂OH and NO₂⁻. Soils rich in phenolic lignin derivatives may favor N₂O formation from NO₂⁻ (Stevenson & Swaby, 1964; Wrage *et al.*, 2001), but may decrease N₂O formation from NH₂OH, as NH₂OH binds readily to carbonyl groups of organic matter to form oximes (Thorn *et al.*, 1992). Anoxic conditions could not only change the availability of mineral N substrates (mainly NO₃⁻, NH₄⁺ and NO₂⁻) (Achnich *et al.*, 1995), and quality of SOM (Achnich *et al.*, 1995; Dassonville & Renault, 2002), but also transition metal redox state. In soil samples with high Fe and Mn content, the oxidized form will promote the conversion of NH₂OH to N₂O, whereas under reduced conditions the formation of N₂O from NO₂⁻ will be favored (Heil *et al.*, 2016).

1.4 Objectives and outline of the thesis

The aim of this thesis was to explore the coupled biotic-abiotic mechanisms of N₂O production involving the nitrification intermediates NH₂OH and NO₂⁻, with a particular focus on the mechanisms of abiotic N₂O production from NH₂OH. As it has been summarized above, NH₂OH is an intermediate of the oxidation of NH₃ to NO₂⁻ in ammonia oxidizers. The quantification of the release of NH₂OH during NH₃ oxidation, the determination of NH₂OH in natural soils, the relationship between NH₂OH content and N₂O production in natural soils and the impact factors affecting the abiotic conversion of NH₂OH to N₂O would be essential to explore the mechanisms of the coupled biotic-abiotic N₂O formation from NH₂OH. As another reactive N intermediate during nitrification and the end product of NH₃ oxidation by

AOA and AOB, the processes of NO_2^- -related N_2O production have been studied for a long time as the so-called “chemodenitrification” (van Cleemput & Baert, 1984; van Cleemput & Samater, 1995; van Cleemput, 1998; Venterea, 2007). Therefore, in this thesis, the study on NO_2^- -related N_2O production mainly focused on the comparison of the contribution of NO_2^- and NH_2OH on biotic and abiotic N_2O production in soils with oxic and anoxic pre-incubation, and the role of NO_2^- on N_2O production during rewetting events.

The main questions that this thesis aimed to resolve were the following:

- (1) Do ammonia oxidizers of different ammonia oxidizing guilds release NH_2OH ?
- (2) Is it possible to detect NH_2OH in natural soil samples?
- (3) How is soil NH_2OH content correlated with aerobic N_2O production at the ecosystem scale?
- (4) What are the main factors responsible for the abiotic conversion of NH_2OH to N_2O ?
- (5) Which reactive N species, NH_2OH or NO_2^- , is more important for soil abiotic N_2O production, considering basic soil properties and redox conditions?
- (6) What is the role of reactive N in N_2O production during rewetting events?

Chapter 2

Abiotic conversion of extracellular NH₂OH contributes to N₂O emission during ammonia oxidation

Based on:

Liu, S., Han, P., Hink, L., Prosser, J., Wagner, M. and Brüggemann, N. Abiotic conversion of extracellular NH₂OH contributes to N₂O emission during ammonia oxidation. *Environmental Science & Technology*, accepted.

2.1 Introduction

Nitrous oxide is an important greenhouse gas and is currently the third largest contributor to global warming, after CO₂ and methane CH₄. N₂O also has deleterious effects in the stratosphere, where it is split photolytically and catalyzes the destruction of atmospheric ozone (IPCC, 2013). In the past two centuries, the atmospheric N₂O concentration has increased by about 20% from pre-industrial levels of 270 ppbv to the current level of 324 ppbv (WMO, 2010). In addition to denitrification and dissimilatory nitrate reduction to ammonia, aerobic ammonia (NH₃) oxidation contributes significantly to N₂O production in soil (Huang *et al.*, 2014). Traditionally, two different biochemical routes are proposed for N₂O production during NH₃ oxidation in AOB. The first is the oxidation of NH₂OH to NO by HAO and subsequent reduction to N₂O catalyzed by NO reductase (Ritchie & Nicholas, 1972). The second pathway is the so-called nitrifier-denitrification, by which NO₂⁻ is reduced to NO and N₂O by nitrite reductase (NIR) and NOR, respectively (Ritchie & Nicholas, 1972; Poth & Focht, 1985; Shaw *et al.*, 2006). However, recent studies revealed two other routes for the N₂O production from the AOB *N. europaea* under anaerobic conditions. One is the direct oxidation of NH₂OH to N₂O by the enzyme cytochrome (cyt) P460 (Caranto *et al.*, 2016), and nitrification intermediate NO (Caranto *et al.*, 2017). Nitrifier-denitrification has been suggested to play a crucial role in N₂O formation at low O₂ and low pH (Wrage *et al.*, 2001), whereas pathways related to biological or chemical reactions of ammonia oxidation intermediates (NH₂OH, nitroxyl (HNO)) and/or its product (NO₂⁻) may be more important for N₂O production at high ammonium (NH₄⁺) levels and sufficient O₂ supply (Wunderlin *et al.*, 2012). However, not all AOB share the same route for N₂O production. *N. communis*, for example, has no homologues of genes encoding a canonical copper-containing NirK (Kozłowski *et al.*, 2016b). Thus, it is unlikely to be able to conduct canonical nitrifier-denitrification, even though low production of N₂O has been detected in an *N. communis* culture (Kozłowski *et al.*, 2016c). Furthermore, a recent study revealed that NH₂OH can also be oxidized directly to N₂O by the enzyme cytochrome (cyt) P460 from the AOB *N. europaea* under anaerobic conditions (Caranto *et al.*, 2016). Most studies on AOB N₂O production pathways have focused on *N. europaea* ATCC 19718 (Ritchie & Nicholas, 1972; Poth & Focht, 1985; Yu & Chandran, 2010) and different biochemical routes responsible for N₂O production in other AOB cannot be excluded.

In recent years, ammonia oxidation-related N₂O production by several AOA strains has been reported (Santoro *et al.*, 2011; Jung *et al.*, 2014; Stieglmeier *et al.*, 2014) and AOA abundance

exceeds that of AOB by several orders of magnitude in some ecosystems (Leininger *et al.*, 2006; He *et al.*, 2007). However, the mechanism(s) of N₂O production by AOA appear to differ from that of AOB, as AOA lack genes encoding a canonical HAO and NOR, which are involved in N₂O production by AOB (Walker *et al.*, 2010; Tourna *et al.*, 2011; Spang *et al.*, 2012). Recent research showed that the soil AOA *Nitrososphaera viennensis* is indeed not able to generate N₂O through nitrifier-denitrification (Stieglmeier *et al.*, 2014). Instead, hybrid N₂O formation from NH₄⁺ and NO₂⁻ in *Nitrososphaera viennensis* was demonstrated in ¹⁵N-labeling experiments (Stieglmeier *et al.*, 2014), indicating an N₂O production pathway from NO₂⁻ and an intermediate of ammonia oxidation, e.g. NH₂OH or NO. Recently, for this AOA species it could be confirmed that N₂O formation under anoxic conditions results from the abiotic reaction of NO with medium or cellular components (Kozłowski *et al.*, 2016a). However, the mechanism of N₂O production by AOA under oxic conditions remains unclear. Furthermore, complete bacterial nitrifiers (comammox) of the genus *Nitrospira* that perform NH₃ oxidation via NO₂⁻ to NO₃⁻ have recently been enriched (Daims *et al.*, 2015; van Kessel *et al.*, 2015), but nothing is yet known about the N₂O production by these microorganisms.

Hydroxylamine has long been known as an important intermediate of chemolithoautotrophic AOB (Lees, 1952) and was reported to be an intermediate of the marine AOA *Nitrosopumilus maritimus* (Vajjala *et al.*, 2013). Surprisingly, genes homologous to those encoding the AOB-like HAO complex have not been found in AOA genomes (Walker *et al.*, 2010; Tourna *et al.*, 2011), indicating that AOA either encode a novel enzyme for NH₂OH oxidation or form during NH₃ oxidation an initial oxidation product other than NH₂OH, e.g. HNO (Walker *et al.*, 2010). Recent research showed that in *N. viennensis* NO₂⁻ can be formed after addition of NH₂OH, leading to the proposal of a novel mechanism for the production of NO₂⁻ via the reactions between NH₂OH and NO in AOA (Kozłowski *et al.*, 2016a).

Hydroxylamine may play a crucial role in N₂O production from soils under oxic conditions (Bremner, 1997; Liu *et al.*, 2014; Heil *et al.*, 2015; Liu *et al.*, 2016), as indicated by the close relationship between NH₂OH concentration and N₂O formation observed in forest soil (Liu *et al.*, 2014; Liu *et al.*, 2016). Further support for this hypothesis comes from the intramolecular distribution of ¹⁵N within the linear, asymmetric NNO molecule, the so-called ¹⁵N SP (Toyoda & Yoshida, 1999), which is distinctly different between N₂O produced via denitrification and nitrification (Ostrom & Ostrom, 2011). In pure cultures of different nitrifiers and denitrifiers, Sutka *et al.* (2006) found SP values near 0‰ for N₂O formed by

NO_2^- and NO_3^- reduction (via classical denitrification and nitrifier denitrification), while SP values were approximately 33‰ for N_2O produced during aerobic NH_3 and NH_2OH oxidation by both guilds, which is similar to SP values reported by Heil *et al.* (2014) for N_2O produced by chemical reactions of NH_2OH with Fe^{3+} , Cu^{2+} and NO_2^- . Santoro *et al.* (2011) also reported an SP value of ~30‰ for N_2O produced by an enrichment culture of a marine AOA, although soil AOA showed different SP values with a range of 13-30‰ (Jung *et al.*, 2014). Recently, Soler-Jofra *et al.* (2016) observed a significant contribution of the abiotic reaction between NH_2OH and NO_2^- to N_2O formation in a full-scale nitrification reactor. All these findings indicate that chemical reactions involving NH_2OH may play an important role in N_2O production during chemolithoautotrophic NH_3 oxidation under oxic conditions. However, this would require the availability of free NH_2OH , either in the growth medium or, potentially, in the periplasm, for abiotic N_2O formation through chemical reactions with substances such as NO_2^- , MnO_2 and Fe^{3+} . Quantification of extracellular NH_2OH from AOB, AOA and comammox may, therefore, provide important information on the feasibility of coupled biotic–abiotic N_2O production during microbial NH_3 oxidation.

In this study, we aimed to answer several important questions regarding N_2O formation by ammonia oxidizing microbes: (1) What are the extracellular concentrations of NH_2OH during NH_3 oxidation by different ammonia oxidizers? (2) If these concentrations are significant, what is the NH_2OH :final product ratio for AOB, AOA, and comammox? (3) Can we estimate the contribution of extracellular NH_2OH to abiotic N_2O production during NH_3 oxidation? (4) What is the role of NO_2^- in stabilizing NH_2OH and in the abiotic conversion of NH_2OH to N_2O ? To address these questions, temporal changes in NH_2OH concentration were determined during incubation of pure and enriched cultures of chemolithoautotrophic AOB, AOA and comammox (obtained from soil and aquatic environments) at high (2 mM) and low (0.5 mM) NH_4^+ concentrations. These experiments were complemented by measurement of abiotic NH_2OH decay rates and abiotic N_2O production involving NH_2OH in different media and at different incubation temperatures and NO_2^- concentrations. These analyses were performed to calculate extracellular NH_2OH production ratios on a final product basis, to quantify the coupled biotic-abiotic NH_4^+ - NH_2OH - N_2O conversion rate of AOB, AOA and comammox, and to explore the role of NO_2^- in the abiotic NH_4^+ - NH_2OH - N_2O conversion. We hypothesize that the coupled biotic-abiotic N_2O production is an important mechanism of N_2O production during NH_4^+ oxidation, at least in some ammonia oxidizers.

2.2 Materials and methods

2.2.1 Strains and cultivation

This study involved four AOB (*Nitrosomonas europaea* ATCC 19718, *Nitrospira multiformis* ATCC 25196, *Nitrosomonas nitrosa* Nm90, *Nitrosomonas communis* Nm2), three AOA (*Nitrososphaera gargensis*, *Nitrososphaera viennensis* and *Ca. Nitrosotalea* sp. Nd2), one AOA enrichment (*Ca. Nitrosotenuis uzonensis*) and one comammox enrichment (*Ca. Nitrospira inopinata*). *N. europaea*, *N. multiformis*, *N. communis*, *N. viennensis* and *Ca. N. sp. Nd2* were isolated from soil (Koops *et al.*, 1991; Shaw *et al.*, 2006; Tourna *et al.*, 2011; Lehtovirta-Morley *et al.*, 2014); *N. nitrosa* Nm90 was isolated from industrial sewage (Koops *et al.*, 1991); *N. gargensis* and *Ca. N. uzonensis* were isolated from thermal springs (Lebedeva *et al.*, 2013; Palatinszky *et al.*, 2015); *Ca. N. inopinata* was enriched from a hot water outflow of a deep oil exploration well (Daims *et al.*, 2015).

N. europaea and *N. multiformis* were maintained at 30 °C in modified Skinner and Walker (S&W) medium (Skinner & Walker, 1961), containing 0.2 g KH₂PO₄, 0.04 g CaCl₂·2 H₂O, 0.04 g MgSO₄·7 H₂O, 1 mL FeNaEDTA (7.5 mM), 1 mL phenol red (0.05%) as pH indicator, 10 mL L⁻¹ HEPES buffer (1 M HEPES, 0.6 M NaOH) and 4 mM (NH₄)₂SO₄ L⁻¹. The pH was regularly adjusted to 7.7 by the addition of sterilized 5% (w/v) Na₂CO₃. The acidophilic AOA *Ca. N. sp. Nd2* and the AOA *N. viennensis* were maintained in freshwater medium at 35 and 37 °C, respectively, according to Tourna *et al.* (2011). The pH for the *Ca. N. sp. Nd2* was adjusted to 5.0-5.3 with HCl and the NH₄⁺ concentration was kept at 0.5 mM by routinely adding the NH₄Cl stock solution. The pH for *N. viennensis* was adjusted to 7.5 by the addition of 10 mL L⁻¹ HEPES buffer (1 M HEPES, 0.6 M NaOH). *N. viennensis* was supplied with 1 mM NH₄Cl and 0.1 mM pyruvate. The AOB *N. nitrosa* and *N. communis*, the AOA *N. gargensis*, and the enrichments containing *Ca. N. uzonensis* and *Ca. N. inopinata* were maintained at 37, 28, 46, 46 and 37 °C, respectively, in AOA medium modified from Lebedeva *et al.* (2013) containing (L⁻¹) 75 mg KCl, 50 mg KH₂PO₄, 584 mg NaCl, 50 mg MgSO₄ · 7 H₂O, 1 mL of trace element solution (AOA-TES), 1 mL of selenium-tungsten solution (SWS), 4 g CaCO₃ (mostly undissolved, acting as a solid buffer reservoir and growth surface) and 5 ml of NH₄Cl (from an autoclaved 0.2 M stock solution). For a detailed description of the composition of TES and SWS please refer to Widdel (1980).

2.2.2 Incubation experiments

Metabolically active cultures were concentrated and washed twice using fresh medium without NH_4^+ by centrifugation (Table S2.1), and resuspended in fresh medium containing 0.5 or 2 mM NH_4^+ . Note that the added NH_4^+ concentrations were not optimal for all strains tested, but the use of the same concentrations for all strains maximized comparability of the chemical factors contributing to the N_2O formation in the various growth media. *Ca. N. sp. Nd2* was incubated with 0.5 mM NH_4^+ only, as this culture grew extremely slowly and is inhibited by high nitrous acid concentration formed under acidic conditions. Cultures were incubated under different conditions and for different periods depending on their different growth characteristics (Table S2.1). All treatments were carried out with 4-6 replicates. Only *N. communis* (90 rpm, New Brunswick™ Innova® 42 Shaker) and *N. nitrosa* (90 rpm, GFL 3019 shaker) cultures were shaken during incubation. Before each sampling, bottles of all cultures were mixed by shaking by hand. Samples (3 mL) for chemical and protein analyses were taken at 0, 2, 5, 8 and 13 h on the first day, and thereafter every 12 or 24 h, and transferred to 2-mL and 1.5-mL autoclaved Eppendorf tubes, respectively. The tubes were centrifuged immediately at 8000 *g* (4 °C) for 10 min and 1.2 mL of supernatant was transferred to two 1.5-mL Eppendorf tubes containing 75 μL 480 mM (for 2 mM NH_4^+ treatment) or 160 mM (for 0.5 mM NH_4^+ treatment) sulfanilamide in 0.8 M HCl for quantification of NH_2OH (see below). Another 0.2 mL supernatant was transferred to a 1.5-mL Eppendorf tube for NH_4^+ and NO_2^- analyses (see below) and the remaining liquid and pellet were frozen at -20 °C for protein quantification (see below). To prevent any potential effect of phenol red on NH_2OH analysis, *N. europaea* and *N. multiformis* were grown in parallel in media buffered with HEPES without and with phenol red to facilitate maintenance of pH between pH 7.5 and 8 by the addition of sterilized 5% (w/v) Na_2CO_3 . *Ca. N. sp. Nd2* cultures were not buffered and pH was determined daily by pH measurement of 2-mL samples. For cultures buffered with CaCO_3 , pH was stable at ~8.2 throughout the incubation period.

2.2.3 Determination of abiotic NH_2OH decay rates under ambient air conditions

Abiotic NH_2OH decay was quantified in S&W (with HEPES buffer) and modified AOA (with CaCO_3 buffer) media used in this study at the respective growth temperatures. The freshwater medium for *Ca. N. sp. Nd2* and *N. viennensis* were not tested for abiotic NH_2OH decay since no extracellular NH_2OH was observed during NH_3 oxidation by these cultures. Well-aerated medium (40 mL) was added to 120-ml glass serum bottles followed by different amounts (4, 8,

20 and 40 μL) of 5 mM NH₂OH to reach final concentrations of 0.5, 1, 2.5 and 5 μM , respectively. Subsequently, 1.6 mL 50 mM NO₂⁻ was added to give a final concentration of 2 mM to simulate abiotic NH₂OH decay in the presence of NO₂⁻. Bottles were then capped with aluminum foil and incubated at 30, 37 and 46 °C. Samples (1.2 mL) were taken after 0, 1, 2, 5 and 8 h and transferred to 1.5-mL Eppendorf tubes containing 75 μL 480 mM (for 2 mM NO₂⁻ treatment) or 160 mM (for the treatment without NO₂⁻ addition) sulfanilamide in 0.8 M HCl. Samples were frozen at -20 °C until quantification of NH₂OH (see below).

2.2.4 Chemical assays

Hydroxylamine concentration was estimated according to the method of Liu *et al.* (2014). Briefly, 1.2 mL of sample, thawed at room temperature, was transferred to a 22-mL glass vial and 4.8 mL deionized water was added, yielding a pH of ~2. Then, 0.6 mL of 25 mM FeCl₃ was added to the vial, which was immediately closed gas-tight with a crimping tool. Control vials contained sample and water only to assess N₂O in the headspace and dissolved in the sample. The vials were shaken for 3 h at 200 rpm and then transferred to an autosampler for gas chromatography (GC) analysis with an electron capture detector (ECD) as described in Liu *et al.* (2014). NH₂OH calibration in the range 0 - 1 μM was performed before each measurement. Since N₂O background increased by about 10 ppb in the control vials for the culture samples of *N. communis* and *N. nitrosa* during NH₂OH determination, NH₂OH concentrations <0.06 μM were defined as not detectable. NO₂⁻ and NH₄⁺ concentrations were determined colorimetrically in 96-well plates using sulfanilamide and N-(1-naphthyl)ethylenediamine dihydrochloride for NO₂⁻ (Strickland & Parsons, 1972), and the indophenol method described by Kandeler & Gerber (1988) for NH₄⁺. Protein concentration was determined with the Pierce BCA protein assay kit (Thermo Fisher Scientific).

2.2.5 Calculation of the NH₂OH:final product ratio

Total extracellular NH₂OH concentrations by AOB, AOA and comammox during consumption of available NH₄⁺ was evaluated as the NH₂OH:final product ratios (final product was NO₃⁻ in the case of comammox and NO₂⁻ in all other cases), taking into account the abiotic decay rate of the very reactive NH₂OH, which followed first-order reaction kinetics:

$$C = C_0 e^{-kt} \quad (2.1)$$

where C is the NH_2OH concentration (μM) at decay time t (h), C_0 is the initial NH_2OH concentration (μM) and k is the first-order rate constant.

The NH_2OH :final product ratio was calculated as:

$$r = \frac{[C_{t_2} - C_{t_1} + \sum_{i=t_1}^{t_2-1} C_i \cdot (1 - e^{-k \cdot 1})]}{C'_{t_2} - C'_{t_1}} \quad (2.2)$$

where r (dimensionless) is the NH_2OH :final product ratio between t_1 and t_2 , C_{t_1} and C_{t_2} (μM) are the measured NH_2OH concentrations at t_1 and t_2 , respectively, C_i (μM) is the interpolated NH_2OH concentration between times t_1 and t_2 ($t_2 - t_1 = 1$ hour), C'_{t_1} and C'_{t_2} (μM) are the NO_2^- or (for comammox) NO_3^- concentrations at t_1 and t_2 , and k is the average value of the measured kinetic constant for abiotic NH_2OH decay in the range of 0.5–2.5 (for HEPES buffered medium) or 0.5–5 (for CaCO_3 buffered medium) μM initial NH_2OH concentrations. Note that the presence of NO_2^- in the medium would also decrease k . As k was determined in the absence or presence of 2 mM NO_2^- , loss of NH_2OH was calculated using an average value of k determined at 0 or 2 mM NO_2^- when NO_2^- concentration in the medium was <1 mM or >1 mM, respectively. As NO_2^- concentration increased gradually with time, this definition of k would have led to overestimation or underestimation of NH_2OH when NO_2^- concentration was <1 mM or >1 mM, respectively. However, the total NH_2OH :final product ratio was very likely underestimated since higher NH_2OH concentration was detected during late growth when NO_2^- concentration was mostly >1 mM. For the comammox, NO_2^- concentration was low (<0.033 mM) at all time points and had a negligible effect on the calculation of NH_2OH :final product ratio.

2.2.6 Calculation of the fraction of NH_4^+ converted to N_2O during incubation

The fraction of NH_4^+ converted to N_2O through incubation was calculated by determining the overall abiotic N_2O product ratios (r_i in equation 2.3) at different NH_2OH and NO_2^- concentrations for different media and incubation temperatures. For this, 1.2 mL of HEPES and CaCO_3 medium, respectively, was added to 22-ml glass vials, followed by 0, 12 and 24 μL of 100 mM NO_2^- and 12, 24 and 60 μL of 50 μM NH_2OH . The final NO_2^- concentrations were 0, 1 and 2 mM and final NH_2OH concentrations were 0.5, 1 and 2.5 μM . Vials were then incubated for 24 h at 30, 37 and 46 $^\circ\text{C}$ according to the cultivation conditions of the respective microorganisms and headspace gas was analyzed for N_2O by GC. The fraction of NH_4^+ converted to N_2O over the whole NH_3 oxidation process (R) was then calculated as follows:

$$R = \frac{\sum_{i=1}^n C_i r_i}{C} \quad (2.3)$$

where C_i is the concentration of NH₂OH during the i^{th} and $(i+1)^{\text{th}}$ sampling, r_i is the theoretical abiotic N₂O production ratio determined as described in section 2.2.6, and C is the concentration of NH₄⁺ consumed during incubation. Note that r_i was strongly dependent on NO₂⁻ concentration. Abiotic N₂O production within a certain time period when NO₂⁻ concentration was >1 mM, 1 - 1.5 mM and >1.5 mM was calculated using r_i values for NO₂⁻ concentrations of 0, 1 and 2 mM, respectively. As r_i increased with increasing NO₂⁻ concentration, this definition of r_i may have led to underestimation or overestimation of abiotic N₂O production when NO₂⁻ concentration was < or >1.5 mM, respectively.

2.2.7 Data analyses

Abiotic NH₂OH decay was fitted to first-order reaction equations by the R software package (version 3.1.0). The coefficients of determination (R^2) were larger than 0.99. Paired t-tests (R, version 3.1.0) were used to identify significant differences in NH₂OH concentrations between two time points during culture incubation.

2.3 Results and discussion

2.3.1 Extracellular NH₂OH from autotrophic ammonia oxidizers

The NH₂OH concentration in the medium during NH₃ oxidation differed significantly among AOB cultures (Fig. 2.1) and was greatest for *N. multiformis* on initial NH₄⁺ concentrations of 0.5 and 2 mM. NH₂OH release was also observed for *N. europaea*, albeit at lower concentrations than for *N. multiformis*. No NH₂OH was detectable for *N. nitrosa* Nm90 or *N. communis* at both tested NH₄⁺ concentrations. Initial increases in NH₂OH concentration in cultures of *N. multiformis* and *N. europaea* were associated with increases in NO₂⁻ concentration, but eventually reached a plateau or decreased before NO₂⁻ concentration reached a maximum. The largest measured NH₂OH concentrations in the medium were 2.2 and 0.78 μM, from *N. multiformis* and *N. europaea*, respectively, during incubation with 2 mM NH₄⁺.

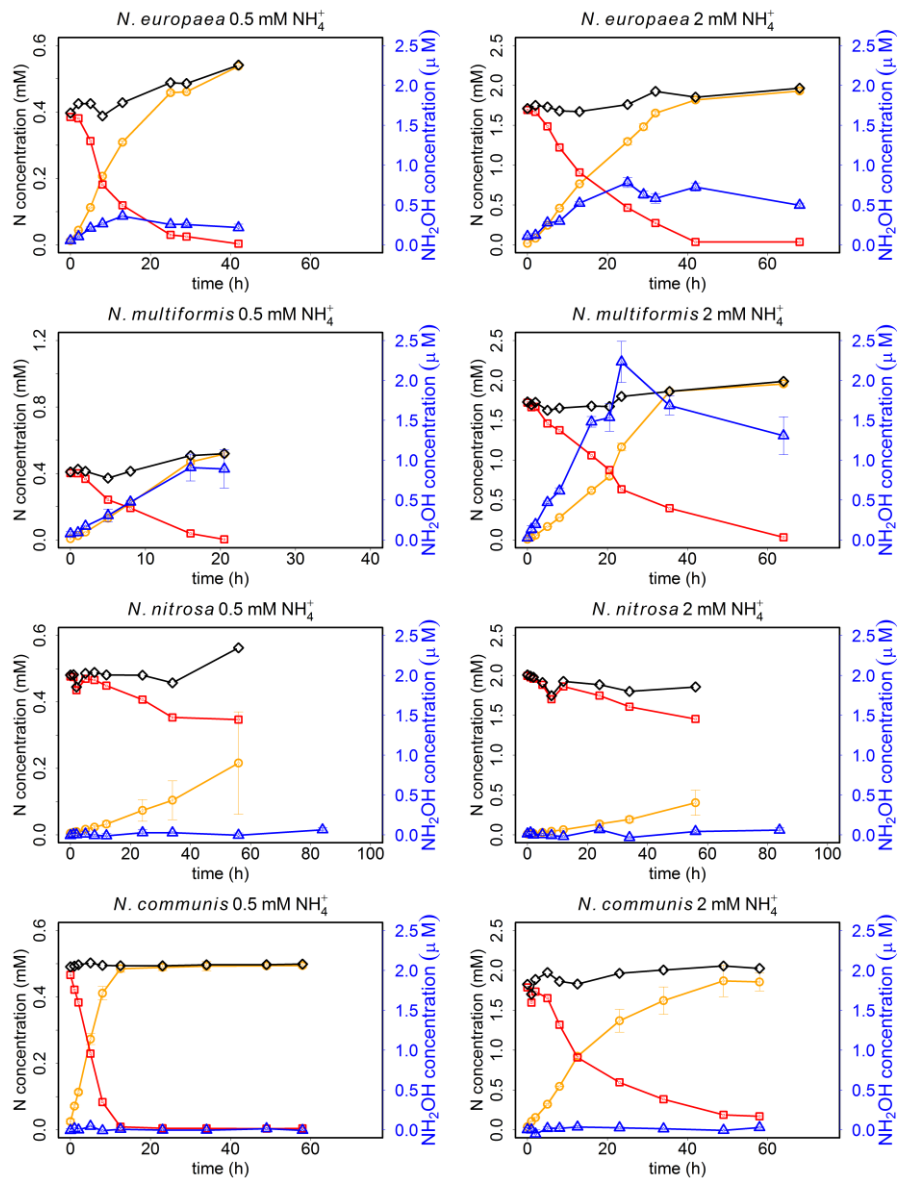


Figure 2.1 Dynamics of NH_4^+ (red squares), NO_2^- (yellow circles), NH_2OH (blue triangles) and total N (sum of NO_2^- and NH_4^+ , black diamonds) concentrations during incubation of four ammonia oxidizing bacteria. NH_4^+ , NO_2^- and total N are plotted using the left y-axis, while NH_2OH is plotted using the right y-axis. Please note that the left y-axes and the x-axes, respectively, are not always scaled identically to improve data presentation. The values are presented as mean \pm standard error (SE).

Several studies have determined NH_2OH concentrations in the medium during NH_3 oxidation by pure cultures of the AOB *N. europaea*. Stüven *et al.* (1992) observed 0.2 - 1.7 μM NH_2OH during NH_3 oxidation (10 mM) and Yu & Chandran (2010) reported 0.2–3.2 μM NH_2OH during growth of *N. europaea* 19718 on 20 mM NH_4^+ . These findings are consistent with the NH_2OH concentrations detected for *N. europaea* in our study, where NH_2OH concentrations were about three orders of magnitude smaller than those of the produced NO_2^- . NH_2OH

production by *N. europaea* during NH₃ oxidation in our study was also consistent with data reported by Yu & Chandran (2010) for *N. europaea* 19718, although they did not specify whether they measured NH₂OH in supernatant (as in our study) or in untreated cultures. In our experiments, *N. multiformis* NH₂OH concentrations were even larger than for *N. europaea*. The exact reason for this phenomenon remains unclear. One possible explanation is that *N. multiformis* biomass consumed NH₄⁺ faster (for the 0.5 mM NH₄⁺ treatment) than *N. europaea* and faster NH₃ oxidation might have led to the higher NH₂OH release. However, the *N. communis* biomass in the batch experiments showed no detectable NH₂OH release into the medium even though it had the highest NH₃ oxidation rates. Since *N. communis* is considered eutrophic and prefers higher concentrations of NH₄⁺ (10-50 mM) (Prosser *et al.*, 2014), the absence of NH₂OH could be due to complete consumption by HAO and conversion to NO₂⁻, assuming that the V_{max} of HAO in *N. communis* is larger than in other AOB. Moreover, *N. communis* is unable to tolerate >100 μM NH₂OH in contrast to tolerance of 250 μM NH₂OH by *N. europaea* and *N. multiformis* (Kozłowski *et al.*, 2016c), which may relate to the absence of NH₂OH in the medium of *N. communis*, although the exact mechanism for the low tolerance of NH₂OH by *N. communis* is still not clear. NH₃ oxidation by *N. nitrosa* Nm90 was lower than by the other tested AOB strains, possibly explaining the lack of detectable NH₂OH release.

Among the three AOA pure cultures, NH₂OH release was detected from the thermal spring isolate *N. gargensis* growing on 2 mM initial NH₄⁺, but not on 0.5 mM NH₄⁺. The pattern of NH₂OH release by *N. gargensis* differed from that of AOB, with a small but rather constant increase in NH₂OH during incubation on 2 mM NH₄⁺, resulting in a final NH₂OH concentration of 0.33 μM in the medium after 58 h. In contrast, NH₃ oxidation by the soil AOA *N. viennensis* and *Ca. N. sp. Nd2* was not associated with the detectable NH₂OH release (Fig. 2.2). The NO₂⁻ production rate by the AOA enrichment *N. uzonensis* (~0.3 mM NO₂⁻ produced within 104 h) was similar at the two initial NH₄⁺ concentrations, but more NH₂OH (0.34 μM) was observed at the end of the incubation at 2 than 0.5 mM NH₄⁺ initial concentration.

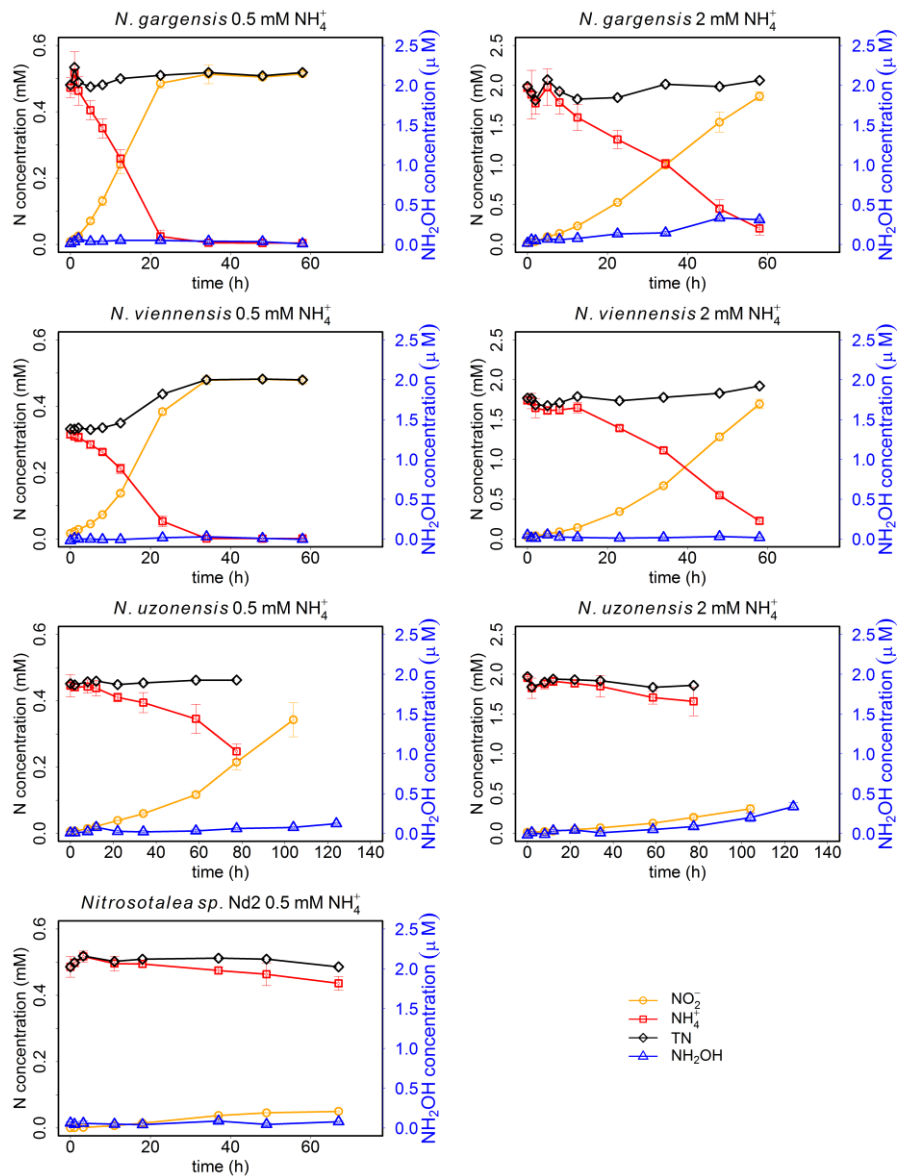


Figure 2.2 Dynamics of NH_4^+ (red squares), NO_2^- (yellow circles), NH_2OH (blue triangles) and total N (sum of NO_2^- and NH_4^+ , black diamonds) concentrations in the batch experiments with four ammonia oxidizing archaea. NH_4^+ , NO_2^- and total N are plotted using the left y-axis, while NH_2OH is plotted using the right y-axis. Please note that the left y-axes and the x-axes, respectively, are not always scaled identically to improve data presentation. The values are present as mean \pm standard error (SE).

No published AOA genomes contains an obvious homologue of AOB-like HAO, or of cytochromes c554 and cM552 that are considered critical for energy conversion (Walker *et al.*, 2010), initially casting some doubt on the role of NH_2OH as an intermediate in NO_2^- formation by AOA (Walker *et al.*, 2010). However, Vajrala *et al.* (2013) reported the production of NH_2OH in the marine AOA *N. maritimus* during NH_3 oxidation. Furthermore, Kozłowski *et al.* (2016a) showed that the addition of NH_2OH to a culture of *N. viennensis*

resulted in respiration and NO₂⁻ formation and thus the most current model of AOA physiology postulates a yet undiscovered novel NH₂OH-converting enzyme. The data from the *N. uzonensis* enrichment culture, that does not contain any known AOB (Lebedeva *et al.*, 2013), confirms the *N. gargensis* data in showing that some AOA release NH₂OH. Also, in a preliminary experiment, *N. gargensis* could convert NH₂OH to NO₂⁻ biotically, especially at lower NH₂OH levels (Fig. S2.1). Stieglmeier *et al.* (2014) observed aerobic N₂O production by *N. viennensis* and attributed this to the hybrid formation of N₂O via an N-nitrosating reaction. Kozłowski *et al.* (2016a) later reported that N₂O formation from *N. viennensis* could be attributed to abiotic reactions between NO and medium substances during growth, especially under anoxic conditions. It is tempting to speculate that the aerobic hybrid formation of N₂O in *N. viennensis* could also stem from the well-known chemical reaction between NH₂OH and NO₂⁻. However, we failed to observe NH₂OH in the medium of *N. viennensis*, which could reflect (i) lack of NH₂OH release by this culture (indicating that the coupling between AMO and the archaeal HAO-like enzyme is more efficient than in some AOB) or (ii) rapid chemical NH₂OH conversion in the medium (which could only mask small amounts of released NH₂OH), as the medium response of *N. viennensis* was different from that of *N. gargensis* in terms of the nitrogenous gas production from abiotic NH₂OH decay (Fig. S2.2). Also for *Ca. N. sp. Nd2*, NH₂OH was not detectable, possibly due to low NH₃ oxidation rates.

The comammox organism *Nitrospira inopinata* oxidized NH₄⁺ to NO₃⁻ (Fig. 2.3). After 48 h of incubation, *N. inopinata* produced 0.46 mM NO₃⁻ with 2 mM initial NH₄⁺ concentration, while it produced 0.27 mM NO₃⁻ when fed with 0.5 mM NH₄⁺. The release of the NH₂OH into the medium by *N. inopinata* was similar for both NH₄⁺ levels, but unlike the other cultures, increasing mainly at the beginning of the incubation, decreasing and then increasing again in parallel with increasing NO₃⁻ concentration to reach 0.43 μM at the end of the incubation period. This decreasing and increasing trend was significant ($P < 0.025$) for the culture growing on 2 mM NH₄⁺. Consistent with the detection of NH₂OH, previous genomic analysis had shown that *N. inopinata* encodes a predicted octaheme cytochrome c protein resembling the HAO of AOB, and an AMO that is relatively closely related to the AMO of the betaproteobacterial AOB (Daims *et al.*, 2015). *N. inopinata* lacks canonical NO reductases but encodes enzymes for dissimilatory nitrate reduction to ammonia (Kits *et al.*, 2017). Whether the latter enzymes are also expressed and active under aerobic conditions and might contribute to N₂O formation has not yet been investigated.

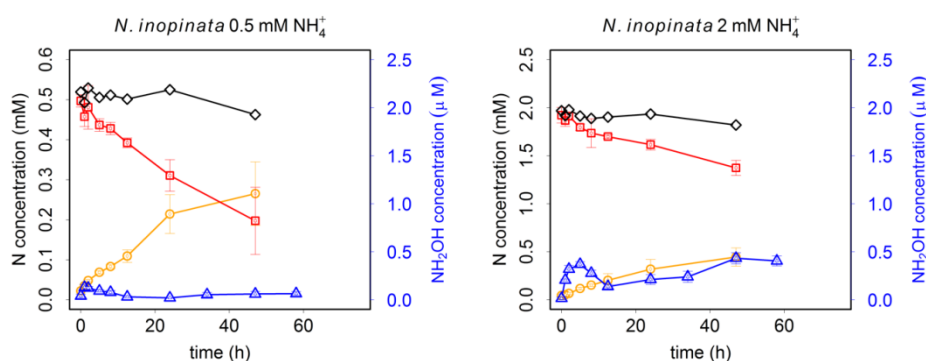


Figure 2.3 Dynamics of NH_4^+ (red squares), NO_3^- (yellow circles), NH_2OH (blue triangles) and total N (sum of NO_3^- and NH_4^+ , black diamonds) concentrations during the incubation of the comammox organism *N. inopinata*. NH_4^+ , NO_3^- and total N are plotted using the left y-axis, while NH_2OH is plotted using the right y-axis. The values are present as mean \pm standard error (SE).

2.3.2 NH_2OH abiotic decay and NH_2OH :final product ratios during NH_3 oxidation

To better understand the presence of extracellular NH_2OH during ammonia oxidation of the tested organisms, a series of NH_2OH abiotic decay experiments were conducted with different media, incubation temperatures and NO_2^- concentrations (Fig. 2.4). All three factors, i.e., medium type, temperature, and NO_2^- concentration, had strong effects on the rate of abiotic NH_2OH decay. The decay rate was faster in CaCO_3 than in HEPES-buffered media: 0.5 to 2.5 μM NH_2OH decayed abiotically at 30 °C within ~8 h and ~30 h in the CaCO_3 and HEPES-buffered media, respectively. Consequently, the first-order rate constants for abiotic NH_2OH decay were much higher in the CaCO_3 than in the HEPES-buffered media, with an average value approximately fourfold larger in the former (0.71 vs. 0.16) (Table S2.2). The temperature increased the rate of abiotic NH_2OH decay (with a single exception, Table S2.2). The decay time at 46 °C (~4 h) was half that at 30 °C (~8 h) for the CaCO_3 medium, and the average first-order rate constant was ~80% greater at 46 °C (1.31) than at 30 °C (0.71). NO_2^- , however, unexpectedly inhibited abiotic NH_2OH decay in both media tested (Figure 2.4, Table S2.2), although NO_2^- is known to oxidize NH_2OH to N_2O , albeit preferentially at low pH (e.g., Heil *et al.*, 2014). This stabilizing effect of NO_2^- was particularly pronounced at higher temperatures for the CaCO_3 medium, where the first-order rate constant decreased by 52% for 2 mM NO_2^- at 46 °C compared to the absence of NO_2^- . To exclude the possibility of abiotic conversion of NO_2^- to NH_2OH by components of the medium, an additional test was conducted using the more active CaCO_3 -buffered medium (compared to the HEPES-buffered medium) at the highest culture incubation temperature, but no abiotic conversion of NO_2^- to

NH_2OH occurred (data not shown). An additional $^{15}\text{N}\text{-NO}_2^-$ experiment showed that NO_2^- did not interfere with the NH_2OH analysis (Table S2.3). Under alkaline conditions, one product of NH_2OH abiotic decay is NO_2^- (Butler & Gordon, 1986), which has been also observed in abiotic NH_2OH decay experiments in the CaCO_3 -buffered medium in this study (Fig. S2.3). In addition to NO_2^- and N_2O , nitrogen dioxide (NO_2), but almost no NO , was observed during the NH_2OH abiotic decay (Fig. S2.2). The presence of NO_2 may explain the observation of abiotic NH_2OH -to- NO_2^- conversion as NO_2 is highly reactive and can hydrolyze to nitric acid (HNO_2) and nitrous acid (HNO_3) in aqueous solution. Consequently, NO_2^- , N_2O , and NO_2 comprised approximately 18.5%, 9.8% and 32.1%, respectively, of the abiotically decayed NH_2OH in the CaCO_3 -buffered medium (Fig. S2.2, S2.3). Therefore, a possible reason for the inhibitory effects of NO_2^- on abiotic NH_2OH decay could be that the presence of NO_2^- slowed down the transformation of NH_2OH to NO_2^- by inhibiting the disproportionation of NO_2 , one of the primary decay products of NH_2OH , to HNO_3 and HNO_2 .

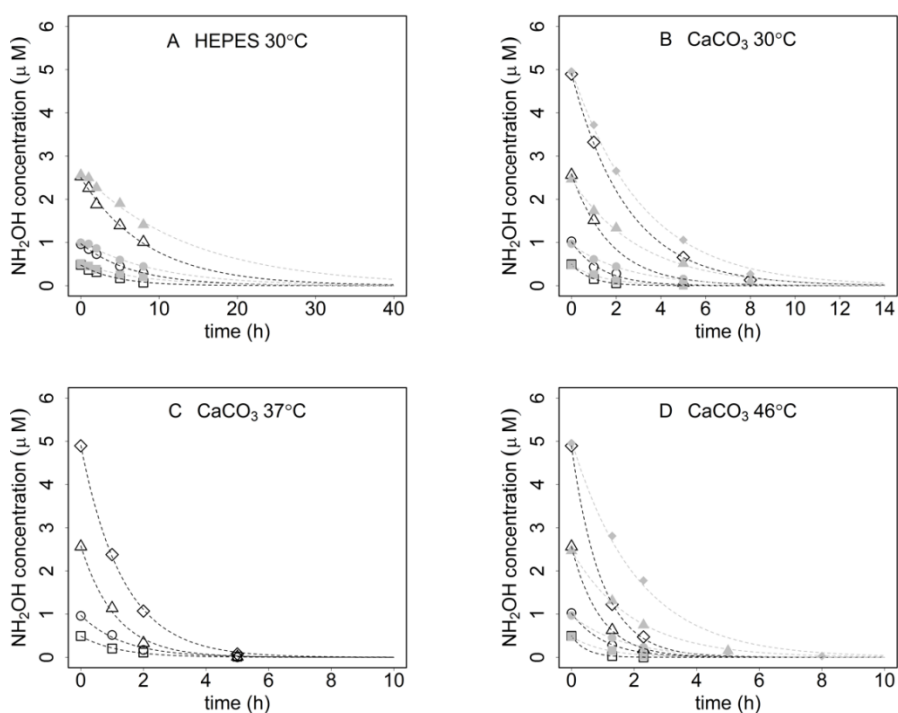


Figure 2.4 Abiotic decay of NH_2OH in the absence (hollow) or presence (solid) of 2 mM NO_2^- in HEPES-buffered and CaCO_3 -buffered media at different incubation temperatures. The NH_2OH concentrations were 0.5 (square), 1 (circle), 2.5 (triangle), and 5 (diamond) μM . Mean values of three replicates are presented. The relative standard deviation (RSD) of all data is smaller than 10%. Please note that the x-axes are not always scaled identically to improve data presentation.

The effect of temperature on abiotic NH_2OH decay was as expected, as NH_2OH is extremely unstable and reactive, especially at higher temperatures (Butler & Gordon, 1986). The exact reason for the difference of abiotic NH_2OH decay between the two media (HEPES- and CaCO_3 -buffered) is not obvious. The media differ mainly in terms of pH, the composition, and concentrations of the trace metals and the buffer (HEPES vs. CaCO_3). Both pH and redox active trace metals are known to have a strong effect on abiotic NH_2OH decay. Acidic pH stabilizes NH_2OH in the absence of redox active trace metals, while trace metals such as Cu^{2+} , Fe^{3+} and Mn^{4+} can stimulate NH_2OH decomposition (Butler & Gordon, 1986). Therefore, higher pH and the presence of trace metals could lead to greater abiotic NH_2OH decay in the CaCO_3 -buffered medium than in HEPES-buffered medium.

First-order kinetic rate constants and Equation 2.2 were used to estimate both instantaneous and total NH_2OH :final product ratios during NH_3 oxidation by those cultures producing relatively high NH_2OH concentrations, i.e. *N. europaea*, *N. multiformis*, *N. gargensis* and *N. inopinata* (Fig. S2.4 and Table 2.1). For the three pure cultures (*N. europaea*, *N. multiformis* and *N. gargensis*), instantaneous NH_2OH :final product ratios were in the range 0.1 to 0.6% during early phases of the incubation experiments, but several-fold higher as the substrate NH_4^+ was nearly consumed, e.g., as high as about 4% for *N. multiformis* (Fig. S2.4). For the comammox organism *N. inopinata*, instantaneous NH_2OH :final product ratios were in the range 0.1 to 2.6% and 0.9 to 5.7% at 0.5 and 2 mM initial NH_4^+ concentration, respectively, also with higher values at the end of incubation (Fig. S2.4). Generally, *N. inopinata* had the largest total NH_2OH :final product ratio of all cultures tested, with ratios of 0.63% and 1.92% after incubation for 60 h at 0.5 and 2 mM initial NH_4^+ concentration, respectively (Table 2.1). In contrast, *N. gargensis* had a total $\text{NH}_2\text{OH}:\text{NO}_2^-$ ratio of 0.46% at 2 mM initial NH_4^+ concentration after 60 h, whereas *N. multiformis* and *N. europaea* had total NH_2OH :final product ratios of 0.34-0.56% and 0.24-0.33%, respectively, depending on the initial NH_4^+ concentration.

Table 2.1 Total NH₂OH:final product (NO₂⁻ or NO₃⁻) ratios for different ammonia oxidizers. [§] For *N. inopinata* (a comammox organism), NO₃⁻ is the final product of NH₃ oxidation. [#] The NH₂OH concentration here is the total extracellular NH₂OH including the calculated concentration of NH₂OH that was abiotically converted during incubation.

Cultures	Initial NH ₄ ⁺ concentration (mM)	Final NO ₂ ⁻ or NO ₃ ⁻ [§] concentration (μM)	NH ₂ OH [#] concentration (μM)	NH ₂ OH:final product ratio (%)
<i>N. multiformis</i>	0.5	516	1.8	0.34
	2	1955	11.0	0.56
<i>N. europaea</i>	0.5	537	1.8	0.33
	2	1930	4.7	0.24
<i>N. gargensis</i>	2	1860	7.1	0.46
<i>N. inopinata</i>	0.5	280	1.8	0.63
	2	490	9.4	1.92

2.3.3 Estimating the fraction of NH₄⁺ converted to N₂O during NH₃ oxidation under ambient air conditions

For an informed estimate of the fraction of NH₄⁺ that was converted to N₂O by the different ammonia oxidizers under ambient air incubation conditions over the whole incubation period, it is essential to consider abiotic N₂O production from different NH₂OH concentrations, at different incubation temperatures, and at different concentrations of NO₂⁻. In the environment, additional factors such as organic matter content, pH, and content of suitable oxidants like MnO₂ and Fe³⁺ will also affect the chemical N₂O conversion ratio from NH₂OH (Bremner, 1997; Liu *et al.*, 2016). The abiotic N₂O:NH₂OH conversion ratio was 12-14% for the HEPES-buffered medium at 30 °C in the absence of NO₂⁻, and between 18% and 37% for the same medium with 1 and 2 mM NO₂⁻, respectively (Table 2.2). The ratio in the CaCO₃-buffered medium at 30 °C was larger, with values of 15-28%, 32.2-46.9%, and 37.6-48.9% at 0, 1 and 2 mM NO₂⁻, respectively, for the NH₂OH range from 0.5 to 2.5 μM. The contribution of NO₂⁻ to N₂O production involving NH₂OH was even larger at a higher temperature, e.g. 46 °C (Table 2.2). The stimulated conversion of NH₂OH to N₂O by NO₂⁻ is likely caused by the hybrid reaction of NO₂⁻ and NH₂OH. However, another mechanism could be inhibition of NH₂OH conversion to NO₂/NO₂⁻ by NO₂⁻, thereby channeling NH₂OH to N₂O indirectly via other mechanisms.

Table 2.2 Fraction (%) of N₂O abiotically produced from the added NH₂OH in the different media at various levels of NH₂OH (0.5, 1 and 2.5 μM) and NO₂⁻ (0, 1 and 2 mM).

NH ₂ OH (μM)	0 mM NO ₂ ⁻			1 mM NO ₂ ⁻			2 mM NO ₂ ⁻		
	0.5	1	2.5	0.5	1	2.5	0.5	1	2.5
HEPES (30 °C)	14.1	13.7	12.0	29.3	20.0	18.4	36.6	33.1	23.4
CaCO₃ (30 °C)	15.0	20.9	28.0	33.2	32.2	46.9	45.0	37.6	48.9
CaCO₃ (37 °C)	6.7	5.6	6.7	36.2	31.0	43.7			
CaCO₃ (46 °C)	6.3	4.6	12.5	29.5	22.4	36.1	38.8	46.0	57.1

The total fraction of NH₄⁺ converted to N₂O through extracellular NH₂OH and substances in the medium over the whole incubation period was then calculated according to Equation 2.3 (Table 2.3). The total fraction of NH₄⁺ converted to N₂O by this mechanism was 0.05% and 0.12% for *N. multiformis* incubated at 0.5 and 2 mM initial NH₄⁺, respectively, which is consistent with that emitted as N₂O (0.05-0.1%) during aerobic incubation of a *Nitrosospira* strain (Jiang & Bakken, 1999; Shaw *et al.*, 2006). The fraction of NH₄⁺ converted to N₂O by *N. europaea* was lower than that of *N. multiformis*, but still consistent with that converted to N₂O by *N. europaea* reported by other studies, e.g., 0.05-1.95% (Remde & Conrad, 1990) and 0.05-0.15% (Hynes & Knowles, 1984). Dundee & Hopkins (2001) also reported that *N. multiformis* produced more N₂O than *N. europaea* at greater dissolved O₂ concentrations, while *N. europaea* produced much more N₂O during nitrifier-denitrification than *N. multiformis*, which is consistent with our finding that the fraction of NH₄⁺ converted to N₂O was larger for *N. multiformis* than for *N. europaea* under ambient air conditions.

Table 2.3 Estimated fraction of NH₄⁺ converted to N₂O from the abiotic reactions between the biologically produced extracellular NH₂OH and substances in the medium for different ammonia oxidizers.

Cultures	Initial NH ₄ ⁺ concentration (μM)	Estimated fraction of NH ₄ ⁺ converted to N ₂ O (%)
<i>N. multiformis</i>	500	0.05
	2000	0.12
<i>N. europaea</i>	500	0.05
	2000	0.07
<i>N. gargensis</i>	2000	0.08
<i>N. inopinata</i>	500	0.06
	2000	0.14

The AOA *N. viennensis* and *N. maritimus* are reported to be incapable of nitrifier-denitrification at reduced O_2 concentration, but produce N_2O via hybrid formation, as revealed by ^{15}N -labeling (Stieglmeier *et al.*, 2014). In the present study, potential abiotic N_2O production was approximately 0.08% of the total substrate turnover during aerobic NH_3 oxidation by AOA. Albeit this value was found only in *N. gargensis*, it was close to the values reported for *N. viennensis* (0.09%) and *N. maritimus* (0.05%) by Stieglmeier *et al.* (2014). The fraction of NH_4^+ calculated to be converted to N_2O by the comammox organism *N. inopinata* was even higher (in the range of 0.06–0.14%), but no measured data on N_2O emissions from comammox organisms are yet available for comparison.

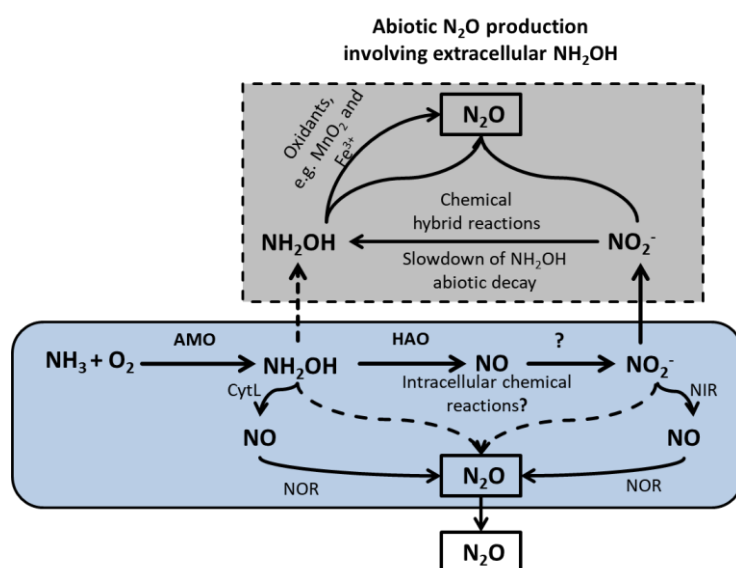


Figure 2.5 Schematic representation of N_2O production pathways during NH_3 oxidation involving NH_2OH and NO_2^- (AMO, ammonia monooxygenase; HAO, hydroxylamine dehydrogenase; NIR, nitrite reductase; NOR, NO reductase). Please note that the schematic cell drawing includes the periplasm.

2.4 Conclusions

We show that extracellular NH_2OH is formed in growth media during aerobic NH_3 oxidation in batch incubations by AOB, AOA and comammox cultures, but with large differences between the different organisms and incubation conditions. The calculated fraction of NH_4^+ converted to N_2O by abiotic reactions between extracellular NH_2OH and substances in the growth medium during aerobic NH_3 oxidation, was in the range of values reported previously for the conversion of substrate to N_2O for various AOB and AOA. The presence of NO_2^- in the medium not only offers a reactant for hybrid N_2O formation from NH_2OH , but also delays

overall NH_2OH abiotic decay further stimulating the conversion of NH_2OH to N_2O . In view of the new results presented here and in recent studies (Stieglmeier *et al.*, 2014; Heil *et al.*, 2016; Kozłowski *et al.*, 2016a; Liu *et al.*, 2017a,b; Terada *et al.*, 2017), it is tempting to speculate that at least for some strains extracellular NH_2OH might contribute significantly to aerobic ammonia-oxidizer associated N_2O formation (as indicated in the gray area in Fig. 2.5). In others, e.g. *N. viennensis*, no extracellular NH_2OH was observed during NH_3 oxidation but aerobic N_2O production has been reported (Stieglmeier *et al.*, 2014), indicating a different mechanism, e.g. the abiotic reactions between intracellular NH_2OH and periplasmic substances.

Chapter 3

A highly sensitive method for the determination of hydroxylamine in soils

Based on:

Liu, S., Vereecken, H. and Brüggemann, N. (2014). A highly sensitive method for the determination of hydroxylamine in soils. *Geoderma*. **232-234**, 117-122.

3.1 Introduction

Hydroxylamine is a short-lived and reactive intermediate in the natural nitrogen cycle. It is formed during microbial nitrification, where NH_4^+ is oxidized via NH_2OH to NO_2^- and NO_3^- (Lees, 1952). NH_2OH appears particularly interesting as it is not only an essential intermediate of nitrification, but also a potential participant in soil N_2O formation (Ritchie & Nicholas, 1972; Bremner *et al.*, 1980; Schreiber *et al.*, 2012).

Certain nitrifiers, e.g. *Nitrosomonas europaea* and *Alcaligenes faecalis*, can produce N_2O during the oxidation of NH_3 and NH_2OH (Ritchie & Nicholas, 1972; Otte *et al.*, 1999). NH_2OH can also react with NO_2^- during denitrification and produce hybrid N_2O in denitrifiers, e.g. *Pseudomonas sp.* (Spott & Stange, 2011). Furthermore, large N_2O emissions from sterilized soil were observed after NH_2OH addition, indicating that chemical reactions between NH_2OH and other soil constituents may also play a crucial role in N_2O production (Bremner *et al.*, 1980). In general, there are three chemical ways of NH_2OH oxidation to N_2O :

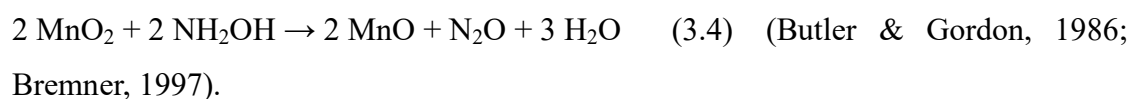
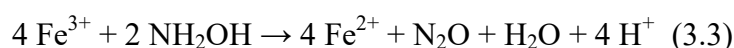
- (i) the oxidation of NH_2OH by O_2 :



- (ii) the reaction between NH_2OH and NO_2^- :



- (iii) the reactions between NH_2OH and metal ions or metal oxides:



Methods for NH_2OH determination have been developed since the 1950s (Dias *et al.*, 1979). However, none of these methods have been widely accepted partly due to the inevitable disadvantages (Dias *et al.*, 1979). An alternative approach, which involves oxidation of NH_2OH to N_2O by Fe^{3+} and the subsequent measurement of N_2O by GC with GC-ECD, was formerly developed for the determination of NH_2OH in seawater (von Breyman *et al.*, 1982; Butler & Gordon, 1986). Compared to the former methods, this alternative approach is much more sensitive and can detect NH_2OH in water at concentrations as low as 5 nM, thereby exceeding the sensitivity of the spectrophotometric methods by at least an order of magnitude

(von Breymann *et al.*, 1982; Butler & Gordon, 1986). Until now, this GC method has been successfully used for the determination of NH_2OH in marine and pharmaceutical aqueous samples (Guzowski Jr *et al.*, 2003; Schweiger *et al.*, 2007; Kock & Bange, 2013). Due to its high sensitivity, it appeared to be a very promising approach for the detection of NH_2OH in soils.

In contrast to water samples, soil is a much more complex matrix, containing potentially large amounts of organic matter, metal ions and, occasionally, NO_2^- , which could interfere with NH_2OH detection. As NH_2OH is highly reactive, fast extraction of soil NH_2OH is crucial for reliable quantification of NH_2OH concentrations in soils. Different extraction conditions – such as temperature, pH, extraction method and time – may affect the determination of NH_2OH concentrations.

As no successful attempt to extract NH_2OH from natural soil samples has been reported until now, the first aim of the study was to test different methods for NH_2OH extraction from soils and identify the most suitable conditions for highest NH_2OH recovery from the soil samples. Another challenge was to minimize the potential interference of soil NO_2^- with N_2O formation from NH_2OH oxidation, as NO_2^- can artificially increase N_2O formation due to its reaction with NH_2OH by contributing one of the two nitrogen atoms of N_2O . Kock & Bange (2013) reported that already $5 \mu\text{M}$ NO_2^- could significantly bias NH_2OH analysis in water samples, but this bias could be eliminated by the use of $100 \mu\text{M}$ sulfanilamide (SA). Therefore, the second aim of this study was to explore the effect of NO_2^- at concentrations as high as $100 \mu\text{M}$ on NH_2OH detection via N_2O , as well as to identify the SA concentration sufficient for its elimination. Motivated by the hypothesis that there might be a close link between soil NH_2OH concentrations and N_2O formation in soils under aerobic conditions, the third aim of this study was to apply the new method to natural soil samples and compare their NH_2OH content with their N_2O emission rates.

3.2 Materials and methods

3.2.1 Soils

Soil samples were collected at 44 locations in a Norway spruce forest site (Wüstebach, $50^\circ 30' 10''$ N, $6^\circ 19' 50''$ E) in the Eifel National Park, Germany which is part of the Terrestrial

Environmental Observatories (TERENO) initiative (Zacharias *et al.*, 2011; Bogena *et al.*, 2013). At each sampling point, samples of organic (O) and mineral (A) horizons were collected between June 24 and 28, 2013. Soil of one of the sampling points was chosen for the development of soil NH_2OH analysis. At this point, litter layer (L) of Norway spruce was also collected. Litter was cut with scissors, and all samples were passed through a 2 mm sieve. The samples of the chosen point were put in open plastic bags and stored in a refrigerator (4 °C) until the beginning of the experiments. The other soil samples were stored in closed plastic bags in a freezer at -18°C until analysis with the final method. Before analysis, the frozen soil samples were taken out of the freezer, opened and kept at room temperature (21 ± 1 °C, applied for the whole paper) for 3 d for reactivation of microbial activity. Soil samples were passed through 2 mm sieve during the reactivation period. The basic properties of the soil and litter samples are shown in Table 3.1.

Table 3.1 Characteristics of the soil used in the experiments of this study ($n = 3$, \pm sd).

	C	N	Fe*	Mn*	Ca*	K*	Mg*	pH
Samples	(%)	(%)	(%)	(%)	(%)	(%)	(%)	
Litter	45.7 \pm 0.1	2.02 \pm 0.02	0.52	0.024	0.29	0.21	0.09	3.40 \pm 0.06
Oh	29.3 \pm 0.1	1.43 \pm 0.03	2.05	<0.01	0.11	0.73	0.13	2.93 \pm 0.06
Ah	14.1 \pm 0.1	0.72 \pm 0.011	3.34	<0.01	0.05	1.15	0.17	3.12 \pm 0.05

* The relative error was 3% for values $>1\%$, 20% for values $<0.1\%$, and 10% for the other values.

3.2.2 Principle of the assay

Hydroxylamine was determined using the method described by Butler & Gordon (1986), where NH_2OH was oxidized to N_2O by Fe^{3+} at acidic conditions according to equation (3.3). The final concentration of NH_2OH was calculated as follows (Gebhardt *et al.*, 2004):

$$[\text{NH}_2\text{OH}] = 2 \cdot r^{-1} \cdot ([\text{N}_2\text{O}] - [\text{N}_2\text{O}]') \quad (3.5)$$

$$[\text{N}_2\text{O}] = (S \cdot N \cdot P \cdot V_{wp} + N \cdot P \cdot V_{hs} / RT) / V_{wp} \cdot 10^{-6} \quad (3.6)$$

where $[\text{N}_2\text{O}]$ is the concentration of N_2O produced by the reaction between NH_2OH and Fe^{3+} at a certain pH; $[\text{N}_2\text{O}]'$ is the background concentration of N_2O of the solution without NH_2OH and Fe^{3+} addition; r stands for the conversion rate, which is defined as the ratio of measured and theoretical NH_2OH concentration, determined by adding different known amounts of NH_2OH to deionized water samples; S is the solubility of N_2O (nmol L^{-1}) as a

function of T and salinity of the sample at 1.01×10^5 Pa according to Weiss and Price (1980); N is the measured mole fraction of N_2O (ppb) in the headspace of vials; P is the pressure in the headspace (1.01×10^5 Pa); V_{wp} is the volume of water phase (mL); V_{hs} is the volume of headspace (mL); R is the gas constant ($8.31441 \text{ J K}^{-1} \text{ mol}^{-1}$); and T is the equilibration temperature (room temperature) in Kelvin.

All samples were analyzed for their headspace N_2O concentrations using an automatic headspace sampler (TurboMatrix 110, PerkinElmer, Germany) and a GC-ECD system (Clarus 580, PerkinElmer, Rodgau, Germany) with dinitrogen (99.999%, Air Liquide, Germany) and a mixture of argon/methane (90/10, Air Liquide, Germany) as carrier gas (flow 7 mL min^{-1}) and make up gas (flow 25 mL min^{-1}), respectively. The ECD column was filled with Elite-PLOT Q (30 m, 0.53 mmID, and 20 μm df, USA) and run at 375°C . The temperature of the oven was 30°C . Signal processing and chromatogram integration was carried out with Totalchrom (Clarus 580, PerkinElmer, Germany) software. The GC was calibrated by three different N_2O standard gas mixtures in the range between 240 to 746 ppb N_2O in nitrogen (99.999%), in which the detector showed a linear response ($r^2 > 0.99$). All experiments and analyses were carried out in 22-mL GC glass vials (VWR International, Darmstadt, Germany). For N_2O analysis of the headspace, the vials were crimped gas-tight with aluminum caps with butyl rubber seal (VWR International). If not indicated differently, the vials were then shaken on a rotary shaker at 250 rpm for 3 h. Preliminary experiments had shown that this time was sufficient for the full reaction between NH_2OH and Fe^{3+} at pH 3.

3.2.3 Experimental design

3.2.3.1 Soil NH_2OH extractions

The extraction procedures were showed in Fig. 3.1. Four grams of fresh, field-moist soil or 2 g litter was first added to a 100 mL conical flask. Then, 25 mL of 2 mM SA solution in 0.02 M HCl (pH 1.7) and 0.002 M HCl (pH 2.7) was added, respectively. The extraction was tested at 4°C and 25°C , respectively, using two different extraction types (magnetic stirring and shaking), and testing different extraction times. After extraction, the mixture of soil and extractant was centrifuged at 3500 rpm for 15 min in a 50 mL polypropylene centrifuge tube (VWR International). Every treatment was duplicated or triplicated.

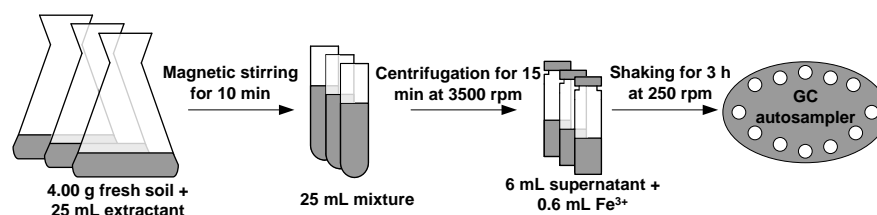


Figure 3.1 The final workflow of NH_2OH extraction in this study.

The extracted soil NH_2OH was determined by adding 6 mL supernatant into a GC vial, followed by 0.6 mL 25 mM $\text{FeCl}_3 \cdot 6\text{H}_2\text{O}$. Another 6.6 mL of supernatant was transferred into a separate GC vial for the determination of the N_2O background. NH_2OH concentration of the soil extract was calculated according to equation (3.5). NH_2OH -to- N_2O conversion rate (r) from each soil supernatant was determined by adding 5.5 mL supernatant into a GC vial, followed by 0.55 mL of 10 μM NH_2OH solution and 0.6 mL of 25 mM Fe^{3+} solution.

Hydroxylamine recovery from soil was determined by extracting 4 g of soil or 2 g of litter with 25 mL 2 mM SA, containing 1 μM NH_2OH , thereby adding in total 25 nmol NH_2OH . The soil NH_2OH extraction and measurement were carried out as mentioned above. The recovery factor was calculated according to the following equation:

$$\text{Recovery factor (f)} = (C_1 - C_0) / C \quad (3.7)$$

where C_1 is the measured NH_2OH concentration in soil samples after addition of 25 mL of 1 μM NH_2OH ; C_0 is the measured NH_2OH concentration without NH_2OH addition; and C stands for the added NH_2OH concentration (1 μM).

3.2.3.2 Nitrite removal

Nitrite interference was tested first in deionized water. Five mL 0.05 M acetic acid solution (pH 3) was first transferred into GC vials, followed by 0.5 mL of either deionized water, 100 μM or 1000 μM NaNO_2 solution, resulting in a final NO_2^- concentration of 0, 9.1 and 91 μM , respectively (for the ease of use labeled as 0, 10 and 100 μM NO_2^-). Half of the vials were immediately amended with 60 μL of 0.2 M SA in 1 M HCl, and allowed to stand for 30 min. Noted that 1 M HCl, instead of 2 M HCl was used, because the pH of soil supernatant was around 2 due to the counteraction of soil alkali ions after extraction. The other vials were amended with 60 μL of 1 M HCl only. Then 0.55 mL of 0.1, 0.5, 1 and 10 μM NH_2OH

solution were added to the vials, respectively, followed by 0.6 mL of 25 mM Fe³⁺ solution. Each combination of NO₂⁻ and NH₂OH concentrations was analyzed in triplicate.

Nitrite interference in soil was tested by adding 25 mL 0.05 M acetic acid with 100 μM NO₂⁻ to 4 g fresh soil each. Then 0.25 mL 0.2 M SA in 2 M HCl was added to half of the soil samples, and the other half was amended with 0.25 mL 2 M HCl. The soil solutions were stirred magnetically for 10 min. After centrifugation at 3500 rpm for 15 min, 5.5 mL supernatant was transferred into GC vials, and 0.55 mL NH₂OH with either 0.1, 0.5, 1 or 10 μM were added to the vials, followed by 0.6 mL 25 mM Fe³⁺. Again, all analyses were carried out in triplicate.

3.2.3.3 Soil N₂O emission

Three grams of field-moist soil each was weighed into GC vials. Then, the vials were crimped gas-tight and incubated at room temperature for 1, 3.5, 6 and 8 h, respectively. The N₂O concentration in the vial headspace was subsequently measured with the same GC-ECD system described in section 3.2.2. The N₂O emission rate (μg N kg⁻¹ dry soil h⁻¹) was calculated from the linear slope of N₂O headspace concentration change with time (ppb h⁻¹) according to the following equation:

$$E = v \cdot V \cdot V_m \cdot 2 \cdot M / W_{ds} \quad (3.8)$$

where E is the N₂O emission rate (μg N kg⁻¹ dry soil h⁻¹); v is the slope of the change of N₂O mixing ratio in the vial headspace (ppb h⁻¹); V is the volume of vial headspace (L); V_m is the molar volume of N₂O at standard pressure and room temperature (L mol⁻¹); M is molar mass of nitrogen (g mol⁻¹); W_{ds} is the mass of the dry soil (g).

3.2.4 Statistical analyses

All statistical analyses were carried out with Origin Pro. 8. Two-sample t-tests were performed to compare the differences in NH₂OH concentration between 10-min magnetic stirring and 2.5-h shaking, between 0 and 10 μM NO₂⁻ addition, and between 10 μM NO₂⁻ + SA and 10 μM NO₂⁻ only addition treatments.

3.3 Results and discussion

3.3.1 Soil NH₂OH extractions

Although pH 3 had been previously identified as a suitable condition for conversion of NH₂OH to N₂O, and for storage of NH₂OH with micromolar concentrations (Butler & Gordon, 1986; Kock & Bange, 2013), this pH condition could not guarantee NH₂OH extraction from soil, even with addition of SA solution and only 10-min magnetic stirring. Moreover, the recovery of NH₂OH was also extremely small (nearly 0) with the addition of 25 nM under this pH condition (Table 3.2). One explanation for the quick disappearance of NH₂OH could be the consumption of NH₂OH by soil microorganisms. Brierley & Wood (2001) reported that heterotrophic nitrifiers, such as *Arthrobacter sp.* may be actively nitrifying at pH 3 in acid forest soil similar to the soil used in this study. Moreover, due to the fact that NH₂OH is extremely reactive, it could also quickly react with carboxyl groups of organic matter or with metal cations in the soil, such as Fe³⁺ or Mn⁴⁺ (Thorn *et al.*, 1992; Bremner, 1997; Schreiber *et al.*, 2012). Our experiments showed that NH₂OH could not be completely recovered even in sterilized soil samples (data not shown), indicating that the chemical reactions between NH₂OH and other soil constituents play a crucial role in the quick disappearance of NH₂OH in the soil samples.

Table 3.2 pH and temperature effect on NH₂OH extraction during 10 min magnetic stirring at 4 °C (n = 3, ± sd).

Treatment	Measured NH ₂ OH concentration (μM)			
	L	Oh	L + 1 μM NH ₂ OH	Oh + 1 μM NH ₂ OH
pH 3[†]	n.d.*	n.d.	n.d.	n.d.
pH 1.7[‡]	0.053 ± 0.003	0.021 ± 0.001	0.67 ± 0.029	0.50 ± 0.022

* n.d. = not detectable

[†] pH 3 extractant was 0.05 M acetic acid.

[‡] pH 1.7 extractant was 0.05 M acetic acid with 0.02 M HCl.

In contrast to negligible NH₂OH extraction at pH 3, NH₂OH could be extracted from the forest soil samples at pH 1.7. For L and Oh layers, NH₂OH concentrations of the extracts at pH 1.7 amounted to 95 and 28 nM after shaking for 2.5 h at 4 °C, respectively (Fig. 3.2a). The recovery of 25 nmol NH₂OH added to the L and Oh samples with the extractant were 40.7% and 15.5%, respectively, after 2.5 h shaking. In contrast, 53 and 21 nM NH₂OH have been

extracted already after 10-min magnetic stirring, with recovery factors of 61.3% and 49.3% for L and Oh layers, respectively (Fig. 3.2b), indicating that the extraction efficiency of magnetic stirring was better than that of shaking. However, with increasing extraction time, the NH_2OH recovery factor decreased significantly for both extraction methods, i.e. shaking and magnetic stirring, suggesting that NH_2OH is extremely reactive and unstable (Fig. 3.2a, b). Therefore, despite the lower absolute amount of NH_2OH extracted as compared to 2.5 h shaking, magnetic stirring for 10 min was chosen as the appropriate extraction method for soil NH_2OH extraction due to its significantly higher NH_2OH recovery factor, especially for the Oh layer samples.

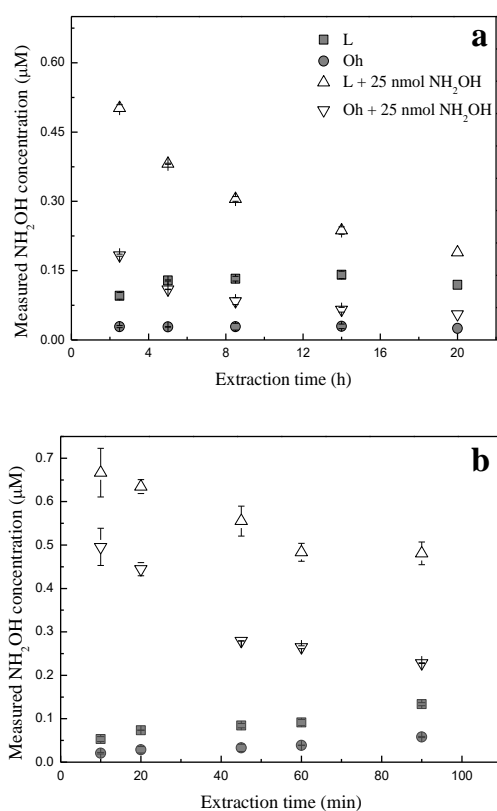


Figure 3.2 Effects of extraction time on NH_2OH concentration of the extract with shaking (a) and magnetic stirring (b) at 4 °C. Error bars indicate the range of measured concentrations ($n = 2$).

We also explored the effect of temperature on soil NH_2OH extraction. Our results showed that the concentration of the extracted NH_2OH was the same or even higher at room temperature as compared to 4 °C (data not shown). Therefore, NH_2OH extraction at room temperature was selected as the routine extraction condition.

3.3.2 Nitrite removal

Nitrite could significantly bias NH_2OH detection with this method due to the reaction according to equation (3.2), especially at low pH. Kock & Bange (2013) reported a significant bias even when NO_2^- concentration was as low as $5 \mu\text{M}$. Although NO_2^- concentration has been found to be relatively low in most forest soils (Su *et al.*, 2011), i.e. the main research object in the present study, it could be as high as $100 \mu\text{M}$ (ca. $17.4 \text{ mg N kg}^{-1}$ soil) in agricultural soils after fertilization (Shen *et al.*, 2003). Therefore, to ensure versatility of the newly developed method, NO_2^- concentrations of 10 and $100 \mu\text{M}$ were used to explore the effect of NO_2^- on the r value (Fig. 3.3a, b).

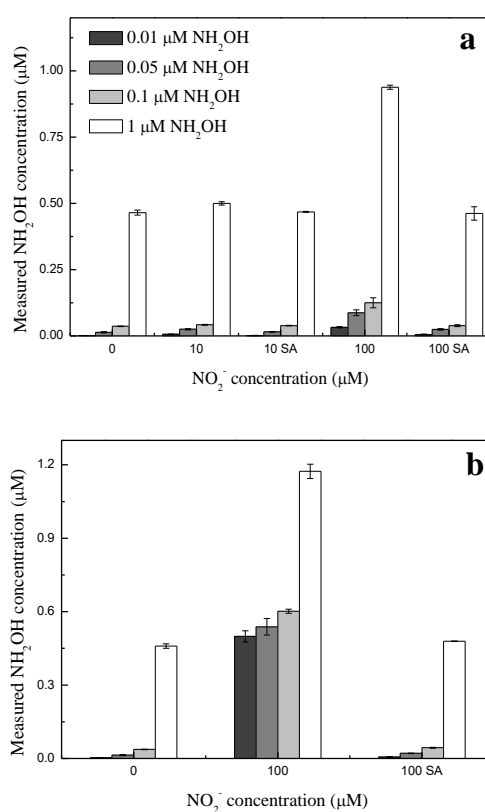


Figure 3.3 Effect of 10 and $100 \mu\text{M}$ NO_2^- on NH_2OH conversion with and without sulfanilamide (SA) in 0.05 M acetic acid + 0.01 M HCl solution (a) and soil extracts (b) at pH 2 and room temperature. Error bars indicate the standard deviation of the mean ($n = 3$).

We found that $10 \mu\text{M}$ NO_2^- had a negligible effect on the NH_2OH -to- N_2O conversion rate, especially when NH_2OH concentration was higher than $0.05 \mu\text{M}$. In contrast, $100 \mu\text{M}$ NO_2^- increased the NH_2OH -to- N_2O conversion rate in deionized water by about 50% (Fig. 3.3a), revealing substantial N_2O formation by the reaction of NO_2^- with NH_2OH . Furthermore, NO_2^-

biased NH_2OH measurements more significantly in soil samples, especially at lower NH_2OH concentrations, e.g. 37-fold at $0.05 \mu\text{M}$ NH_2OH (Fig. 3.3b). Kock and Bange (2013) suggested $100 \mu\text{M}$ SA to remove the effect of $5 \mu\text{M}$ NO_2^- . Therefore, in this study we assumed that 2 mM SA should be sufficient to remove the bias of $100 \mu\text{M}$ NO_2^- .

Our results showed that 2 mM SA was adequate for the complete removal of the bias of $10 \mu\text{M}$ NO_2^- on NH_2OH -to- N_2O conversion, and also to fully eliminate the effect of $100 \mu\text{M}$ NO_2^- at NH_2OH concentrations above, but not below $0.05 \mu\text{M}$. This could have been due to the fact that 2 mM SA was not completely sufficient for the removal of $100 \mu\text{M}$ NO_2^- . We then tried 5 mM SA in the subsequent experiment, but failed to find any significant difference between these two SA concentration treatments (data not shown), which suggested that the bias of $100 \mu\text{M}$ NO_2^- on the determination of nM NH_2OH concentrations was inevitable. Nevertheless, our results also showed that the concentration bias was linearly correlated with the amount of NO_2^- in the range of $10\text{--}100 \mu\text{M}$ (Fig. 3.4). Thus, the NO_2^- bias could be corrected for using this linear relationship after determination of the NO_2^- concentration of the soil samples.

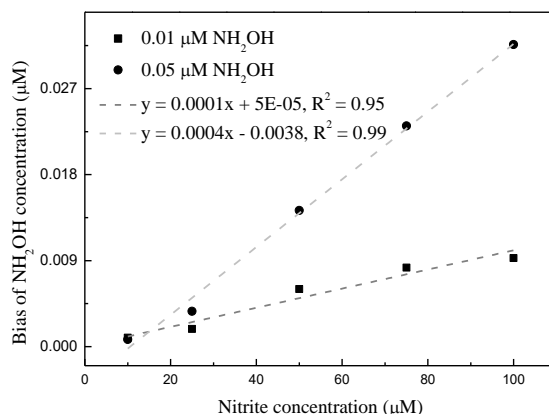


Figure 3.4 Effect of different NO_2^- concentrations on NH_2OH determination in the presence of 2 mM sulfanilamide (SA) at pH 2 in 0.05 M acetic acid + 0.01 M HCl solution ($n = 3$).

3.3.3 NH_2OH concentration in forest soil samples and its correlation with aerobic N_2O emission rate

The analysis of NH_2OH concentrations in soil samples from Wüstebach forest with the newly developed method revealed a range of $0.3\text{--}34.8 \mu\text{g N kg}^{-1}$ dry soil (Fig. 3.5). This is approximately three orders of magnitude lower than the concentrations of NH_4^+ and NO_3^- in forest soil samples, but still comparable to the concentration of NO_2^- , for which e.g. a range of

2.8–11.2 $\mu\text{g N kg}^{-1}$ was found for northern hardwood forests (Venterea *et al.*, 2003). NH_2OH concentration decreased with the depth of soil profiles, in the order of $\text{L} > \text{Oh} > \text{Ah}$ (Fig. 3.2b and Fig. 3.5). NH_2OH concentration in the L layer was usually twice as high as in the Oh layer (Fig. 3.2b), while in the Ah horizon, the NH_2OH concentration was rarely above 5 $\mu\text{g N kg}^{-1}$ dry soil (Fig. 3.5). This trend was consistent with the trends of NH_4^+ and NO_3^- in forest soil profiles (Tietema *et al.*, 1992), indicating that higher mineralization and nitrification rates probably occur in the litter layer, leading to higher NH_2OH production.

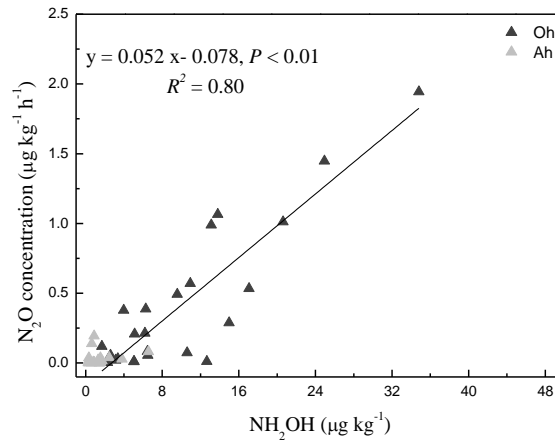


Figure 3.5 Correlation between soil NH_2OH content and aerobic N_2O emission rates at room temperature of soil samples collected from Wüstebach forest ($n = 44$).

Nitrous oxide emission rates from ranged from 0–1.9 $\mu\text{g N kg}^{-1}$ dry soil h^{-1} from Oh and Ah with a higher value in Oh than that in Ah (Fig. 3.5). Moreover, the N_2O emission rate from the L of the chosen point was around 2.9 $\mu\text{g N kg}^{-1}$ dry soil h^{-1} (data not shown). These results corresponded well with the findings of Martikainen & de Boer (1993), who observed an N_2O emission rate of 3 $\mu\text{g N kg}^{-1}$ dry soil h^{-1} in an aerobic incubation of acid forest litter from a fir stand in the Netherlands. Moreover, The same trend of $\text{L} > \text{Oh} > \text{Ah}$ was observed for the soil of a Finnish coniferous forest, where ammonia oxidizers were assumed to play an important role in aerobic N_2O production in these acid soils (Martikainen *et al.*, 1993). In other forest soils across Europe, however, denitrification was considered as the main source of N_2O emission due to the lower aeration of the fresh litter layer especially in deciduous forests (Ambus *et al.*, 2006). By using $^{15}\text{NH}_4^-$ and $^{15}\text{NO}_3^-$ as substrates, Ambus *et al.* (2006) identified NO_3^- as a significant source of N_2O in most forests, except for two spruce forest soils, indicating that the source of N_2O may differ between forest types.

Hydroxylamine stimulated N₂O production during nitrifier pure-culture studies (Ritchie & Nicholas, 1972; Otte *et al.*, 1999), most likely due to reactions between NH₂OH and other substances, such as MnO₂ and NO₂⁻ (Bremner, 1997). The potential role of NH₂OH in soil N₂O production has been emphasized in several recent reviews (Wrage *et al.*, 2001; Schreiber *et al.*, 2012; Butterbach-Bahl *et al.*, 2013). However, the relationship between soil NH₂OH and N₂O emission has not been explored so far due to the lack of sufficiently sensitive determination methods for NH₂OH in soil up to now. In this study, we indeed found a significant correlation between soil NH₂OH concentration and N₂O emission rate (Fig. 3.5). This finding suggests NH₂OH, the intermediate of nitrification, as a significant source of N₂O formation in the Wüstebach spruce forest soil. Moreover, the linear relationship was more obvious in the Oh than that in the Ah. This could be due to that both the NH₂OH concentration and N₂O emission rate were considerably smaller in the Ah than that in the Oh. Additionally, the less aerobic condition in Ah layer could also contribute to the less obvious relationship.

3.4 Conclusions

The newly developed method for soil NH₂OH extraction and analysis is very sensitive, and its applicability to soils has been shown. The appropriate extraction conditions for soil NH₂OH were identified as 10-min magnetic stirring at room temperature with an aqueous extractant of pH 1.7 (0.05 M acetic acid with 0.02 M HCl), containing 2 mM SA. Soil NH₂OH concentration was found to be significantly correlated with soil N₂O emission, indicating that nitrification plays a crucial role in soil N₂O formation in the Norway spruce forest soil examined in this study. Future work should focus on the analysis of different soil properties and their control on soil NH₂OH concentrations and N₂O emission.

Chapter 4

The contribution of hydroxylamine content to spatial variability of N₂O formation in soil of a Norway spruce forest

Based on:

Liu, S., Herbst, M., Bol, R., Gottselig, N., Pütz, T., Weymann, D., Wiekenkamp, I., Vereecken, H. and Brüggemann, N. (2016). The contribution of hydroxylamine content to spatial variability of N₂O formation in soil of a Norway spruce forest. *Geochimica et Cosmochimica Acta*, **178**, 76–86.

4.1 Introduction

Nitrous oxide is one of the most important greenhouse gasses, with a global warming potential 298 times that of CO₂ within a timeframe of 100 years and including climate–carbon feedbacks (IPCC, 2013). Soils are estimated to contribute 60% of the total annual N₂O emissions to the atmosphere, of which about 60% originate from natural soils and the remainder from agricultural soils as a result of excessive nitrogen fertilizer application (IPCC 2013). However, the estimate of total soil N₂O emissions is still highly uncertain due to the spatial heterogeneity and temporal variability, even at a smaller scale. To quantify N₂O emissions more accurately, a comprehensive understanding of the spatio-temporal variation of soil N₂O emissions as well as of the controlling factors and underlying mechanisms is required.

Nitrous oxide is mainly produced by the microbial processes of nitrification and denitrification (Baggs, 2008). Denitrification is a process by which NO₃⁻ is stepwise reduced to molecular nitrogen via the chain NO₃⁻ – NO₂⁻ – NO – N₂O – N₂, while nitrification – including heterotrophic nitrification, nitrifier denitrification, as well as abiotic chemodenitrification – starts with NH₃ as a substrate (Brierley & Wood, 2001; Wrage *et al.*, 2001; Baggs, 2011). Denitrification is traditionally considered as the most important source of soil N₂O emissions (Wolf & Brumme, 2003; Ambus *et al.*, 2006). However, nitrification has increasingly been identified as a relevant source of N₂O in forest ecosystems, especially at pH values below 5 (Brierley & Wood, 2001; Mørkved *et al.*, 2007). One potential explanation is that the first intermediate of nitrification, i.e., NH₂OH, might play a crucial role in N₂O formation as a direct precursor (Bremner, 1997; Schreiber *et al.*, 2012; Butterbach-Bahl *et al.*, 2013) (see below).

Commonly, it is assumed that the aerobic oxidation of NH₂OH to N₂O is a biological process, involving the enzyme HAO (Stein, 2011). Using metabolic modeling analysis, Law *et al.* (2013) predicted that the key N₂O production pathway of an AOB culture is the biological oxidation of NH₂OH. Rathnayake *et al.* (2013) reported that 65% of the N₂O was produced through NH₂OH oxidation in an autotrophic partial nitrification reactor. However, N₂O formation from NH₂OH under oxic conditions has also been observed for some methane-oxidizing alphaproteobacteria that co-metabolize NH₃ along with methane, but do not have a corresponding HAO (Sutka *et al.*, 2004; Stein, 2011), pointing to a hitherto unknown N₂O production mechanism.

One possible alternative mechanism of aerobic N₂O production could be the chemical oxidation of NH₂OH excreted by or leaked from nitrifying soil microorganisms by redox active soil cations, such as Fe³⁺ and Mn⁴⁺, especially at acidic conditions, since at higher, more neutral pH the unprotonated NH₂OH can undergo a multitude of chemical reactions with SOM (Thorn *et al.*, 1992) and is then no longer available for oxidation by transition metals. The occurrence of this oxidation reaction was documented previously (Bremner, 1997; Schreiber *et al.*, 2012). Although the importance of NH₂OH for N₂O emissions has received more attention along with progress in the analysis of the isotopic composition of N₂O and its isotopologues from purely chemical reactions and from wastewater treatment plants (Stein, 2011; Law *et al.*, 2013; Wunderlin *et al.*, 2013; Heil *et al.*, 2014), studies of the role of NH₂OH in soil N₂O emissions have only rarely been carried out until now (Bremner *et al.*, 1980) due to difficulties with detecting small quantities of the reactive intermediate NH₂OH in the complex soil environment. However, a highly sensitive method for the determination of the NH₂OH content of soils has been developed recently (Liu *et al.*, 2014), which enables analysis of the correlation between NH₂OH content and N₂O emissions in natural soils.

The spatial variability of soil N₂O emissions has been studied in agricultural, grassland, pasture or forest ecosystems (Velthof *et al.*, 2000; Yanai *et al.*, 2003; Turner *et al.*, 2008). Forest ecosystems have been reported to be a large source of N₂O, especially in regions with water-logged soils or with large water table fluctuations (Ahmed & De Marsily, 1987; Lamers *et al.*, 2007; Rütting *et al.*, 2013). Given that chamber measurements will remain an important methodology for the quantification of N₂O emissions from soils, but that the number of chambers employed – and hence the spatial representativeness – is usually comparatively low, it is crucial to find a supporting tool for assessing spatial N₂O emission patterns and to understand its controlling factors. Only in this way can the uncertainty caused by the choice of chamber locations be reduced and the prediction of soil N₂O emissions at larger scales be improved. Therefore, the goals of this study were to explore the contribution of soil NH₂OH content to potential soil N₂O emissions in a spruce forest ecosystem in association with other soil basic properties, and to elucidate the spatial variability of and the relationship between potential soil N₂O emission rates and NH₂OH content.

4.2 Materials and methods

4.2.1 Experimental site

The soil used in this study was sampled at the TERENO site Wüstebach (50° 30' 10" N, 6° 19' 50" E, elevation 630 m a.m.s.l.). This site is located in the German low mountain ranges within the National Park Eifel near the German-Belgian border (Fig. 4.1). The site was dominated by Norway spruce (*Picea abies* (L.) H. Karst), planted in 1946, and covers an area of approximately 27 ha in a forested catchment of a small tributary (Wüstebach creek) of the river Rur, with an average and maximum slope of 3.6% and 10.4%, respectively (Bogena *et al.*, 2015). The sampling locations were based on the existing geospatial design of the SoilNet network (Bogena *et al.*, 2010). On the hillslopes, cambisols and planosols prevailed, whereas gleysols and histosols dominated the riparian zone at the valley bottom (Fig. 4.1). The main soil texture was silty clay loam. In most of the area, the organic soil layers consisted of a litter layer (L), a fermented litter horizon (Of) and humus rich layer (Oh). The L, Of and Oh layers had an average thickness of 3 cm to 5 cm in total, and the average A horizon was about 6 cm thick. The ground vegetation was species-poor and scantily developed (mainly fern, grass, and moss species, with a few interspersed shrubs and bushes). The climate of the area is temperate maritime with an annual mean temperature of around 7°C and an annual precipitation of approximately 1200 mm (Bogena *et al.*, 2010). The growing season is short (130-135 days) due to the prevailing cold westerlies.

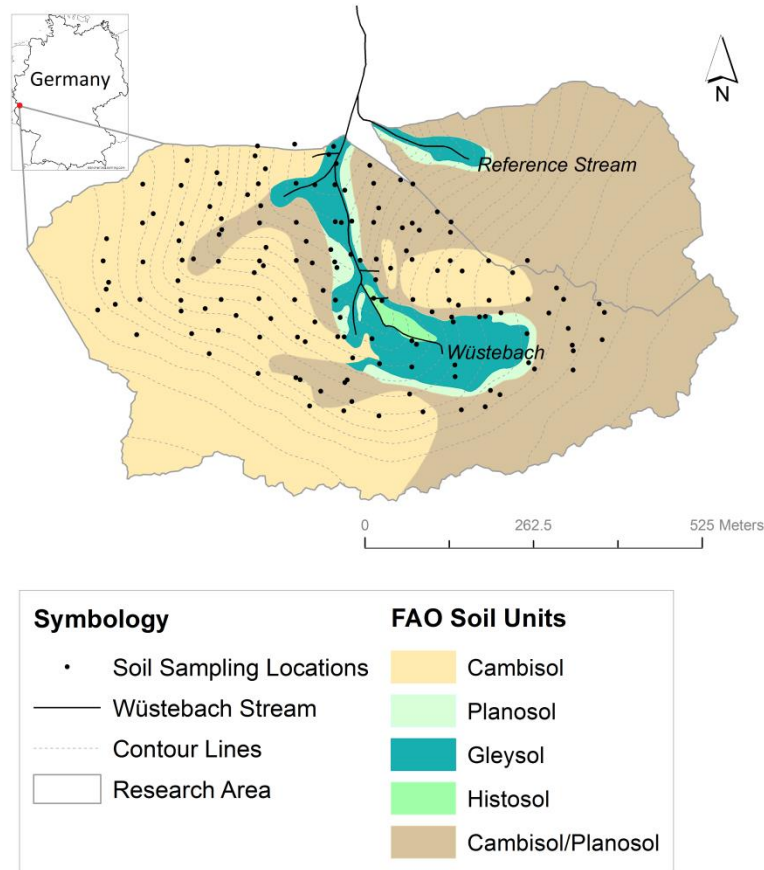


Figure 4.1 Map showing the location of the sampling area and the exact position of the sampling points within the Wüstebach catchment.

4.2.2 Soil sampling

In the period of June 24 to 28, 2013, bags with disturbed soil samples were collected from O and A horizons at 150 sampling points within the experimental area (Fig. 4.1). Soil samples were stored in closed plastic bags in a freezer at -18°C until analysis for NH_2OH content and N_2O emissions under oxic conditions. Homogenized aliquots of the soil samples (ca. 300 g) were analyzed for soil basic properties, i.e. pH, soil water content (SWC), C, N, P, S, Na, K, Ca, Mn, Fe, NH_4^+ and NO_3^- content by a commercial laboratory (Landwirtschaftliches Labor Dr. Janssen GmbH, Gillersheim, Germany) (see section 4.2.3.3 for details). Three days before the analysis of NH_2OH and N_2O , the samples were taken out of the freezer, opened at room temperature for reactivation of microbial activity, and then passed through a 2 mm sieve. The SWC had changed only negligibly after two days of storage at room temperature (data not shown).

4.2.3 Analytical methods

4.2.3.1 Hydroxylamine extraction and analysis

Soil NH_2OH content was determined as described in Liu *et al.* (2014). Briefly, 25 mL of 2 mM sulfanilamide solution in a mixture of 0.02 M HCl and 0.05 M acetic acid (pH 1.7) was added to 4 g of thawed, field-moist soil. The mixture was then magnetically stirred for 10 min and centrifuged at 3500 rpm for 15 min. Six ml supernatant was subsequently transferred to a 22-mL glass vial (VWR International, Darmstadt, Germany), and 0.6 mL of 25 mM $\text{FeCl}_3 \cdot 6 \text{H}_2\text{O}$ in deionized water was added. The vials were immediately closed gas-tight after Fe^{3+} addition and shaken for 3 h on a rotary shaker (250 rpm) at 21°C. N_2O production in the headspace of the vials was measured afterwards by using a GC-ECD (Clarus 580, PerkinElmer, Rodgau, Germany). Afterwards, the NH_2OH content of the soil extract was calculated according to equations described in Liu *et al.* (2014).

4.2.3.2 Potential soil N_2O emission rates

Three grams of field-moist soil were weighed into 22-mL GC vials. Then, the vials were crimped gas-tight and incubated at constant temperature (21°C) for 67, 209, 354 and 496 min, respectively, with three replicates for each point in time. The N_2O concentration in the vial headspace was subsequently measured with the same GC-ECD system used for NH_2OH measurement. The N_2O emission rate ($\mu\text{g N kg}^{-1}$ dry soil h^{-1}) was calculated according to Liu *et al.* (2014).

4.2.3.3 Soil basic properties

Topographic attributes were obtained from a digital elevation model with 1 m resolution (Land Surveying Office of North Rhine-Westphalia, Germany). Exact elevation and slope of each sampling point were calculated in ArcGIS (version 9.3.1, ESRI, Redlands, CA, USA). The distance between the nearest superficially visible root and each sampling point was determined with a measuring tape. Soil pH was determined in H_2O (pH₁) and 0.01 M CaCl_2 (pH₂) according to the standard procedures DIN 38404 and DIN ISO 10390, respectively. Extractable inorganic P (P₁) and K were extracted with a mixture of 0.05 M calcium lactate and 0.3 M calcium acetate (1:20, soil to liquid) according to Schüller (1969), and analyzed by inductively coupled plasma optical emission spectrometry (ICP-OES). Mn, Fe and Na were extracted with a mixture of 0.1 M CaCl_2 and 0.002 M diethylenetriaminepentaacetic acid

(pentetic acid, DPTA) (1:10, soil to liquid) according to VDLUFA A6.4.1 (Hoffmann, 1991) and analyzed by ICP-OES. C and N were determined by dry combustion at 950 °C according to DIN ISO 10694 and DIN ISO 13878, respectively, and analyzed by a CHN analyzer. Total P (P₂), S and Ca were extracted by aqua regia (3:1 (v/v) mixture of 12 M hydrochloric acid and 14.4 M nitric acid) digestion according to DIN 38406-22 and analyzed by ICP-OES. NH₄⁺ and NO₃⁻ were determined after extraction with 0.01 M CaCl₂ (1:1, soil to liquid) according to VDLUFA A6.4.1 (Hoffmann, 1991), and analyzed with a continuous-flow analyzer.

4.2.4 Data analyses

Frequency distributions and skewness of the data were analyzed with histograms, using the R statistical software package (version 3.1.0). Soil variables that were not normally distributed were log-transformed prior to the geostatistical analysis. The spatial autocorrelation of each soil variable was quantified using the semivariance (γ). A semivariogram displays the semivariance plotted against the lag distances between pairs of samples. The variance increases with distance until a maximum (sill, c) if the data is spatially auto-correlated and 2nd order stationary. The distance corresponding to the sill is called the range (a_1). The y-intercept of a semivariogram is the nugget (c_0), which represents the variance caused by measurement error and subscale spatial variability, while the variance between c_0 and c shows the variance of the spatial structure, i.e. spatial variance that is given by $(c-c_0)/c$. Spherical variogram models were fitted to the experimental semivariograms with the VESPER software (Minasny *et al.*, 2005).

Stepwise multiple linear regressions were performed to predict potential soil N₂O emission rates from all the determined soil properties (NH₂OH, NO₃⁻, C, N, C/N, SWC, Mn, Fe, pH₁, pH₂, P₁, P₂, Na, K, S, Ca) for the Oh and Ah layer, respectively (R version 3.1.0). Variables were stepwise eliminated during the regression procedure to determine a minimum subset of variables with a maximum explanatory power, and to get rid of explanatory variables' inter-correlation. R² was used to quantify the variation of potential soil N₂O emission rates that was explained by the variation of the independent variables. R²_{adj} is a more appropriate criterion by relating the explained variation to the number of the variables. As a final criterion for model selection, we used the Akaike information criterion (AIC) in the multiple linear regressions, where the smallest AIC means that the optimum regression model is closest to the 'true' model (Akaike, 1998).

The KT3D-routine of the Geostatistical Software Library (Deutsch & Journel, 1998) was applied to perform the spatial estimation by Kriging. The mean absolute error (MAE) and the root mean square error (RMSE), determined by a cross validation procedure, were used to indicate the goodness of the Kriging estimates. Ordinary Kriging (OK) was extended to external-drift Kriging (EDK) by using spatial regression estimates as auxiliary data (Ahmed & De Marsily, 1987). The improvement index (I_r) of MAE and RMSE was used to evaluate the improvement of the EDK compared to the OK simulation. To preserve the probability density function and the spatial autocorrelation of the original measured point data, conditional stochastic simulation (CSS) was performed with the Simulated Annealing Algorithm (SASIM, Deutsch & Journel, 1998) based on the potential N₂O emission measurements and the regression estimates as auxiliary spatial information (Goovaerts, 2000; Bourennane *et al.*, 2007). In contrast to the Kriging approaches, CSS reproduces the semivariogram and the frequency distribution of the target variable. Further details on the Kriging estimation and stochastic simulation approaches can be found in Herbst *et al.* (2012).

4.3 Results

4.3.1 Potential soil N₂O emission rates, NH₂OH content and basic properties

The basic properties of the Ah and Oh layers are displayed in Table 4.1. Of all soil properties, potential N₂O emission rates showed the largest variation, followed by NH₂OH, NO₃⁻ and Mn content. The potential N₂O emission rates ranged from 0–2.9 and 0–0.49 µg N kg⁻¹ dry soil h⁻¹ in the Oh and Ah layer, respectively, with the mean value of the Oh tenfold higher than that of the Ah. The potential N₂O emission rates were highly variable, with coefficients of variation of 260% and 439% for the Ah and Oh layer, respectively, and were left-skewed distributed. The NH₂OH concentrations showed a pattern similar to that of potential soil N₂O emission rates, ranging from 0.3–37.0 and 0.02–6.6 µg N kg⁻¹ dry soil in the Oh and Ah, respectively. On a dry weight basis, the mean NH₂OH content in the Oh was about sixfold larger than in the Ah, with less variation (CV ≈ 100%) compared to potential N₂O emission rates. The NH₂OH content was approximately three orders of magnitude lower than the NO₃⁻ content of the forest soil samples (Table 4.1).

Table 4.1 Descriptive statistics of potential N₂O emission rates, NH₂OH concentrations and other soil variables of the Ah and Oh soil horizons.

Soil properties	Ah					Oh				
	μ	σ	CV (%)	n ¹	D	μ	σ	CV (%)	n	D
N ₂ O (μg ⁻¹ N kg ⁻¹ dry soil h ⁻¹)	0.07	0.21	295.5	98	LD	0.64	2.81	438.5	126	LD
NH ₂ OH (μg ⁻¹ N kg ⁻¹ dry soil)	1.72	1.86	108.4	119	LD	11.1	14.3	128.7	131	LD
NO ₃ ⁻ (mg N kg ⁻¹ dry soil)	2.87	3.26	113.7	139	LD	19.9	33.0	166.0	118	LD
NH ₄ ⁺ (mg N kg ⁻¹ dry soil)	- [§]	-	-	-	-	94.5	89.2	94.4	118	LD
C (%)	10.2	5.0	49.4	139	LD	23.1	7.5	32.5	118	ND
N (%)	0.56	0.24	43.0	139	LD	1.12	0.33	29.1	118	ND
C/N	18.1	2.5	14.0	139	LD	20.5	2.6	12.5	118	ND
pH ₁ (H ₂ O)	4.26	0.32	7.5	139	LD	3.93	0.36	9.1	121	LD
pH ₂ (CaCl ₂)	3.27	0.25	7.5	139	LD	3.10	0.26	8.5	129	LD
SWC (g g ⁻¹ wet soil)	43.6	9.6	22.0	139	ND	59.7	8.4	14.0	120	ND
Mn (mg kg ⁻¹ dry soil)	29.4	42.7	145.1	138	LD	40.2	40.2	100.0	126	LD
Fe (mg kg ⁻¹ dry soil)	1294	300	23	138	ND	946	235	25	126	ND
P ₁ (mg P kg ⁻¹ dry soil)	17.0	8.4	49.3	139	LD	52.5	22.0	41.9	129	LD
P ₂ (%)	0.07	0.02	23.8	139	ND	0.09	0.01	16.0	136	ND
Na (mg kg ⁻¹)	23.2	12.0	51.6	138	LD	35.6	20.3	57.0	126	LD
Ca (%)	0.05	0.03	62.9	139	LD	0.12	0.09	74.7	136	LD
S (%)	0.05	0.03	50.6	139	LD	0.11	0.03	30.9	136	ND
K (mg K kg ⁻¹ dry soil)	19.6	37.8	193.0	139	LD	119	104	87	129	LD

μ: mean, σ: standard deviation of the left-deviated parameters, calculated by the following equation: $\mu = \exp(\mu_1 + 0.5 \sigma^2)$, variance = $\sigma^2 = [\exp(2 \mu_1 + \sigma_1^2)] [\exp(\sigma_1^2) - 1]$. μ and σ² represent the mean and variance of the random variable X (in original units), whereas μ₁ and σ₁² are the mean and variance of its log-transformation, given by Y = ln(X) (Singh *et al.*, 1997); n: number of valid data used for data analysis. There are generally three kinds of distribution (D): LD = left deviation, RD = right deviation, and ND = normal distribution; SWC: soil gravimetric water content.

¹ Soil properties of some sampling points are missing because the amount of soil material was not sufficient for all analyses for those sampling points.

[§] Soil NH₄⁺ data of Ah layer was missing due to experimental errors during NH₄⁺ determination.

Soil NO₃⁻ content was also remarkably higher in the Oh than in the Ah layer, with considerable spatial variation (Table 4.1). The mean C content of the Oh layer was twice as high as that of the Ah layer, whereas the mean C/N ratios of the two layers were nearly the same. Owing to the topography and soil variability in the Wüstebach catchment, also SWC varied considerably in the sampling area. The mean pH of about 4 (H₂O) and of slightly above 3 (CaCl₂) was typical for an acidic spruce forest soil. In general, the Oh layer was more acidic than the Ah layer. At certain sampling points, the Mn content was as high as 366 mg kg⁻¹ in the Ah layer, whereas the mean value was about 30 mg kg⁻¹ for the Ah, and around 40 mg kg⁻¹ for the Oh layer. Of all soil properties, only Fe content and pH were larger in the Ah than in the Oh.

4.3.2 Spatial patterns

Semivariograms were used to analyze spatial variance and spatial auto-correlations of potential N_2O emission rates as well as NH_2OH and NO_3^- content of the spruce forest soil. The semivariograms for potential soil N_2O emission rates showed similar ranges (approx. 100 m) for Ah and Oh layers, but with a large difference in spatial variance (22.5% vs. 53.4%) due to the difference in spatial auto-correlation in both layers (Fig. 4.2). The NH_2OH and NO_3^- content showed an opposite pattern for ranges and spatial variances in the two soil layers. For the Ah, the semivariogram of NH_2OH exhibited a smaller range (113.2 m) than for NO_3^- (179.0 m), but a larger spatial variance (55.0%) than for NO_3^- (31.9%). For the Oh, however, the range of NH_2OH was larger, associated with a smaller spatial variance, compared to NO_3^- (Fig. 4.2).

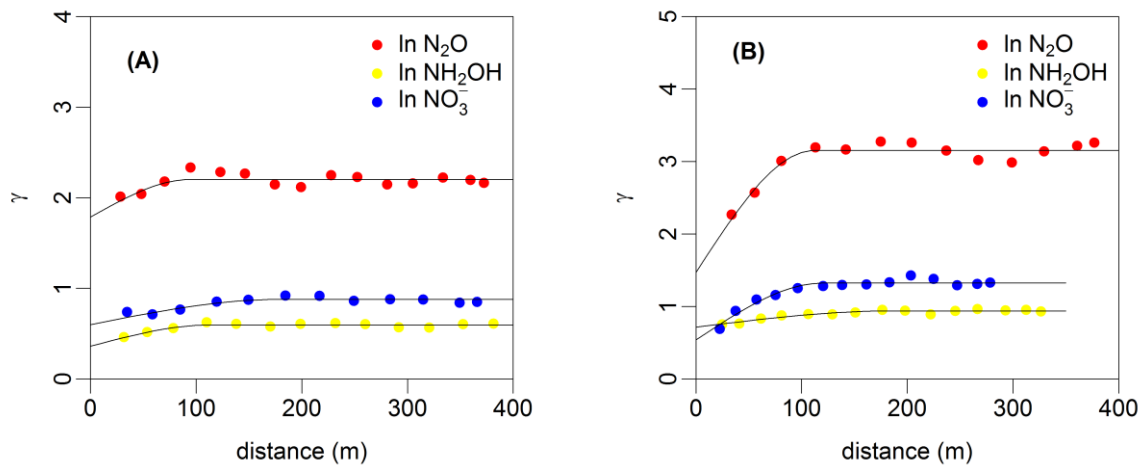


Figure 4.2 Semivariograms of log-transformed N_2O emission rates $[\ln (\mu\text{g}^{-1} \text{N kg}^{-1} \text{ dry soil h}^{-1})]^2$, NH_2OH content $[\ln (\mu\text{g}^{-1} \text{N kg}^{-1} \text{ dry soil})]^2$ and NO_3^- content $[\ln (\text{mg N kg}^{-1} \text{ dry soil})]^2$ in the Ah (A) and Oh (B) of the sampling area.

Ordinary Kriging was applied to estimate the spatial patterns of soil NH_2OH , soil NO_3^- and potential N_2O emission rates. A large spatial variability was observed for potential N_2O emission rates for both Ah and Oh layer (Fig. 4.3). The spatial distributions of potential N_2O emission rates were similar for both layers and were highly dependent on SWC, with larger potential N_2O emission rates at sampling points close to the headwater of the Wüstebach creek. For example, the average potential soil N_2O emission rates were 0.04 and $0.7 \mu\text{g N kg}^{-1} \text{ dry soil h}^{-1}$ for Ah and Oh layer, respectively, in the area of the headwater of the Wüstebach

creek (Fig. 4.3), which was several times larger than at a greater distance from the creek. However, N₂O emission hotspots were also observed at sampling points with a thick litter layer or high root density, whereas N₂O emissions at positions with grass cover and no tree nearby were hardly detectable.

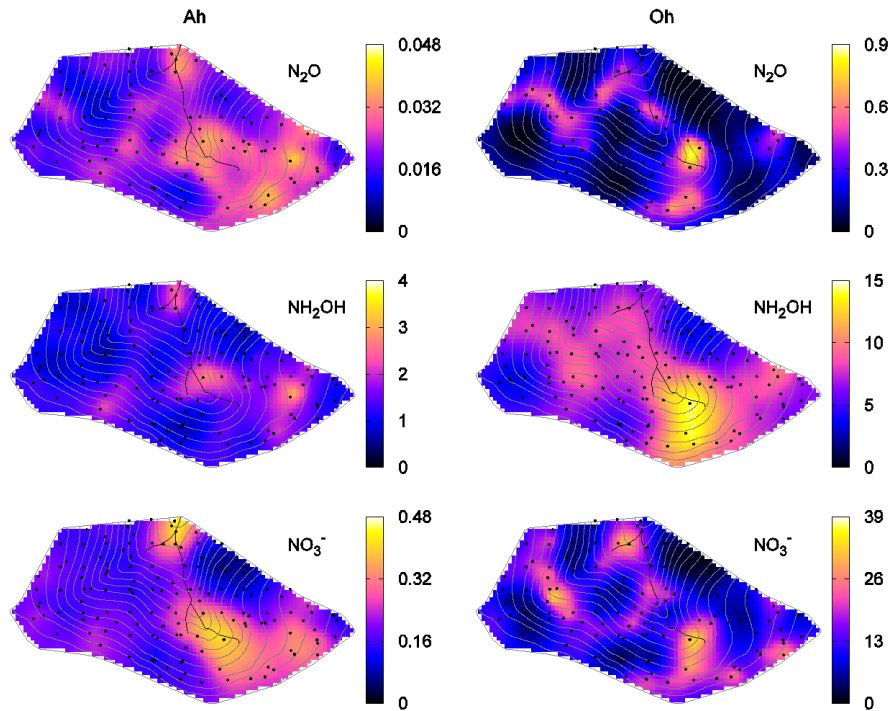


Figure 4.3 Spatial patterns of potential N₂O emission rates ($\mu\text{g}^{-1} \text{N kg}^{-1} \text{dry soil h}^{-1}$), NH₂OH content ($\mu\text{g}^{-1} \text{N kg}^{-1} \text{dry soil}$) and NO₃⁻ content ($\text{mg N kg}^{-1} \text{dry soil}$) estimated using ordinary Kriging (OK) for the Ah and Oh layers of the sampling area. The grey smooth lines in the maps are contour lines. The black line represents the Wüstebach creek. The black points indicate the sampling points with valid data for each soil property.

Also, soil NH₂OH and NO₃⁻ content showed large spatial variability across the whole study area. Their spatial patterns were similar to that of potential soil N₂O emission rates. Especially NH₂OH content featured almost the same hotspots as potential soil N₂O emission rates, even in the area with high SWC (up to 80% WFPS) (Fig. 4.3). However, all of the extreme values of soil properties were underestimated by OK, probably as a result of the high spatial variability and the smoothing effect of the interpolation.

4.3.3 Correlations and multiple stepwise regressions

As soil C and N content as well as pH and SWC are commonly considered as important drivers of soil N₂O emissions, the correlation analysis focused on these parameters. The log-

transformed potential soil N₂O emission rates were highly and positively correlated with C and inorganic N content in both Ah and Oh layer (Table 4.2). Soil NH₂OH content alone explained 39% and 63% of the potential N₂O emission rates of the Ah and Oh, respectively, which was similar to the explanatory power of NO₃⁻ content in the Ah (40%) and Oh layer (58%). However, NH₄⁺ was less strongly correlated with potential soil N₂O emission rates, although highly correlated with soil C and N content. Potential soil N₂O emission rates showed no significant correlations with soil pH, while a negative correlation ($P < 0.05$) was observed between soil pH₁ and NH₂OH.

Table 4.2 Spearman's rank correlation coefficients of the correlations of N₂O emission rates with NH₂OH, NO₃⁻, NH₄⁺, C, N, C/N, pH₁ (H₂O), pH₂ (CaCl₂) and soil water content (SWC) in the Oh (grey area) and Ah (white area) layer, respectively.

Oh Ah	ln N ₂ O	ln NH ₂ OH	ln NO ₃ ⁻	ln NH ₄ ⁺	C	N	C/N	pH ₁	pH ₂	SWC
ln N ₂ O		0.796*	0.761*	0.234*	0.109	0.128	0.021	-0.173	-0.097	0.295*
ln NH ₂ OH	0.626*		0.598*	0.364*	0.240*	0.222*	0.152	-0.248*	-0.251*	0.323*
ln NO ₃ ⁻	0.633*	0.490*		0.137	0.050	0.098	-0.070	-0.224*	-0.251*	0.238*
ln NH ₄ ⁺	-	-	-		0.738*	0.738*	0.258*	-0.011	-0.091	0.751*
ln C	0.349*	0.496*	0.423*	-		0.929*	0.475*	-0.126	-0.037	0.665*
ln N	0.447*	0.536*	0.5535*	-	0.948*		0.161	-0.079	0.068	0.715*
ln C/N	0.025	0.155	-0.145	-	0.512*	0.282*		-0.151	-0.290*	0.035
pH ₁	-0.146	-0.075	0.019	-	-0.080	-0.047	-0.209*		0.527*	0.083
pH ₂	-0.174	0.239*	0.101	-	-0.214*	-0.118	-0.464*	0.527*		0.128
SWC	0.356*	0.331*	0.363*	-	0.693*	0.697*	0.239*	0.005	0.028	

In contrast to the correlation analysis, stepwise multiple regressions were carried out by using all the basic soil properties depicted in Table 4.1 as variables for the prediction of potential soil N₂O emission rates. As preliminary results showed that soil K, S, Ca and Na content did not contribute significantly to explaining the spatial variance of potential N₂O emission rates, they were excluded from the multiple regression models. In contrast, NH₂OH and NO₃⁻ content strongly contributed to the variance of N₂O (Table 4.3). Soil C content and SWC were the second most important variables explaining potential soil N₂O emission rates from the Ah, followed by soil pH₁ and Mn content. Soil Fe and P₁ content also featured small, but insignificant contributions to potential soil N₂O emission rates. Also for the Oh layer, soil NH₂OH and NO₃⁻ content were the most important variables explaining the variance of potential N₂O emission rates, but followed by total P and soil Mn content. Soil Fe content,

again, showed a small but not significant contribution. The best model could explain 60% of the variance of potential soil N₂O emission rates for the Ah layer, while it could explain about 80% for the Oh layer (Table 4.3).

Table 4.3 Stepwise multiple regression equations of potential N₂O emission rates in the Oh and Ah layer, respectively. The Akaike Information Criterion (AIC) was used for the model selection in the multiple linear regressions.

Soil layer	Multiple regression equation	R ²	R ² _{adj}	AIC
Ah (n = 84)	$\ln N_2O = -2.292 + 1.007 \ln NH_2OH^{***} + 0.513 \ln NO_3^{-**}$ $- 1.111 \ln C^* + 0.042 SWC^* - 0.896 pH_1^* + 0.257 \ln$ $Mn^* - 0.0006 Fe + 0.826 \ln P_1$	0.636	0.601	3.05
Oh (n = 84)	$\ln N_2O = -8.569^{***} + 0.851 \ln NH_2OH^{***} + 0.738 \ln NO_3^-$ $^{***} + 21.07 P_2^{**} + 0.250 \ln Mn^* + 0.0006 Fe$	0.794	0.781	-29.2

Asterisks indicate the significance of the respective variable or y-intercept in the multiple regression models at a level of $P < 0.05$ (*), $P < 0.01$ (**), $P < 0.001$ (***) .

n = number of soil samples for which values for all the co-variables were available.

4.3.4 Improvement of spatial estimation

External-drift Kriging (EDK) was used to estimate the spatial patterns of potential soil N₂O emission rates by adding the information of covariates identified by the multiple regression analysis (Fig. 4.4). Compared with the spatial patterns based on OK, the EDK simulation showed a more complex and sharpened spatial structure for both Ah and Oh layer. Using EDK instead of OK led to a greater improvement of MAE and RMSE for the Oh layer than for the Ah layer, with an improvement of 45.2% and 41.3 % for the MAE and RMSE for the Oh, and 27.6% and 23.9% for the Ah, respectively (Table 4.4). A similar spatial pattern was observed between CSS and EDK (Fig. 4.4). Even though the CSS approach produced a noisier pattern, it exhibited a wider data range compared to EDK (see color bar range of Fig. 4.4) and provides a more realistic pattern. Additionally, the pattern of potential soil N₂O emission rates of the Oh layer derived from CSS showed less noise in comparison to that of the Ah layer, as a result of the higher spatial variance of the Oh layer compared to the Ah layer (see Section 4.3.2).

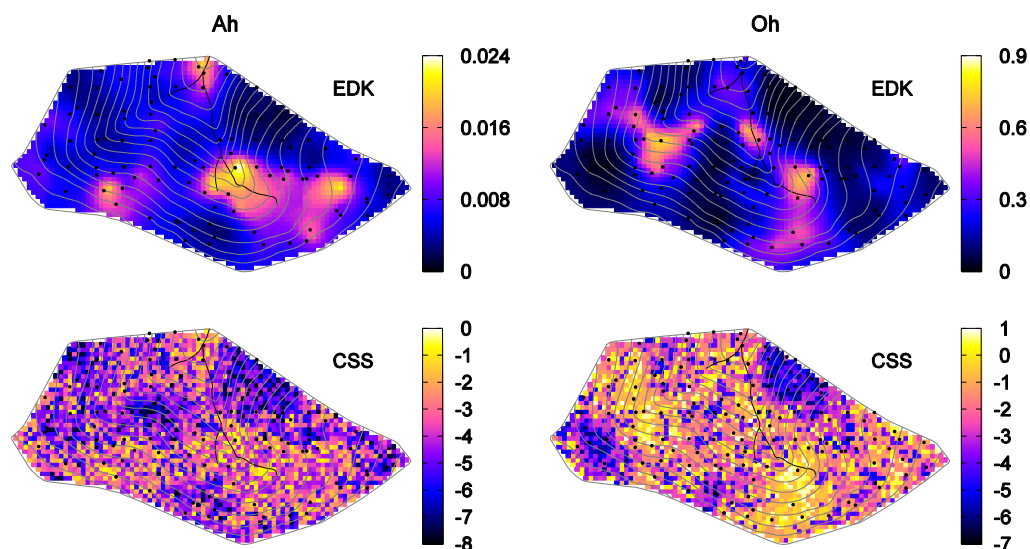


Figure 4.4 Spatial patterns of potential N_2O emission rates estimated using external-drift Kriging (EDK) and conditional stochastic simulations (CSS) for the Ah and Oh layers. The EDK estimation is an extension of ordinary Kriging (OK) by using spatial regression estimates based on the regression models as auxiliary data. The CSS estimation is an estimation based on the spatial variability and spatial structure by checking the cumulative probability density function. The color code of the EDK maps represents N_2O emission rates in $\mu\text{g}^{-1} \text{N kg}^{-1} \text{dry soil h}^{-1}$, while the color code of the CSS maps represents the logarithm of N_2O emission rates in $\mu\text{g}^{-1} \text{N kg}^{-1} \text{dry soil h}^{-1}$.

Table 4.4 Mean absolute error (MAE), root mean square error (RMSE), χ^2 and the improvement (I_r) percentage for the interpolation maps of ordinary Kriging (OK) and external drift Kriging (EDK).

	MAE	RMSE	χ^2
Ah ($n = 96$)			
OK	1.220	1.480	88.588
EDK	0.884	1.127	42.920
I_r (%)	27.6	23.9	
Oh ($n = 125$)			
OK	1.344	1.612	868.45
EDK	0.736	0.947	141.46
I_r (%)	45.2	41.3	

4.4 Discussion

4.4.1 Spatial patterns of potential soil N₂O emission rates and soil NH₂OH content

A high spatial variability of potential N₂O emissions was observed in the Wüstebach sampling area. Topographic conditions, such as slope and elevation, have been reported as important factors of spatial variability of soil N₂O emissions (Velthof *et al.*, 2000; Nishina *et al.*, 2009; Konda *et al.*, 2010). However, although slope and elevation ranged between 0.75–8.27% and 595–627 m, respectively, in the sampling area of this study, we did not observe a significant correlation between N₂O emissions and these two variables, neither for the Ah nor for the Oh layer (data not shown). Tree density and aboveground vegetation may contribute to the spatial variability of soil N₂O emissions, as the abundant input of organic matter from litter can support microbial activity in the topsoil. In addition, tree distance and root density may also have an influence on soil N₂O emissions, on the one hand due to their impact on soil water fluxes and hence on SWC, and on the other hand due to root litter input and root exudates that can serve as substrates for soil microbial N turnover processes (Butterbach-Bahl *et al.*, 2002). We observed that SOM was abundant at the sampling points with high root density, and we found a weak negative, but significant correlation ($r = -0.264$, $p < 0.05$) between the distance of the nearest superficially visible root to the sampling point and the respective potential soil N₂O emission rates of the Oh layer of this point (data not shown).

In addition to the influence of vegetation, the Wüstebach creek flowing through the sampling area might have also contributed to the spatial variability of potential soil N₂O emission rates, mainly by causing – in combination with the specific topographical conditions – a large spatial variability of SWC in this area (Bol *et al.*, 2015). Hotspots of potential N₂O emission rates were observed in the headwater of the creek for both the Oh and Ah layer. This finding is consistent with McSwiney *et al.* (2001), who found that soil N₂O emissions increased dramatically at the slope-riparian interface and continued to increase through the floodplain and the riverbank. The change in SWC is associated with a change in the soil O₂ and substrate availability, and with the formation of different soil types, e.g. *Cambisols* (well-aerated) and *Gleysols* (water-logged). Lamers *et al.* (2007) demonstrated that the N₂O fluxes from (water-logged) *Gleysols* were much larger than those from an (upland) *Cambisol* in a spruce forest in Central Germany, which is consistent with our research. Increased SWC may decrease O₂ availability in soil but can increase the solubility of iron. In a recent study, large concentrations of iron were found in the headwater of Wüstebach creek (Bol *et al.*, 2015). As

iron can be an important driver of soil N₂O emissions, either through the oxidation of NH₂OH by iron (III) or through the reduction of NO₂⁻ by iron (II) (Zhu *et al.*, 2013b), the increased iron concentration in the *Gleysols* induced by high water content may contribute to the larger N₂O emissions in the headwater of the Wüstebach forest.

The NH₂OH content of the soil ranged from 0.02–6.6 µg N kg⁻¹ dry soil in the Ah layer, but was on average tenfold larger in the Oh layer, probably due to the large organic matter content and therefore higher microbial activity in this layer. The average soil NH₂OH content was approximately three orders of magnitude lower than the average content of NH₄⁺ and NO₃⁻ in forest soil samples, but the spatial pattern of soil NH₂OH content was similar to that of potential soil N₂O emission rates and soil NO₃⁻ content. The hotspots of soil NH₂OH content along the headwater of the Wüstebach creek were unexpected, since the conditions in such areas are less favorable for autotrophic nitrifying bacteria, which is presumably the most likely source process of soil NH₂OH. Bol *et al.* (2015) found the lowest pH value in water samples taken in the hotspot area of this study, which could have contributed to the accumulation of NH₂OH in this location since NH₂OH is more stable at low pH. This could have also promoted the activity of AOA, which have recently been shown to be also involved in N₂O formation in soils under oxic conditions (Jung *et al.*, 2014; Stieglmeier *et al.*, 2014). While the formation mechanism of N₂O in this class of microorganisms is still unclear, NH₂OH has been shown to be an intermediate of ammonia oxidation by AOA (Vajjala *et al.*, 2013). However, at the present stage the source process of NH₂OH in the *Gleysol* area of this study remains unknown and needs further investigation.

4.4.2 The contribution of NH₂OH to soil potential N₂O emission

Models for the N₂O production in forest soils have been developed using functions and parameters for nitrification, denitrification and chemodenitrification (Li *et al.*, 2000; Parton *et al.*, 2001). But the role of NH₂OH on soil N₂O emissions in a natural ecosystem has not been confirmed before, even though it is an important intermediate of nitrification.

Although NH₂OH and the responsible source processes have recently received more attention as potential determinants of soil N₂O emissions (Wrage *et al.*, 2001; Schreiber *et al.*, 2012; Butterbach-Bahl *et al.*, 2013), a strong correlation of NH₂OH with potential N₂O emission rates, as in this study, has not been observed before for natural ecosystems. In contrast, large contributions (up to 65%) of NH₂OH to N₂O emissions have been observed in wastewater

treatment plants (Law *et al.*, 2013; Rathnayake *et al.*, 2013). Until now, soil NH₄⁺, NO₃⁻ and water content have been considered as the most crucial factors affecting soil N₂O emission in forest soils (Wolf & Brumme, 2003; Schindlbacher *et al.*, 2004; Pilegaard *et al.*, 2006), as well as soil pH (Klemedtsson *et al.*, 2005; Mørkved *et al.*, 2007; Gharahi Ghehi *et al.*, 2012) and soil C/N ratio (Ambus *et al.*, 2006). However, Bremner *et al.* (1980) demonstrated that the addition of NH₂OH to sterilized soil immediately led to soil N₂O emission. Chemical formation of soil N₂O emissions has also been assumed in acidic soils (Martikainen *et al.*, 1993; Gharahi Ghehi *et al.*, 2012).

There are mainly two potential pathways for the oxidation of NH₂OH to N₂O: the biological reaction by the enzyme HAO or methanotrophic bacteria, and the chemical oxidation by nitrite or redox active metal cations (Bremner, 1997; Campbell *et al.*, 2011; Stein, 2011). The redox reaction between NH₂OH and Mn⁴⁺ ($2 \text{ MnO}_2 + 2 \text{ NH}_2\text{OH} \rightarrow 2 \text{ MnO} + \text{N}_2\text{O} + 3 \text{ H}_2\text{O}$) has been demonstrated to play an important role in soil N₂O emissions (Bremner, 1997). In this study, by using multiple regression analysis, we also found that Mn was an important factor explaining N₂O emission rates (Table 4.3), emphasizing the importance of the oxidation of NH₂OH by MnO₂ to N₂O in this Norway spruce forest ecosystem. In addition, we also observed a negative correlation between N₂O emission rates with soil pH and soil C content (Table 4.3). This could be explained by the fact that unprotonated NH₂OH can react with organic carbonyl groups to oximes (Thorn *et al.*, 1992). As higher soil pH leads to a decreasing degree of NH₂OH protonation (pK_a = 5.95), it will become more reactive with organic matter, and thus less available for the oxidation by MnO₂ to N₂O.

The prediction of soil N₂O emissions for larger areas is usually difficult due to high spatial variability, not least due to the complex topographic, hydrologic and edaphic conditions. Static chambers are widely used for the estimation of soil N₂O emissions from terrestrial ecosystems and provide valuable information for assessing the spatial variability (Velthof *et al.*, 2000; Yanai *et al.*, 2003; Konda *et al.*, 2010). Because the area enclosed by a chamber is typically smaller than 1 m², it is necessary to use a large number of chambers to get a representative estimate of the fluxes at the field scale. The decision of how many chambers should be used and where the chambers should be put in a terrestrial ecosystem with high spatial variability is quite difficult due to high spatial and temporal variability and the limited number of chambers that can be employed. For example, the required number for a spatially representative observation of soil N₂O emission in the sampling area of this study would be as

high as 532, using the method by Herbst *et al.* (2009), which is impossible to realize with a practical experimental design. A supporting tool, as suggested here, is to elucidate key control variables of soil N₂O emission that can be relatively easily measured, to determine these variables at a large number of sampling points and to calculate the respective N₂O emission rates for these points.

4.5 Conclusions

In this study, potential soil N₂O emission rates showed a large spatial variability, which could be chiefly explained with the spatial variability of soil NH₂OH and NO₃⁻ contents. Hotspots of all three soil parameters were observed in the headwater of the Wüstebach creek. This finding suggests that NH₂OH plays a crucial role in explaining spatial variability of N₂O emissions under a range of soil conditions in a heterogeneous catchment and indicates that a spatially representative determination of soil NH₂OH content, along with other co-variables, is a promising way to reduce the uncertainty of soil N₂O emission estimates for complex ecosystems. The approach demonstrated in this study could also facilitate field measurements of N₂O with chambers in terms of a spatially optimized sampling design which reflects best the spatial N₂O emission patterns.

Chapter 5

Interactive effects of MnO₂, organic matter and pH on abiotic formation of N₂O from hydroxylamine in artificial soil mixtures

Based on:

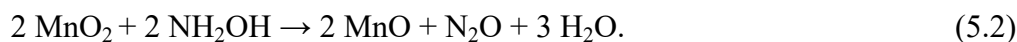
Liu, S., Berns, A. E., Vereecken, H., Wu, D. and Brüggemann, N. (2017). Interactive effects of MnO₂, organic matter and pH on abiotic formation of N₂O from hydroxylamine in artificial soil mixtures. *Scientific Reports*, **7**, 39590

5.1 Introduction

Nitrous oxide is a potent greenhouse gas that can be formed by several soil processes, such as microbial nitrification and denitrification. The N₂O production from nitrification, especially from its reactive intermediate NH₂OH, has received increasing attention in the recent past, fostered by the development of analytical techniques for the determination of the ¹⁵N site preference in the N₂O molecule that allows for constraining the contribution of different source processes to total N₂O formation (Sutka *et al.*, 2006; Stein, 2011; Wunderlin *et al.*, 2012; Rathnayake *et al.*, 2013). Also, increasing knowledge from molecular biological and genetic studies has contributed to elucidating the different N₂O formation mechanisms during nitrification (Stein, 2011). Still, the role of NH₂OH in N₂O formation in the soil is insufficiently understood. While there is evidence, e.g., from measurements in wastewater treatment systems that NH₂OH can contribute about 65% of total N₂O formation (Rathnayake *et al.*, 2013), the formation of N₂O from NH₂OH in soil and its controlling factors have rarely been studied (Bremner *et al.*, 1980; Heil *et al.*, 2015).

Hydroxylamine was first identified by Lees (1952) as an intermediate of the first step of nitrification by AOB, in which NH₃ is oxidized to NO₂⁻. The knowledge of understanding the nitrification process in AOA, however, is much more fragmentary, but NH₂OH has been identified as an intermediate of ammonia oxidation also in AOA (Vajrala *et al.*, 2013). In most circumstances, NH₂OH is quickly oxidized to nitrite in the periplasm of the AOB, and N₂O may be produced as a side product during this process (Stein, 2011). However, also a leakage of NH₂OH from the periplasm across the outer membrane of the AOB into the soil matrix, followed by a chemical reaction with soil constituents yielding N₂O, could be a potential mechanism of the N₂O formation during nitrification. This assumption is supported by the fact that AOB can take up NH₂OH from the surrounding medium (Schmidt *et al.*, 2004a) as well as by the observation that the medium of AOB cultures contains measurable amounts of NH₂OH. The latter was found for *Nitrosomonas europaea* under oxic conditions, both for wild-type *N. europaea* and even more so for NirK and NorB-deficient mutants (Schmidt *et al.*, 2004b). In accordance with this assumption, a positive relationship between NH₂OH content of the soil and soil N₂O emissions under oxic conditions has been detected in natural forest soil samples Liu *et al.* (2014). In addition, also the abiotic formation of N₂O from NH₂OH has been observed in sterilized soil samples from different ecosystems (Heil *et al.*, 2015).

In soil, N₂O can be formed chemically, among other possibly reactions, according to the following equations (Bremner, 1997):



Owing to its high oxidization potential, manganese dioxide (MnO₂) acts as a strong oxidant in the soil that plays an important role not only in the turnover of organic substances (Lehmann *et al.*, 1987; Li *et al.*, 2012), but also in the N cycle (Luther & Popp, 2002), even under anoxic conditions (Hulth *et al.*, 1999; Hulth *et al.*, 2005). SOM plays a crucial role in the storage and release of N as well as in the emission of N₂O from soils. Quick disappearance of NO₂⁻ and NO₃⁻ within a few hours after addition has been observed in forest soils (Dail *et al.*, 2001; Davidson *et al.*, 2003; Schmidt & Matzner, 2009), whereas NH₂OH disappeared completely in soil several minutes after addition (Bremner *et al.*, 1980; Liu *et al.*, 2014). Abiotic reactions of SOM and inorganic N may contribute to the quick disappearance, as nitrite and nitrate can react with SOM or dissolved organic carbon (DOC), leading to the formation of organic N, such as nitroso and nitro compounds (El Azhar *et al.*, 1986; Thorn & Mikita, 2000), while NH₂OH can also react with carbonyl groups to form oximes (Nelson, 1977; Thorn *et al.*, 1992):



The quality of SOM, or more specifically the C/N ratio and the type and abundance of functional groups, influence the bonding of inorganic N to SOM (Thorn & Mikita, 2000). Phenolic lignin derivatives, an important constituent of SOM, can covalently bind reactive N compounds and thereby stabilize N in soil (Olk *et al.*, 2006; Halvorson & Gonzalez, 2008). The N binding form can be affected by the plant species from which the SOM is derived due to the different characteristics of phenolic compounds, e.g. condensed or hydrolyzable tannin (Kraus *et al.*, 2004).

Soil pH is another key factor influencing most nitrogen transformations in soil. High soil N₂O emissions have been observed in acid forest soils (Martikainen *et al.*, 1993; Šimek & Cooper, 2002). The effect of pH on enzyme activities during denitrification and nitrification was suggested as the main reason (Liu *et al.*, 2010). However, also chemical reactions that produce N₂O in the soil, such as the reaction of nitrite with SOM and the reaction of NH₂OH with

MnO_2 , are subject to a strong pH dependence and can contribute substantially to N_2O emissions under acidic conditions (van Cleemput, 1998; Venterea, 2007; Samarkin *et al.*, 2010).

The aim of this study was to quantify the interactive effects of the major control factors of abiotic N_2O formation from NH_2OH in soil, i.e. MnO_2 content, pH and OM quantity and quality, by means of experiments with artificial soil mixtures. We hypothesized that the control factors interact with each other in the following way: At higher pH, unprotonated NH_2OH would react more readily with carbonyl groups of OM, leading to oxime formation and making NH_2OH less available for oxidation to N_2O by MnO_2 . Lower soil pH would lead to increased protonation of NH_2OH , making NH_2OH more stable against the reaction with carbonyl groups of OM and more prone to the reaction with MnO_2 , leading to the higher N_2O formation from the same amount of NH_2OH (Fig. 5.1). To test these hypotheses, we performed a series of laboratory experiments with artificial soil mixtures, which were produced from pure quartz sand, quartz powder, kaolin clay, MnO_2 powder and different plant-derived organic materials, resembling SOM of different quality, at different mixing ratios. In these experiments, the N_2O formation was determined after NH_2OH addition to the different mixtures at different pH levels and related to the different control factors.

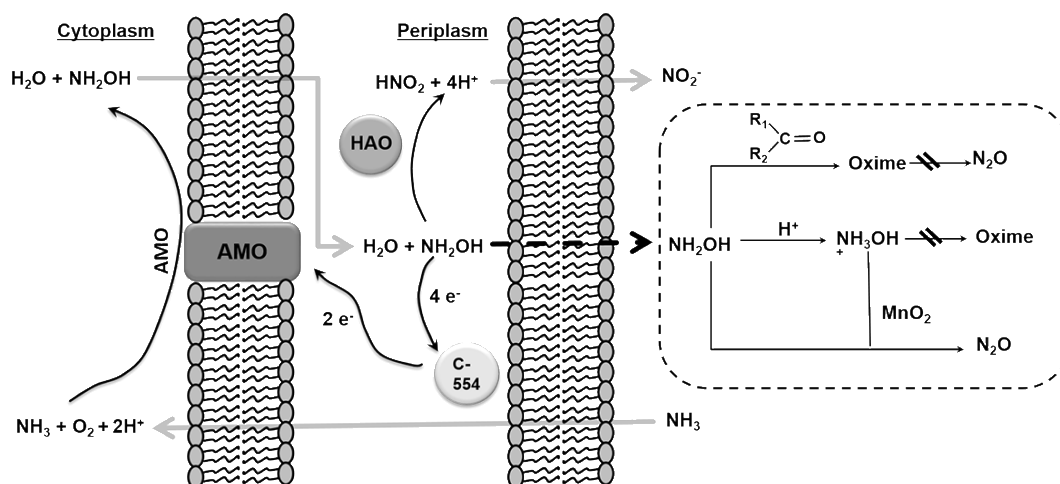


Figure 5.1 Hypothetical model of NH_2OH release by ammonia-oxidizing bacteria to the soil environment and potential reactions of NH_2OH with MnO_2 and organic matter in the soil at different pH conditions ($\text{R}_1\text{R}_2\text{C}=\text{O}$ represents carbonyl groups of SOM). AMO is ammonia monooxygenase; HAO is hydroxylamine oxidoreductase.

5.2 Methods

5.2.1 Preparation of the artificial soil mixtures

The artificial soil mixtures consisted of 15% (expressed as percentage of dry weight) fine quartz sand (50% of the particles 0.05-0.2 mm), representing the sand fraction, 65% quartz powder (0.002-0.063 mm), representing the silt fraction, and 20% kaolin clay (≤ 0.002 mm), representing the clay fraction, mimicking the soil texture of the agricultural TERENO field site Selhausen (Bornemann *et al.*, 2011). Freeze-dried, finely ground and sieved (< 0.75 mm) peat moss (*Sphagnum magellanicum*, collected from Dürres Maar, Eifel, Germany) was amended as SOM to the artificial soil mixtures at levels of 0%, 1%, 2.5%, 5%, 10% dry weight, while the relative amount of sand, clay and silt was reduced according to the amount of peat moss added. The water holding capacity (WHC) was determined for each of the artificial soil mixtures. The WHC increased with increasing organic matter (OM) content, and amounted to 29%, 44%, 55%, 76%, and 132% for the five OM contents, respectively. Each of those artificial soil mixtures was amended with MnO₂ (Merck, Darmstadt, Germany) at five different levels (0%, 0.01%, 0.025%, 0.05%, 0.1% Mn), then the ingredients were thoroughly homogenized.

5.2.2 Preparation of artificial soil mixtures with different OM qualities

Organic materials with different C/N ratios (Table 5.1) were derived from two different plant species, i.e. watermilfoil (*Myriophyllum spec.*) and clover (*Trifolium repens*), and from a cyanobacterium (*Spirulina platensis*). Watermilfoil and clover had been collected previously on the campus of Forschungszentrum Juelich GmbH (2004 and 2014, respectively), while the cyanobacterium material had been purchased in 2006 (Concept Vitalprodukte, Schwerte, Nordrhein-Westfalen, Germany). The finely ground and sieved (< 0.75 mm) OM was amended to the inorganic quartz-kaolin mixture as described above at a rate of 2.5% dry weight, while the relative amount of sand, clay, and silt was reduced accordingly. Also for this experiment, each of the artificial soil mixtures was amended with MnO₂ at five different levels (0%, 0.01%, 0.025%, 0.05%, 0.1% Mn), and again mixed thoroughly to obtain a homogeneous composition.

Table 5.1 Basic elemental properties of the organic materials used in this study.

	C [§]	N	C/N	Al	Ca	Fe	K	Mg	Mn	Na	P	Si
Peat moss	41.3 [†]	0.61	67.2	0.034	0.13	0.055	0.055	0.071	< 0.01	0.014	0.029	0.083
Watermilfoil	35.4	2.08	17.0	0.12	2.26	0.11	1.21	0.25	0.031	0.666	0.124	0.213
Clover	41.4	3.67	11.3	< 0.01	1.10	0.011	2.68	0.20	< 0.01	< 0.01	0.338	0.031
Cyanobacterium	44.9	9.90	4.5	0.017	0.31	0.089	1.22	0.31	< 0.01	1.359	0.920	0.065

[§] All elements are reported as % of dry weight.

[†] The standard deviation is 3% for the values larger than 1%, 20% for the values smaller than 0.1%, and 10% for the values in the range of 0.1% to 3%.

5.2.3 Addition of NH₂OH to the artificial soil mixtures and analysis of the N₂O formed

One gram of each artificial soil mixture was weighed into individual 22-mL GC vials. Subsequently, NH₂OH in different buffer solutions was added to each vial to obtain a soil water content of 50% WHC, which required addition of varying volumes of buffer solution to the different soil mixtures depending on the OM content, and adaptation of the NH₂OH concentration of each of the buffer solutions accordingly. The total amount of NH₂OH added to each of the soil mixtures was always 5 nmol (equivalent to 70 µg N per kg dry material). The pH buffer solutions at pH 3, 4, 5 and 6 were prepared with citric acid (0.1 M) and sodium citrate (0.1 M) according to Gomori (1955), whereas the buffer at pH 7 was prepared with tris(hydroxymethyl)aminomethane and maleate (Tris-maleate buffer). There were totally two experiments conducted, with one experiment with totally three treatments (pH×5 levels, MnO₂ ×5 levels, OM amount×5 levels) and the other one with also three treatments (pH×5 levels, MnO₂ ×5 levels, OM quality×4 levels, OM amount 2.5%). The experiments included totally four treatments (pH×5 levels, MnO₂ ×5 levels, OM amount×5 levels and OM quality×4 levels), with three replicates for each level. The vials were closed immediately after NH₂OH addition. After 10 h of incubation, the N₂O concentration in the headspace of the vials was measured with a GC equipped with an electron capture detector (Clarus 580, PerkinElmer, Rodgau, Germany) (Liu *et al.*, 2014).

5.2.4 Calculation of the NH₂OH-to-N₂O conversion ratio

The NH₂OH-to-N₂O conversion ratio ($R_{\text{NH}_2\text{OH-to-N}_2\text{O}}$, moles N₂O-N per mole NH₂OH-N, %) was determined according to the following equation:

$$R_{\text{NH}_2\text{OH-to-N}_2\text{O}} = (c_1 - c_0) \cdot V / V_m \cdot 2 / n \cdot 100 \quad (5.4)$$

where c_0 is the background N₂O mixing ratio in the headspace of the control without NH₂OH addition (nL L⁻¹); c_1 is the N₂O mixing ratio in the headspace of the sample with NH₂OH addition (nL L⁻¹); the factor 2 represents the molar N ratio of N₂O and NH₂OH; V is the volume of the vial headspace (0.022 L); V_m is the molar volume of N₂O at standard pressure and room temperature (24.465 L mol⁻¹); n is the amount of NH₂OH added to the sample vials (5 nmol).

5.2.5 Determination of the basic properties of the organic materials

Three replicates of each organic material were analyzed to determine its basic properties. The C and N content of the different organic materials was analyzed by weighing 200-300 µg dry material into tin capsules, followed by combustion at 1080°C in an elemental analyzer (EuroEA, EuroVector, Milan, Italy) interfaced to an isotope-ratio mass spectrometer (Isoprime, Isoprime Ltd, Stockport, United Kingdom). The C and N content were determined through peak integration of m/z 44 (CO₂) and 28 (N₂), respectively, and calibrated against elemental standards.

The elemental composition of the organic materials was analyzed by using ICP-OES in the central analytical laboratory (ZEA-3) of Forschungszentrum Jülich. Briefly, 100 mg of sample material were mixed with 3 mL HNO₃ and 2 mL H₂O₂, heated in the microwave at 800 W for 30 min. The mixtures were subsequently filled up to 14 mL and diluted 10-fold with deionized water followed by the ICP-OES measurement.

For the determination of characteristic molecule structures and functional groups of the different organic materials used in the experiments, ¹³C and ¹⁵N cross-polarisation magic-angle spinning (CPMAS) nuclear magnetic resonance (NMR) spectra were obtained. ¹³C CPMAS spectra were obtained on a 7.05 T Varian INOVATM Unity (Varian Inc., Palo Alto, CA, USA) at a ¹³C resonance frequency of 75.4 MHz. ¹⁵N CPMAS spectra were obtained on a 14.09 T Varian NMR system (Varian Inc., Palo Alto, CA, USA) at a ¹⁵N resonance frequency of 60.8 MHz. Samples were packed into 6 mm diameter cylindrical zirconia rotors with Vespel® drive tips and spun at 8000 ± 3 Hz in an HX Apex probe. The spectra were collected with a sweep width of 25 kHz and an acquisition time of 20 ms. In preliminary experiments, the optimal contact time and recycle delay for the cross-polarization experiment were determined. A contact time of 1 ms and a 5 s recycle delay time were used for ¹³C, whereas a contact time of 1 ms and a 1 s recycle delay time were used for ¹⁵N. During cross-polarization

the ^1H radio frequency (RF) field strength was set to 47 kHz for ^{13}C and to 33.7 kHz for ^{15}N , respectively. The ^{13}C and ^{15}N RF field strength were set to 41 and 41.7 kHz, respectively. An ascending ramp of 15 and 12.2 kHz on the ^1H -RF field was used for ^{13}C and ^{15}N during contact time to account for inhomogeneities of the Hartmann-Hahn condition, respectively (Berns & Conte, 2011). Proton decoupling was done using a spinal sequence with a ^1H field strength of 50 and 35.6 kHz, a phase of 4.5° and 5.5° , and a pulse length of 12 and 9.5 μs , respectively.

The free induction decays (FID) were recorded with VnmrJ (Version 1.1 RevisionD, Varian Inc., Palo Alto, CA, USA) and processed with Mestre-C (Version 4.9.9.9, Mestrelab Research, Santiago de Compostela, Spain). All FIDs were Fourier-transformed with an exponential filter function with a line broadening of 20 to 50 Hz. Baseline correction was done using the manual baseline correction function of Mestre-C.

The ^{13}C chemical shifts are reported relative to tetramethylsilane (= 0 ppm) using adamantane as an external reference. The relative intensities of the regions were determined using the integration routine of the MestRe-C software. The ^{15}N chemical shifts are reported relative to ammonium nitrate ($\text{NH}_4^+ = 0$ ppm).

5.2.6 Data analyses

Analysis of variance (ANOVA) was performed in the two series of experiments, main controlling factors pH, MnO_2 and SOM content, or pH, MnO_2 and SOM quality, respectively. and their interactive effects was performed, followed by a Tukey honest significant difference (HSD) test. The effects of pH, MnO_2 and OM on $R_{\text{NH}_2\text{OH-to-N}_2\text{O}}$ were quantified by multiple regression model analysis. All analyses were performed with the R software package (version 3.1.0, R Development Core Team, 2013) (R Development Core Team, 2013).

5.3 Results and discussion

5.3.1 $R_{\text{NH}_2\text{OH-to-N}_2\text{O}}$ at different pH, MnO_2 and OM contents (%)

In the present study all three factors, i.e. pH, MnO_2 and OM content, affected $R_{\text{NH}_2\text{OH-to-N}_2\text{O}}$ from peat moss significantly (Fig. 5.2, S5.1 and S5.2). The $R_{\text{NH}_2\text{OH-to-N}_2\text{O}}$ increased greatly with an increase in MnO_2 content from 0% to 0.1% (Fig. 5.2). This finding is consistent with Bremner *et al.* (1980) who studied 19 soils with a wide range of properties and found that the

formation of N₂O by decomposition of NH₂OH was highly correlated with oxidized Mn content of the soils. The fact that NH₂OH was used in the past for the selective extraction of Mn oxides from soil samples (Chao, 1972) indicates that NH₂OH can efficiently reduce Mn(IV) to Mn(II) or Mn(III) (and in turn is oxidized to N₂O) in natural soil samples. With increasing OM content, R_{NH₂OH-to-N₂O} decreased remarkably, especially at high pH (Fig. 5.2). For example, an increase in OM by only 1% at 0.01% MnO₂ led to about 50% and 80% decrease in N₂O emissions at pH 3 and pH 7, respectively (Fig. 5.2, S5.2). This could be caused by the oxime-forming reaction between NH₂OH and carbonyl groups of OM, such as in quinones. The oximes may undergo a tautomeric equilibrium with their corresponding nitrosophenol forms (Thorn *et al.*, 1992). In fact, NH₂OH has been used in a number of previous studies to determine the carbonyl content of humic substances (Gierer & Söderberg, 1959), indicating a high affinity of NH₂OH to OM that contains carbonyl groups. In the absence of OM and MnO₂, increasing pH led to a slight increase in R_{NH₂OH-to-N₂O} due to the self-decomposition of NH₂OH at high pH, whereas in the presence of OM and absence of MnO₂ nearly no NH₂OH was converted to N₂O (Fig. 5.2, S5.2). In contrast, the effect of increasing pH on R_{NH₂OH-to-N₂O} became negative already in the presence of 0.01% MnO₂ (Fig. 5.2, S5.2). This finding suggests that acidic conditions are favorable for the redox reaction between NH₂OH and MnO₂.

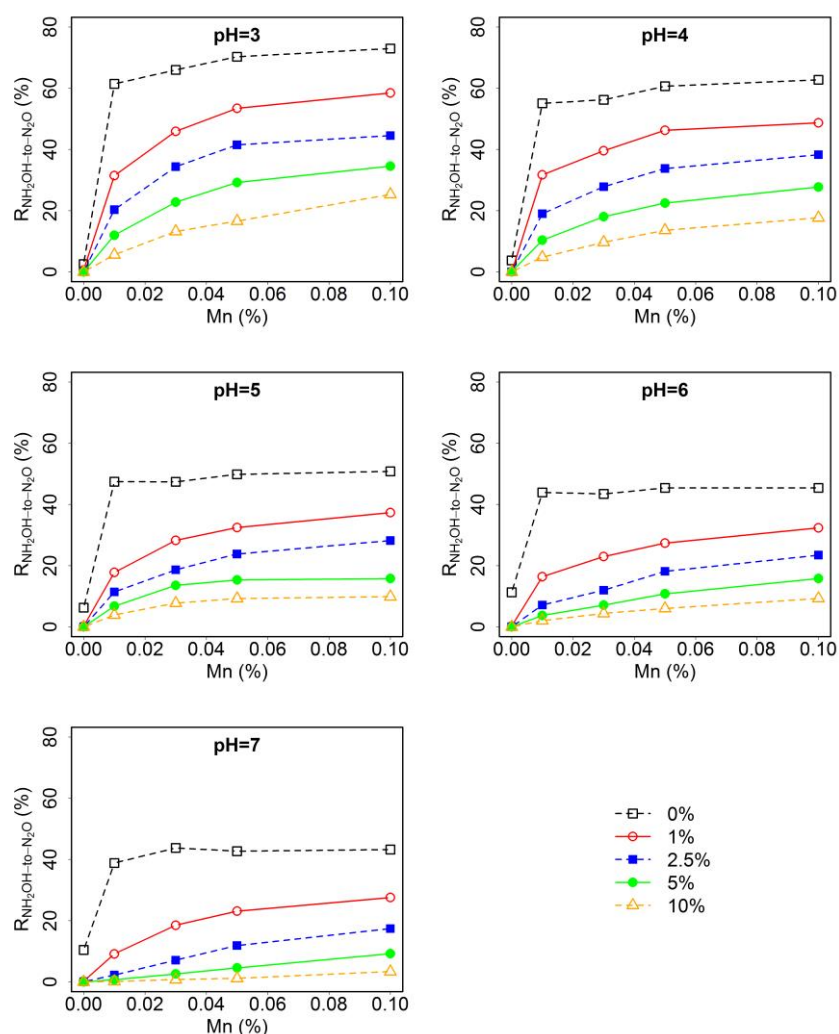


Figure 5.2 NH_2OH -to- N_2O conversion ratios ($R_{\text{NH}_2\text{OH-to-N}_2\text{O}}$) in artificial soil mixtures at different pH as well as MnO_2 and organic matter (OM, peat moss) contents. The total amount of NH_2OH added was 5 nmol. Different symbols represent $R_{\text{NH}_2\text{OH-to-N}_2\text{O}}$ at different OM content.

The interactive effects of pH and MnO_2 , pH and OM, and OM and MnO_2 were significant ($P < 0.01$). The largest $R_{\text{NH}_2\text{OH-to-N}_2\text{O}}$ found in the present experiment was 81.5% in the absence of SOM at pH 3, and with a MnO_2 content of 0.1%, while the lowest $R_{\text{NH}_2\text{OH-to-N}_2\text{O}}$ was about 9%, when SOM content was 10% in the presence of 0.1% MnO_2 at pH 7. This suggests that even at the highest MnO_2 level and otherwise optimal conditions a small fraction of NH_2OH had not been converted to N_2O , but to some other unidentified product.

In the treatments without OM, MnO_2 had only a small effect on $R_{\text{NH}_2\text{OH-to-N}_2\text{O}}$ at all pH conditions, while it had a larger effect especially at higher OM content (Fig. 5.2, S5.1), suggesting a strong competition between OM and MnO_2 for NH_2OH . The competition was

biased by pH, with lower pH favouring the reaction of NH₂OH and MnO₂, while higher pH favoured the reaction of NH₂OH with OM. These findings confirmed our hypothesis that at low pH NH₂OH is more protected against reaction with OM and more available for the oxidation by MnO₂ due to the higher degree of NH₂OH protonation at lower pH.

5.3.2 R_{NH₂OH-to-N₂O} at different pH, MnO₂ content, and OM quality

Organic matter quality had a clear influence on R_{NH₂OH-to-N₂O} in this study (Fig. 5.3, S5.3, and S5.4). Most of the OM types were associated with a significantly lower R_{NH₂OH-to-N₂O} compared to the mixtures without OM within the pH range of the experiment. In general, the inhibitory effect of the organic materials on the conversion of NH₂OH to N₂O conversion showed a clear pH dependency, but not a C/N ratio dependency as we assumed (Fig. 5.3, S5.3). At acid conditions (pH 3-4), peat moss and watermilfoil which own the relatively larger C/N ratio, inhibited the R_{NH₂OH-to-N₂O} least, while cyanobacterium and clover inhibited the R_{NH₂OH-to-N₂O} although they have relatively smaller C/N ratio. The differences between peat moss, cyanobacterium and watermilfoil material as OM became smaller at higher pH, and were no longer significant at pH 7 in the presence of 0.01% MnO₂ (Fig. S5.4), while clover showed always the smallest R_{NH₂OH-to-N₂O} for all the pH levels. In the absence of MnO₂, all OM forms showed a R_{NH₂OH-to-N₂O} close to zero, except for the watermilfoil material that was associated with a R_{NH₂OH-to-N₂O} significantly above zero at the pH range 3-6 (Fig. 5.3, S5.3, S5.4). A possible explanation could be the fact that, in contrast to the other OM sources, the watermilfoil material contained about 0.03% Mn (Table 5.1), which could have caused the N₂O emission after NH₂OH addition even without external MnO₂ addition.

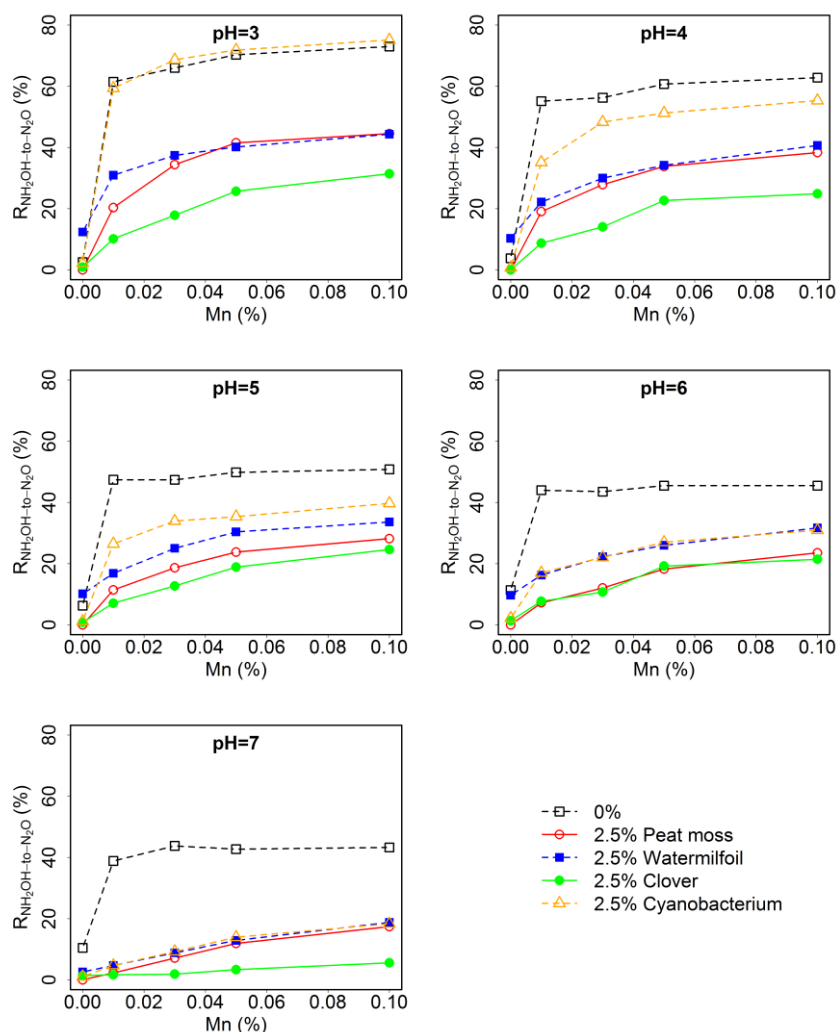


Figure 5.3 NH_2OH -to- N_2O conversion ratios ($R_{\text{NH}_2\text{OH-to-N}_2\text{O}}$) in artificial soils at different pH and MnO_2 content, and for organic matter of different origins at a fixed content of 2.5% (w/w). The total amount of NH_2OH added was 5 nmol. Different symbols represent $R_{\text{NH}_2\text{OH-to-N}_2\text{O}}$ for the artificial soil mixtures with the different organic materials.

We assumed that $R_{\text{NH}_2\text{OH-to-N}_2\text{O}}$ would be a function of the C/N ratio of the different SOM types, as larger C/N ratios would be indicative of a lower degree of N-containing functional groups, i.e. leaving a higher chance for NH_2OH to react with SOM and not to be converted to N_2O . However, we did not observe any clear relationship between C/N ratio and $R_{\text{NH}_2\text{OH-to-N}_2\text{O}}$, e.g. peat moss had the largest C/N ratio, but did not lead to the lowest $R_{\text{NH}_2\text{OH-to-N}_2\text{O}}$. Instead, clover with a much lower C/N ratio had the largest inhibitory effect on $R_{\text{NH}_2\text{OH-to-N}_2\text{O}}$. The addition of 2.5% dry clover powder (C/N ratio = 11.3) to the artificial soil mixture decreased $R_{\text{NH}_2\text{OH-to-N}_2\text{O}}$ by 48% at pH 3 (Fig. 5.3), which was similar to the effect of 10% peat moss

(C/N ratio = 67.2) at the same pH (Fig. 5.2). The reason for this observation could lie in the differences in functional groups between the different organic materials used in this study.

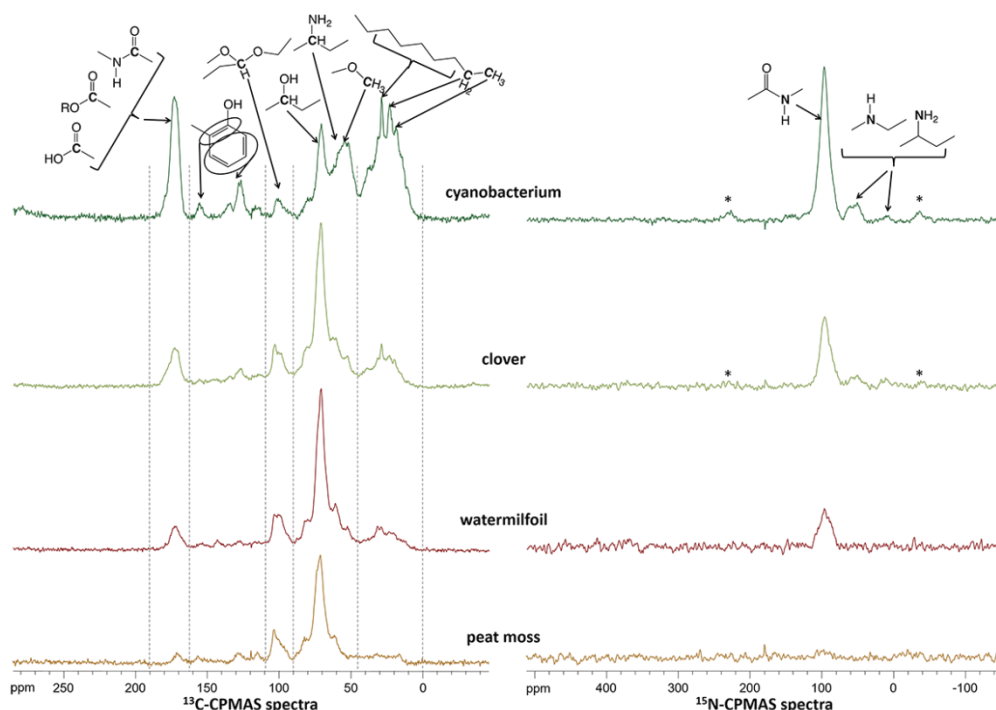


Figure 5.4 The ¹³C- and ¹⁵N-CPMAS-NMR spectra of the different organic materials (cyanobacterium, clover, watermilfoil, peat moss) used in the experiment.

A better insight into the effects of C and N functional groups of the different organic materials was obtained from NMR analysis. The peat moss OM had the lowest proportion of ester or amide carbonyl at around 170 ppm of all materials (Fig. 5.4, Table 5.2). This is in accordance with the observation that – despite having the largest C/N ratio – peat moss OM had a lower inhibitory effect on $R_{\text{NH}_2\text{OH-to-N}_2\text{O}}$ compared to clover and watermilfoil OM (if the background MnO₂ effect was subtracted), i.e. the lack of almost any carbonyl groups in peat moss was clearly visible in its chemical behaviour toward NH₂OH. In addition, peat moss OM exhibited the largest proportion of O-substituted aliphatic compounds, which might have also contributed to the relatively low inhibitory effect on $R_{\text{NH}_2\text{OH-to-N}_2\text{O}}$ in comparison to clover and watermilfoil OM. In contrast, cyanobacterium OM had the highest proportion of acid/amide carbonyl of all four organic materials, suggesting the highest inhibitory effect on $R_{\text{NH}_2\text{OH-to-N}_2\text{O}}$ due to the competitive reaction of carbonyl groups with NH₂OH. The clover material, however, contained lower amounts of O-substituted aliphatics and di-O-substituted C in comparison to peat moss and watermilfoil OM, which may have increased its affinity for

NH₂OH. For the proportion of unsaturated C no clear trend emerged across the different materials, suggesting that the effect of unsaturated C on $R_{\text{NH}_2\text{OH-to-N}_2\text{O}}$ is of minor importance.

Table 5.2 The chemical structures and their relative proportions derived from ¹³C CPMAS NMR spectra of the different plant materials.

Spectral range (ppm)	Chemical structures	Found in	Cyanobacterium (%)	Clover (%)	Watermilfoil (%)	Peat moss (%)
45 – 0	Aliphatic compounds	waxes, suberin, cutin, cyanophycin, chlorophyll (a,b,d)	40.5	17.1	14.8	11.0
64.5 – 45	N- and O-substituted aliphats	amino acids, amino sugars, lignin, cyanophycin	19.4	13.7	13.8	11.6
90 – 64.5	O-substituted aliphats	polysaccharides, cellulose, hemi-cellulose, starch, pectin, lignin	14.2	37.8	42.1	49.1
109 – 90	di-O-substituted C	polysaccharides, cellulose, hemi-cellulose, starch, pectin	2.5	10.5	12.0	13.5
162 – 109	unsaturated C, aromatic C	suberin, lignin, chlorophyll	6.9	11.1	10.0	11.4
190 – 162	acid, ester, amid	cutin, proteins, cyanophycin, chlorophyll	16.6	9.8	7.4	3.5

5.3.3 Development of a stepwise multiple regression model from the artificial soil mixtures and application to natural soils

A stepwise multiple regression model for $R_{\text{NH}_2\text{OH-to-N}_2\text{O}}$ was developed on the basis of the co-variables pH, MnO₂ and SOM using the data in Fig. 5.2 ($R_{\text{NH}_2\text{OH-to-N}_2\text{O}} = 45.9 - 3.1 \text{ SOM} + 241.1 \text{ MnO}_2 - 4.5 \text{ pH}$, $R^2 = 0.62$, $P < 0.01$). This model obtained from the peat moss experiments could explain about 62% variation of $R_{\text{NH}_2\text{OH-to-N}_2\text{O}}$, and the contributions of pH, Mn and SOM content to the model's performance were all significant ($P < 0.01$). It could well explain the observations (Fig. 5.3) for peat moss, watermilfoil and clover OM (R^2 around 0.80, $P < 0.01$, Fig. 5.5), which could be due to the fact that the cyanobacterium material had a high N content, a higher ratio of aliphatic C and a lower C/N ratio than the plant materials. This demonstrated the general applicability of the model for the OM derived from the different plant species, with different N content, aliphatic C and C/N ratio. In contrast, the model proved to be not appropriate for the artificial soil mixture without any MnO₂, indicated by the decreased goodness of the simulation.

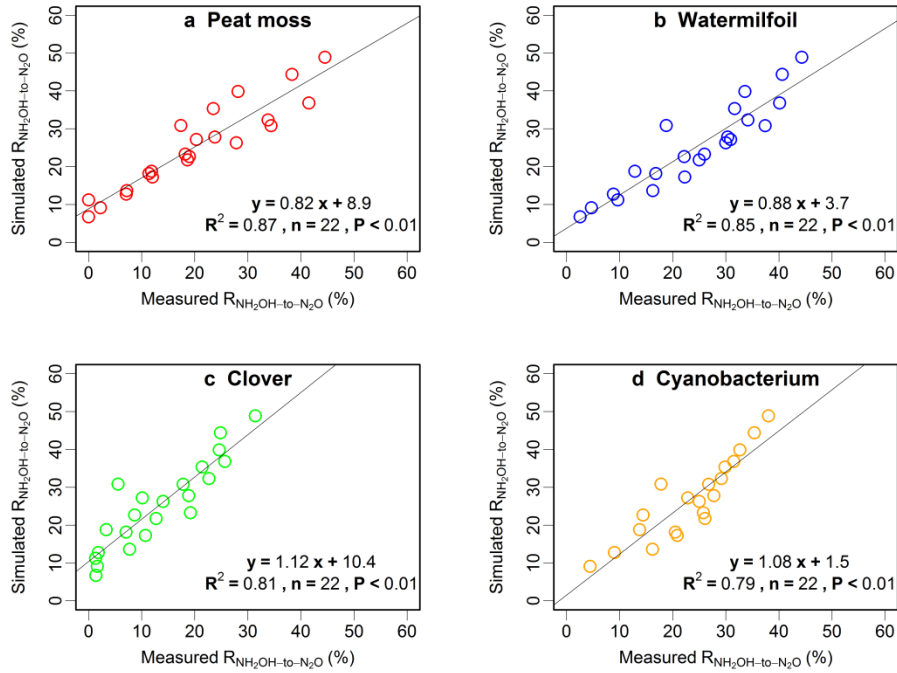


Figure 5.5 Results of the application of the artificial soil regression model for the $\text{NH}_2\text{OH-to-N}_2\text{O}$ conversion ratios ($R_{\text{NH}_2\text{OH-to-N}_2\text{O}}$) to artificial soil mixtures amended with the different organic materials ($n=22$). The three points for which $R_{\text{NH}_2\text{OH-to-N}_2\text{O}}$ was determined at pH 3, 4, and 5 without MnO_2 addition were excluded for a better simulation.

In addition, $R_{\text{NH}_2\text{OH-to-N}_2\text{O}}$ was simulated with the same regression model for the natural soils described in Heil *et al.* (2015). The results showed that the application of the model to natural soils was promising, no matter if it was applied to fumigated or fresh soils (Fig. 5.6). The simulated $R_{\text{NH}_2\text{OH-to-N}_2\text{O}}$ explained more than 90% of the observed rates, especially for cropland, grassland, and deciduous forest soils. However, the model failed at correctly predicting $R_{\text{NH}_2\text{OH-to-N}_2\text{O}}$ for the spruce forest soil of Heil *et al.* (2015), which could be related to the high SOM and relatively low MnO_2 content of the spruce soil as compared to the other soils. This finding suggests that there is a threshold value for the SOM content of 10% above which – and a MnO_2 content of 0.01% below which – the model fails to predict the correct $R_{\text{NH}_2\text{OH-to-N}_2\text{O}}$ values.

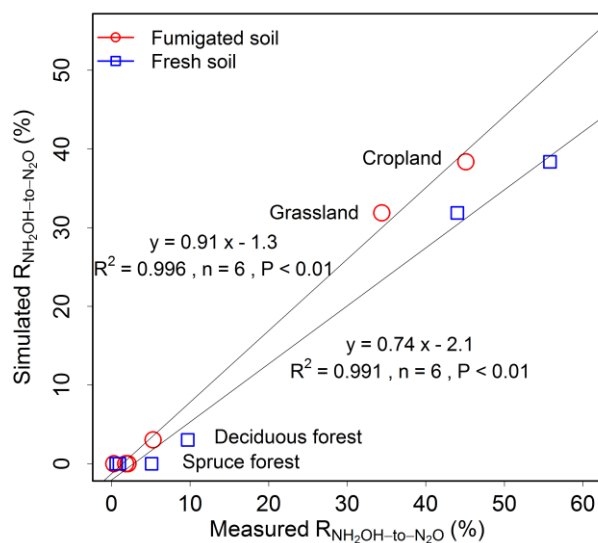


Figure 5.6 Application of the artificial soil regression model for the calculation of NH_2OH -to- N_2O conversion ratios to six natural fresh and fumigated soils as reported in Heil *et al.* (2015).

Soil pH, MnO_2 , and SOM content were identified as crucial control variables of $R_{\text{NH}_2\text{OH-to-N}_2\text{O}}$, i.e. the conversion ratio of NH_2OH to N_2O in the artificial soil experiments of this study. Organic matter derived from different plant species and a cyanobacterium also affected $R_{\text{NH}_2\text{OH-to-N}_2\text{O}}$ due to the differences in composition, type, and abundance of functional groups, as more carbonyl C leads to higher reactivity of NH_2OH with organic matter, thereby lowering its availability for the oxidation to N_2O by MnO_2 . The multiple regression model of pH, MnO_2 and OM developed here could explain about 60% of the variance of $R_{\text{NH}_2\text{OH-to-N}_2\text{O}}$ in the artificial soil mixtures, and proved also to be promising for the prediction of $R_{\text{NH}_2\text{OH-to-N}_2\text{O}}$ of chemical N_2O production from NH_2OH in natural soils, when SOM content was below 10% and Mn content was larger than 0.01%. If these findings can be confirmed for other soils from different ecosystems, this improved understanding of the controls of N_2O formation from the reactive nitrification intermediate NH_2OH in soils can have large implications for developing appropriate management options, such as adding organic amendments with suitable chemical characteristics, for mitigating N_2O emissions from agricultural land, the largest anthropogenic source of N_2O to the atmosphere.

Chapter 6

Effect of nitrite and hydroxylamine on N₂O production depends on the soil type and preceding redox condition

Based on:

Liu S., Schloter M., Hu R., Vereecken H. and Brüggemann N. Effect of nitrite and hydroxylamine on N₂O production depends on the soil type and preceding redox condition. Submitted to *Geoderma*.

6.1 Introduction

The mechanisms of soil N₂O formation have been studied extensively in recent years due to the large impact of N₂O on global warming and ozone depletion (Bremner, 1997; Baggs, 2011; Schreiber *et al.*, 2012; Butterbach-Bahl *et al.*, 2013). Soil biological processes, such as nitrification and denitrification, and abiotic processes involving the reactive intermediates of nitrification, i.e. NH₂OH and NO₂⁻, and of denitrification, i.e. NO₂⁻, such as the reactions between NO₂⁻ and organic matter (van Cleemput & Samater, 1995; van Cleemput, 1998) and between NH₂OH and MnO₂ (Bremner, 1997), contribute to soil N₂O formation. Different terrestrial ecosystem types (e.g., grassland, cropland, and forest), various environmental factors (e.g., temperature, water content, and O₂ availability) and soil constituents (e.g., quality and quantity of organic carbon and pH) have strong effects on soil N₂O formation.

Nitrite and NH₂OH are important nitrification intermediates responsible for soil N₂O production. Both are very reactive with relatively high self-decomposition rates dependent on pH and soil composition. In oxic soils without any artificial (e.g., fertilizer) or natural (e.g., drought) interference, NO₂⁻ is rarely accumulated due to the faster oxidation of NO₂⁻ to NO₃⁻ than oxidation of NH₃ to NO₂⁻ during nitrification (Robertson & Groffman, 2007). However, high NO₂⁻ concentrations can be found after fertilizer application and drought (Gelfand & Yakir, 2008; Ma *et al.*, 2015). The other reactive nitrification intermediate, NH₂OH, is even more reactive and unstable in its natural environment. At neutral or slightly alkaline pH, about 30% of NH₂OH degrade within 3 h at room temperature in seawater samples at micromolar concentrations (Butler & Gordon, 1986). Nevertheless, NH₂OH has been detected in cultures of heterotrophic nitrifiers and ammonia oxidizers (Daum *et al.*, 1998; Liu *et al.*, 2017b) and acid forest soils (Liu *et al.*, 2014).

The two reactive N intermediates can produce N₂O both biologically and chemically during nitrification. NO₂⁻ can be reduced biologically to N₂O either by NO₂⁻ reductase through a pathway called “nitrifier denitrification” (Wrage *et al.*, 2001), as well as biologically or chemically by Fe²⁺ with the help of iron oxidizers and other microorganisms (Kampschreur *et al.*, 2011). Moreover, soil organic matter fractions, e.g. fulvic acids, lignin-building units and phenolic compounds can also react chemically with NO₂⁻ to form N₂O (Stevenson & Swaby, 1964). From NH₂OH, N₂O can be formed both biologically by the enzyme NH₂OH oxidoreductase (Ritchie & Nicholas, 1972) and chemically by O₂ and several soil oxidants (e.g., MnO₂ and Fe³⁺) (Bremner, 1997; Heil *et al.*, 2016). The role of abiotic N₂O formation

from NH₂OH in different soils has been demonstrated previously (Heil *et al.*, 2015), while the contribution of NO₂⁻ to the abiotic N₂O formation in the same soils remains unclear.

Different soil types and environmental conditions may have a strong impact on biotic and abiotic N₂O formation from NO₂⁻ and NH₂OH in soil. For example, quality and quantity of SOM, especially the reactive part of SOM, i.e. dissolved organic matter (DOM), may have strong effects on N₂O formation from NH₂OH and NO₂⁻. Soils rich in DOM, especially in phenolic lignin derivatives, may favor N₂O formation from NO₂⁻ (Stevenson & Swaby, 1964; Wrage *et al.*, 2001), but may decrease N₂O formation from NH₂OH, as NH₂OH binds readily to carbonyl groups of organic matter to form oximes (Thorn *et al.*, 1992). Moreover, the content and oxidation state of transition metals may also affect the formation of N₂O from NO₂⁻ and NH₂OH. In soil samples with high Fe and Mn content, the oxidized form will promote the conversion of NH₂OH to N₂O, whereas under reduced conditions the formation of N₂O from NO₂⁻ will be favored (Heil *et al.*, 2016). In addition to the transition metal redox state, it has been demonstrated that anoxic condition could change the composition of the microbial community (Pett-Ridge *et al.*, 2006), availability of mineral N substrates (mainly NO₃⁻, NH₄⁺ and NO₂⁻) (Achnich *et al.*, 1995), and quality of SOM (Achnich *et al.*, 1995; Dassonville & Renault, 2002).

The aim of this study was to: (1) compare the importance of NO₂⁻ and NH₂OH for N₂O formation in different soils; (2) explore the effect of preceding soil redox condition on the N₂O production from NO₂⁻ and NH₂OH addition; and (3) assess the contribution of the abiotic pathways to the formation of N₂O from NO₂⁻ and NH₂OH. For this purpose, different soil samples from forest, grassland and cropland with large ranges of C and Mn contents and pH were collected, and oxic or anoxic pre-incubations were carried out. The effect of sterilization with γ -irradiation was scrutinized to quantify the relevance of abiotic processes. We hypothesized that (1) NH₂OH plays a more important role in soil N₂O production in soils with higher Mn and lower SOM content, whereas NO₂⁻ contributes more to N₂O formation in soils with higher SOM and Fe content; (2) anoxic pre-incubation increases the contribution of NO₂⁻ to soil N₂O formation, but decreases the contribution of NH₂OH to soil N₂O formation; (3) the contribution of NH₂OH to N₂O formation is mainly from abiotic processes, while there is a mixed contribution of biotic and abiotic processes to N₂O formation from NO₂⁻.

6.2 Materials and methods

6.2.1 Soil collection

Soil material was collected from the three field sites of the TERENO (www.tereno.net) from the Eifel/Lower Rhine Valley, Germany, i.e. coniferous forest (Wüstebach; 50°30'10" N, 6°19'50" E), extensive grassland (Rollesbroich; 50°37'18" N, 6°18'15" E) and cropland (Selhausen; 50°52'10" N, 6°27'4" E). The coniferous forest site is situated in the low mountain ranges of the Eifel National Park, with a sub-catchment of the river Rur basin flowing through it. The site was dominated by Norway spruce (*Picea abies* (L.) H. Karst). The hillslopes are characterized by Cambisol and Planosols, whereas the riparian zone is dominated by Gleysol and Histosol. The main soil texture at this site is silty clay loam. The mean annual precipitation of the coniferous forest is about 1400 mm. The height above sea level (a.s.l.) of the forest site is 630 m and the mean annual temperature is around 7 °C. The grassland site is located in the Northern Eifel region with smooth meadow grassland. Dominant soils at this site are (gleyic) Cambisol, Stagnosol, and Cambisol-Stagnosol with a silt loam texture. Mean annual temperature and precipitation at the grassland site are 7.7 °C and 1033 mm, respectively. The agricultural site is dominated also by (gleyic) Cambisol and (gleyic) Luvisol with a silt loam texture, and regularly cultivated with sugar beet, wheat, and oilseed rape, depending on the year. Mean annual temperature and precipitation at the cropland site are 9.8 °C and 690 mm, respectively.

Due to the strong spatial heterogeneity in soil basic properties of the forest site of this study (Liu *et al.*, 2016), fresh soils (~ 3 kg) were sampled in January 2016 from the humus-rich layer (Oa horizon, depth 3–5 cm) of five sampling points (F1, F2, F3, F4 and F5) of the forest upland area, and one sample from the forest riparian zone (FR) in the area of approximately 27 ha of the forested Wüstebach catchment. For the grassland (G) and cropland (C) sites, five soil samples (~ 1.5 kg each) in one hectare were collected from the soil top 15 cm layers of the two sites, respectively in January 2016. As the spatial variability of the grassland and cropland sites was smaller compared to the forest site, the fresh soil samples were mixed directly in a large plastic bag after soil sampling in both the grassland and cropland sites, and were transferred to the laboratory with the forest soil samples at the same day. In the laboratory, fresh samples (except for the FR sample) were passed through a 2-mm sieve, and coarse plant residues (including roots) and stones were manually removed. After that, soil

samples were put into open plastic bags and stored in a refrigerator (4 °C) until the beginning of the experiment.

6.2.2 Oxic and anoxic pre-treatment of soil

For the anoxic pre-treatment, about 600 g fresh soil from each sampling site was put into a 1-litre glass bottles and sealed with a rubber plug within a plastic lid. The water content (*w/w*) of the fresh soils was around 59–108%, 22% and 10% for the forest, grassland and cropland, respectively. The bottles were then evacuated and refilled with He to 0.4 bar overpressure. This procedure was repeated three times. Then the bottles were incubated with He as headspace gas at ambient pressure at room temperature for one week. For the oxic pre-treatment, another about 600 g fresh soil was put in large open plastic bags and kept under oxic conditions at room temperature for one week. All plastic bags were stored in a large plastic box to reduce air flow and further reduce soil water evaporation. All soil samples were freeze-dried immediately after the oxic/anoxic pre-incubations to preserve the chemical status of the soil samples until further treatment. One side effect of freeze-drying could have been that this process led to a disruption of soil aggregates, which would have made more of the substrates soluble when the solution was added, and would have led to an overestimation of the N₂O production from NO₂⁻ (via both biotic and abiotic pathways), but an underestimation of the N₂O production from NH₂OH (via abiotic pathways). All plastic bags were stored in a large plastic box to reduce air flow and further reduce soil water evaporation. After the oxic/anoxic pre-incubations, soil samples were freeze-dried for about one week and stored at room temperature. After freeze-drying, half of the soil samples were transferred to 50-ml falcon tubes and sterilized with γ -irradiation (Best Theratronics, Canada) for 14 hours (total dose: 11 kGy). The success of the sterilization process was checked by plating soil slurries after the sterilization on R2A medium and incubated for 24 h at 25 °C. No growth of bacteria or fungi was observed (data not shown).

6.2.3 Addition of reactive N to freeze-dried soils

About 1.4 g of freeze-dried soil with or without γ -irradiation were weighed into 22-ml GC vials (VWR International, Darmstadt, Germany), followed by the addition of H₂O, NO₂⁻, NH₂OH and NH₂OH + MnO₂ (Merck, Darmstadt, Germany) to reach around 40% WHC to resemble nitrification conditions. The MnO₂ was added to the soil to explore the effect of MnO₂ on abiotic NH₂OH-to-N₂O production in soil with either oxic or anoxic pre-treatment.

The concentration of the added N solutions was adjusted accordingly, so that 1 mg N kg⁻¹ dry soil was added to each bottle. The added N amount corresponded to NO₂⁻ content in soil with fertilizer application (Shen *et al.*, 2003; Venterea *et al.*, 2003), and was assumed also reasonable for NH₂OH in soils with fertilizer application as concentration level of 0.3–34.8 µg N kg⁻¹ dry soil had been observed in natural forest soils (Liu *et al.*, 2014). The added Mn amount amounted to 0.1% (w/w) of soil dry weight, while the natural Mn content of the soil samples of this study ranged between 0.015–0.194% (w/w) (Table 6.1). The vials were closed gas-tight immediately after addition of the solution with butyl septa and aluminum crimp caps (VWR International) and incubated at room temperature for 1 and 7 h. Each treatment was carried out in triplicate.

Table 6.1 Basic properties of the soils used in this study. For the determination of total C, N, Fe and Mn content, soils with oxic pre-incubation were used. Values are presented as mean of three replicates. The coefficient of variation of all data was smaller than 10% and is therefore not shown. For the determination of pH, DOC, DTN, A₂₅₄, NH₄⁺ and NO₃⁻, soils with both oxic and anoxic pre-incubation were used, and only one extraction was carried out.

	C (%)	N (%)	C/N	Fe (%)	Mn (%)	pH		DOC (mg kg ⁻¹ dry soil)		DTN (mg kg ⁻¹ dry soil)		A ₂₅₄ (cm ⁻¹ g ⁻¹ dry soil)		NH ₄ ⁺ (mg kg ⁻¹ dry soil)		NO ₃ ⁻ (mg kg ⁻¹ dry soil)	
						oxic	anoxic	oxic	anoxic	oxic	anoxic	oxic	anoxic	oxic	anoxic	oxic	anoxic
F1	27.4	1.4	19.3	1.62	0.015	2.88	2.92	2865	3650	155	207	1.42	2.00	7.6	24.5	7.2	n.d.
F2	26.8	1.5	18.0	2.02	0.027	3.13	3.12	2215	3090	145	168	1.24	1.61	13.2	30.4	13.4	n.d.
F3	21.0	1.1	20.0	2.44	0.026	3.26	3.23	3175	3720	253	220	1.16	1.68	19.8	35.7	32.4	n.d.
F4	25.7	1.3	19.2	1.92	0.018	2.99	3.05	2390	3350	126	158	1.24	1.64	2.4	19.6	6.4	n.d.
F5	23.7	1.1	21.2	2.81	0.194	3.67	3.71	1510	1590	135	121	0.61	0.80	6.3	38.9	17.3	1.6
FR	9.7	0.5	18.1	1.57	0.024	4.14	4.13	–	930	–	86	–	0.52	3.8	n.d.	n.d.	n.d.
G	5.3	0.5	9.9	2.39	0.097	5.45	5.82	720	1023	133	126	0.41	0.62	16.0	97.5	19.5	n.d.
C	1.3	0.1	9.2	2.10	0.074	5.87	6.19	226	236	24	19	0.29	0.37	2.2	4.5	3.1	n.d.

n.d.: not detectable; –: value is missing due to shortage of material.

6.2.4 N₂O analysis

The gas in the headspace of the sample vials was analyzed for N₂O using a gas chromatograph (Clarus 580, PerkinElmer, Rodgau, Germany) equipped with an ECD and flame ionization detector (FID) for N₂O and CO₂ detection, respectively, as described in Liu *et al.* (2014). The instrument was calibrated each day using five different standard gasses with 0.25, 0.50, 0.75, 1.00 and 5.00 ppm N₂O, balanced with N₂ (99.999% purity, Linde, Munich, Germany).

6.2.5 Soil chemical analyses

Total C and N contents were determined with an elemental analyzer (vario EL Cube, Elementar Analysensysteme GmbH, Hanau, Germany). The elemental composition of the organic materials was analyzed by using ICP-OES. Briefly, 100 mg of sample material were

mixed with 3 mL HNO₃ and 2 ml H₂O₂, heated in the microwave at 800 W for 30 min. The mixtures were subsequently filled up to 14 ml and diluted 10-fold with deionized water followed by the ICP-OES measurement.

Additionally, mineral N and the quality and quantity of soil DOM were analyzed to determine the effects of anoxic pre-treatment on the DOM dynamics. The mineral N (NH₄⁺ and NO₃⁻) contents were analyzed with ion chromatography (IC, Dionex ICS-3000 for NO₂⁻ and NO₃⁻, Dionex DX-500 for NH₄⁺). NH₄⁺ and NO₃⁻ were extracted with 1 M KCl (dry soil: solution = 1:10 w/w) and shaken for 24 h. DOC and dissolved total nitrogen (DTN) were extracted with deionized water (dry soil: water = 1:2.5 for grassland and cropland soils, and 1:5 for forest and riparian soils) by shaking for 1 h at 200 rpm. DOC and DTN were then analyzed with a TOC-TN analyzer (Shimadzu Corp., Kyoto, Japan). In addition, for characterization of the aromatic substances the absorbance of the DOC extract at 254 nm (A₂₅₄) was determined with UV-VIS spectrometry (DU 800, Beckman Coulter, Inc., United States) and a path length of 1 cm.

6.2.6 Data analyses

The effects of NO₂⁻ and NH₂OH on N₂O emission were calculated by subtracting N₂O emission after water addition only (as control) from the N₂O emission in response to NO₂⁻ and NH₂OH addition. N₂O emission was calculated according to Equation 8 in Liu *et al.* (2014). Spearman's correlation analysis was performed with Origin 7.0. Student's t-test was used to identify significant ($P < 0.05$) differences in N₂O production between oxic or anoxic pre-treatment, with or without γ -irradiation and different soil samples.

6.3 Results

6.3.1 Effect of reactive N addition on N₂O production in different soils

Nitrite addition to the freeze-dried soil samples after oxic pre-treatment was associated with large N₂O production in the grassland soil, whereas it was only minor in the other soil samples (Fig. 6.1A). In the grassland soil with oxic pre-treatment, 80% of the NO₂⁻ had been converted to soil N₂O within 7 h, assuming that all the N₂O came from the added NO₂⁻. For the forest soils, the N₂O formation after NO₂⁻ addition amounted to about 30 $\mu\text{g N kg}^{-1}$ dry soil after 1 h, which was 25% of the grassland soil N₂O production within 1 h, but did not

increase significantly after 7 h, except for the soil from sampling point F2. Although the N_2O production from the riparian (FR) and cropland (C) soils increased with incubation time after NO_2^- addition, it was the smallest among the different soil samples.

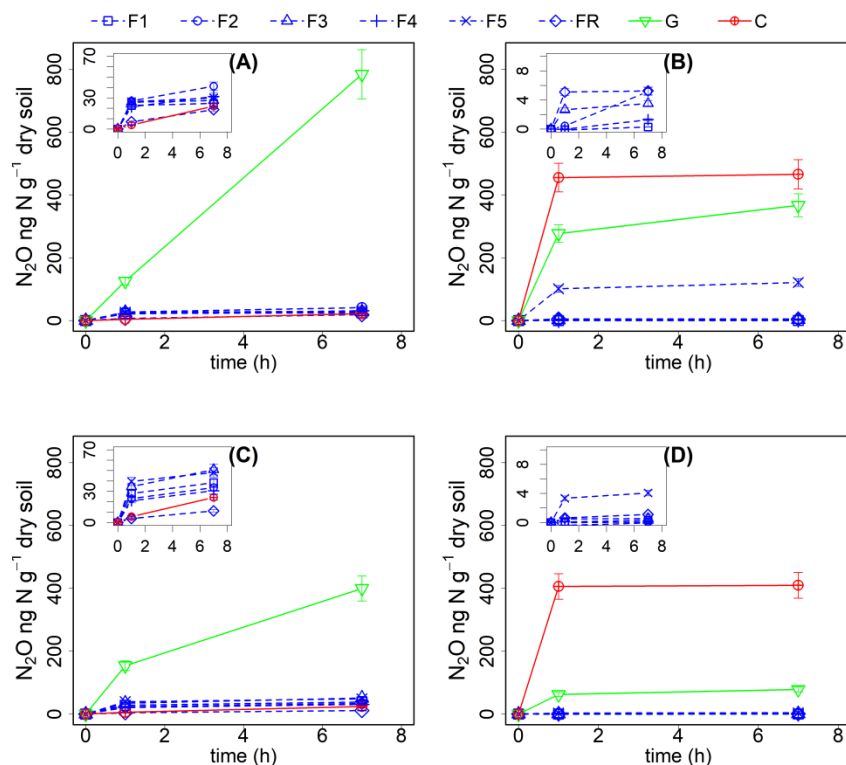


Figure 6.1 Net N_2O (ng N g^{-1} dry soil) production in forest (F1, F2, F3, F4, F5 and FR), grassland (G) and cropland (C) soils after NO_2^- (A: oxic, C: anoxic pre-incubation) and NH_2OH (B: oxic, D: anoxic pre-incubation) addition. Net N_2O production was calculated by subtracting N_2O emission after addition of pure water (as control) from the N_2O emission after addition of NO_2^- or NH_2OH solution. The values are presented as mean \pm standard deviation (SD).

In contrast, NH_2OH addition induced the highest N_2O production in cropland soil, followed by the grassland soil and the forest soil from sampling point F5 in the soil samples with oxic pre-treatment. The conversion ratio from the added NH_2OH to N_2O was 47%, 37% and 12% for the cropland, grassland, and F5 forest soils within 7 h, respectively, assuming that all the N_2O came from the added NH_2OH . NH_2OH addition had only a minor effect on the other forest soil samples during the whole incubation period (Fig. 6.1B). Comparing to the effect of NO_2^- , NH_2OH had a larger effect on N_2O production in cropland and F5 forest soils. Moreover, N_2O was produced very quickly in the first 1 h after NH_2OH addition, accounting for about 95%, 75% and 85% of the N_2O emission after 7 h for the cropland, grassland, and F5 forest soils, respectively.

6.3.2 Effect of anoxic pre-incubation on N₂O production from reactive N addition

Anoxic pre-incubation increased soil NH₄⁺ concentration up to sevenfold, with the largest NH₄⁺ concentration (195 mg N kg⁻¹ dry soil) in the grassland soil (Table 6.1), and decreased NO₃⁻ concentration in most of the soil samples (except forest sample F5) to nearly zero. The quality (reflected in the A₂₅₄ value) and quantity of DOM (reflected in the concentrations of DOC and DTN) varied substantially after anoxic pre-incubation between the different soil samples, with 5-42% higher DOC content compared to soil samples with oxic pre-incubation. The A₂₅₄ value followed a trend very similar to DOC, indicating that more aromatic substances were available in dissolved form after anoxic pre-incubation. The difference in DTN between the different treatments was not as pronounced as for DOC and A₂₅₄. Moreover, the DTN content of soil samples F3 and F5 was even smaller after anoxic pre-incubation compared to samples with oxic pre-incubation

Anoxic pre-treatment of the soil samples had a large effect on soil N₂O emission after addition of reactive N. After anoxic pre-incubation, N₂O production in grassland soil after NO₂⁻ addition was about 25% higher after the first hour of incubation compared to the oxic pre-treatment, but was about 50% lower after 7 h (Fig. 6.1C). Forest soil samples F1, F3 and F5 showed larger N₂O emission after NO₂⁻ addition after anoxic pre-incubation compared to the oxic-pretreatment, while F2 and F4 showed no difference in response (Table 6.2). Anoxic pre-treatment stimulated N₂O emission the most from the soil of sampling point F3 after NO₂⁻ addition, followed by F5, whereas it decreased the effect of NO₂⁻ on N₂O production in the riparian soils.

Table 6.2 Effect of anoxic pre-treatment on soil N₂O emissions after 1 and 7 h of incubation of soils with NO₂⁻ and NH₂OH additions. Values indicate the relative increase (%) in N₂O emission in anoxic vs. oxic pre-treatment. Negative values indicate a decrease.

	F1	F2	F3	F4	F5	FR	G	C
NO₂⁻								
1 h	23.4	-14.8	34.1	-1.7	49.7	-44.1	22.8	49.0
7 h	55.5	-18.3	85.0	-2.2	61.3	-39.6	-49.0	9.8
NH₂OH								
1 h	-	-81.4	-	-96.7	-100.3	-87.5	-77.5	-10.7
7 h	-	-84.4	-104.5	-96.6	-98.6	-78.5	-78.6	-12.0

–: relative increase could not be calculated correctly due to negligible N₂O emission after NH₂OH addition.

In terms of NH₂OH, anoxic pre-treatment had a negative effect on the N₂O production after NH₂OH addition in all soil samples, especially in those with a large NH₂OH effect after oxic

pre-incubation, i.e. grassland and F5 forest soils, but had a relatively small effect on the N₂O production after NH₂OH addition in cropland soil (Table 6.2). Anoxic pre-incubation decreased N₂O production in cropland, grassland, and forest soil F5 by about 14%, 80% and 97%, respectively, 7 h after NH₂OH addition (Fig. 6.1D, Table 6.2).

6.3.3 Contribution of abiotic pathways to N₂O production from reactive N addition

Abiotic pathways contributed to 9.1-39.4% of soil N₂O production within 7 h after NO₂⁻ addition from the different soils after oxic pre-incubation, but contributed to 72.5-92.5% of soil N₂O production within 7 h after NH₂OH addition in the cropland, grassland and the F5 soil (Table 6.3). For the soil samples with anoxic pre-incubation, abiotic pathways contributed to 7.0-49.0% of NO₂⁻-induced N₂O production after 7 h, but contributed to 84.5-98.7% of N₂O production only after NH₂OH addition in the grassland, cropland and F5 soil in the same time period. In general, abiotic pathways played a more important role in the N₂O production after NH₂OH addition than that after NO₂⁻ addition in the tested soils.

Table 6.3 Contribution (%) of abiotic pathways to soil N₂O emissions after 7 h incubation of soils with addition of aqueous solutions of NH₂OH or NO₂⁻ to soil samples with oxic or anoxic pre-incubation and freeze-drying treatment. The data of F4 after γ -irradiation treatment is missing due to shortage of material.

		F1	F2	F3	F5	FR	G	C
Oxic	NO ₂ ⁻	9.1	18.9	17.4	16.5	30.2	27.7	39.4
	NH ₂ OH	–	–	85.3	84.2	89.1	72.5	92.5
Anoxic	NO ₂ ⁻	19.6	14.4	49.0	18.3	41.6	35.1	7.0
	NH ₂ OH	84.5	–	–	98.7	–	88.5	93.4

6.3.4 Controls of the effect of reactive N addition on N₂O production in soils after oxic and anoxic pre-incubation

Correlation analysis showed that soil Mn, C and DOC content, and pH were important factors responsible for soil N₂O formation from NH₂OH in the forest soil samples (Table 6.4). The NH₂OH-to-N₂O conversion ratio was positively and significantly correlated with soil Mn content and pH, but negatively and significantly correlated with soil C, N and DOC content, and A₂₅₄. Soil N₂O production after NO₂⁻ addition was found to be only marginally ($P = 0.06$) correlated with soil Fe content after anoxic pre-treatment. No significant correlation was

observed between the NO₂⁻-to-N₂O conversion ratio and any soil basic properties after oxic pre-treatment.

Table 6.4 Spearman's correlation coefficients between soil N₂O emissions and basic soil properties in forest soil samples after 7 h incubation. Asterisks indicate a significant correlation ($P < 0.05$).

	NO ₂ ⁻ addition		NH ₂ OH addition	
	Oxic	Anoxic	Oxic	Anoxic
Fe	0.40	0.69 ($P=0.06$)	0.43	0.43
Mn	0.36	0.38	0.83*	0.69 ($P=0.06$)
C	0.21	0.07	-0.83*	-0.83*
N	0.40	0.13	-0.74*	-0.83*
C/N	-0.07	0.33	-0.55	-0.36
pH	-0.16	-0.07	0.95*	0.90*
DOC	0.24	0.45	-0.86*	-0.71*
DTN	0.31	0.52	-0.52	-0.67
A₂₅₄	0.38	0.40	-0.79*	-0.74*

The addition of MnO₂ increased the NH₂OH-to-N₂O conversion ratio in all soil samples after oxic or anoxic pre-incubation (Fig. 6.2). However, the addition of MnO₂ increased the NH₂OH-to-N₂O conversion ratio more in the soil with oxic pre-incubation (especially during the first hour after NH₂OH addition) compared to the soil with anoxic pre-incubation. Only N₂O emission from soil F3 with anoxic pre-incubation was largely affected by the addition of MnO₂ (as high as 2.5 mg kg⁻¹ N after 7 h), which disappeared completely after γ -irradiation (data not shown). The NH₂OH-to-N₂O conversion ratio of the grassland soil, F5 and other forest soil samples after anoxic pre-incubation also increased after MnO₂ addition, but was still much lower than with NH₂OH addition only after oxic pre-incubation.

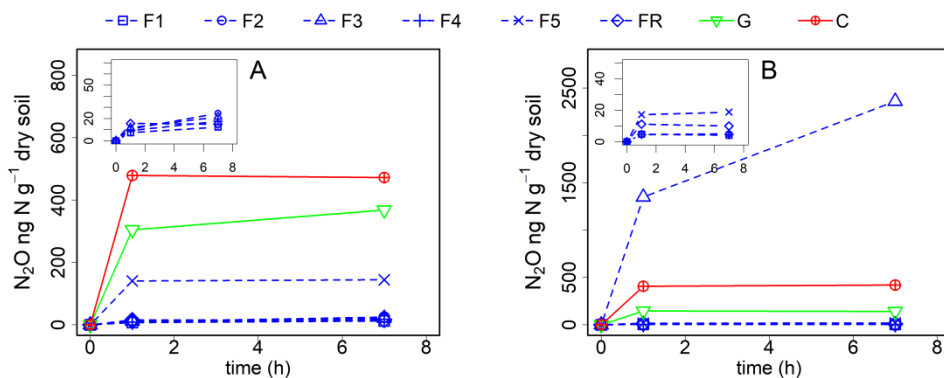


Figure 6.2 Soil N₂O production (ng N g⁻¹ dry soil) after MnO₂ and NH₂OH addition after oxic (A) and anoxic (B) pre-incubation for samples from forest (F1, F2, F3, F4, F5 and FR), grassland (G) and cropland (C).

6.4 Discussion

6.4.1 The importance of NO_2^- and NH_2OH on biotic and abiotic N_2O formation in different soils

Nitrite and NH_2OH are important intermediates of the inorganic N cycle in soil (van Cleemput & Samater, 1995; Bremner, 1997; Zhu-Barker *et al.*, 2015; Heil *et al.*, 2016). Nitrite is involved in soil N_2O production through biological denitrification and nitrifier denitrification, as well as chemodenitrification, while NH_2OH is related to N_2O formation via nitrification and chemical NH_2OH oxidation. Although previous papers reported the importance of NO_2^- and NH_2OH on soil N_2O emissions separately (Bremner *et al.*, 1980; van Cleemput & Samater, 1995; Venterea, 2007; Heil *et al.*, 2015), according to our knowledge no paper has tried to compare the contribution of the two reactive N compounds on soil N_2O emissions at the same time, with consideration of different soil types, biological and abiotic processes, and redox history, which may provide useful information for the exploration of soil N_2O formation mechanisms. Our results showed that the role of NO_2^- and NH_2OH in N_2O was strongly dependent on soil redox history and soil basic properties.

The by far largest amount of N_2O was produced in non- γ -irradiated grassland soil after NO_2^- addition, much higher than in all other soils (Fig. 6.1A and C). About 80% of the added NO_2^- was converted to N_2O in the grassland soil with oxic pre-incubation after 7 h of incubation, assuming that all the N_2O produced came from the added NO_2^- . However, no soil basic property was significantly correlated with N_2O production after NO_2^- addition (Table 6.4), which is not consistent with Venterea *et al.* (2007) who found N_2O production from NO_2^- to be correlated with pH, total nitrogen, and soluble and total C.

This large and quick N_2O pulse could easily lead to the assumption of abiotic pathways, e.g. chemodenitrification, being responsible for the N_2O production upon addition of NO_2^- . However, γ -irradiation decreased the N_2O production after NO_2^- addition to soil with oxic pre-incubation by 72.3%, indicating that biotic pathways played a more important role in N_2O production after NO_2^- addition. It was reported that nitrifier denitrification involving biological NO_2^- reduction can play an important role in soil N_2O emissions, especially in grassland and cropland soil with large nitrifier activity (Wrage *et al.*, 2001; Wrage *et al.*, 2004). Thus, the large pulse of N_2O production with NO_2^- addition in the grassland soil could be due to nitrifier denitrification. In contrast, the smaller effect of NO_2^- addition on N_2O

production in forest soils was at first unexpected, as there was more carbon available in the forest soils than in the grassland soil for biotic (denitrification) and abiotic (chemodenitrification) pathways leading to N₂O. One possible reason responsible for the smaller N₂O production in the forest soils could be that more NO instead of N₂O was produced as it mostly decomposes to NO and NO₂ at low pH (Davidson, 1992; Venterea *et al.*, 2005). This assumption is supported by the fact that in our study (1) the added water amount was small (40% WHC); and (2) the forest soil was acidic with pH values lower than 3.5 for most of the samples. Furthermore, also Goldberg & Gebauer (2009) found a maximum NO emission for a Norway spruce forest at 33% WFPS in the organic layer, and it was reported that chemodenitrification increased at a pH less than 4 (Kesik *et al.*, 2006)

In contrast to NO₂⁻, large N₂O production was observed after NH₂OH addition to cropland, grassland and one forest soil sample (F5), and only negligible amounts of N₂O were produced in other forest soils (Fig. 6.1B and D). Abiotic reactions played a much larger role in the case of NH₂OH addition compared to NO₂⁻ addition. Comparison of the results from the experiments with γ -irradiated and non-irradiated soils revealed that most of the N₂O from NH₂OH was chemically produced, contributing 90.5%, 84.2% and 72.5% to the total conversion of NH₂OH to N₂O for the cropland, F5 and grassland soil, respectively. We found larger Mn content in grassland, cropland and F5 forest sub-sample (Table 6.1), and a positive and significant correlation was observed between soil N₂O production in response to NH₂OH addition and Mn content (Table 6.4). This is in accordance with previous findings, which identified the chemical reaction between MnO₂ and NH₂OH as important factor for abiotic N₂O production in soil (Bremner, 1997; Heil *et al.*, 2015). The, at first sight, contradictory observation that the forest soil with the largest Mn content (F5) had a lower N₂O production upon NH₂OH addition than the grassland and cropland soils can be explained with the inhibitory effect of soil organic matter on the abiotic conversion of NH₂OH to N₂O. The effect of NH₂OH on soil N₂O emissions had been found earlier to be related to SOM quantity, quality and Mn content, with largest NH₂OH-to-N₂O conversion ratio in soils with higher Mn content and lower soil organic C content or, more specifically, lower content of carbonyl groups to which NH₂OH could bind chemically (Liu *et al.*, 2017a).

6.4.2 Effect of soil redox history on N₂O formation from NO₂⁻ and NH₂OH

Despite their reactivity, the two N intermediates NH₂OH and NO₂⁻ may accumulate in soils under anoxic conditions. NH₂OH accumulation in anoxic sediment slurries has been observed

in a preliminary experiment (data not shown), while transient NO_2^- accumulation as well as the absence of NO_3^- have been reported in soil slurries during anaerobic incubation (Clément *et al.*, 2005). In the present study, the NH_4^+ concentration, especially of the grassland soil, increased largely with anoxic pre-incubation (Table 6.1), probably due to dissimilatory nitrate reduction to ammonium and indicating that soil redox potential was smaller than +200 mV (Froelich *et al.*, 1979). SOM quality, transition metal redox state, and pH may change remarkably at this redox potential (Dassonville & Renault, 2002). According to thermodynamic theory, the following sequential reduction of electron acceptors is observed with decreasing redox potential: O_2 , NO_3^- , MnO_2 , Fe_2O_3 , SO_4^{2-} and CO_2 reduction (Froelich *et al.*, 1979) during respiratory or other dissimilatory processes. Thus, Fe^{2+} , Mn^{2+} and the fermented organic matter would accumulate during anoxic pre-incubation. Furthermore, the transient occurrence of reactive C substances could have reversed the effects of NH_2OH and NO_2^- addition, as a transient increase in reactive C rich in carbonyl groups would preferentially react with NH_2OH and decrease N_2O production from abiotic conversion of NH_2OH , while a transient increase in reactive phenolic compounds would lead to preferential reaction with NO_2^- to produce N_2O chemically.

We hypothesized that anoxic pre-incubation would lead to higher N_2O release after NO_2^- addition and less N_2O release after NH_2OH addition due to the accumulation of more reduced substances. Our results appeared that anoxic pre-incubation increased N_2O production in the first hour after NO_2^- addition in most of the soils, but decreased N_2O production afterwards. The stimulatory effect of anoxic pre-incubation on N_2O production in the first hour could be due to the increased contribution of N_2O production via chemodenitrification, as more reduced metal ions, e.g. Fe^{2+} , may accumulate after anoxic pre-incubation and abiotic N_2O production occurred usually very fast. However, since most of the N_2O produced after NO_2^- addition came from biotic pathways, anoxic pre-incubation may have altered the microbial composition, e.g. changed the activity of nitrifiers and related enzymes, leading to negative effects on the longer-term effect of anoxic pre-incubation on N_2O production via NO_2^- in soils.

Anoxic pre-incubation had an even more pronounced effect on N_2O production after NH_2OH addition, with a significant reduction in the forest soil F5 and the grassland soil (79% and 97%, respectively), in accordance with our hypothesis, but with only a small effect (13%) on the cropland soil. As a strong oxidant, most of the MnO_2 should have been reduced to Mn^{2+} during the anoxic pre-incubation period according to the large increase in NH_4^+ and the low

redox potential state (Table 6.1), especially in those soil samples with high C content, which can be used by microorganisms that reduce Fe³⁺ or Mn⁴⁺ instead of oxygen to catabolize organic matter (Lovley *et al.*, 2004). The lower effect of the anoxic pre-treatment on the conversion of NH₂OH to N₂O in the cropland soil could be attributed to the lower C content in this soil, where less Mn⁴⁺ would be reduced to Mn²⁺. To further explore the effect of MnO₂ on the NH₂OH-to-N₂O conversion ratio, we added 0.1% (w/w) MnO₂-Mn (equal to the Mn content of grassland soil) to both the oxic and anoxic pre-treated soil samples. We hypothesized that this amount of MnO₂ addition would increase the NH₂OH-to-N₂O conversion ratio of the anoxically pre-incubated soil samples. However, only the grassland soil and forest soils F3 and F5 showed a larger Mn effect after anoxic pre-treatment, but the added Mn amount could not make up the reduction in N₂O production caused by the anoxic pre-incubation, despite the large increase of N₂O production from F3 with anoxic pre-incubation (Fig. 6.2).

It was reported that large amounts of fermented substances could accumulate during anoxic incubation (Dassonville & Renault, 2002). In the present study, we found more DOC and dissolved aromatic substances (represented as A₂₅₄) in the soil samples with anoxic pre-incubation than with oxic pre-incubation (Table 6.1). The change of soil DOC quality and quantity could be responsible for the difference in N₂O production after NH₂OH addition to soils with different redox history. The increase in DOC and aromatic substances after anoxic pre-incubation would increase the likelihood of fast binding of NH₂OH to organic compounds once added to the soil, and lead to a lower availability of NH₂OH for the reaction with MnO₂ to produce N₂O. Therefore, the absence of a MnO₂ addition effect on the NH₂OH-to-N₂O conversion ratio could be due to the accumulation of fermented substances that can quickly react with NH₂OH.

6.5 Conclusions

In summary, we show that the response of soil N₂O production to the addition of the reactive N intermediates NH₂OH or NO₂⁻ depends on the soil precondition, i.e. oxic vs. anoxic. The addition of NO₂⁻ increased N₂O emissions mainly from biotic processes, while the addition of NH₂OH increased N₂O from abiotic processes. Anoxic pre-incubation decreased N₂O emissions in the NH₂OH treatment, while it increased N₂O emissions in the first hour after

NO_2^- addition. Cropland, forest, and grassland soils showed different responses to the addition of the two N intermediates and soil pre-conditions, e.g. in cropland soil with large MnO_2 content and low C content, more N_2O originated from the abiotic NH_2OH oxidation compared to well-known nitrifier denitrification. This study provides insight into the coupled biotic-abiotic processes involved in N_2O production in soils.

Chapter 7

Accumulation of NO_2^- during drying periods stimulates soil N_2O emissions during subsequent rewetting events

Based on:

Liu S., Schloter M. and Brüggemann N. Accumulation of NO_2^- during drying period stimulates soil N_2O emissions by subsequent rewetting events. *European Journal of Soil Science*, under revision.

7.1 Introduction

As an important greenhouse gas, the emissions of N₂O from soils of various ecosystems under different environmental conditions have been widely studied. Rewetting of soil after longer dry periods is an important event of accelerated soil C and N mineralization (“Birch effect”), as well as soil N₂O emissions (Smith & Parsons, 1985; Rudaz *et al.*, 1991; Ruser *et al.*, 2006). A single wetting event may be responsible for a large fraction of the annual N₂O emission for certain ecosystems (Priemé & Christensen, 2001; Berger *et al.*, 2013). In recent years, numerous studies have focused on the mechanisms of large soil N₂O emissions upon rewetting (Beare *et al.*, 2009; Harrison-Kirk *et al.*, 2013; Snider *et al.*, 2015). Three reasons have been considered responsible for the increased N₂O flux following rewetting: (1) Enhanced microbial metabolism including nitrification and denitrification; (2) abiotic reactions due to the availability of accumulated soluble substrates; (3) physical mechanisms involving infiltration, reduced diffusivity and gas displacement. Soluble substances accumulated in the soil during the drying process play an important role in the abrupt N₂O emissions. To survive drought, microbes must accumulate high concentrations of solutes to retain osmotic pressure and prevent dehydration (Fierer & Schimel, 2002; Schimel *et al.*, 2007). Upon rewetting, however, the accumulated solutes inside the cell may be released during cell rupture after sudden rewetting (Halverson *et al.*, 2000; Fierer & Schimel, 2003). In addition, drought will also shrink soil aggregates, but rapid rewetting with water entering the aggregates quickly can rupture the aggregate (Denef *et al.*, 2001; Fierer & Schimel, 2003). These processes can expose large amounts of soluble substances in the soil for subsequent microbial uptake and turnover as well as fast chemical reactions.

The resilience of microorganisms to the drying-rewetting process is largely dependent on soil type and history of drought (Placella & Firestone, 2013; Thion & Prosser, 2014). In a drought-acclimated upland soil, an increase in the quantity of bacterial ammonia monooxygenase (*amoA*) transcripts was detectable within 1 hour after rewetting and continued until the NH₄⁺ pool began to decrease (Placella & Firestone, 2013). A rapid increase of denitrifying enzyme activity was also observed following rewetting of air-dried soils in laboratory incubations (Rudaz *et al.*, 1991). However, in a grassland soil without drought history, Thion & Prosser (2014) found little evidence for adaptation of bacterial and archaeal ammonia oxidizers, which is in accordance with a cropland field experiment in

Canada, in which no increase in the transcription of functional N cycle genes during the rewetting process was observed (Snider *et al.*, 2015).

Compared to biotic processes, abiotic reactions may play an even more important role in triggering soil N_2O pulses in the wake of rewetting. NH_2OH and NO_2^- are the most important reactive N intermediates involved in abiotic N_2O production (Heil *et al.*, 2016). It is unlikely that NH_2OH would accumulate during soil drying process because of its very reactive nature, especially at dry conditions. Nitrite does usually not accumulate in soil at moist or wet conditions (Robertson & Groffman, 2007), as then the oxidation of NO_2^- to NO_3^- proceeds faster than the conversion of NH_3 to NO_2^- . However, NO_2^- has a great potential to accumulate during soil drying. Davidson (1992) reported that accumulation of soil NO_2^- during drought probably contributes to pulses of NO and N_2O production following rewetting. The accumulation of NO_2^- in soil is very likely caused by a time delay between the turnover of NH_4^+ and NO_2^- because of differences in tolerance towards and recovery from soil environmental change between AOB and NOB, e.g. after pH increase, at high NH_3 levels and during drought stress (Smith *et al.*, 1997; Shen *et al.*, 2003; Gelfand & Yakir, 2008; Placella & Firestone, 2013). Shen *et al.* (2003) reported that more NO_2^- was accumulated at alkaline conditions than at acidic conditions with urea addition in an incubation experiment. Gelfand & Yakir (2008) also observed an unexpected rapid increase in NO_2^- concentration in a forest soil after soil rewetting by the first winter rains, accompanied by a decrease in ammonium and only a slight increase in nitrate concentrations.

Accumulation of NO_2^- in soil does not only provide substrate for biological processes such as denitrification, nitrification and DNRA (Silver *et al.*, 2001; Rütting *et al.*, 2011), but plays also a major role for chemodenitrification, in which NO_2^- reacts with humic substances or phenolic compounds to form nitroso and nitro compounds (Thorn & Mikita, 2000), which in turn can decompose to NO or be reduced by Fe(II) to N_2O (van Cleemput & Samater, 1995; Samarkin *et al.*, 2010). Another important pathway for the N_2O production via chemodenitrification is the direct reaction between NO_2^- and Fe(II), which have been studied widely recently by using the new isotope technology-site preference (SP) (Jones *et al.*, 2015; Grabb *et al.*, 2017).

In order to investigate the processes involved in N_2O emission pulses after rewetting in more detail and to assess the importance of biotic vs. abiotic processes in different soils, we designed a series of rewetting experiments with soil samples from various ecosystems (upland

and riparian forest, grassland and cropland). We sterilized part of the soil samples with γ -irradiation and analyzed the ^{15}N SP of N_2O , i.e., the intramolecular distribution of ^{15}N within the linear NNO molecule, which is considered as an effective tool to assign the source of N_2O formation via biological reactions (i.e. nitrification, nitrifier denitrification, bacterial denitrification and fungal denitrification) and abiotic reactions (chemodenitrification and NH_2OH oxidation). The aim of the experiments was to (1) identify the relevant drivers of soil N_2O pulse emissions caused by rewetting; and (2) quantify the contributions of abiotic and biotic reactions to the N_2O pulse. We hypothesized that (1) the N_2O production with rewetting would be higher from soil samples with more NO_2^- accumulated; (2) abiotic reactions play an important role in N_2O production upon rewetting.

7.2 Materials and methods

7.2.1 Soil collection

Fresh soil samples were collected from three different field sites of the Eifel/Lower Rhine Valley Observatory of the network of TERENO (www.tereno.net): coniferous forest (Wüstebach; 50°30' 10" N, 6°19' 50" E), cropland (Selhausen; 50°52' 10" N, 6°27' 4" E) and grassland (Rollesbroich; 50°37' 18" N, 6°18' 15" E). The coniferous forest site was situated in the low mountain ranges of the Eifel National Park, with a sub-catchment of the river Rur basin flowing through it. The site was dominated by Norway spruce (*Picea abies* (L.) H. Karst). The main soil texture at this site was silty clay loam. The mean annual precipitation of the coniferous forest is about 1400 mm. The height above sea level (a.s.l.) of the forest site is 630 m and the mean annual temperature is around 7 °C. The agricultural site was planted with different crops according to the locally common crop rotation, including sugar beet and wheat. The soil is dominated by (gleyic) Cambisol and (gleyic) Luvisol with a silt loam texture, and the altitude ranges between 102–110 m a.s.l.. Mean annual temperature is 9.8 °C, and the average precipitation amounts to 690 mm per year. The grassland site was located in the Northern Eifel region and planted with smooth meadow-grass. Dominant soils at this site are (gleyic) Cambisol, Stagnosol, and Cambisol-Stagnosol with a silt loam texture, covering an area of 27 ha with altitude ranging between 474 and 518 m a.s.l.. Mean annual temperature and precipitation are 7.7 °C and 1033 mm, respectively (Rötzer *et al.*, 2014).

Forest soil samples (~ 2 kg each) including those from the riparian zone were collected in July 2015. For the forest site, a large spatial variability of N_2O production had been observed in a previous study (Liu *et al.*, 2016) due to the topographic conditions, vegetation and the creek flowing through the sampling area. Hotspots of soil N_2O production were concentrated in several areas where soil basic properties, water conditions and vegetation status were different from the rest of the area. We therefore collected several soil samples including one fermented litter sample (F_{Of}), six humus-rich (Oa horizon) samples (F1, F2, F3, F4, F5 and F6) and one riparian sample (FR) in the area of approximately 27 ha in the Wüstebach forested catchment to explore the N_2O production mechanisms. Fresh soil samples were transferred to the laboratory separately at the same day. At the grassland (G) and cropland (C) sites, five soil samples (~ 1.5 kg each) in one hectare were collected from the soil top 15 cm layers of the two sites, respectively in January 2016. The spatial variability of the grassland and cropland sites were smaller compared to the forest site, therefore we mixed soil samples collected in the grassland and cropland sites to one composite soil sample, which was considered as representative for the whole site. The fresh soil samples were mixed directly in a large plastic bag after soil sampling in both sites, and were transferred to the laboratory on the same day. In the laboratory, fresh samples (except the FR sample) were passed through a 2-mm sieve, and coarse plant residues (including roots) and stones were manually removed to homogenize the soil samples and explore the effects of soil constituents on the rewetting effect. The existence of plant material would have biased the soil effect and might have made the results of this study only comparable for soils with certain plant species composition. After that, soil samples were put into open plastic bags and stored at 4 °C until the beginning of the experiment.

7.2.2 Experimental setup

7.2.2.1 Soil pre-treatment

Fresh soil samples were taken out of the fridge and spread out on aluminum foil to a thin layer of 0.5-1 cm, and kept at room temperature (21 ± 1 °C) for about one month. After that, the air-dried soil samples were put into ziplock bags and stored at room temperature. To explore the effects of air-drying on soil mineral N dynamics, mineral N was measured both fresh and dry soil samples.

7.2.2.2 Soil γ -irradiation

Half of the air-dried soil samples were sterilized using γ -irradiation by a Gammacell Irradiator 4000 (Best Theratronics, Canada), applying a dose of 11 kGy. Plating of the sterilized soil slurries directly after γ -radiation revealed no microbial growth (R2A medium, 24-hour incubation; 25°C; data not shown). To prevent the quick recovery of microorganism after γ -irradiation, soil samples were incubated only up to 7 h after rewetting.

7.2.2.3 Rewetting experiments

Rewetting experiments were performed with both non-irradiated and γ -irradiated air-dried soil. The experiments with γ -irradiated air-dried samples were conducted in a clean bench with all solutions filtered through 0.2 μm filters. 1.4 g of air-dried soil (0.7 g for F_{OF}) were weighed into 22-ml GC vials (VWR international, Darmstadt, Germany), followed by the addition of either H_2O , or NO_2^- , NO_3^- or NH_4^+ solution to reach around 40% WHC and adding 1 $\mu\text{g N g}^{-1}$ dry soil (for NO_2^-) and 100 $\mu\text{g N g}^{-1}$ dry soil (for NH_4^+ and NO_3^-). The vials were closed gastight with butyl septa and aluminum crimp caps (VWR International) immediately after addition of water or solution and incubated at room temperature for 1 and 7 h. Each treatment was carried out in triplicate. The gas sample in the headspace of the sample vials was analyzed using a gas chromatograph (Clarus 580, PerkinElmer, Rodgau, Germany) equipped with an ECD and FID for N_2O and CO_2 , respectively (Liu *et al.*, 2014). The instrument was calibrated using five different standard gases with 0.25, 0.50, 0.75, 1.00 and 5.00 ppm N_2O balanced with N_2 (99.5% purity, Linde, Munich, Germany).

7.2.2.4 Analysis of ^{15}N site preference of N_2O

For the determination of N_2O SP values, 1.4-2.8 g of soil were weighed into 120-ml headspace bottles, and only water was added to the soils to reach about 40% WHC. The bottles were closed immediately after addition of water and transferred to an autosampler that was programmed in a way that sample bottles were incubated for 0.5-6.5 hours prior to analysis. The autosampler was coupled to a pre-concentration unit (TraceGas, Elementar Analysensysteme, Langenselbold, Germany) for online separation and purification of N_2O , which in turn was connected to an isotope ratio mass spectrometer (IRMS, IsoPrime 100, Elementar Analysensysteme). Molecular ions (N_2O^+) and fragment ions (NO^+) were monitored simultaneously with the IRMS at m/z 44, 45, 46, and 30, 31, respectively. The sample values of $\delta^{15}\text{N}^{\text{bulk}}$ and $\delta^{18}\text{O}$ were calculated according to the isotope ratios of m/z 45 to

44, and 46 to 44, respectively, against a working reference gas. A correction for ¹⁷O was performed according to the mass-dependent fractionation of ¹⁷O and ¹⁸O, described by the formula $^{17}\text{R} = 0.00937035 \cdot (^{18}\text{R})^{0.516}$ (Kaiser *et al.*, 2003). The SP is defined as $\text{SP} = \delta^{15}\text{N}^{\alpha} - \delta^{15}\text{N}^{\beta}$ ($\delta^{15}\text{N}^{\alpha}$ and $\delta^{15}\text{N}^{\beta}$ are the $\delta^{15}\text{N}$ at the central and terminal position of the N₂O molecule, respectively). The $\delta^{15}\text{N}^{\alpha}$ was calculated from the isotope ratio m/z 30 and 31. The $\delta^{15}\text{N}^{\beta}$ was calculated according to the following formula: $\delta^{15}\text{N}^{\beta} = 2 \cdot \delta^{15}\text{N}^{\text{bulk}} - \delta^{15}\text{N}^{\alpha}$. Scrambling effects were corrected for assuming an isotopic scrambling of the terminal and central nitrogen atom of about 8% (Kaiser *et al.*, 2004). Pure N₂O (99.999%, Linde, Munich, Germany) was used as working standard ($\delta^{15}\text{N}^{\alpha}$ vs air-N₂ = $3.18 \pm 0.23\text{‰}$, $\delta^{15}\text{N}^{\beta}$ vs air-N₂ = $1.42 \pm 0.21\text{‰}$, $\delta^{18}\text{O}$ vs VSMOW = $39.35 \pm 0.27\text{‰}$) for isotope analysis, and the $\delta^{15}\text{N}^{\text{bulk}}$, $\delta^{15}\text{N}^{\alpha}$, $\delta^{15}\text{N}^{\beta}$ and $\delta^{18}\text{O}$ were calibrated against two reference gases (Ref 1: $\delta^{15}\text{N}^{\alpha}$ vs air-N₂ = $15.70 \pm 0.31\text{‰}$, $\delta^{15}\text{N}^{\beta}$ vs air-N₂ = $-3.21 \pm 0.37\text{‰}$, $\delta^{18}\text{O}$ vs VSMOW = $35.16 \pm 0.35\text{‰}$; Ref 2: $\delta^{15}\text{N}^{\alpha}$ vs air-N₂ = $5.55 \pm 0.21\text{‰}$, $\delta^{15}\text{N}^{\beta}$ vs air-N₂ = $-12.87 \pm 0.32\text{‰}$, $\delta^{18}\text{O}$ vs VSMOW = $32.73 \pm 0.21\text{‰}$) provided by EMPA (Dübendorf, Switzerland) and as described in Mohn *et al.* (2014). In addition, different amounts of reference N₂O gas were added to the 120-ml bottles and isotope signatures were measured. Strong quadratic relations were observed between N₂O peak height (2.7 to 72 nA) and $\delta^{45}\text{N}_2\text{O}$ vs. ref., $\delta^{46}\text{N}_2\text{O}$ vs. ref. and $\delta^{31}\text{NO}$ vs. ref., with polynomial equations of $y = 0.0032x^2 - 0.1689x + 0.5516$, $R^2 = 0.93$, $y = 0.0054x^2 - 0.2643x + 39.3$, $R^2 = 0.92$ and $y = 0.0014x^2 + 0.4489x - 0.6767$, $R^2 = 0.99$, respectively. Therefore, all $\delta^{15}\text{N}^{\text{bulk}}$, $\delta^{18}\text{O}$ and SP values in this study were calculated according to the corrected $\delta^{45}\text{N}_2\text{O}$ vs. ref., $\delta^{46}\text{N}_2\text{O}$ vs. ref. and $\delta^{31}\text{NO}$ vs. ref. values by using polynomial equations. For the peak area correction and calibration, no technical replication was performed as the standard deviation for the isotope analysis was very small, i.e. 0.2‰, 0.4‰, 0.3‰, 0.4‰, 0.7‰ and 0.6‰ for $\delta^{15}\text{N}^{\text{bulk}}$ vs. air-N₂, $\delta^{18}\text{O}$ vs. VSMOW, $\delta^{31}\text{N}$ vs. ref., $\delta^{15}\text{N}^{\alpha}$ vs. air-N₂, $\delta^{15}\text{N}^{\beta}$ vs. air-N₂ and SP for a long measurement period, respectively.

7.2.2.5 Soil chemical analyses

Total C and N contents were determined with an elemental analyzer (vario EL Cube, Elementar Analysensysteme GmbH, Hanau, Germany). The elemental composition of the soil samples was analyzed by using ICP-OES. Briefly, 100 mg of sample material were mixed with 3 ml HNO₃ and 2 ml H₂O₂, and heated in a microwave oven at 800 W for 30 minutes. The mixtures were subsequently filled up to 14 ml and diluted 10-fold with deionized water followed by the ICP-OES measurement. The mineral N (NH₄⁺, NO₂⁻ and NO₃⁻) contents were

analyzed with ion chromatography (IC, Dionex ICS-3000 for NO_2^- and NO_3^- , Dionex DX-500 for NH_4^+). NH_4^+ and NO_3^- were extracted with 1 M KCl (dry soil: solution = 1:10 w/w) and shaken for 24 h. Soil pH was measured from the NH_4^+ and NO_3^- extractant. NO_2^- was extracted with water during 15 min magnetic stirring and by using 0.2 M NaOH to keep the pH around 6 during extraction (Homyak *et al.*, 2015). DOC and DTN were extracted with deionized water (dry soil: solution = 1:2.5 w/w for grassland and cropland soils, and 1:5 w/w for forest and riparian soils) by shaking for 1 hour at 200 rpm. DOC and DTN were then analyzed with a TOC-TN analyzer (Shimadzu Corp., Kyoto, Japan). Aromatic substances in the extracted DOC were determined by UV spectrometry (Beckman Coulter DU 800, Beckman Coulter, Inc., California, United States) at a wavelength of 254 nm (A_{254}) with a path length of 1 cm.

7.2.3 Data analyses

The rewetting effects related to NO_2^- , NO_3^- or NH_4^+ were calculated by subtracting N_2O emission after addition of water only (as control) from the N_2O emission after NO_2^- , NO_3^- or NH_4^+ addition. N_2O emission was calculated according to Equation 8 in Liu *et al.* (2014). Isotope signatures ($\delta^{15}\text{N}^{\text{bulk}}$, $\delta^{18}\text{O}$ and SP values) of soil-emitted N_2O (δ_{soil}) were calculated from the total isotope signature of the gas samples (δ_{bottle}) and of ambient air (δ_{air}) using a two-component mixing model: $\delta_{\text{soil}} = (\delta_{\text{bottle}} \times C_{\text{bottle}} - \delta_{\text{air}} \times C_{\text{air}}) / (C_{\text{bottle}} - C_{\text{air}})$, with C_{bottle} representing the N_2O concentration in the sample bottles and C_{air} the N_2O concentration in ambient air. Spearman's correlation analysis was conducted using Origin Pro version 2015.

7.3 Results

7.3.1 Soil basic properties

Soil basic properties, e.g., C content, Mn content and pH varied largely between the soil samples obtained from the different ecosystems (Table 7.1). Soil C content ranged from around 10% to 46% in the forest soil samples, including the F_{Of} and the FR, while it was only ~5% and ~1% for the grassland and cropland soil, respectively. The forest soil was strongly acidic with a pH around 3, while the pH of grassland and cropland soils was much higher (between 5 and 6). Compared to grassland and cropland soil samples, the Mn content of forest soil samples of around 0.02% was relatively low, except for soil samples F5 and F6 that

exhibited the largest Mn content of all forest soil samples. No distinct difference was observed for the Fe content between the soil samples, only the fermented layer (F_{Of}) and riparian soil (FR) had a lower Fe content than the other soil samples.

Table 7.1 Basic properties of air-dried soils. Data values are presented as mean (SD).

	C (%)	N (%)	C/N	pH	Fe (%)	Mn (%)	Ca (%)	K (%)	Mg (%)
F_{Of}	45.72 (0.00)	1.93 (0.00)	23.7	2.85	0.35 (0.01)	0.031 (0.000)	0.33 (0.06)	0.13 (0.01)	0.05 (0.00)
F1	28.70 (0.20)	1.47 (0.01)	19.5	3.05	1.72 (0.05)	0.011 (0.000)	0.10 (0.00)	0.73 (0.01)	0.15 (0.00)
F2	19.80 (0.20)	1.08 (0.03)	18.4	3.27	2.55 (0.02)	0.021 (0.000)	0.20 (0.03)	1.05 (0.01)	0.25 (0.00)
F3	25.87 (0.10)	1.47 (0.02)	17.6	3.35	2.20 (0.1)	0.012 (0.001)	0.13 (0.02)	0.77 (0.03)	0.16 (0.00)
F4	24.57 (0.00)	1.32 (0.00)	18.5	3.03	1.87 (0.02)	0.020 (0.001)	0.14 (0.01)	0.96 (0.01)	0.16 (0.00)
F5	21.38 (0.10)	0.88 (0.06)	24.4	3.92	3.30 (0.2)	0.210 (0.020)	0.19 (0.06)	1.28 (0.06)	0.21 (0.00)
F6	22.23 (0.10)	1.51 (0.00)	14.7	3.78	3.50 (0.2)	0.072 (0.002)	0.09 (0.00)	1.12 (0.01)	0.17 (0.00)
FR	9.65 (0.06)	0.53 (0.01)	18.1	4.23	1.57 (0.08)	0.024 (0.001)	0.13 (0.01)	1.75 (0.08)	0.31 (0.02)
G	5.29 (0.05)	0.53 (0.00)	9.9	5.25	2.39 (0.03)	0.097 (0.003)	0.28 (0.03)	1.65 (0.04)	0.29 (0.02)
C	1.29 (0.01)	0.14 (0.00)	9.2	5.82	2.10 (0.1)	0.074 (0.004)	0.36 (0.03)	1.46 (0.06)	0.32 (0.01)

7.3.2 Mineral N and DOM content before and after drying

The mineral N content (including NH_4^+ and NO_3^-) of the fresh soil differed strongly between the soil samples (Fig. 7.1). Before air-drying, forest soil samples F_{Of} and F4 had the largest NH_4^+ and NO_3^- , while samples F5 and F6 had smaller NH_4^+ but larger NO_3^- content compared to the other forest soil samples. Samples from the riparian zone and from the cropland had the lowest NH_4^+ and NO_3^- content amongst all soil samples, and grassland soil had an intermediate level of NH_4^+ and NO_3^- . After air-drying, the NH_4^+ content decreased for all the soil samples. There was nearly no NH_4^+ detectable in the riparian and cropland soil samples after air-drying.

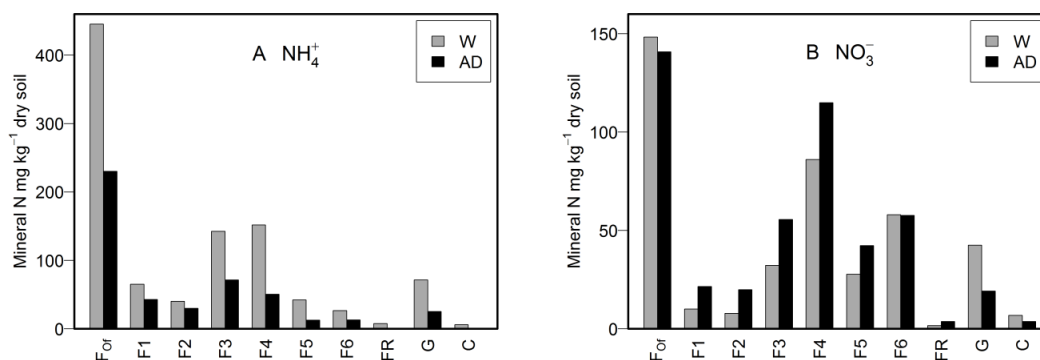


Figure 7.1 Soil NH_4^+ (A) and NO_3^- (B) content before (W, grey) and after air-drying (AD, black) for forest (F_{0f}, F₁, F₂, F₃, F₄, F₅, F₆ and FR), grassland (G) and cropland (C) soil samples. Only one extraction was performed for the determination of soil NH_4^+ and NO_3^- content.

In contrast to NH_4^+ , NO_3^- increased during the drying process in almost all soil samples, except for F_{0f}, F₆, grassland and cropland samples. Forest soil sample F_{0f} had the largest NO_3^- content, followed by F₄ and F₆. The grassland soil had an intermediate NO_3^- content compared to the forest soil samples, while the riparian and cropland soil samples were characterized by the lowest NO_3^- content.

Table 7.2 Soil NO_2^- -N (mg kg⁻¹), dissolved organic carbon (DOC, mg kg⁻¹), dissolved total nitrogen (DTN, mg kg⁻¹) and A_{254} (cm⁻¹ g⁻¹ dry soil) after air-drying for forest, grassland and cropland soil samples. The standard deviation of the NO_2^- assay is about 20% of the values (n.d. = not detectable). Only one extraction was performed for the determination of soil DOC, DTN and A_{254} .

Soils	NO_2^-	DOC	DTN	A_{254}
F _{0f}	0.3	2420	358	1.40
F ₁	0.2	2110	161	1.27
F ₂	n.d.	1680	123	1.00
F ₃	0.3	1825	183	0.78
F ₄	n.d.	1885	221	1.01
F ₅	0.1	555	118	0.41
F ₆	0.3	890	84	0.24
FR	n.d.	575	74	0.42
G	0.2	636	105	0.41
C	0.1	177	21	0.22

Before air-drying, NO_2^- concentrations were below the detection limit for the fresh soil samples (data not shown). However, small amounts of NO_2^- were detectable in several soil samples (Table 7.2). Forest soil samples F_{0f}, F₃ and F₆ had the largest NO_2^- content (0.3 mg

kg^{-1}), followed by grassland and forest soil F1 (0.2 mg kg^{-1}), while no NO_2^- was detectable in soil samples F4, F2 and FR.

The trend of soil DOC and DTN dynamics after air-drying was very similar to that of soil C content, with the largest DOC and DTN contents in soil sample F_{Of} and the smallest in the cropland soil, with the exception of soil sample F5, which had a relatively high C content but the smallest DOC content of all forest soil samples (Table 7.2). The DOC and DTN contents in the grassland soil were also relatively high. Although soil sample F6 featured the second largest total N content, it contained a relatively small amount of DTN. The dynamics of A_{254} (i.e., content of aromatic substances) followed a similar trend as DOC, with the largest value for forest soil sample F_{Of} and the smallest value for the cropland soil.

7.3.3 Rewetting effects on soil N_2O emissions

Rewetting responses of soil N_2O emissions to the water and different N additions were varied between the soils from the different ecosystems (Fig. 7.2A). After rewetting with water only, the grassland soil showed the largest N_2O emission among all soil samples, especially in the first hour after rewetting, with an emission of $64 \mu\text{g N}_2\text{O-N kg}^{-1}$ dry soil. Forest soil samples showed different responses to rewetting with water only, with samples F1 and F3 showing the largest N_2O emissions, while samples F2, F4, F5 and FR exhibited a lower N_2O emission. Unlike the grassland soil, the N_2O emission from forest soil did not increase substantially in the first hour, but increased between 1 and 7 h, and certain forest soil samples even reached the level of the grassland soil after 7 h. In contrast, there was nearly no rewetting effect on soil N_2O emissions detectable for the cropland soil.

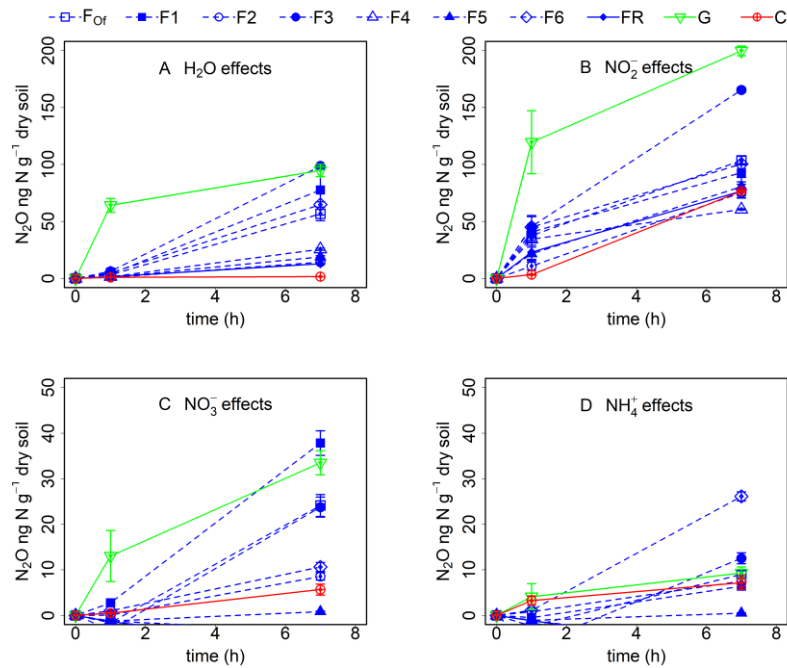


Figure 7.2 Rewetting effects by the addition of water (A), and aqueous solutions of NO_2^- (B), NO_3^- (C) and NH_4^+ (D) on soil N_2O production (ng N g^{-1} dry soil) of forest (F_{Or}, F1, F2, F3, F4, F5, F6 and FR), grassland (G) and cropland (C) soil samples for different (1 and 7 h) incubation times. The values are present as mean \pm standard deviation (SD).

Nitrite addition increased the rewetting effect considerably for all soil samples (Fig. 7.2B). Similar with water rewetting, NO_2^- increased the N_2O emission the most for grassland soil samples, followed by the forest sample F3. The effects of NO_2^- on N_2O production in the other upland forest, riparian zone and cropland samples were very similar. For most soil samples, NO_2^- had a stronger stimulatory effect in the first hour compared to the following 6 h if we assume that the N_2O production was linear between two-time points. The total NO_2^- -to- N_2O turnover rate after 7 h was about 20% for grassland soil, but only between 5-10% for most upland forest, riparian and cropland samples.

Compared to NO_2^- , NO_3^- and NH_4^+ had only small stimulatory effects on soil N_2O production upon rewetting (Fig. 7.2C, 7.2D), even though the added amount of NH_4^+ -N and NO_3^- -N was 100-fold higher than that of NO_2^- . The addition of NO_3^- increased the N_2O production in the grassland soil as well as in forest samples F_{Or}, F1, F3 the most, while the maximum N_2O production after NH_4^+ addition was observed for F6. In contrast, both NO_3^- and NH_4^+ had nearly no effect on N_2O production in cropland and riparian soil samples as well as in forest samples F4 and F5.

7.3.4 Influence of γ -irradiation on soil N_2O and CO_2 emissions after rewetting

The effect of γ -irradiation on soil N_2O emissions upon rewetting was dependent on soil type. In general, γ -irradiation decreased N_2O emission upon rewetting with water only by about 50-90% in most forest soil samples compared to the non-irradiated soil samples, while it unexpectedly stimulated N_2O emissions from grassland and cropland soils by threefold and twofold, respectively, after 7 h of incubation (Fig. 7.3A and Table 7.3). Forest soil samples showed a large variance of γ -irradiation effects. Gamma irradiation inhibited soil N_2O production from F_{Of} the most, followed by the riparian sample and F5, while the N_2O production from samples F1 and F2 were affected by γ -irradiation the least during the incubation.

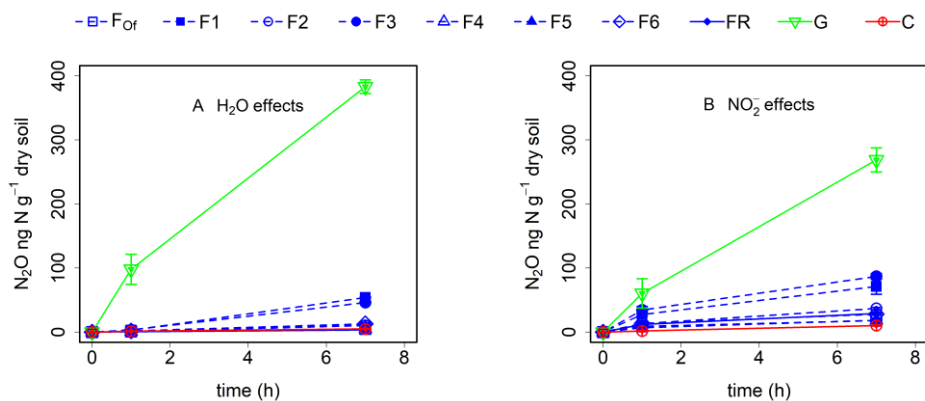


Figure 7.3 Rewetting effects by the addition of water (A) and aqueous NO_2^- (B) solution on soil N_2O production (ng N g^{-1} dry soil) of forest (F_{Of} , F1, F2, F3, F4, F5, F6 and FR), grassland (G) and cropland (C) soil samples for different (1 and 7 h) incubation times after γ -irradiation. The values are present as mean \pm standard deviation (SD).

Also in the NO_2^- rewetting treatment, γ -irradiation increased the N_2O production in grassland soils, but decreased it in forest soils (Fig. 7.3B and Table 7.3). The increase in N_2O production caused by rewetting of the cropland soil with NO_2^- solution was also reduced by 86.7%. In contrast, soil samples F1 and F3 were inhibited the least by γ -irradiation.

Table 7.3 The inhibitory effect (%) of γ -irradiation on soil N_2O and CO_2 emissions after 7 h incubation after rewetting of air-dried soils. Negative values represent a stimulating effect of γ -irradiation.

	F _{Or}	F1	F2	F3	F5	FR	G	C
H₂O addition								
N ₂ O	91.1	30.4	28.0	53.2	73.3	73.4	-304.2	-210.0
CO ₂	13.2	-28.2	-0.8	-12.2	25.8	31.0	53.9	26.0
NO₂⁻ addition								
N ₂ O	82.7	23.2	51.0	47.4	77.1	61.9	-34.6	86.7
CO ₂	21.7	-25.5	1.1	4.9	28.0	24.6	53.2	21.2

Compared to the effects on soil N_2O emissions, γ -irradiation decreased CO_2 production the most in the grassland soil, by about 50% after rewetting with water only, but had an inhibitory effect of only zero to 20% in forest, cropland and riparian soil samples (Table 7.3). In forest soil sample F1, the CO_2 production was even stimulated by γ -irradiation.

7.3.5 Control variables of soil N_2O emission upon rewetting

Soil basic properties play an important role in biotic and abiotic reactions, and may contribute to the pulse N_2O emissions after rewetting. Among all the basic soil properties, N_2O production was only significantly ($P < 0.05$) and positively correlated with NO_2^- content, marginally ($P = 0.056$) correlated with soil NH_4^+ content, but had no statistically significant correlations with other basic soil properties, such as soil C and NO_3^- content (Table 7.4). Within the forest soil samples, N_2O production was also significantly ($P < 0.05$) correlated with soil C and N content (data not shown). Soil NO_2^- itself was only significantly ($P < 0.05$) correlated with total soil N content and N_2O production, but was not correlated with soil mineral N and DTN.

Table 7.4 Spearman's correlation coefficients between soil N₂O emission after 7 h incubation after rewetting and basic soil properties of air-dried soils (excluding Ca, Mg and K) across all soil samples. An asterisk indicates the significance of the respective correlation coefficient at a level of $P < 0.05$.

	N ₂ O	Fe	Mn	C	N	C/N	pH	NO ₂ ⁻	NH ₄ ⁺	NO ₃ ⁻	DOC	DTN	A ₂₅₄
N ₂ O	1.00												
Fe	0.12	1.00											
Mn	-0.28	0.43	1.00										
C	0.53	-0.33	-0.58	1.00									
N	0.55	-0.09	-0.44	0.91*	1.00								
C/N	-0.02	-0.25	-0.19	0.64	0.43	1.00							
pH	-0.28	0.36	0.62	-0.88*	-0.81*	-0.67*	1.00						
NO ₂ ⁻	0.72*	0.08	0.03	0.50	0.64*	-0.10	-0.15	1.00					
NH ₄ ⁺	0.62	-0.30	-0.57	0.82*	0.75*	0.40	-0.84*	0.42	1.00				
NO ₃ ⁻	0.43	-0.01	-0.20	0.81*	0.85*	0.48	-0.77*	0.48	0.74*	1.00			
DOC	0.53	-0.44	-0.70*	0.88*	0.82*	0.47	-0.93*	0.34	0.92*	0.68*	1.00		
DTN	0.47	-0.33	-0.53	0.84*	0.70*	0.64	-0.90*	0.24	0.95*	0.77*	0.88*	1.00	
A ₂₅₄	0.28	-0.62	-0.68*	0.75*	0.57	0.62	-0.88*	0.03	0.81*	0.45	0.91*	0.85*	1.00

7.3.6 Isotopic ratio analyses of N₂O production during rewetting

The $\delta^{15}\text{N}^{\text{bulk}}$ and $\delta^{18}\text{O}$ varied from -42.4 to -24.0‰ and from 9.7 to 32.0 ‰, respectively, for all the soil samples during rewetting, except for soil F3 where $\delta^{18}\text{O}$ was extremely high with a value of 110.6 ‰ (Table 7.5). Both $\delta^{15}\text{N}^{\text{bulk}}$ and $\delta^{18}\text{O}$ decreased with increasing incubation

Table 7.5 ¹⁵N site preference (SP) values of N₂O production (peak height) upon water rewetting with different soil samples and incubation time. The peak height of ambient air and 400 ppb standard N₂O gas was about 1.9 and 2.4 nA, respectively.

Samples	Soil (g)	Incubation time (h)	Peak height (nA)	$\delta^{15}\text{N}^{\text{bulk}}$	$\delta^{18}\text{O}$	SP [‰]
				[‰ vs. air-N ₂]	[‰ vs. VSMOW]	
F _{of}	1.4	6	3.8	-24.0	29.3	1.6
F ₁	1.4	6	2.6	-24.8	32.0	-15.4
F ₃	1.4	6	4.3	-35.6	110.6	2.4
F ₄	2.8	6	3.2	-28.6	24.8	2.4
F ₅	2.8	6	2.3	-42.4	16.0	9.9
F ₆	2.8	6	5.1	-35.7	13.5	-1.0
G	2.8	0.5	11.1	-28.4	12.7	-0.3
G	2.8	3.5	25.7	-33.8	10.4	-1.6
G	2.8	6.5	31.1	-35.1	9.7	-2.1
G (Sterilized)	2.8	0.5	8.5	-24.6	11.7	1.3
G (Sterilized)	2.8	3.5	51.5	-27.0	9.9	-0.3
G (Sterilized)	2.8	6.5	64.9	-29.0	10.9	-0.7

time for the grassland soil, no matter the soil was treated with γ -irradiation in advance or not. Similar ranges of $\delta^{15}\text{N}^{\text{bulk}}$ values were observed for the grassland and forest soils, while $\delta^{18}\text{O}$ of N₂O was higher from the forest soil than from the grassland soil. The SP values of the N₂O

formed after rewetting were close to zero for most of the soil samples (except for F5), independent of the amount of N₂O produced, as indicated by the peak height (Table 7.5), of incubation time and of the sterilization treatment. For the forest soil samples, the SP values ranged between -15.9 and 9.9‰. The SP values for the grassland soil samples ranged from -2.1‰ to 1.3‰ for both γ -irradiated and non-irradiated samples, even though the N₂O production increased largely with incubation time.

7.4 Discussion

Soil rewetting-induced N₂O production has received a lot of attention in recent years due to the potentially large contribution of this fraction of N₂O to the annual N₂O flux (Priemé & Christensen, 2001; Kim *et al.*, 2012; Berger *et al.*, 2013). This rewetting effect was shown to be highly variable in different ecosystems. In this study, we collected soil samples from upland and riparian forest, grassland and cropland and simulated drying and rewetting with either pure water or aqueous solutions with different N substrates (NH₄⁺, NO₂⁻, and NO₃⁻), quantified the N₂O pulses upon rewetting in the different soil samples and identified the main governing factor responsible for the rewetting effect on N₂O production. Our study demonstrated that grassland soil responded to rewetting with pure water most rapidly and had the largest N₂O production in the first hour after rewetting compared to upland forest, riparian forest and cropland soil samples (Fig. 7.2). Nearly 64 $\mu\text{g N}_2\text{O-N kg}^{-1}$ dry soil was emitted from an air-dried grassland soil sample in only 1 hour without γ -irradiation after rewetting (Fig. 7.2). However, seasonal variation, e.g. winter and summer, might have an influence on the N₂O production in different ecosystems (Flessa *et al.*, 1995; Kiese *et al.*, 2003). The collected forest soils could have been affected more by dry summer conditions, leading to more accumulated substrate and certain microorganisms that are resistant to the drying conditions (Bouskill *et al.*, 2013). Therefore, N₂O production during rewetting events could have been overestimated in the forest soil samples compared to the cropland and grassland soils. However, overall our finding was in accordance with the results of Priemé & Christensen (2001) that a greater emission of N₂O was observed upon rewetting of soil from grassland sites compared to arable and forest sites in Germany, Sweden and Finland.

Knowledge about the exact mechanisms and influencing factors of the large N₂O formation upon rewetting from dry soils are still limited. However, soil basic properties, such as C

content, pH and inorganic N content, as well as the soil texture and soil microbial composition were demonstrated to play important roles in the pulse production of N_2O upon rewetting (Ruser *et al.*, 2006; Beare *et al.*, 2009; Harrison-Kirk *et al.*, 2013). In our study, there was a large variation of soil pH, C, N, metal element and inorganic N (NO_3^- and NH_4^+) content between the different soil samples. Generally, forest soils exhibited the largest soil C content (19.8-45.7%) and the lowest soil pH (2.85-3.92) compared to riparian, grassland and cropland soils. Harrison-Kirk *et al.* (2013) reported that more N_2O was produced in soil samples with high soil organic C content. However, in our study the N_2O production from the grassland (with less soil C) was larger than from the forest soil samples (with larger soil C content). Ruser *et al.* (2006) reported that soil compaction and high NO_3^- content were two important factors responsible for the rewetting-induced N_2O production in a cropland soil, as more anoxic sites could develop when water was added to compacted soils. In this study, air-dried grassland soil (1.09 g cm^{-1}) had a much higher bulk density compared to forest soil (0.83 g cm^{-1}) according to former research on these sites (Baatz *et al.*, 2014), which may be one reason for the immediate and large N_2O emission upon rewetting for the grassland soil.

High soil NO_3^- content has been considered as one important factor responsible for rewetting-induced N_2O production, as NO_3^- would favor N_2O production from denitrification (Ruser *et al.*, 2006). During the drying process, soil NO_3^- may accumulate due to the higher resistance of nitrifiers to water limitation compared to denitrifiers (Avrahami *et al.*, 2003; Szukics *et al.*, 2010). In this study, we also observed an increase of soil NO_3^- content with air-drying for all forest soil samples, but not for the grassland and cropland soils (Fig. 7.1). However, there was no significant correlation between soil NO_3^- content of air-dried soil and N_2O production upon rewetting (Table 7.4), and NO_3^- addition did not induce N_2O emission significantly (Fig. 7.2C), which is in accordance with Venterea (2007). These findings indicate that NO_3^- accumulation was not the main contributor to the large N_2O production upon rewetting to around 40% WHC, as done in this study. We assumed that this relatively low water content may favor the N_2O production from nitrification, but addition of NH_4^+ only increased the N_2O production from one forest soil sample (F6), and had no stimulatory effects on the other soil samples.

Soil NO_2^- accumulation has been considered as another important factor for soil N_2O pulse production after rewetting (Davidson, 1992; Venterea, 2007), although NO_2^- was commonly not detected after soil air-drying in previous studies. In this study, where we used a new NO_2^-

extraction method, developed by Homyak *et al.* (2015), which allows to extract NO_2^- at elevated pH, we found detectable NO_2^- concentration levels in air-dried samples F_{Of}, F3 and F6, but no NO_2^- was detectable in the air-dried soil samples F4, F2 and riparian forest.

Despite the low amount of NO_2^- accumulated, a close correlation between NO_2^- content in the air-dried soil and the amount of N_2O produced after rewetting was found (Table 7.4). Addition of NO_2^- also increased soil N_2O production largely within the first hour after rewetting in all the soil samples (Fig. 7.2B). The exact reason responsible for the variation in NO_2^- content among the different soil samples remains unclear, but correlation analysis showed that the NO_2^- concentration was positively correlated with total soil N content (Table 7.4), but had no correlation with soil NO_3^- and NH_4^+ concentrations. There are mainly two sources involved in the release of soil C and N during the rewetting process: (1) disruption of soil aggregates by rapid water addition; (2) the proportion of microorganism died back during drying or by dehydration or cell lysis, and the associated release of labile intracellular substrates with rewetting. Previous study showed that NO_2^- produced from organic N is an important NO_2^- pool in grassland soil (Müller *et al.*, 2006). Therefore, the NO_2^- could originate from soil aggregate (< 2 mm in this study) disruption or the release of labile intracellular substrates during microbial cell lysis.

There are mainly two pathways responsible for the NO_2^- -mediated N_2O production: (1) biological nitrifier-denitrification and denitrification; (2) chemical reactions with organic matter and metal ions (e.g. Fe^{2+}). Stevenson & Swaby (1964) showed that N_2O is chemically produced following NO_2^- addition to acidic soil organic matter fractions. Samarkin *et al.* (2010) found abiotic reactions between NO_2^- and Fe^{2+} -containing minerals derived from the surrounding igneous Ferrar Dolerite, contributing to the N_2O emission from the hypersaline Don Juan Pond in Antarctica. We also explored the contribution of abiotic reactions to NO_2^- -mediated N_2O production during rewetting by sterilizing the soil with a dose of 11 kGy of γ -irradiation. Our results showed a large variability of the effect of γ -irradiation on soil N_2O production in the different soil samples (Table 7.3). In general, γ -irradiation inhibited N_2O production from the forest and riparian soil samples, with the largest inhibition in the soil sample with the fermented organic layer (F_{Of}, 91.1%) and smallest inhibition in soil sample F2 (28%). The range of inhibition by γ -irradiation was consistent with the range reported by Venterea (2007), who also found that N_2O production in γ -irradiated cultivated and

uncultivated soils was 75%, 60% and 31% of N_2O production of their nonsterile counterparts, respectively.

The small effects of γ -irradiation on soil CO_2 emissions in the forest soils were unexpected, as we assumed that negligible CO_2 would be produced in the γ -irradiated soils. One reason responsible for the produced CO_2 could be due to the limited effect of γ -irradiation on soil certain microorganisms, mainly spore forming fungi, even though γ -irradiation is suggested to be highly effective and preferable compared to other sterilization methods due to its smaller effect on soil chemical and physical properties (Stroetmann *et al.*, 1994). Therefore, γ -irradiation might have changed microbial community structure towards a strong fungal dominance, contributing only partially to N_2O production after rewetting in certain forest soil samples (e.g. F1 and F2). However, chemical reactions, e.g. nitrosative decarboxylation reactions, could also produce CO_2 chemically (Thorn & Mikita, 2000), as no microbial growth was detected by plating of the γ -irradiated soil slurries in this study. In contrast, in the grassland and cropland soil samples γ -irradiation increased soil N_2O production threefold and twofold, respectively, even though CO_2 emission was reduced by about 50% after γ -irradiation (Table 7.3). The stimulatory effect of γ -irradiation on N_2O production in the grassland soil samples was surprising, but could indicate an increased contribution of an abiotic mechanism of N_2O production from NO_2^- . It is possible that the death of certain microorganisms by γ -irradiation may have stimulated the activity of other microorganisms that have an exceptionally high production rate of N_2O after rewetting, which might explain the threefold higher N_2O production from the grassland soil after γ -irradiation, but this assumption remains speculative. In contrast, a contribution of abiotic processes to soil N_2O production in the grassland soils seems more likely as γ -irradiation could alter organic matter structure or functional groups involved in nitrosation reactions, which could promote abiotic N_2O production (Venterea, 2007). But still this is at odds with the reduced N_2O formation in the γ -irradiated forest soil samples. Therefore, further research is needed towards elucidating the mechanisms behind stimulation and inhibition of N_2O production from nitrite after γ -irradiation of the different soil samples.

Finally, we measured the isotopic signatures ($\delta^{15}\text{N}^{\text{bulk}}$, $\delta^{18}\text{O}$ and SP values) of N_2O formed during rewetting, as they are thought to reflect the relative contribution of different N_2O sources to certain extent (Yoshida & Toyoda, 2000). There have been a number of recent studies examining N_2O SP from chemodenitrification (Heil *et al.*, 2014; Jones *et al.*, 2015;

Buchwald *et al.*, 2016; Grabb *et al.*, 2017). The measured $\delta^{15}\text{N}^{\text{bulk}}$ in this study falls within the range of denitrification (-40 to -19‰) in pure cultures (Toyoda *et al.*, 2005; Toyoda *et al.*, 2017), while the $\delta^{18}\text{O}$ values were in the range of N_2O produced via nitrification in soils (Snider *et al.*, 2012). SP values have been considered as a more useful tool for N_2O source partitioning than $\delta^{15}\text{N}^{\text{bulk}}$ and $\delta^{18}\text{O}$, since the SP values were found relatively stable for N_2O production from different soil processes, although there was still some overlap found between aerobic nitrification, fungal denitrification and NH_2OH oxidation (Sutka *et al.*, 2006; Heil *et al.*, 2014; Rohe *et al.*, 2014), and denitrification and nitrifier-denitrification (Sutka *et al.*, 2006). In this study, the SP values were close to 0‰ for most of the soil samples after rewetting, except for F5, no matter whether the soils were sterilized by γ -irradiation or not (Table 5), which falls within the SP range (-10...0‰) reported for bacterial denitrification including nitrifier denitrification (Sutka *et al.*, 2006). Snider *et al.* (2015) reported that nitrifier denitrification became a more dominant N_2O source following a rain event in cropland soils by using the $\delta^{15}\text{N}$ of N_2O in their study. In our study, since the addition of NO_3^- did not increase N_2O production significantly and since there was no significant correlation between NO_3^- and N_2O , it was more likely that denitrification by nitrifiers was the dominant contributor of N_2O production during rewetting. However, as we observed a similar SP for sterile and unsterile soil samples, and since previous studies showed that SP values of N_2O production from NO_2^- -mediated chemodenitrification varied widely from -45‰ to 26.5‰ from chemical reactions or soil samples (Samarkin *et al.*, 2010; Peters *et al.*, 2014; Jones *et al.*, 2015; Buchwald *et al.*, 2016; Grabb *et al.*, 2017; Wei *et al.*, 2017a,b), it is likely that also abiotic reactions have contributed substantially to soil N_2O production after soil rewetting.

7.5 Conclusions

Soils from different ecosystems demonstrate various N_2O emissions after rewetting, with grassland soil exhibiting the largest N_2O emissions while cropland and riparian soils showing the smallest N_2O emissions. Among different soil basic properties, soil NO_2^- content was the only significant factor correlated with soil N_2O production. Addition of NO_2^- increased N_2O emissions the most, compared to NH_4^+ and NO_3^- . Although biological reactions might play an important role in N_2O production in the different soil samples, the role of abiotic processes in N_2O formation during the rewetting event cannot be excluded.

Chapter 8

Synopsis, Synthesis & Perspectives

8.1 Synopsis

This thesis was laid out to characterize the abiotic processes of N_2O production in soils involving NH_2OH and NO_2^- , assuming a coupled biotic-abiotic mechanism. The abiotic N_2O formation processes involving NO_2^- have been studied for decades, but are still not well understood, while the N_2O production involving NH_2OH has been widely neglected in most current studies. The first part of the thesis was a general introduction of the current state of knowledge about these coupled biotic-abiotic mechanisms. The experiments conducted in this thesis mainly focused on the proof of NH_2OH release during NH_3 oxidation by ammonia oxidizers, determination of NH_2OH in natural soils, the relationship between NH_2OH and aerobic N_2O production in a forest ecosystem, factors governing abiotic N_2O production from NH_2OH , and the comparison of the roles of NH_2OH and NO_2^- in abiotic N_2O production and (especially for NO_2^-) in pulse N_2O production during rewetting events in soils.

The second chapter of this thesis was an experiment which aimed at exploring the possibility of NH_2OH release by various chemolithoautotrophic ammonia oxidizers (AOB, AOA and comammox). It was observed that certain AOB and AOA as well as the comammox indeed released NH_2OH during NH_3 oxidation. The type of medium, culture incubation temperature and the presence of NO_2^- were found to affect NH_2OH decomposition and abiotic N_2O production during NH_3 oxidation. The NH_2OH :final product ratio varied considerably (0.24-1.92%) dependent on the culture type and NH_4^+ concentration, with the largest ratio observed during the NH_3 oxidation of comammox. Overall, the fractions of NH_4^+ converted to N_2O via NH_2OH release during incubations ranged from 0.05% to 0.14%, and were consistent with published NH_4^+ -to- N_2O conversion ratios for certain ammonia oxidizers. NO_2^- played an important role in abiotic decay of NH_2OH and conversion of NH_2OH to N_2O during NH_3 oxidation, with negative effects on the abiotic NH_2OH decay, but positive effects on the abiotic N_2O production.

After proving the existence of NH_2OH release in chemoautotrophic ammonia oxidizers during NH_3 oxidation, in the second experiment, presented in chapter three, a method for the determination of NH_2OH in natural soils was newly developed and successfully applied. The determination of NH_2OH in natural soil samples had not been possible before due to the highly reactive nature of NH_2OH . Only with the fast extraction and determination method newly developed in this work was it possible for the first time to detect NH_2OH in soils. The method allowed extraction of NH_2OH from a spruce forest soil with acidic solution (pH = 1.7)

and 10 min magnetic stirring. This highly sensitive NH_2OH determination method was based on the oxidation of NH_2OH to N_2O with Fe^{3+} at $\text{pH} = 3$ in glass vials and analysis of N_2O formed in the vial headspace with GC. NO_2^- at concentrations larger than $10 \mu\text{M}$ could bias this method, but the addition of 2 mM sulfanilamide was found to remove the effect of even $100 \mu\text{M}$ NO_2^- effectively. By using this newly developed method, the NH_2OH concentration in the spruce forest soil samples determined with this new method ranged from 0.3 to $34.8 \mu\text{g N kg}^{-1}$ dry soil, which is comparable with the NO_2^- concentration in the forest soil samples.

A further experiment, described in the fourth chapter, studied the spatial variability of NH_2OH content and potential N_2O emission rates of humic organic (Oh) and mineral (Ah) soil layers of a Norway spruce forest, using the developed analytical method for the determination of soil NH_2OH content described in chapter three, combined with a geostatistical Kriging approach. Potential soil N_2O emission rates were determined in laboratory incubations under oxic conditions. Soil basic properties, such as C, N, pH, Mn, Fe, and mineral N (NH_4^+ and NO_3^-) were also analyzed. The results demonstrated that the soil N_2O emission rates were spatially highly correlated with soil NH_2OH content. The hotspots of soil N_2O emission rates in the forest were the same or similar as those of soil NH_2OH content. According to the multiple regression models developed for the two soil horizons, soil NH_2OH content contributed to soil N_2O emission rates the most, followed by soil NO_3^- and Mn content. The addition of the co-variable information of soil NH_2OH and NO_3^- content improved the Kriging map of soil N_2O emission rates in the study area markedly.

The fifth chapter presents an experiment testing a conceptual model of abiotic N_2O formation from NH_2OH released to the soil matrix by changing relevant soil environmental factors determined in the previous experiment with natural soil, i.e. pH, SOM and MnO_2 content, in artificial soil mixtures. The three factors were shown to indeed affect abiotic conversion of NH_2OH to N_2O interactively. High SOM content lowered the abiotic N_2O formation from NH_2OH , while a higher MnO_2 content increased the abiotic conversion of NH_2OH to N_2O . Lower pH stimulated abiotic N_2O formation from NH_2OH by MnO_2 , but made NH_2OH more stable in the absence of MnO_2 . The multiple regression model set up with the three factors could explain 62% of the abiotic conversion of NH_2OH to N_2O . Further work revealed that also SOM quality, and not just SOM quantity, played an important role in the abiotic NH_2OH oxidation to N_2O . Soil SOM with more carbonyl groups or phenolic compounds would bind

more NH_2OH , leading to less N_2O production compared to soil SOM with fewer carbonyl groups and phenolic compounds.

The subsequent experiment, presented in chapter six, studied the abiotic N_2O production process by comparing the role of the two nitrification intermediates NH_2OH and NO_2^- in soils from three ecosystems (forest, grassland, and cropland) with oxic or anoxic pre-incubation. Fresh soil samples were incubated under oxic or anoxic conditions prior to the main experiment for one week and then freeze-dried. Gamma radiation was applied to half of the freeze-dried soil samples, followed by the addition of NH_2OH and NO_2^- . The experiment revealed that NO_2^- played an important role in the N_2O production in grassland soil, followed by the forest and cropland soils, while NH_2OH played an important role in the N_2O production in cropland soil, followed by the grassland and forest soils. The contribution of NO_2^- to N_2O production was mostly biotic, while the contribution of NH_2OH on N_2O production was mainly abiotic, particularly in soil samples with large Mn content and low soil SOC content. The anoxic pre-incubation increased the N_2O production from NO_2^- shortly after NO_2^- addition, but decreased the N_2O production from NH_2OH greatly. Moreover, the effect of anoxic pre-incubation was dependent on SOC content. In cropland soil with lower SOC, the effect of anoxic pre-incubation on N_2O production from NH_2OH was the least.

The last experiment, presented in chapter seven, explored the mechanism of large pulse N_2O production caused by rewetting in soils from three ecosystems (forest, grassland, and cropland), involving the nitrification intermediates NO_2^- and NH_2OH . Since NH_2OH is not likely to accumulate in soils during the drying process due to its very reactive nature, the accumulation of NO_2^- during air-drying and the effect of NO_2^- addition on N_2O production during rewetting was explored in this experiment. The results demonstrated that grassland soil exhibited the largest pulse N_2O production after rewetting, followed by forest and cropland soils. The N_2O production during rewetting was positively correlated with NO_2^- concentration of the air-dried soils, and the addition of NO_2^- to air-dried soil samples increased N_2O production the most compared to NH_4^+ and NO_3^- addition.

8.2 Synthesis

In this thesis, a series of experiments were designed and conducted, providing strong evidence that NH_2OH -related abiotic processes are important contributors to N_2O production during nitrification in pure nitrifier cultures as well as in natural soils. Soil basic properties, such as SOC and Mn content as well as pH, affect the N_2O production via NH_2OH during nitrification. The other nitrification intermediate, NO_2^- , also played an important role in soil N_2O production, especially during rewetting events. With the obtained results, the presence of coupled biotic-abiotic mechanisms of N_2O production during nitrification in natural soils has been proved and elucidated.

The first experiment, as presented in chapter two, proved the possibility of NH_2OH release in certain AOB, AOA and the comammox and gave strong evidence for a substantial contribution of a coupled biotic-abiotic mechanism involving NH_2OH to N_2O production during NH_3 oxidation. Although the determination of NH_2OH concentration from one AOB culture *Nitrosomonas europaea* had been conducted in several former studies (Stüven *et al.*, 1992; Yu & Chandran, 2010), the experiment in this thesis showed the variability of NH_2OH release in various AOB. For example, more NH_2OH excretion was observed in *Nitrosospira multiformis*, while no NH_2OH release was observed in *Nitrosomonas communis* and *Nitrosomonas nitrosa*. The exact reason responsible for the variability of NH_2OH release capacity remains unclear, but these results may indicate a versatile contribution of NH_2OH to abiotic N_2O production in different ecosystems. For the first time, this experiment also showed the NH_2OH release capacity in AOA. AOA have received increasing attention regarding nitrification-related N_2O production due to the observed N_2O production capacity of several AOA strains (Jung *et al.*, 2014; Stieglmeier *et al.*, 2014) and an AOA abundance that exceeds that of AOB by orders of magnitude in certain ecosystems (Leininger *et al.*, 2006; He *et al.*, 2007) in recent years. The observation of NH_2OH release in one AOA pure culture and one AOA enrichment showed that N_2O production in AOA could also stem from the well-known chemical reaction between NH_2OH and NO_2^- . Even though the NH_2OH :final product ratios were smaller than 1% for most of the cultures except comammox, the released amount of NH_2OH cannot be ignored considering the fact that the total N_2O production from N fertilizer application is around 1% (De Klein *et al.*, 2006) via both pathways of nitrification and denitrification. NH_3 oxidation can contribute above 80% to soil N_2O emissions under certain conditions, which means that up to 0.8% of the added N would be lost as N_2O through

the NH_3 oxidation process. The total NH_2OH :final product excretion ratio of the soil NH_3 oxidizer *N. multiformis* was found to be as high as 0.6%. If the conversion of NH_2OH to N_2O can reach 80%, which is realistic for certain soil samples containing large amounts of oxidants, e.g., Mn, a relatively low pH and a relatively small amount of SOC (Liu *et al.*, 2017a), the contribution of NH_2OH to N_2O formation could be around 0.5% after N application.

Before the second experiment, no successful attempt to extract NH_2OH from natural soil samples had been reported, probably due to the reactive nature of NH_2OH . Different extraction conditions – such as temperature, pH, extraction method and time – may affect the determination of NH_2OH concentrations. As NH_2OH decomposes faster at neutral and alkaline conditions, the acidic condition is beneficial for the conservation of NH_2OH . The results of this experiment indeed showed a quick turnover of NH_2OH during the extraction process. With water, instead of acid (pH = 1.7) solution, no NH_2OH could be extracted, indicating the strong reactivity of NH_2OH at neutral or alkaline conditions, as NH_2OH reacts with a range of soil constituents, such as SOM, Mn oxides and ferric iron (Bremner *et al.*, 1980). Moreover, it has been known that a high NO_2^- concentration can bias the determination of NH_2OH in water samples by the well-known hybrid reactions between NO_2^- and NH_2OH (Kock & Bange, 2013). This experiment proved the effectiveness of application of sulfanilamide for removing the NO_2^- effect on NH_2OH determination in soil samples. Another interesting result in this experiment was that even though the NH_2OH concentrations measured in the forest samples were approximately three orders of magnitude lower than the concentrations of ammonium and nitrate, they were still comparable to common concentration values of nitrite in soil.

A further experiment was carried out to apply the newly developed NH_2OH determination method combined with GC microincubation for the analysis of the relationship between soil NH_2OH content and aerobic N_2O production in a Norway spruce forest ecosystem with high spatial heterogeneity. This forest ecosystem was characterized by various topographic conditions, with slope and elevation ranging between 0.75–8.27% and 595–627 m, respectively, in the sampling area of this study. Besides, one small creek flowed through the study site, which made the ecosystem more complex. The complexity of the ecosystem with its upland and wetland soil areas allowed the identification of hotspots of NH_2OH concentration, which were similar to the hotspots of aerobic N_2O production rates, indicating a close correlation between the two parameters.

There are mainly two potential pathways for the oxidation of NH_2OH to N_2O : the biological reaction by the enzyme HAO or methanotrophic bacteria, and the chemical oxidation by nitrite or redox active metal cations (Bremner, 1997; Campbell *et al.*, 2011; Stein, 2011). The redox reaction between NH_2OH and Mn^{4+} ($2 \text{MnO}_2 + 2 \text{NH}_2\text{OH} \rightarrow 2 \text{MnO} + \text{N}_2\text{O} + 3 \text{H}_2\text{O}$) has been demonstrated to play an important role in soil N_2O emissions (Bremner, 1997). In this study, by using multiple regression analysis, we also found that Mn was an important factor explaining N_2O emission rates despite a much higher Fe concentration in the forest soils, emphasizing the importance of the oxidation of NH_2OH by MnO_2 to N_2O in soil, which is due to the higher position of the $\text{Mn}^{4+}/\text{Mn}^{2+}$ pair in the redox chain compared to $\text{Fe}^{3+}/\text{Fe}^{2+}$. Moreover, this experiment in this thesis provided a supporting tool to elucidate key control variables of soil N_2O emission that can be relatively easily measured, to determine these variables and to calculate the respective N_2O emission rates for the different sampling points.

From the former experiments, several control factors, i.e. SOC content (or more specifically C/N ratio), pH and Mn content, were assumed to affect the abiotic N_2O production involving NH_2OH . The conceptual model hypothesized that the released NH_2OH would react with different soil constituents, e.g. SOM and MnO_2 . At higher pH, unprotonated NH_2OH would react more readily with carbonyl groups of SOM, leading to oxime formation and making NH_2OH less available for oxidation to N_2O by MnO_2 . Lower soil pH would lead to increased protonation of NH_2OH , making NH_2OH more stable against the reaction with carbonyl groups of SOM and more prone to the reaction with MnO_2 , leading to higher N_2O formation from the same amount of NH_2OH . The results of chapter five verified this conceptual model, and the interactive effects of the major control factors of abiotic N_2O formation from NH_2OH in soil, i.e. MnO_2 content, pH and OM quantity and quality, could be quantified by developing a regression model.

Although previous papers reported the importance of NO_2^- and NH_2OH on soil N_2O emissions separately (Bremner *et al.*, 1980; Venterea, 2007; Heil *et al.*, 2015), according to our knowledge no study has tried to compare the contribution of the two reactive N compounds on soil N_2O emissions at the same time, with consideration of different soil types, biological and abiotic processes, and redox history. The results of the sixth experiment also proved the former studies that abiotic NH_2OH -to- N_2O conversion is positively correlated with soil Mn content, but negatively correlated with SOC content. However, since most of the N_2O produced from NO_2^- came from the biotic pathway, soil properties that can stimulate the

microbial or enzyme activity in soils would be more important for N₂O production from NO₂⁻. However, the stimulating factors for N₂O production from NO₂⁻ could still not be fully identified in this study. Moreover, this study also showed that redox conditions are important for the contribution of these two reactive nitrification intermediates to N₂O production. When soil is at a reduced state, more reduced metal ions, e.g. Mn²⁺ and Fe²⁺, as well as DOC will be released, which would bind with NH₂OH and lead to less N₂O production from this pathway. However, a reduced state of soil would probably increase the contribution of N₂O from NO₂⁻ by increasing the abiotic reactions between NO₂⁻ and reduced iron.

Since it is unlikely that NH₂OH would accumulate during soil drying because of its very reactive nature, especially at dry conditions, the last experiment only studied the contribution of NO₂⁻, NO₃⁻ and NH₄⁺ on soil N₂O production during rewetting. The results of this experiment showed a positive and significant correlation between the NO₂⁻ concentration in the air-dried soil samples at the time of rewetting and the soil N₂O production after rewetting. Moreover, the effect of the biotic and abiotic processes on the N₂O produced from NO₂⁻ was dependent on soil types. Gamma radiation confirmed that abiotic processes contributed about 20-30% of N₂O production from NO₂⁻ during rewetting of forest soil samples, while for the grassland soil an even higher N₂O production was found after the gamma-radiation treatment.

8.3 Perspectives

Through the experiments of this thesis, a clearer picture of the coupled biotic-abiotic mechanisms of N₂O production during nitrification could be developed. Thus, the results of the thesis can help to extend our current understanding of the biotic and abiotic N₂O production mechanisms and improve the estimation of N₂O emissions in different soils under different environmental conditions. However, a range of questions are still left open due to the finite time that was available for this dissertation:

8.3.1 The release of NH₂OH during NH₃ oxidation in ammonia oxidizers enriched from different soils in various ecosystems

Even though this dissertation has demonstrated the existence of NH₂OH release in various chemoautotrophic ammonia oxidizers, only two of the studied AOB were enriched from soils. In addition, NH₂OH release has not been observed in the two newly enriched soil AOA strains (*Ca. Nitrosotalea* sp. Nd2 and *Nitrososphaera viennensis*). Recent research demonstrated that the range of ¹⁵N site preference (SP) values, one promising indicator to partition the sources of N₂O production, of soil AOA strains was 13-30‰ (Jung *et al.*, 2014), indicating that N₂O production from soil AOA may originate from different production pathways, leaving the question about the importance of the coupled biotic-abiotic mechanism of N₂O production in soil AOA open. Moreover, other microorganisms, such as heterotrophic nitrifiers, fungal denitrifiers and methanotrophic (methane-oxidizing) bacteria may play a crucial role in NH₃ oxidation in certain ecosystems (Stein, 2011; Rohe *et al.*, 2014; Zhang *et al.*, 2015b). However, NH₂OH release rates have not been determined yet for these microorganisms. Moreover, even though the N₂O production from the coupled biotic-abiotic mechanisms has been estimated in this dissertation, further studies should quantify the real N₂O production during NH₃ oxidation in pure cultures and compare the N₂O production rate with the calculated N₂O production rate by the coupled biotic-abiotic mechanism. The importance of this mechanism in N₂O production during NH₃ oxidation in pure cultures should also be further studied under different environmental conditions, e.g. different levels of O₂ availability and pH.

8.3.2 The importance of the coupled biotic-abiotic mechanisms in soil of other ecosystems

This dissertation has demonstrated the possibility of NH_2OH analysis and a positive correlation between NH_2OH concentration and aerobic N_2O production in spruce forest soil. However, the determination of NH_2OH in other soils is still necessary to fully elucidate the importance of this mechanism of N_2O production in general. Moreover, soil environmental factors, such as pH, MnO_2 and SOC content have been demonstrated as important contributors to the coupled biotic-abiotic mechanism based on the studies on one grassland, cropland and various soils from a spruce forest. Further studies are needed, though, to refine the regression model of the abiotic conversion of NH_2OH to N_2O by considering the three factors (pH, MnO_2 and SOC) in other soils.

In addition, the role of NO_2^- in the coupled biotic-abiotic mechanism and the impact factors of NO_2^- -related abiotic N_2O production in soils could not be fully elucidated in this dissertation. Although the importance of NO_2^- in abiotic N_2O production, also called chemodenitrification, has been noticed for a long time, and number of studies have been carried out (van Cleemput & Samater, 1995; Venterea, 2007; Müller *et al.*, 2014), the exact mechanisms, such as the role of chemical properties of SOM, pH and metal ions in chemodenitrification are still not fully understood. Further studies should also develop a model, like the one developed in this dissertation, with consideration of soil basic properties and environmental factors for both NH_2OH and NO_2^- -related abiotic N_2O production.

8.3.4 Developing effective measures to mitigate soil N_2O emissions considering the mechanism of coupled biotic-abiotic N_2O production in soils

Currently, measures to mitigate soil N_2O emissions are mainly dependent on biological N_2O production pathways, such as inhibiting the enzyme activity of NOR and AMO. However, the mechanism of coupled biotic-abiotic production can provide a new stimulus for the development of N_2O mitigation measures by changing the reaction conditions between NH_2OH , NO_2^- and soil constituents. For example, increasing pH has been shown as an effective measure to reduce N_2O emissions in certain ecosystems by increasing the nitrous oxide reductase activity. However, increasing soil pH can also decrease the chemical production of N_2O from NH_2OH , but foster the production of N_2 and NO_2^- . Addition of organic soil amendments with suitable functional groups (e.g., carbonyl groups) to soils,

accompanied by the application of ammonia fertilizer, could potentially lead to a higher binding rate of released NH_2OH to SOM, thereby reducing the availability of NH_2OH for chemical oxidation to N_2O during nitrification. However, addition of organic soil amendments could also increase the activity of denitrifiers, which in turn could lead to an increase in N_2O production from denitrification. Thus, further studies on the potentially counteractive effects of soil management options on the range of biotic and abiotic N_2O production pathways in soils are needed to develop more effective N_2O mitigation measures.

References

- Achtnich, C., Bak, F. and Conrad, R. (1995). Competition for electron donors among nitrate reducers, ferric iron reducers, sulfate reducers, and methanogens in anoxic paddy soil. *Biology and Fertility of Soils*, **19**, 65-72.
- Ahmed, S. and De Marsily, G. (1987). Comparison of geostatistical methods for estimating transmissivity using data on transmissivity and specific capacity. *Water Resources Research*, **23**, 1717-1737.
- Akaike, H. 1998. A new look at the statistical model identification. In: *Selected Papers of Hirotugu Akaike* (eds. Parzen, E., Tanabe, K. & Kitagawa, G.), pp. 215-222. Springer New York.
- Ambus, P., Zechmeister-Boltenstern, S. and Butterbach-Bahl, K. (2006). Sources of nitrous oxide emitted from European forest soils. *Biogeosciences*, **3**, 135-145.
- Arnold, P.W. (1954). Losses of nitrous oxide from soil. *European Journal of Soil Science*, **5**, 116-128.
- Avrahami, S., Liesack, W. and Conrad, R. (2003). Effects of temperature and fertilizer on activity and community structure of soil ammonia oxidizers. *Environmental Microbiology*, **5**, 691-705.
- Baatz, R., Bogaen, H.R., Hendricks Franssen, H.J., Huisman, J.A., Qu, W., Montzka, C. and Vereecken, H. (2014). Calibration of a catchment scale cosmic-ray probe network: A comparison of three parameterization methods. *Journal of Hydrology*, **516**, 231-244.
- Baggs, E.M. (2008). A review of stable isotope techniques for N₂O source partitioning in soils: recent progress, remaining challenges and future considerations. *Rapid communications in mass spectrometry*, **22**, 1664-1672.
- Baggs, E.M. (2011). Soil microbial sources of nitrous oxide: recent advances in knowledge, emerging challenges and future direction. *Current Opinion in Environmental Sustainability*, **3**, 321-327.
- Bakken, L.R., Bergaust, L., Liu, B. and Frostegård, Å. (2012). Regulation of denitrification at the cellular level: a clue to the understanding of N₂O emissions from soils. *Philosophical Transactions of the Royal Society B: Biological Sciences*, **367**, 1226-1234.
- Bateman, E. and Baggs, E. (2005). Contributions of nitrification and denitrification to N₂O emissions from soils at different water-filled pore space. *Biology and Fertility of Soils*, **41**, 379-388.
- Beare, M., Gregorich, E. and St-Georges, P. (2009). Compaction effects on CO₂ and N₂O production during drying and rewetting of soil. *Soil Biology and Biochemistry*, **41**, 611-621.
- Berger, S., Jung, E., Köpp, J., Kang, H. and Gebauer, G. (2013). Monsoon rains, drought periods and soil texture as drivers of soil N₂O fluxes – Soil drought turns East Asian temperate deciduous forest soils into temporary and unexpectedly persistent N₂O sinks. *Soil Biology and Biochemistry*, **57**, 273-281.
- Berns, A.E. and Conte, P. (2011). Effect of ramp size and sample spinning speed on CPMAS ¹³C NMR spectra of soil organic matter. *Organic Geochemistry*, **42**, 926-935.
- Bhatia, A., Sasmal, S., Jain, N., Pathak, H., Kumar, R. and Singh, A. (2010). Mitigating nitrous oxide emission from soil under conventional and no-tillage in wheat using nitrification inhibitors. *Agriculture, Ecosystems & Environment*, **136**, 247-253.
- Bogaen, H.R., Bol, R., Borchard, N., Brüggemann, N., Diekkrüger, B., Drüe, C., Groh, J., Gottselig, N., Huisman, J.A., Lücke, A., Missong, A., Neuwirth, B., Pütz, T., Schmidt, M., Stockinger, M., Tappe, W., Weihermüller, L., Wiekenkamp, I. and Vereecken, H. (2015). A terrestrial observatory approach to the integrated investigation of the effects of deforestation on water, energy, and matter fluxes. *Science China Earth Sciences*, **58**, 61-75.
- Bogaen, H.R., Herbst, M., Huisman, J.A., Rosenbaum, U., Weuthen, A. and Vereecken, H. (2010). Potential of wireless sensor networks for measuring soil water content variability. *Vadose Zone Journal*, **9**, 1002-1013.
- Bogaen, H.R., Huisman, J.A., Baatz, R., Hendricks Franssen, H.J. and Vereecken, H. (2013). Accuracy of the cosmic-ray soil water content probe in humid forest ecosystems: The worst case scenario. *Water Resources Research*, **49**, 5778-5791.

- Bol, R., Lücke, A., Tappe, W., Kummer, S., Krause, M., Weigand, S., Pütz, T. and Vereecken, H. (2015). Spatio-temporal variations of dissolved organic matter in a German forested mountainous headwater catchment. *Vadose Zone Journal*, **14**.
- Bonner, F.T., Dzelzkalns, L.S. and Bonucci, J.A. (1978). Properties of nitroxyl as intermediate in the nitric oxide-hydroxylamine reaction and in trioxodinitrate decomposition. *Inorganic Chemistry*, **17**, 2487-2494.
- Bornemann, L., Herbst, M., Welp, G., Vereecken, H. and Amelung, W. (2011). Rock Fragments Control Size and Saturation of Organic Carbon Pools in Agricultural Topsoil. *Soil Science Society of America Journal*, **75**, 1898-1907.
- Bourennane, H., King, D., Couturier, A., Nicoulaud, B., Mary, B. and Richard, G. (2007). Uncertainty assessment of soil water content spatial patterns using geostatistical simulations: an empirical comparison of a simulation accounting for single attribute and a simulation accounting for secondary information. *Ecological Modelling*, **205**, 323-335.
- Bouskill, N. J., Lim, H. C., Borglin, S., Salve, R., Wood, T. E., Silver, W. L. and Brodie, E. L. (2013). Pre-exposure to drought increases the resistance of tropical forest soil bacterial communities to extended drought. *The ISME journal*, **7**, 384.
- Bouwman, A., Beusen, A., Griffioen, J., Van Groenigen, J., Hefting, M., Oenema, O., Van Puijenbroek, P., Seitzinger, S., Slomp, C. and Stehfest, E. (2013). Global trends and uncertainties in terrestrial denitrification and N₂O emissions. *Philosophical Transactions of the Royal Society of London B: Biological Sciences*, **368**, 20130112.
- Bouwman, A., Boumans, L. and Batjes, N. (2002). Emissions of N₂O and NO from fertilized fields: Summary of available measurement data. *Global Biogeochemical Cycles*, **16**.
- Braker, G. and Conrad, R. (2011). Diversity, structure, and size of N₂O-producing microbial communities in soils—what matters for their functioning? *Advances in applied microbiology*, **75**, 33-70.
- Bremner, J.M. (1997). Sources of nitrous oxide in soils. *Nutrient Cycling in Agroecosystems*, **49**, 7-16.
- Bremner, J.M., Blackmer, A.M. and Waring, S.A. (1980). Formation of nitrous oxide and dinitrogen by chemical decomposition of hydroxylamine in soils. *Soil Biology and Biochemistry*, **12**, 263-269.
- Brierley, E.D.R. and Wood, M. (2001). Heterotrophic nitrification in an acid forest soil: isolation and characterisation of a nitrifying bacterium. *Soil Biology and Biochemistry*, **33**, 1403-1409.
- Buchwald, C., Grabb, K., Hansel, C.M. and Wankel, S.D. (2016). Constraining the role of iron in environmental nitrogen transformations: Dual stable isotope systematics of abiotic NO₂⁻ reduction by Fe (II) and its production of N₂O. *Geochimica et Cosmochimica Acta*, **186**, 1-12.
- Butler, J.H. and Gordon, L.I. (1986). An improved gas chromatographic method for the measurement of hydroxylamine in marine and fresh waters. *Marine Chemistry*, **19**, 229-243.
- Butterbach-Bahl, K., Baggs, E.M., Dannenmann, M., Kiese, R. and Zechmeister-Boltenstern, S. (2013). Nitrous oxide emissions from soils: how well do we understand the processes and their controls? *Philosophical Transactions of the Royal Society of London B: Biological Sciences*, **368**.
- Butterbach-Bahl, K., Rothe, A. and Papen, H. (2002). Effect of tree distance on N₂O and CH₄-fluxes from soils in temperate forest ecosystems. *Plant and Soil*, **240**, 91-103.
- Campbell, M.A., Nyerges, G., Kozlowski, J.A., Poret-Peterson, A.T., Stein, L.Y. and Klotz, M.G. (2011). Model of the molecular basis for hydroxylamine oxidation and nitrous oxide production in methanotrophic bacteria. *FEMS Microbiology Letters*, **322**, 82-89.
- Caranto, J.D., Vilbert, A.C. and Lancaster, K.M. (2016). *Nitrosomonas europaea* cytochrome P460 is a direct link between nitrification and nitrous oxide emission. *Proceedings of the National Academy of Sciences of the United States of America*, **113**, 14704-14709.
- Caranto, J.D. and Lancaster, K.M. (2017). Nitric oxide is an obligate bacterial nitrification intermediate produced by hydroxylamine oxidoreductase. *Proceedings of the National Academy of Sciences of the United States of America*, **114**, 8217-8222.
- Chao, T.T. (1972). Selective Dissolution of Manganese Oxides from Soils and Sediments with Acidified Hydroxylamine Hydrochloride. *Soil Science Society of America Journal*, **36**, 764-768.

- Clément, J.-C., Shrestha, J., Ehrenfeld, J.G. and Jaffé, P.R. (2005). Ammonium oxidation coupled to dissimilatory reduction of iron under anaerobic conditions in wetland soils. *Soil Biology and Biochemistry*, **37**, 2323-2328.
- Dail, D., Davidson, E. and Chorover, J. (2001). Rapid abiotic transformation of nitrate in an acid forest soil. *Biogeochemistry*, **54**, 131-146.
- Daims, H., Lebedeva, E.V., Pjevac, P., Han, P., Herbold, C., Albertsen, M., Jehmlich, N., Palatinszky, M., Vierheilig, J. and Bulaev, A. (2015). Complete nitrification by *Nitrospira* bacteria. *Nature*, **528**, 504-509.
- Dassonville, F. and Renault, P. (2002). Interactions between microbial processes and geochemical transformations under anaerobic conditions: a review. *Agronomie*, **22**, 51-68.
- Daum, M., Zimmer, W., Papen, H., Kloos, K., Nawrath, K. and Bothe, H. (1998). Physiological and Molecular Biological Characterization of Ammonia Oxidation of the Heterotrophic Nitrifier *Pseudomonas putida*. *Current Microbiology*, **37**, 281-288.
- Davidson, E.A. (1992). Pulses of nitric oxide and nitrous oxide flux following wetting of dry soil: An assessment of probable sources and importance relative to annual fluxes. *Ecological Bulletins*, 149-155.
- Davidson, E.A. (2009). The contribution of manure and fertilizer nitrogen to atmospheric nitrous oxide since 1860. *Nature Geoscience*, **2**, 659-662.
- Davidson, E.A. (2012). Representative concentration pathways and mitigation scenarios for nitrous oxide. *Environmental Research Letters*, **7**, 024005.
- Davidson, E.A., Chorover, J. and Dail, D.B. (2003). A mechanism of abiotic immobilization of nitrate in forest ecosystems: the ferrous wheel hypothesis. *Global Change Biology*, **9**, 228-236.
- De Klein, C., Novoa, R.S., Ogle, S., Smith, K., Rochette, P., Wirth, T., McConkey, B., Mosier, A., Rypdal, K. and Walsh, M. (2006). N₂O emissions from managed soils, and CO₂ emissions from lime and urea application. *IPCC Guidelines for National Greenhouse Gas Inventories, Prepared by the National Greenhouse Gas Inventories Programme*, **4**, 1-54.
- Denef, K., Six, J., Bossuyt, H., Frey, S.D., Elliott, E.T., Merckx, R. and Paustian, K. (2001). Influence of dry-wet cycles on the interrelationship between aggregate, particulate organic matter, and microbial community dynamics. *Soil Biology and Biochemistry*, **33**, 1599-1611.
- Deutsch, C. and Journel, A. 1998. GSLIB: Geostatistical software library and user's guide, 2nd edn., p. 369. Oxford University Press, New York.
- Di, H.J., Cameron, K.C., Sherlock, R.R., Shen, J.-P., He, J.-Z. and Winefield, C.S. (2010). Nitrous oxide emissions from grazed grassland as affected by a nitrification inhibitor, dicyandiamide, and relationships with ammonia-oxidizing bacteria and archaea. *Journal of Soils and Sediments*, **10**, 943-954.
- Dias, F., Olojola, A.S. and Jaselskis, B. (1979). Spectrophotometric determination of micro amounts of hydrazine and hydroxylamine alone and in the presence of each other. *Talanta*, **26**, 47-49.
- Dundee, L. and Hopkins, D.W. (2001). Different sensitivities to oxygen of nitrous oxide production by *Nitrosomonas europaea* and *Nitrosolobus multififormis*. *Soil Biology and Biochemistry*, **33**, 1563-1565.
- El Azhar, S., Verhe, R., Proot, M., Sandra, P. and Verstraete, W. (1986). Binding of nitrite-N on polyphenols during nitrification. *Plant and Soil*, **94**, 369-382.
- Fierer, N. and Schimel, J.P. (2002). Effects of drying-rewetting frequency on soil carbon and nitrogen transformations. *Soil Biology and Biochemistry*, **34**, 777-787.
- Fierer, N. and Schimel, J.P. (2003). A proposed mechanism for the pulse in carbon dioxide production commonly observed following the rapid rewetting of a dry soil. *Soil Science Society of America Journal*, **67**, 798-805.
- Firestone, M.K. and Davidson, E.A. (1989). Microbiological basis of NO and N₂O production and consumption in soil. *Exchange of trace gases between terrestrial ecosystems and the atmosphere*, **47**, 7-21.

- Flessa, H., Dörsch, P. and Beese, F. (1995). Seasonal variation of N₂O and CH₄ fluxes in differently managed arable soils in southern Germany. *Journal of Geophysical Research: Atmospheres*, **100**, 23115-23124.
- Froelich, P.N., Klinkhammer, G.P., Bender, M.L., Luedtke, N.A., Heath, G.R., Cullen, D., Dauphin, P., Hammond, D., Hartman, B. and Maynard, V. (1979). Early oxidation of organic matter in pelagic sediments of the eastern equatorial Atlantic: suboxic diagenesis. *Geochimica et Cosmochimica Acta*, **43**, 1075-1090.
- Galloway, J.N., Townsend, A.R., Erisman, J.W., Bekunda, M., Cai, Z., Freney, J.R., Martinelli, L.A., Seitzinger, S.P. and Sutton, M.A. (2008). Transformation of the nitrogen cycle: recent trends, questions, and potential solutions. *Science*, **320**, 889-892.
- Gebhardt, S., Walter, S., Nausch, G. and Bange, H.W. (2004). Hydroxylamine (NH₂OH) in the Baltic Sea. *Biogeosciences Discussion*, **1**, 709-724.
- Gelfand, I. and Yakir, D. (2008). Influence of nitrite accumulation in association with seasonal patterns and mineralization of soil nitrogen in a semi-arid pine forest. *Soil Biology and Biochemistry*, **40**, 415-424.
- Gharahi Ghehi, N., Werner, C., Cizungu Ntaboba, L., Mbonigaba Muhinda, J.J., Van Ranst, E., Butterbach-Bahl, K., Kiese, R. and Boeckx, P. (2012). Spatial variations of nitrogen trace gas emissions from tropical mountain forests in Nyungwe, Rwanda. *Biogeosciences*, **9**, 1451-1463.
- Gierer, J. and Söderberg, S. (1959). Über die Carbonylgruppen des Lignins. *Acta Chemica Scandinavica*, **13**, 1.
- Gödde, M. and Conrad, R. (1999). Immediate and adaptational temperature effects on nitric oxide production and nitrous oxide release from nitrification and denitrification in two soils. *Biology and Fertility of Soils*, **30**, 33-40.
- Goldberg, S. D., and Gebauer, G. (2009). N₂O and NO fluxes between a Norway spruce forest soil and atmosphere as affected by prolonged summer drought. *Soil Biology and Biochemistry*, **41**, 1986-1995.
- Gomori, G. 1955. [16] Preparation of buffers for use in enzyme studies. In: *Methods In Enzymology*, pp. 138-146. Academic Press.
- Goovaerts, P. (2000). Estimation or simulation of soil properties? An optimization problem with conflicting criteria. *Geoderma*, **97**, 165-186.
- Grabb, K.C., Buchwald, C., Hansel, C.M. and Wankel, S.D. (2017). A dual nitrite isotopic investigation of chemodenitrification by mineral-associated Fe(II) and its production of nitrous oxide. *Geochimica et Cosmochimica Acta*, **196**, 388-402.
- Guzowski Jr, J.P., Golanoski, C. and Montgomery, E.R. (2003). A gas chromatographic method for the indirect determination of hydroxylamine in pharmaceutical preparations: conversion into nitrous oxide. *Journal of Pharmaceutical and Biomedical Analysis*, **33**, 963-974.
- Halverson, L.J., Jones, T.M. and Firestone, M.K. (2000). Release of intracellular solutes by four soil bacteria exposed to dilution stress. *Soil Science Society of America Journal*, **64**, 1630-1637.
- Halvorson, J.J. and Gonzalez, J.M. (2008). Tannic acid reduces recovery of water-soluble carbon and nitrogen from soil and affects the composition of Bradford-reactive soil protein. *Soil Biology and Biochemistry*, **40**, 186-197.
- Harrison-Kirk, T., Beare, M., Meenken, E. and Condrón, L. (2013). Soil organic matter and texture affect responses to dry/wet cycles: effects on carbon dioxide and nitrous oxide emissions. *Soil Biology and Biochemistry*, **57**, 43-55.
- He, J.z., Shen, J.p., Zhang, L.m., Zhu, Y.g., Zheng, Y.m., Xu, M.g. and Di, H. (2007). Quantitative analyses of the abundance and composition of ammonia - oxidizing bacteria and ammonia - oxidizing archaea of a Chinese upland red soil under long - term fertilization practices. *Environmental Microbiology*, **9**, 2364-2374.
- Heil, J., Liu, S., Vereecken, H. and Brüggemann, N. (2015). Abiotic nitrous oxide production from hydroxylamine in soils and their dependence on soil properties. *Soil Biology and Biochemistry*, **84**, 107-115.

- Heil, J., Vereecken, H. and Brüggemann, N. (2016). A review of chemical reactions of nitrification intermediates and their role in nitrogen cycling and nitrogen trace gas formation in soil. *European Journal of Soil Science*, **67**, 23-39.
- Heil, J., Wolf, B., Brüggemann, N., Emmenegger, L., Tuzson, B., Vereecken, H. and Mohn, J. (2014). Site-specific ^{15}N isotopic signatures of abiotically produced N_2O . *Geochimica et Cosmochimica Acta*, **139**, 72-82.
- Herbst, M., Bornemann, L., Graf, A., Welp, G., Vereecken, H. and Amelung, W. (2012). A geostatistical approach to the field-scale pattern of heterotrophic soil CO_2 emission using covariates. *Biogeochemistry*, **111**, 377-392.
- Herbst, M., Prolingheuer, N., Graf, A., Huisman, J.A., Weihermüller, L. and Vanderborght, J. (2009). Characterization and understanding of bare soil respiration spatial variability at plot scale. *Vadose Zone Journal*, **8**, 762-771.
- Hoben, J.P., Gehl, R.J., Millar, N., Grace, P.R. and Robertson, G.P. (2011). Nonlinear nitrous oxide (N_2O) response to nitrogen fertilizer in on-farm corn crops of the US Midwest. *Global Change Biology*, **17**, 1140-1152.
- Hoffmann, G. (1991). Handbuch der landwirtschaftlichen Versuchs-und Untersuchungs-anstalten (Methodenhandbuch) Band 1: Die Untersuchung von Böden. *VDUFLA-Verlag, Darmstadt*, 1740.
- Homyak, P.M., Vasquez, K.T., Sickman, J.O., Parker, D.R. and Schimel, J.P. (2015). Improving nitrite analysis in soils: Drawbacks of the conventional 2 M KCl extraction. *Soil Science Society of America Journal*, **79**, 1237-1242.
- Hu, H.-W., Chen, D. and He, J.-Z. (2015). Microbial regulation of terrestrial nitrous oxide formation: understanding the biological pathways for prediction of emission rates. *FEMS microbiology reviews*, **39**, 729-749.
- Huang, T., Gao, B., Hu, X.-K., Lu, X., Well, R., Christie, P., Bakken, L. R. and Ju, X.-T. (2014) Ammonia-oxidation as an engine to generate nitrous oxide in an intensively managed calcareous Fluvo-aquic soil. *Scientific Reports*, **4**, 3950.
- Hulth, S., Aller, R.C., Canfield, D.E., Dalsgaard, T., Engström, P., Gilbert, F., Sundbäck, K. and Thamdrup, B. (2005). Nitrogen removal in marine environments: Recent findings and future research challenges. *Marine Chemistry*, **94**, 125-145.
- Hulth, S., Aller, R.C. and Gilbert, F. (1999). Coupled anoxic nitrification/manganese reduction in marine sediments. *Geochimica et Cosmochimica Acta*, **63**, 49-66.
- Hynes, R.K. and Knowles, R. (1984). Production of nitrous oxide by *Nitrosomonas europaea*: effects of acetylene, pH, and oxygen. *Canadian Journal of Microbiology*, **30**, 1397-1404.
- IPCC. 2013. Climate Change 2013: The Physical Science Basis. Contribution of Working Group I to the Fifth Assessment Report of the Intergovernmental Panel on Climate Change (ed. Stocker, T.F., D. Qin, G.-K. Plattner, M. Tignor, S.K. Allen, J. Boschung, A. Nauels, Y. Xia, V. Bex and P.M. Midgley), p. 1552. Cambridge University Press, Cambridge, United Kingdom and New York, USA.
- Ishijima, K., Sugawara, S., Kawamura, K., Hashida, G., Morimoto, S., Murayama, S., Aoki, S. and Nakazawa, T. (2007). Temporal variations of the atmospheric nitrous oxide concentration and its $\delta^{15}\text{N}$ and $\delta^{18}\text{O}$ for the latter half of the 20th century reconstructed from firn air analyses. *Journal of Geophysical Research: Atmospheres*, **112**.
- Jiang, Q. and Bakken, L.R. (1999). Nitrous oxide production and methane oxidation by different ammonia-oxidizing bacteria. *Applied and Environmental Microbiology*, **65**, 2679-2684.
- Jones, L.C., Peters, B., Lezama Pacheco, J.S., Casciotti, K.L. and Fendorf, S. (2015). Stable isotopes and iron oxide mineral products as markers of chemodenitrification. *Environmental science & technology*, **49**, 3444-3452.
- Jung, M.-Y., Well, R., Min, D., Giesemann, A., Park, S.-J., Kim, J.-G., Kim, S.-J. and Rhee, S.-K. (2014). Isotopic signatures of N_2O produced by ammonia-oxidizing archaea from soils. *The ISME Journal*, **8**, 1115-1125.

- Kaiser, J., Park, S., Boering, K.A., Brenninkmeijer, C.A.M., Hilker, A. and Röckmann, T. (2004). Mass spectrometric method for the absolute calibration of the intramolecular nitrogen isotope distribution in nitrous oxide. *Analytical and Bioanalytical Chemistry*, **378**, 256–269.
- Kaiser, J., Röckmann, T. and Brenninkmeijer, C.A. (2003). Complete and accurate mass spectrometric isotope analysis of tropospheric nitrous oxide. *Journal of Geophysical Research: Atmospheres*, **108**.
- Kampschreur, M.J., Kleerebezem, R., de Vet, W.W.J.M. and van Loosdrecht, M.C.M. (2011). Reduced iron induced nitric oxide and nitrous oxide emission. *Water Research*, **45**, 5945-5952.
- Kandeler, E. and Gerber, H. (1988). Short-term assay of soil urease activity using colorimetric determination of ammonium. *Biology and Fertility of Soils*, **6**, 68-72.
- Kesik, M., Blagodatsky, S., Papen, H., and Butterbach - Bahl, K. (2006). Effect of pH, temperature and substrate on N₂O, NO and CO₂ production by *Alcaligenes faecalis* p. *Journal of Applied Microbiology*, **101**, 655-667.
- Kiese, R., Hewett, B., Graham, A. and Butterbach - Bahl, K. (2003). Seasonal variability of N₂O emissions and CH₄ uptake by tropical rainforest soils of Queensland, Australia. *Global Biogeochemical Cycles*, **17**.
- Kim, D.G., Vargas, R., Bond-Lamberty, B. and Turetsky, M.R. (2012). Effects of soil rewetting and thawing on soil gas fluxes: a review of current literature and suggestions for future research. *Biogeosciences*, **9**, 2459-2483.
- Kits, K. D., Sedlacek, C. J., Lebedeva, E. V., Han, P., Bulaev, A., Pjevac, P., Daebeler, A., Romano, S., Albertsen, M., Stein, L. Y., Daims, H. and Wagner, M. (2017) Kinetic analysis of a complete nitrifier reveals an oligotrophic lifestyle. *Nature*, **549**, 269-272.
- Klemetsson, L., Von Arnold, K., Weslien, P. and Gundersen, P. (2005). Soil CN ratio as a scalar parameter to predict nitrous oxide emissions. *Global Change Biology*, **11**, 1142-1147.
- Kock, A. and Bange, H.W. (2013). Nitrite removal improves hydroxylamine analysis in aqueous solution by conversion with iron(III). *Environmental Chemistry*, **10**, 64-71.
- Konda, R., Ohta, S., Ishizuka, S., Heriyanto, J. and Wicaksono, A. (2010). Seasonal changes in the spatial structures of N₂O, CO₂, and CH₄ fluxes from Acacia mangium plantation soils in Indonesia. *Soil Biology & Biochemistry*, **42**, 1512-1522.
- Kool, D.M., Dolfing, J., Wrage, N. and Van Groenigen, J.W. (2011). Nitrifier denitrification as a distinct and significant source of nitrous oxide from soil. *Soil Biology and Biochemistry*, **43**, 174-178.
- Koops, H.P., Böttcher, B., Möller, U.C., Pommerening-Röser, A. and Stehr, G. (1991). Classification of eight new species of ammonia-oxidizing bacteria: *Nitrosomonas communis* sp. nov., *Nitrosomonas ureae* sp. nov., *Nitrosomonas aestuarii* sp. nov., *Nitrosomonas marina* sp. nov., *Nitrosomonas nitrosa* sp. nov., *Nitrosomonas eutropha* sp. nov., *Nitrosomonas oligotropha* sp. nov. and *Nitrosomonas halophila* sp. nov. *Microbiology*, **137**, 1689-1699.
- Kozłowski, J.A., Kits, K.D. and Stein, L.Y. (2016b). Genome sequence of *Nitrosomonas communis* strain Nm2, a mesophilic ammonia-oxidizing bacterium isolated from mediterranean soil. *Genome announcements*, **4**, e01541-01515.
- Kozłowski, J.A., Kits, K.D. and Stein, L.Y. (2016c). Comparison of nitrogen oxide metabolism among diverse ammonia-oxidizing bacteria. *Frontiers in Microbiology*, **7**.
- Kozłowski, J.A., Stieglmeier, M., Schleper, C., Klotz, M.G. and Stein, L.Y. (2016a). Pathways and key intermediates required for obligate aerobic ammonia-dependent chemolithotrophy in bacteria and Thaumarchaeota. *The ISME Journal*, **10**, 1836-1845.
- Kraus, T.E.C., Zasoski, R.J., Dahlgren, R.A., Horwath, W.R. and Preston, C.M. (2004). Carbon and nitrogen dynamics in a forest soil amended with purified tannins from different plant species. *Soil Biology and Biochemistry*, **36**, 309-321.
- Lamers, M., Ingwersen, J. and Streck, T. (2007). Nitrous oxide emissions from mineral and organic soils of a Norway spruce stand in South–West Germany. *Atmospheric Environment*, **41**, 1681-1688.
- Law, Y., Lant, P. and Yuan, Z. (2013). The confounding effect of nitrite on N₂O production by an enriched ammonia-oxidizing culture. *Environmental Science & Technology*, **47**, 7186-7194.

- Lebedeva, E.V., Hatzenpichler, R., Pelletier, E., Schuster, N., Hauzmayer, S., Bulaev, A., Grigor'eva, N.V., Galushko, A., Schmid, M. and Palatinszky, M. (2013). Enrichment and genome sequence of the group I. 1a ammonia-oxidizing Archaeon "*Ca. Nitrosotenuis uzonensis*" representing a clade globally distributed in thermal habitats. *PLoS One*, **8**, e80835.
- Lees, H. (1952). Hydroxylamine as an intermediate in nitrification. *Nature*, **169**, 156-157.
- Lehmann, R.G., Cheng, H.H. and Harsh, J.B. (1987). Oxidation of phenolic acids by soil iron and manganese oxides. *Soil Science Society of America Journal*, **51**, 352-356.
- Lehtovirta-Morley, L.E., Ge, C., Ross, J., Yao, H., Nicol, G.W. and Prosser, J.I. (2014). Characterisation of terrestrial acidophilic archaeal ammonia oxidisers and their inhibition and stimulation by organic compounds. *FEMS Microbiology Ecology*, **89**, 542-552.
- Leininger, S., Urich, T., Schloter, M., Schwark, L., Qi, J., Nicol, G.W., Prosser, J.I., Schuster, S.C. and Schleper, C. (2006). Archaea predominate among ammonia-oxidizing prokaryotes in soils. *Nature*, **442**, 806-809.
- Li, C., Aber, J., Stange, F., Butterbach-Bahl, K. and Papen, H. (2000). A process-oriented model of N₂O and NO emissions from forest soils: 1. Model development. *Journal of Geophysical Research: Atmospheres*, **105**, 4369-4384.
- Li, C., Zhang, B., Ertunc, T., Schaeffer, A. and Ji, R. (2012). Birnessite-induced binding of phenolic monomers to soil humic substances and nature of the bound residues. *Environmental Science & Technology*, **46**, 8843-8850.
- Liu, B., Mørkved, P.T., Frostegård, Å. and Bakken, L.R. (2010). Denitrification gene pools, transcription and kinetics of NO, N₂O and N₂ production as affected by soil pH. *FEMS Microbiology Ecology*, **72**, 407-417.
- Liu, S., Berns, A.E., Vereecken, H., Wu, D. and Brüggemann, N. (2017a). Interactive effects of MnO₂, organic matter and pH on abiotic formation of N₂O from hydroxylamine in artificial soil mixtures. *Scientific Reports*, **7**, 39590.
- Liu, S., Han, P., Hink, L., Prosser, J. I., Wagner, M. and Brüggemann, N. (2017b). Abiotic conversion of extracellular NH₂OH contributes to N₂O emission during ammonia oxidation. *Environmental Science & Technology*. doi: 10.1021/acs.est.7b02360.
- Liu, S., Herbst, M., Bol, R., Gottselig, N., Pütz, T., Weymann, D., Wiekenkamp, I., Vereecken, H. and Brüggemann, N. (2016). The contribution of hydroxylamine content to spatial variability of N₂O formation in soil of a Norway spruce forest. *Geochimica et Cosmochimica Acta*, **178**, 76-86.
- Liu, S., Vereecken, H. and Brüggemann, N. (2014). A highly sensitive method for the determination of hydroxylamine in soils. *Geoderma*, **232**, 117-122.
- Lovley, D.R., Holmes, D.E. and Nevin, K.P. (2004). Dissimilatory Fe(III) and Mn(IV) Reduction. In: *Advances in Microbial Physiology*, pp. 219-286. Academic Press.
- Luther, G., III and Popp, J. (2002). Kinetics of the abiotic reduction of polymeric manganese dioxide by nitrite: an anaerobic nitrification reaction. *Aquatic Geochemistry*, **8**, 15-36.
- Ma, L., Shan, J. and Yan, X. (2015). Nitrite behavior accounts for the nitrous oxide peaks following fertilization in a fluvo-aquic soil. *Biology and Fertility of Soils*, **51**, 563-572.
- Martikainen, P.J. and de Boer, W. (1993). Nitrous oxide production and nitrification in acidic soil from a dutch coniferous forest. *Soil Biology and Biochemistry*, **25**, 343-347.
- Martikainen, P.J., Lehtonen, M., Lång, K., De Boer, W. and Ferm, A. (1993). Nitrification and nitrous oxide production potentials in aerobic soil samples from the soil profile of a Finnish coniferous site receiving high ammonium deposition. *FEMS Microbiology Ecology*, **13**, 113-121.
- McSwiney, C., McDowell, W. and Keller, M. (2001). Distribution of nitrous oxide and regulators of its production across a tropical rainforest catena in the Luquillo Experimental Forest, Puerto Rico. *Biogeochemistry*, **56**, 265-286.
- Minasny, B., McBratney, A. and Whelan, B. (2005). VESPER version 1.62. *Australian Centre for Precision Agriculture, University of Sydney, New South Wales*, **5**, 25.
- Mohn, J., Wolf, B., Toyoda, S., Lin, C.T., Liang, M.C., Brüggemann, N., Wissel, H., Steiker, A.E., Dyckmans, J. and Szewc, L. (2014). Interlaboratory assessment of nitrous oxide isotopomer

- analysis by isotope ratio mass spectrometry and laser spectroscopy: current status and perspectives. *Rapid Communications in Mass Spectrometry*, **28**, 1995-2007.
- Mørkved, P.T., Dörsch, P. and Bakken, L.R. (2007). The N₂O product ratio of nitrification and its dependence on long-term changes in soil pH. *Soil Biology & Biochemistry*, **39**, 2048-2057.
- Müller, C., Laughlin, R.J., Spott, O. and Rütting, T. (2014). Quantification of N₂O emission pathways via a ¹⁵N tracing model. *Soil Biology and Biochemistry*, **72**, 44-54.
- Müller, C., Stevens, R. and Laughlin, R. (2006). Sources of nitrite in a permanent grassland soil. *European Journal of Soil Science*, **57**, 337-343.
- Nelson, D. 1977. Transformations of hydroxylamine in soils. In: *Proceedings of the Indiana Academy of Science*, pp. 409-413.
- Nishina, K., Takenaka, C. and Ishizuka, S. (2009). Spatiotemporal variation in N₂O flux within a slope in a Japanese cedar (*Cryptomeria japonica*) forest. *Biogeochemistry*, **96**, 163-175.
- Nömmik, H. (1956). Investigations on denitrification in soil. *Acta Agriculturae Scandinavica*, **6**, 195-228.
- Olk, D.C., Cassman, K.G., Schmidt-Rohr, K., Anders, M.M., Mao, J.D. and Deenik, J.L. (2006). Chemical stabilization of soil organic nitrogen by phenolic lignin residues in anaerobic agroecosystems. *Soil Biology and Biochemistry*, **38**, 3303-3312.
- Ostrom, N.E. and Ostrom, P.H. 2011. The isotopomers of nitrous oxide: analytical considerations and application to resolution of microbial production pathways. In: *Handbook of Environmental Isotope Geochemistry, Advances in Isotope Geochemistry* (ed. Baskaran, M.), pp. 453-476. Springer Berlin Heidelberg.
- Otte, S., Schalk, J., Kuenen, J.G. and Jetten, M.S.M. (1999). Hydroxylamine oxidation and subsequent nitrous oxide production by the heterotrophic ammonia oxidizer *Alcaligenes faecalis*. *Applied Microbiology and Biotechnology*, **51**, 255-261.
- Palatinszky, M., Herbold, C., Jehmlich, N., Pogoda, M., Han, P., von Bergen, M., Lagkouvardos, I., Karst, S.M., Galushko, A., Koch, H., Berry, D., Daims, H. and Wagner, M. (2015). Cyanate as an energy source for nitrifiers. *Nature*, **524**, 105-108.
- Parton, W.J., Holland, E.A., Del Grosso, S.J., Hartman, M.D., Martin, R.E., Mosier, A.R., Ojima, D.S. and Schimel, D.S. (2001). Generalized model for NO_x and N₂O emissions from soils. *Journal of Geophysical Research: Atmospheres*, **106**, 17403-17419.
- Parton, W.J., Mosier, A.R., Ojima, D.S., Valentine, D.W., Schimel, D.S., Weier, K. and Kulmala, A.E. (1996). Generalized model for N₂ and N₂O production from nitrification and denitrification. *Global Biogeochemical Cycles*, **10**, 401-412.
- Peters, B., Casciotti, K.L., Samarkin, V.A., Madigan, M.T., Schutte, C.A. and Joye, S.B. (2014). Stable isotope analyses of NO₂⁻, NO₃⁻, and N₂O in the hypersaline ponds and soils of the McMurdo Dry Valleys, Antarctica. *Geochimica et Cosmochimica Acta*, **135**, 87-101.
- Pett-Ridge, J., Silver, W.L. and Firestone, M.K. (2006). Redox fluctuations frame microbial community impacts on N-cycling rates in a humid tropical forest soil. *Biogeochemistry*, **81**, 95-110.
- Pilegaard, K., Skiba, U., Ambus, P., Beier, C., Brüggemann, N., Butterbach-Bahl, K., Dick, J., Dorsey, J., Duyzer, J. and Gallagher, M. (2006). Factors controlling regional differences in forest soil emission of nitrogen oxides (NO and N₂O). *Biogeosciences*, **3**, 651-661.
- Placella, S.A. and Firestone, M.K. (2013). Transcriptional response of nitrifying communities to wetting of dry soil. *Applied and Environmental Microbiology*, **79**, 3294-3302.
- Poth, M. and Focht, D.D. (1985). ¹⁵N kinetic analysis of N₂O production by *Nitrosomonas europaea*: an examination of nitrifier denitrification. *Applied and Environmental Microbiology*, **49**, 1134-1141.
- Priemé, A. and Christensen, S. (2001). Natural perturbations, drying-wetting and freezing-thawing cycles, and the emission of nitrous oxide, carbon dioxide and methane from farmed organic soils. *Soil Biology and Biochemistry*, **33**, 2083-2091.
- Prosser, J.I., Head, I.M. and Stein, L.Y. 2014. The Family Nitrosomonadaceae. In: *The Prokaryotes: Alphaproteobacteria and Betaproteobacteria* (eds. Rosenberg, E., DeLong, E.F., Lory, S., Stackebrandt, E. & Thompson, F.), pp. 901-918. Springer Berlin Heidelberg, Berlin, Heidelberg.

- R Development Core Team. (2013). R: A language and environment for statistical computing. R Foundation for Statistical Computing. Vienna, Austria. ISBN 3-900051-07-0, URL <http://www.R-project.org/>.
- Rathnayake, R.M.L.D., Song, Y., Tumendelger, A., Oshiki, M., Ishii, S., Satoh, H., Toyoda, S., Yoshida, N. and Okabe, S. (2013). Source identification of nitrous oxide on autotrophic partial nitrification in a granular sludge reactor. *Water Research*, **47**, 7078-7086.
- Remde, A. and Conrad, R. (1990). Production of nitric oxide in *Nitrosomonas europaea* by reduction of nitrite. *Archives of Microbiology*, **154**, 187-191.
- Richardson, D., Felgate, H., Watmough, N., Thomson, A. and Baggs, E. (2009). Mitigating release of the potent greenhouse gas N₂O from the nitrogen cycle—could enzymic regulation hold the key? *Trends in biotechnology*, **27**, 388-397.
- Ritchie, G.A.F. and Nicholas, D.J.D. (1972). Identification of the sources of nitrous oxide produced by oxidative and reductive processes in *Nitrosomonas europaea*. *Biochemical Journal*, **126**, 1181-1191.
- Robertson, G. and Groffman, P. (2007). Nitrogen transformations. *Soil microbiology, Ecology, and Biochemistry*, **3**, 341-364.
- Roeckmann, T. and Levin, I. (2005). High - precision determination of the changing isotopic composition of atmospheric N₂O from 1990 to 2002. *Journal of Geophysical Research: Atmospheres*, **110**.
- Rohe, L., Anderson, T.H., Braker, G., Flessa, H., Giesemann, A., Lewicka - Szczebak, D., Wrage - Mönnig, N. and Well, R. (2014). Dual isotope and isotopomer signatures of nitrous oxide from fungal denitrification – a pure culture study. *Rapid Communications in Mass Spectrometry*, **28**, 1893-1903.
- Rötzer, K., Montzka, C., Bogena, H., Wagner, W., Kerr, Y.H., Kidd, R. and Vereecken, H. (2014). Catchment scale validation of SMOS and ASCAT soil moisture products using hydrological modeling and temporal stability analysis. *Journal of Hydrology*, **519, Part A**, 934-946.
- Rudaz, A.O., Davidson, E.A. and Firestone, M.K. (1991). Sources of nitrous oxide production following wetting of dry soil. *FEMS Microbiology Letters*, **85**, 117-124.
- Ruser, R., Flessa, H., Russow, R., Schmidt, G., Buegger, F. and Munch, J. (2006). Emission of N₂O, N₂ and CO₂ from soil fertilized with nitrate: effect of compaction, soil moisture and rewetting. *Soil Biology and Biochemistry*, **38**, 263-274.
- Rütting, T., Boeckx, P., Müller, C. and Klemedtsson, L. (2011). Assessment of the importance of dissimilatory nitrate reduction to ammonium for the terrestrial nitrogen cycle. *Biogeosciences*, **8**, 1779-1791.
- Rütting, T., Huygens, D., Boeckx, P., Staelens, J. and Klemedtsson, L. (2013). Increased fungal dominance in N₂O emission hotspots along a natural pH gradient in organic forest soil. *Biology and Fertility of Soils*, **49**, 715-721.
- Samarkin, V.A., Madigan, M.T., Bowles, M.W., Casciotti, K.L., Priscu, J.C., McKay, C.P. and Joye, S.B. (2010). Abiotic nitrous oxide emission from the hypersaline Don Juan Pond in Antarctica. *Nature Geoscience*, **3**, 341-344.
- Santoro, A.E., Buchwald, C., McIlvin, M.R. and Casciotti, K.L. (2011). Isotopic signature of N₂O produced by marine ammonia-oxidizing archaea. *Science*, **333**, 1282-1285.
- Schimel, J., Balsler, T.C. and Wallenstein, M. (2007). Microbial stress - response physiology and its implications for ecosystem function. *Ecology*, **88**, 1386-1394.
- Schindlbacher, A., Zechmeister-Boltenstern, S. and Butterbach-Bahl, K. (2004). Effects of soil moisture and temperature on NO, NO₂, and N₂O emissions from European forest soils. *Journal of Geophysical Research: Atmospheres*, **109**, D17302.
- Schmidt, B.M. and Matzner, E. (2009). Abiotic reaction of nitrite with dissolved organic carbon? Testing the Ferrous Wheel Hypothesis. *Biogeochemistry*, **93**, 291-296.
- Schmidt, I., Look, C., Bock, E. and Jetten, M.S.M. (2004a). Ammonium and hydroxylamine uptake and accumulation in *Nitrosomonas*. *Microbiology*, **150**, 1405-1412.

- Schmidt, I., van Spanning, R.J.M. and Jetten, M.S.M. (2004b). Denitrification and ammonia oxidation by *Nitrosomonas europaea* wild-type, and NirK- and NorB-deficient mutants. *Microbiology*, **150**, 4107-4114.
- Schreiber, F., Wunderlin, P., Udert, K.M. and Wells, G.F. (2012). Nitric oxide and nitrous oxide turnover in natural and engineered microbial communities: biological pathways, chemical reactions and novel technologies. *Frontiers in Microbiology*, **3**.
- Schüller, H. (1969). Die CAL-Methode, eine neue Methode zur Bestimmung des pflanzenverfügbaren Phosphates in Böden. *Zeitschrift für Pflanzenernährung und Bodenkunde*, **123**, 48-63.
- Schweiger, B., Hansen, H.P. and Bange, H.W. (2007). A time series of hydroxylamine (NH₂OH) in the southwestern Baltic Sea. *Geophysical Research Letters*, **34**, L24608.
- Shaw, L.J., Nicol, G.W., Smith, Z., Fear, J., Prosser, J.I. and Baggs, E.M. (2006). *Nitrosospira* spp. can produce nitrous oxide via a nitrifier denitrification pathway. *Environmental Microbiology*, **8**, 214-222.
- Shcherbak, I., Millar, N. and Robertson, G.P. (2014). Global metaanalysis of the nonlinear response of soil nitrous oxide (N₂O) emissions to fertilizer nitrogen. *Proceedings of the National Academy of Sciences*, **111**, 9199-9204.
- Shen, Q.R., Ran, W. and Cao, Z.H. (2003). Mechanisms of nitrite accumulation occurring in soil nitrification. *Chemosphere*, **50**, 747-753.
- Silver, W.L., Herman, D.J. and Firestone, M.K. (2001). Dissimilatory Nitrate reduction to ammonium in upland tropical forest soils. *Ecology*, **82**, 2410-2416.
- Šimek, M. and Cooper, J.E. (2002). The influence of soil pH on denitrification: progress towards the understanding of this interaction over the last 50 years. *European Journal of Soil Science*, **53**, 345-354.
- Singh, A.K., Singh, A. and Engelhardt, M. (1997). The lognormal distribution in environmental applications. *Washington, DC: US Environmental Protection Agency, Office of Solid Waste and Emergency Response*.
- Skinner, F.A. and Walker, N. (1961). Growth of *Nitrosomonas europaea* in batch and continuous culture. *Archiv für Mikrobiologie*, **38**, 339-349.
- Smith, M.S. and Parsons, L.L. (1985). Persistence of denitrifying enzyme activity in dried soils. *Applied and Environmental Microbiology*, **49**, 316-320.
- Smith, R.V., Burns, L.C., Doyle, R.M., Lennox, S.D., Kelso, B.H.L., Foy, R.H. and Stevens, R.J. (1997). Free ammonia inhibition of nitrification in river sediments leading to nitrite accumulation. *Journal of Environmental Quality*, **26**, 1049-1055.
- Snider, D., Thompson, K., Wagner-Riddle, C., Spoelstra, J. and Dunfield, K. (2015). Molecular techniques and stable isotope ratios at natural abundance give complementary inferences about N₂O production pathways in an agricultural soil following a rainfall event. *Soil Biology and Biochemistry*, **88**, 197-213.
- Soler-Jofra, A., Stevens, B., Hoekstra, M., Picioeanu, C., Sorokin, D., van Loosdrecht, M.C.M. and Pérez, J. (2016). Importance of abiotic hydroxylamine conversion on nitrous oxide emissions during nitrification of reject water. *Chemical Engineering Journal*, **287**, 720-726.
- Spang, A., Poehlein, A., Offre, P., Zumbärgel, S., Haider, S., Rychlik, N., Nowka, B., Schmeisser, C., Lebedeva, E.V., Rattei, T., Böhm, C., Schmid, M., Galushko, A., Hatzepichler, R., Weinmaier, T., Daniel, R., Schleper, C., Spieck, E., Streit, W. and Wagner, M. (2012). The genome of the ammonia-oxidizing Candidatus *Nitrososphaera gargensis*: insights into metabolic versatility and environmental adaptations. *Environmental Microbiology*, **14**, 3122-3145.
- Spott, O. and Stange, F.C. (2011). Formation of hybrid N₂O in a suspended soil due to co-denitrification of NH₂OH. *Journal of Plant Nutrition and Soil Science*, **174**, 554-567.
- Stein, L.Y. 2011. 6 Surveying N₂O-Producing Pathways in Bacteria. In: *Methods in Enzymology* (ed. Klotz, M.G.), pp. 131-152. Elsevier

- Stevenson, F. and Swaby, R. (1964). Nitrosation of soil organic matter: I. Nature of gases evolved during nitrous acid treatment of lignins and humic substances. *Soil Science Society of America Journal*, **28**, 773-778.
- Stieglmeier, M., Mooshammer, M., Kitzler, B., Wanek, W., Zechmeister-Boltenstern, S., Richter, A. and Schleper, C. (2014). Aerobic nitrous oxide production through N-nitrosating hybrid formation in ammonia-oxidizing archaea. *The ISME Journal*, **8**, 1135-1146.
- Strickland, J.D. and Parsons, T.R. 1972. *A practical handbook of seawater analysis*. Fisheries Research Board of Canada, Ottawa.
- Stroetmann, I., Kämpfer, P. and Dott, W. (1994). [The efficiency of sterilization methods for different soils]. *Zentralblatt für Hygiene und Umweltmedizin= International journal of hygiene and environmental medicine*, **195**, 111-120.
- Stüven, R., Vollmer, M. and Bock, E. (1992). The impact of organic matter on nitric oxide formation by *Nitrosomonas europaea*. *Archives of Microbiology*, **158**, 439-443.
- Su, H., Cheng, Y., Oswald, R., Behrendt, T., Trebs, I., Meixner, F.X., Andreae, M.O., Cheng, P., Zhang, Y. and Pöschl, U. (2011). Soil Nitrite as a Source of Atmospheric HONO and OH Radicals. *Science*, **333**, 1616-1618.
- Sutka, R.L., Ostrom, N., Ostrom, P., Breznak, J., Gandhi, H., Pitt, A. and Li, F. (2006). Distinguishing nitrous oxide production from nitrification and denitrification on the basis of isotopomer abundances. *Applied and Environmental Microbiology*, **72**, 638-644.
- Sutka, R.L., Ostrom, N.E., Ostrom, P.H., Gandhi, H. and Breznak, J.A. (2004). Nitrogen isotopomer site preference of N₂O produced by *Nitrosomonas europaea* and *Methylococcus capsulatus* Bath. *Rapid Communications in Mass Spectrometry*, **18**, 1411-1412.
- Syakila, A. and Kroeze, C. (2011). The global nitrous oxide budget revisited. *Greenhouse Gas Measurement and Management*, **1**, 17-26.
- Szukics, U., Abell, G.C.J., Hödl, V., Mitter, B., Sessitsch, A., Hackl, E. and Zechmeister-Boltenstern, S. (2010). Nitrifiers and denitrifiers respond rapidly to changed moisture and increasing temperature in a pristine forest soil. *FEMS Microbiology Ecology*, **72**, 395-406.
- Terada, A., Sugawara, S., Hojo, K., Takeuchi, Y., Riya, S., Harper, W.F., Yamamoto, T., Kuroiwa, M., Isobe, K., Katsuyama, C., Suwa, Y., Koba, K. and Hosomi, M. (2017). Hybrid nitrous oxide production from a partial nitrifying bioreactor: hydroxylamine interactions with nitrite. *Environmental Science & Technology*, **51**, 2748-2756.
- Thion, C. and Prosser, J.I. (2014). Differential response of nonadapted ammonia-oxidising archaea and bacteria to drying–rewetting stress. *FEMS Microbiology Ecology*, **90**, 380-389.
- Thorn, K. and Mikita, M. (2000). Nitrite fixation by humic substances nitrogen-15 nuclear magnetic resonance evidence for potential intermediates in chemodenitrification. *Soil Science Society of America Journal*, **64**, 568-582.
- Thorn, K.A., Arterburn, J.B. and Mikita, M.A. (1992). Nitrogen-15 and carbon-13 NMR investigation of hydroxylamine-derivatized humic substances. *Environmental Science & Technology*, **26**, 107-116.
- Tietema, A., De Boer, W., Riemer, L. and Verstraten, J. (1992). Nitrate production in nitrogen-saturated acid forest soils: vertical distribution and characteristics. *Soil Biology and Biochemistry*, **24**, 235-240.
- Tourna, M., Stieglmeier, M., Spang, A., Könneke, M., Schintlmeister, A., Urich, T., Engel, M., Schlöter, M., Wagner, M., Richter, A. and Schleper, C. (2011). *Nitrososphaera viennensis*, an ammonia oxidizing archaeon from soil. *Proceedings of the National Academy of Sciences*, **108**, 8420-8425.
- Toyoda, S. and Yoshida, N. (1999). Determination of nitrogen isotopomers of nitrous oxide on a modified isotope ratio mass spectrometer. *Analytical Chemistry*, **71**, 4711-4718.
- Turner, D.A., Chen, D., Galbally, I.E., Leuning, R., Edis, R.B., Li, Y., Kelly, K. and Phillips, F. (2008). Spatial variability of nitrous oxide emissions from an Australian irrigated dairy pasture. *Plant and Soil*, **309**, 77-88.

- Vajrala, N., Martens-Habbena, W., Sayavedra-Soto, L.A., Schauer, A., Bottomley, P.J., Stahl, D.A. and Arp, D.J. (2013). Hydroxylamine as an intermediate in ammonia oxidation by globally abundant marine archaea. *Proceedings of the National Academy of Sciences*, **110**, 1006-1011.
- van Cleemput, O. (1998). Subsoils: chemo-and biological denitrification, N₂O and N₂ emissions. *Nutrient Cycling in Agroecosystems*, **52**, 187-194.
- van Cleemput, O. and Baert, L. (1984). Nitrite: a key compound in N loss processes under acid conditions? *Plant and Soil*, **76**, 233-241.
- van Cleemput, O. and Samater, A.H. (1995). Nitrite in soils: accumulation and role in the formation of gaseous N compounds. *Fertilizer Research*, **45**, 81-89.
- van Kessel, M.A., Speth, D.R., Albertsen, M., Nielsen, P.H., den Camp, H.J.O., Kartal, B., Jetten, M.S. and Lückner, S. (2015). Complete nitrification by a single microorganism. *Nature*, **528**, 555-559.
- Velthof, G.L., van Groenigen, J.W., Gebauer, G., Pietrzak, S., Jarvis, S.C., Pinto, M., Corré, W. and Oenema, O. (2000). Temporal stability of spatial patterns of nitrous oxide fluxes from sloping grassland. *Journal of Environmental Quality*, **29**, 1397-1407.
- Venterea, R.T. (2007). Nitrite - driven nitrous oxide production under aerobic soil conditions: kinetics and biochemical controls. *Global Change Biology*, **13**, 1798-1809.
- Venterea, R.T., Groffman, P.M., Verchot, L.V., Magill, A.H., Aber, J.D. and Steudler, P.A. (2003). Nitrogen oxide gas emissions from temperate forest soils receiving long-term nitrogen inputs. *Global Change Biology*, **9**, 346-357.
- Venterea, R.T., Rolston, D.E.E. and Cardon, Z.G. (2005). Effects of Soil Moisture, Physical, and Chemical Characteristics on Abiotic Nitric Oxide Production. *Nutrient Cycling in Agroecosystems*, **72**, 27-40.
- von Breyman, M.T., De Angelis, M.A. and Gordon, L.I. (1982). Gas chromatography with electron capture detection for determination of hydroxylamine in seawater. *Analytical Chemistry*, **54**, 1209-1210.
- Walker, C., De La Torre, J., Klotz, M., Urakawa, H., Pinel, N., Arp, D., Brochier-Armanet, C., Chain, P., Chan, P. and Gollabgir, A. (2010). *Nitrosopumilus maritimus* genome reveals unique mechanisms for nitrification and autotrophy in globally distributed marine crenarchaea. *Proceedings of the National Academy of Sciences*, **107**, 8818-8823.
- Wei J., Amelung W., Lehndorff E., Schloter M., Vereecken H. and Brüggemann N. (2017a). N₂O and NO_x emissions by reactions of nitrite with soil organic matter of a Norway spruce forest. *Biogeochemistry* **132**, 325–342.
- Wei J., Zhou M., Vereecken H. and Brüggemann N. (2017b). Large variability of CO₂ and N₂O emissions and of ¹⁵N site preference of N₂O from reactions of nitrite with lignin and its derivatives at different pH. *Rapid Communications in Mass Spectrometry*, **31**, 1333-1343.
- Weiss, R.F. and Price, B.A. (1980). Nitrous oxide solubility in water and seawater. *Marine Chemistry*, **8**, 347-359.
- Widdel, F. (1980). Anaerober Abbau von Fettsäuren und Benzoesäure durch neu isolierte Arten Sulfat-reduzierender Bakterien. *Dissertation, Universität Göttingen*, 1-443.
- WMO. (2010). WMO Greenhouse gas bulletin: the state of greenhouse gases in the atmosphere based on observations through 2009. See <http://www.wmo.int/gaw/>.
- Wolf, I. and Brumme, R. (2003). Dinitrogen and nitrous oxide formation in Beech forest floor and mineral soils. *Soil Science Society of America Journal*, **67**, 1862-1868.
- Wrage, N., Velthof, G.L., Laanbroek, H.J. and Oenema, O. (2004). Nitrous oxide production in grassland soils: assessing the contribution of nitrifier denitrification. *Soil Biology and Biochemistry*, **36**, 229-236.
- Wrage, N., Velthof, G.L., van Beusichem, M.L. and Oenema, O. (2001). Role of nitrifier denitrification in the production of nitrous oxide. *Soil Biology and Biochemistry*, **33**, 1723-1732.
- Wunderlin, P., Lehmann, M.F., Siegrist, H., Tuzson, B., Joss, A., Emmenegger, L. and Mohn, J. (2013). Isotope signatures of N₂O in a mixed microbial population system: constraints on N₂O producing pathways in wastewater treatment. *Environmental Science & Technology*, **47**, 1339-1348.

- Wunderlin, P., Mohn, J., Joss, A., Emmenegger, L. and Siegrist, H. (2012). Mechanisms of N₂O production in biological wastewater treatment under nitrifying and denitrifying conditions. *Water Research*, **46**, 1027-1037.
- Yanai, J., Sawamoto, T., Oe, T., Kusa, K., Yamakawa, K., Sakamoto, K., Naganawa, T., Inubushi, K., Hatano, R. and Kosaki, T. (2003). Spatial variability of nitrous oxide emissions and their soil-related determining factors in an agricultural field. *Journal of Environment Quality*, **32**, 1965-1977.
- Yoshida, N. and Toyoda, S. (2000). Constraining the atmospheric N₂O budget from intramolecular site preference in N₂O isotopomers. *Nature*, **405**, 330-334.
- Yu, R. and Chandran, K. (2010). Strategies of *Nitrosomonas europaea* 19718 to counter low dissolved oxygen and high nitrite concentrations. *BMC Microbiology*, **10**, 1-11.
- Zacharias, S., Bogena, H., Samaniego, L., Mauder, M., Fuß, R., Pütz, T., Frenzel, M., Schwank, M., Baessler, C., Butterbach-Bahl, K., Bens, O., Borg, E., Brauer, A., Dietrich, P., Hajnsek, I., Helle, G., Kiese, R., Kunstmann, H., Klotz, S., Munch, J.C., Papen, H., Priesack, E., Schmid, H.P., Steinbrecher, R., Rosenbaum, U., Teutsch, G. and Vereecken, H. (2011). A Network of Terrestrial Environmental Observatories in Germany. *Vadose Zone Journal*, **10**, 955-973.
- Zhang, J., Müller, C. and Cai, Z. (2015b). Heterotrophic nitrification of organic N and its contribution to nitrous oxide emissions in soils. *Soil Biology and Biochemistry*, **84**, 199-209.
- Zhang, X., Davidson, E.A., Mauzerall, D.L., Searchinger, T.D., Dumas, P. and Shen, Y. (2015a). Managing nitrogen for sustainable development. *Nature*, **528**, 51-59.
- Zhu-Barker, X., Cavazos, A.R., Ostrom, N.E., Horwath, W.R. and Glass, J.B. (2015). The importance of abiotic reactions for nitrous oxide production. *Biogeochemistry*, **126**, 251-267.
- Zhu, X., Burger, M., Doane, T.A. and Horwath, W.R. (2013a). Ammonia oxidation pathways and nitrifier denitrification are significant sources of N₂O and NO under low oxygen availability. *Proceedings of the National Academy of Sciences of the United States of America*, **110**, 6328-6333.
- Zhu, X., Silva, L.C.R., Doane, T.A. and Horwath, W.R. (2013b). Iron: The Forgotten Driver of Nitrous Oxide Production in Agricultural Soil. *PLoS One*, **8**, e60146.

Appendix

Figure S2.1

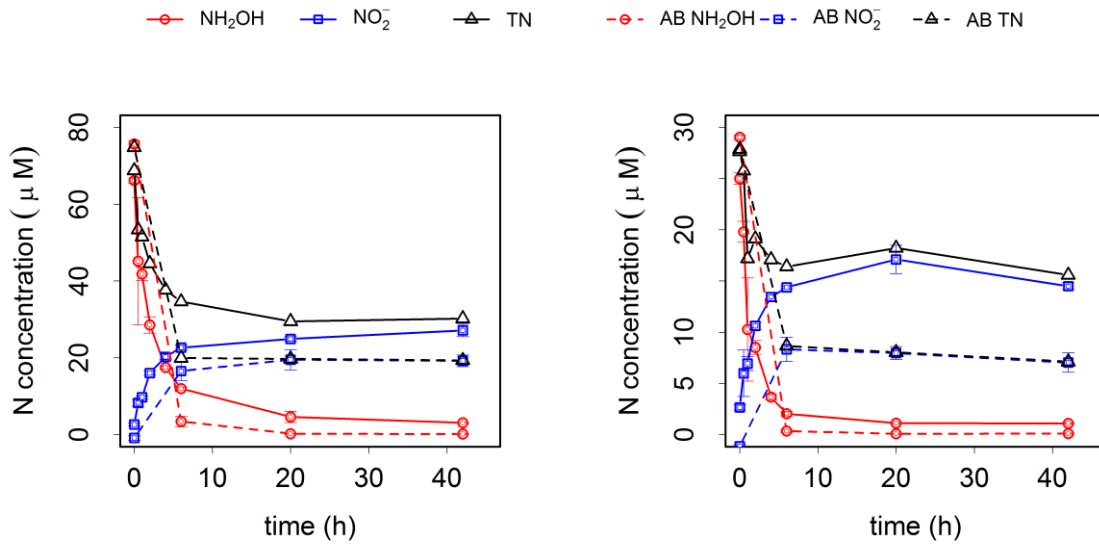


Figure S2.1 Dynamics of NH₂OH, NO₂⁻ and total N (TN) during incubation of the AOA *N. gargensis* (Ng) or only CaCO₃ medium (abiotic control, AB) after addition of NH₂OH (30/right panel or 80/left panel μM). The values are presented as mean ± standard deviation (SD). The differences of NO₂⁻ between the abiotic and biotic treatments are significant ($P < 0.01$, mixed model repeated measures) for both 30 and 80 μM NH₂OH addition.

Figure S2.2

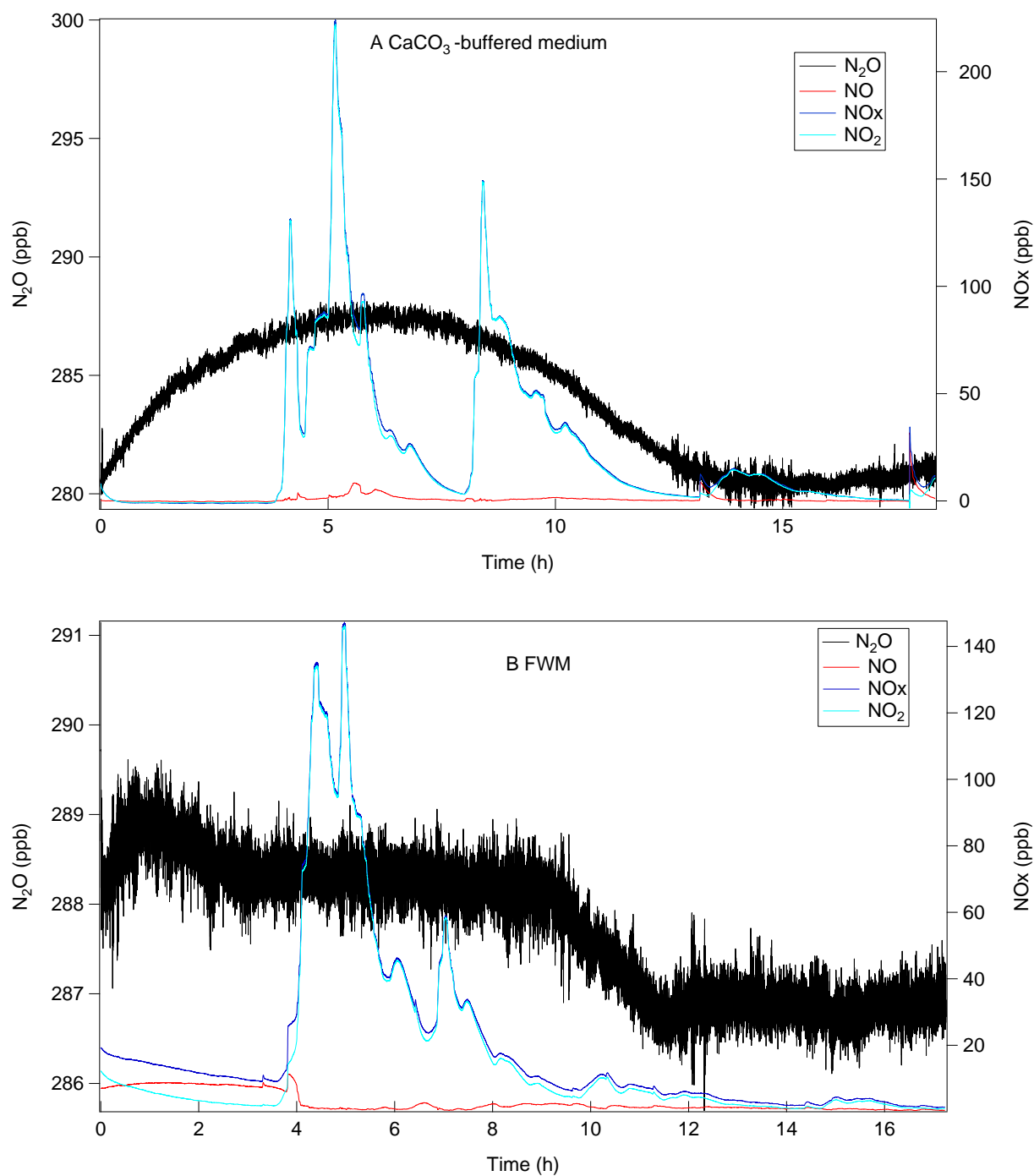


Figure S2.2 Mixing ratios (ppb) of N_2O (left y-axis) and NO_x (right y-axis) during NH_2OH (0.08 mM) abiotic decay at 37 °C using an infrared laser absorption spectrometer for online real-time analysis of N_2O mixing ratio and a chemoluminescence NO_x analyzer.

Figure S2.3

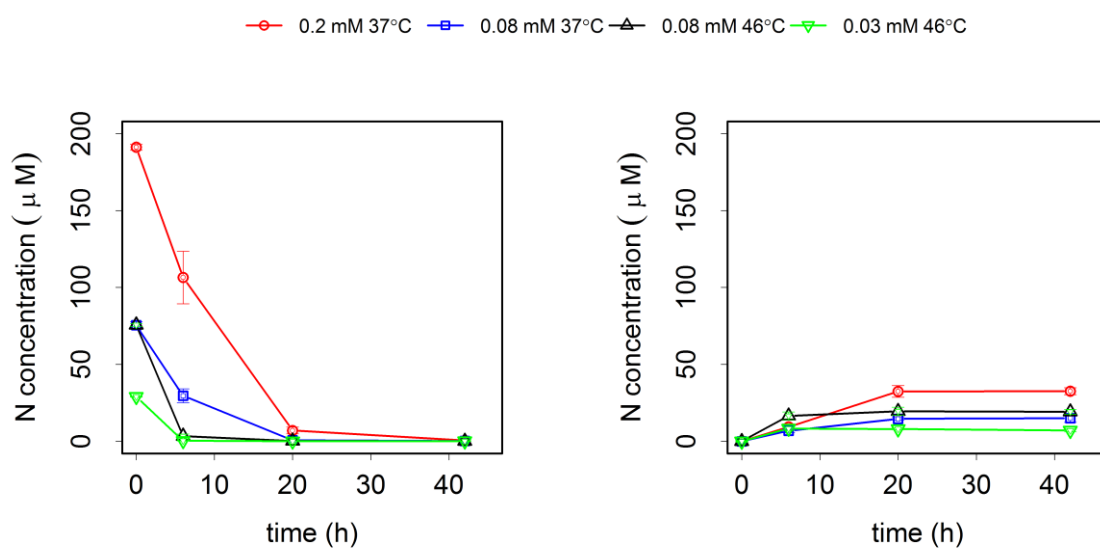


Figure S2.3 Changes in NH_2OH (left panel) and NO_2^- (right panel) following addition of different concentrations (0.03, 0.08 and 0.2 mM) of NH_2OH to CaCO_3 -buffered medium at two temperatures (37 and 46 °C) levels. The values are presented as mean \pm standard deviation (SD).

Figure S2.4

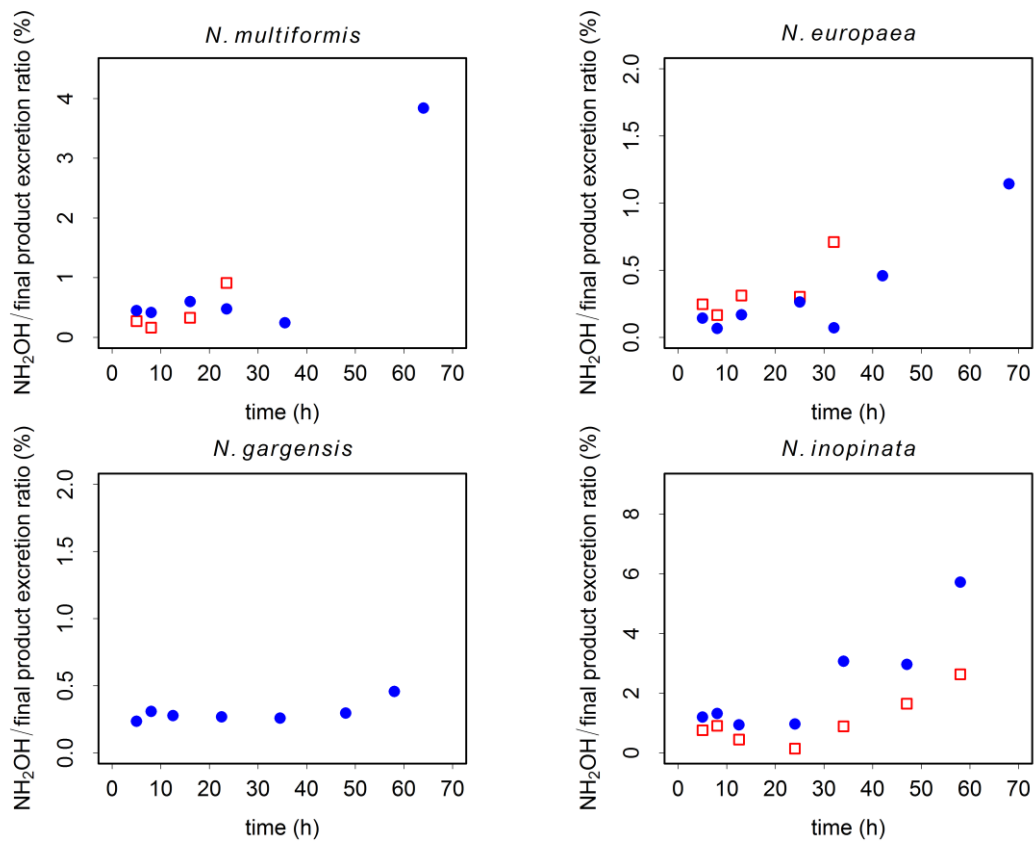


Figure S2.4 NH_2OH :final product ratios (%) during incubation at two different initial NH_4^+ concentrations (0.5 mM, square; 2 mM, circle) for four different cultures of ammonia-oxidizers. Please note that the y-axes are not always scaled identically to improve data presentation.

Figure S5.1

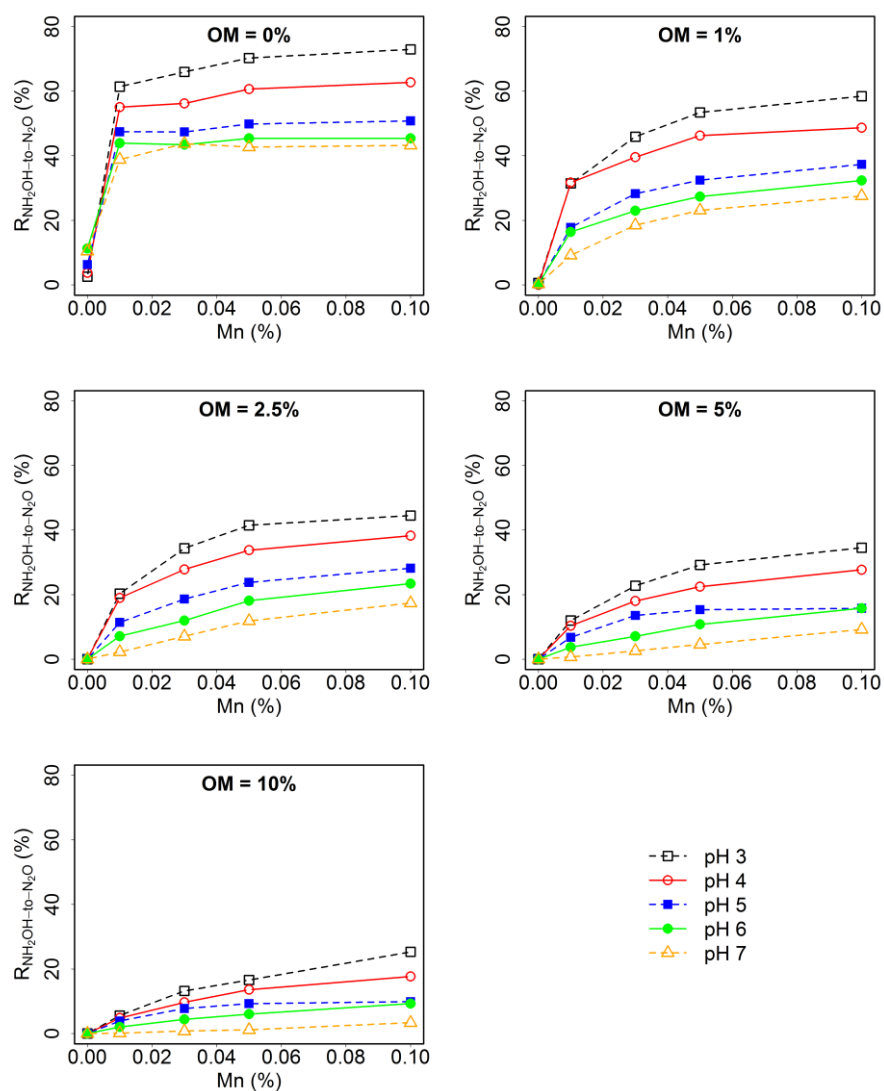


Figure S5.1 NH_2OH -to- N_2O conversion ratios ($R_{\text{NH}_2\text{OH-to-N}_2\text{O}}$) in artificial soil mixtures at different pH as well as MnO_2 and organic matter (OM, peat moss) contents. The total amount of NH_2OH added was 5 nmol. Different symbols represent $R_{\text{NH}_2\text{OH-to-N}_2\text{O}}$ at different pH levels.

Figure S5.2

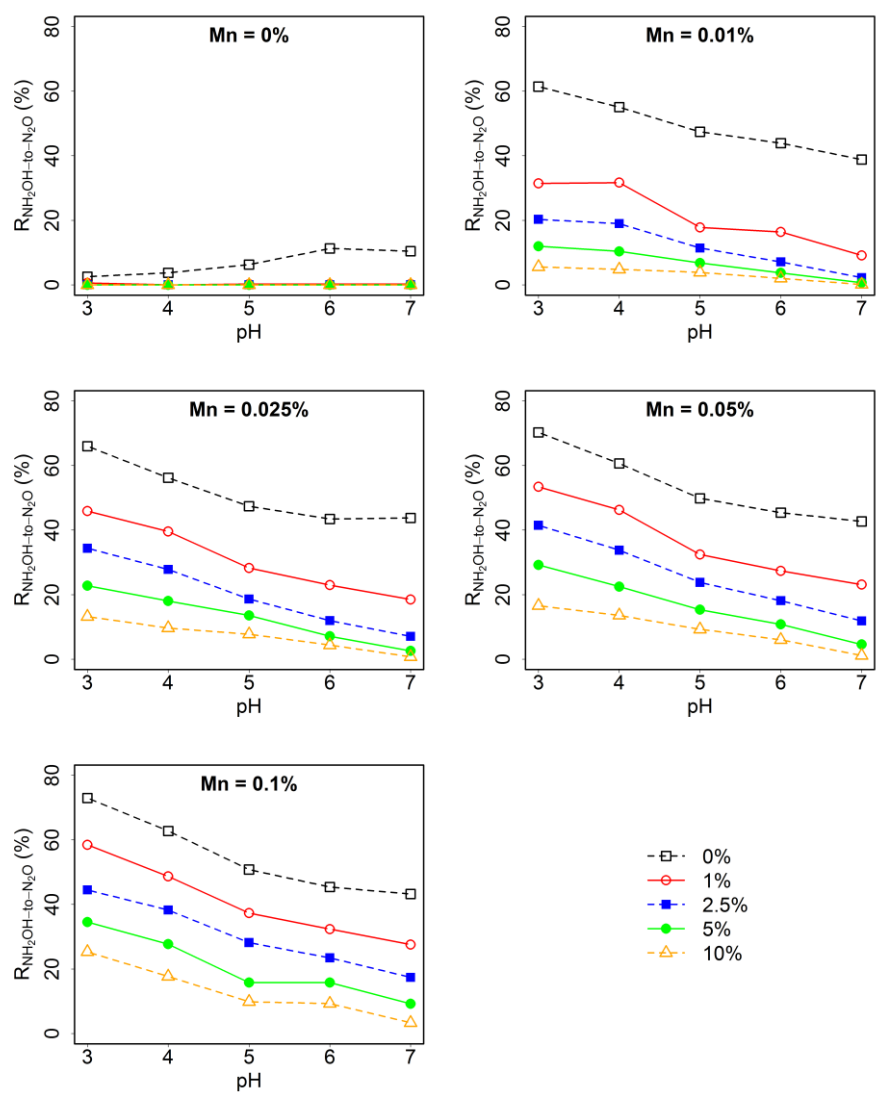


Figure S5.2 $\text{NH}_2\text{OH-to-N}_2\text{O}$ conversion ratios ($R_{\text{NH}_2\text{OH-to-N}_2\text{O}}$) in artificial soil mixtures at different pH as well as MnO_2 and organic matter (OM, peat moss) contents. The total amount of NH_2OH added was 5 nmol. Different symbols represent $R_{\text{NH}_2\text{OH-to-N}_2\text{O}}$ at different OM contents.

Figure S5.3

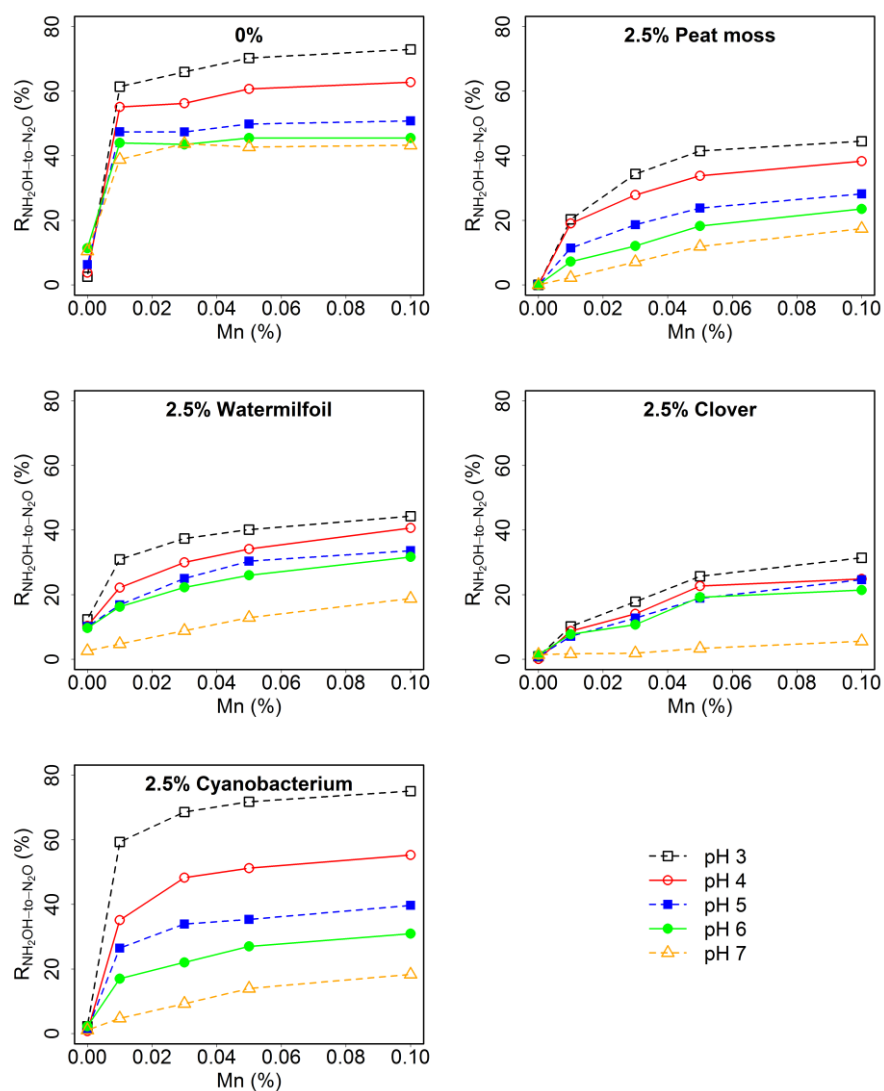


Figure S5.3 NH_2OH -to- N_2O conversion ratios ($R_{\text{NH}_2\text{OH-to-N}_2\text{O}}$) in artificial soils at different pH and MnO_2 content, and for organic matter (OM) of different origins at a fixed content of 2.5% (w/w). The total amount of NH_2OH added was 5 nmol. Different symbols represent $R_{\text{NH}_2\text{OH-to-N}_2\text{O}}$ for the artificial soil mixtures under different pH levels.

Figure S5.4

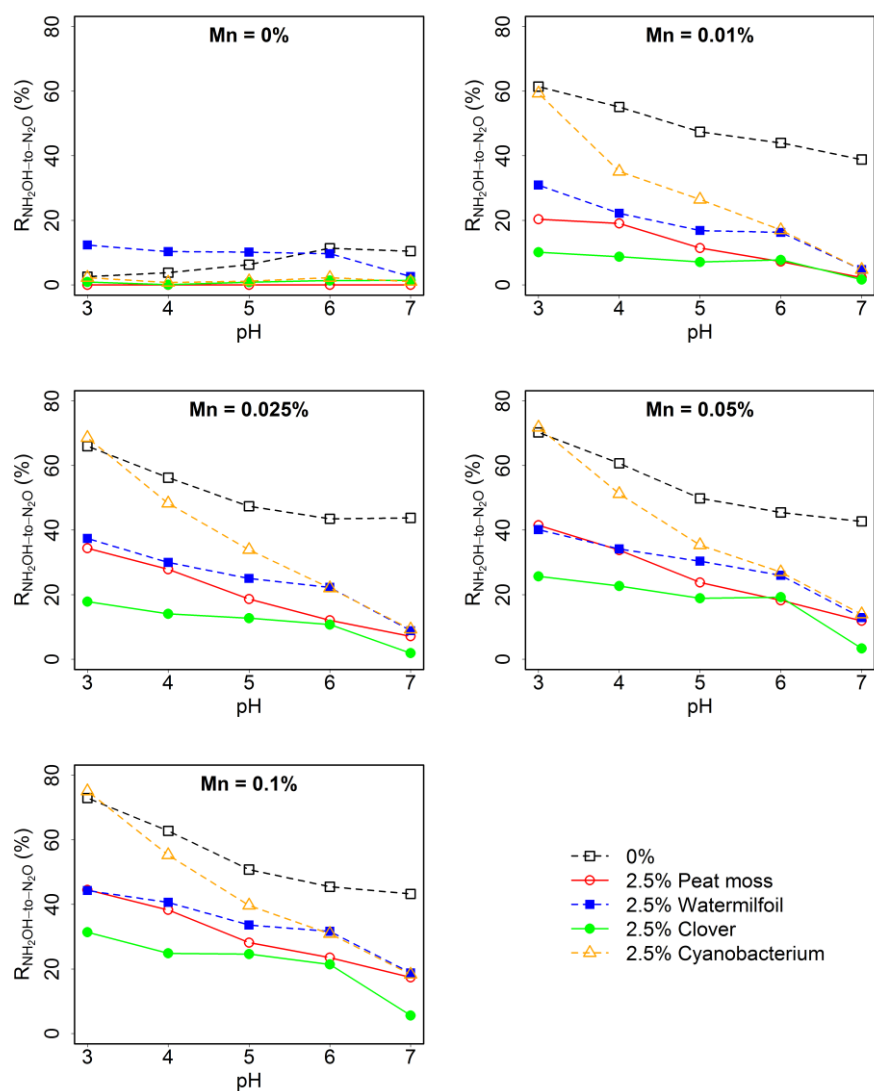


Figure S5.4 NH₂OH-to-N₂O conversion ratios ($R_{\text{NH}_2\text{OH-to-N}_2\text{O}}$) in artificial soils at different pH and MnO₂ content, and for organic matter (OM) of different origins at a fixed content of 2.5% (w/w). The total amount of NH₂OH added was 5 nmol. Different symbols represent $R_{\text{NH}_2\text{OH-to-N}_2\text{O}}$ for the artificial soil mixtures with different OM origins.

Table S2.1**Table S2.1** Centrifugation and incubation conditions for the ammonia-oxidizing strains tested.

Culture type	Strain	Centrifugation conditions (g, min)	Incubation bottles (culture and bottle volume (ml), type)	Initial protein in each bottle ($\mu\text{g ml}^{-1}$)	Incubation conditions ($^{\circ}\text{C}$, shaking or not)	Incubation time (h)
	<i>Nitrosomonas europaea</i> ATCC 19718	8000, 30	60, 120, Serum	3.5	30, no	68
	<i>Nitrospira multiformis</i> ATCC 25196	8000, 30		3.3	30, no	64
AOB pure culture	<i>Nitrosomonas communis</i> Nm2	8000, 20	50, 100, Schott	3.29	28, yes	58
	<i>Nitrosomonas nitrosa</i> Nm90	7830, 20		1.64	37, yes	84
AOA pure culture	<i>Nitrososphaera gargensis</i>	7830, 20	50, 100, Schott	4.64	46, no	58
	<i>Nitrososphaera viennensis</i>	8000, 20		0.72	37, no	58
	<i>Ca. N. sp.</i> Nd2	8000, 30	60, 120, Serum	0.4	35, no	67
AOA enrichment	<i>Ca. N. uzonensis</i>	8000, 20	50, 100, Schott	1.43	46, no	124
Comam-mox enrichment	<i>Ca. N. inopinata</i>	7830, 30	50, 100, Schott	1.74	37, no	58

Table S2.2**Table S2.2** First-order rate constant (k) of abiotic NH_2OH decay in different media at different NH_2OH (0.5, 1, 2.5 and 5 μM) and NO_2^- (0 and 2 mM) concentrations.

NO_2^- (mM)	0				2			
	NH_2OH (μM)	0.5	1	2.5	5	0.5	1	2.5
HEPES (30 $^{\circ}\text{C}$)	0.22	0.15	0.12	-	0.13	0.10	0.07	-
CaCO_3 (30 $^{\circ}\text{C}$)	1.13	0.74	0.56	0.40	0.69	0.39	0.33	0.32
CaCO_3 (37 $^{\circ}\text{C}$)	0.81	0.74	0.89	0.74	-	-	-	-
CaCO_3 (46 $^{\circ}\text{C}$)	2.11	0.96	1.09	1.05	0.93	0.61	0.51	0.48

Table S2.3

Table S2.3 $\delta^{15}\text{N}$ values of N_2O produced by the reaction of NH_2OH and Fe(III) during the NH_2OH assay in the presence of 2 mM ^{15}N -labeled nitrite ($\delta^{15}\text{N} = 1185 \pm 2 \text{‰}$).

Samples	N_2O (ppb)	$\delta^{15}\text{N}$ (‰ vs. air-N_2)
CaCO_3 0h	257	3.09
HEPES 0h	312	3.83
CaCO_3 2h	110	5.12
HEPES 2h	220	4.25
CaCO_3 8h	7.3	6.13
HEPES 8h	16.5	4.07